

AD-A151 946

A MODERN CONTROL DESIGN METHODOLOGY WITH APPLICATION TO
THE CH-47 HELICOPTER(U) AIR FORCE INST OF TECH
WRIGHT-PATTERSON AFB OH R D HOLDRIDGE JAN 85

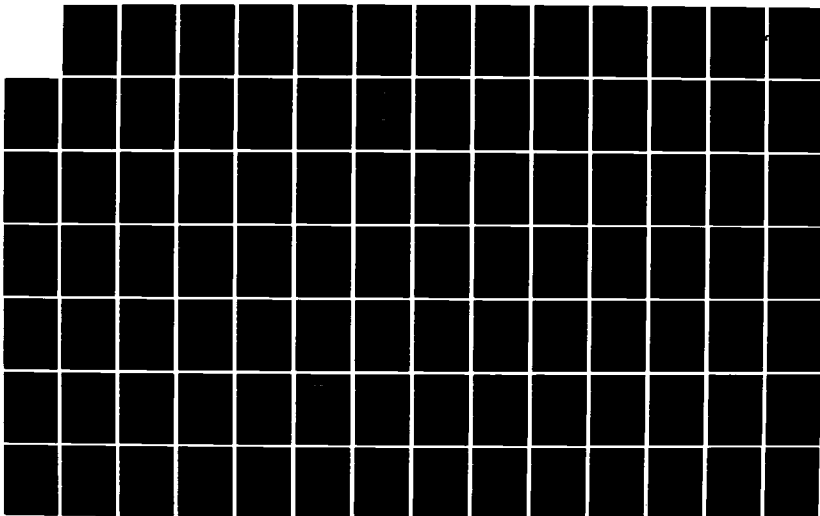
1/3

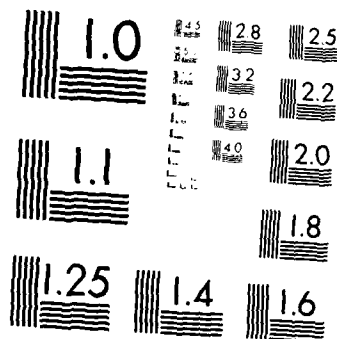
UNCLASSIFIED

AFIT/CI/NR-85-33D

F/G 1/4

NL





MICROCOPY RESOLUTION TEST CHART
NATIONAL BUREAU OF STANDARDS 1963-A

UNCLASS

SECURITY CLASSIFICATION OF THIS PAGE (When Data Entered)

AD-A151 946

1

REPORT DOCUMENTATION PAGE

READ INSTRUCTIONS
BEFORE COMPLETING FORM

1. REPORT NUMBER

AFIT/CI/NR 85-330

2. ACCESSION NUMBER

3. REPORT TYPE, CATALOG NUMBER

4. TITLE (and Subtitle)

A Modern Control Design Methodology With
Application To The CH-47 Helicopter

5. TYPE OF REPORT & PERIOD COVERED

THESIS/DISSERTATION

6. PERFORMING ORG. REPORT NUMBER

7. AUTHOR(s)

Richard D. Holdridge

8. CONTRACT OR GRANT NUMBER(s)

9. PERFORMING ORGANIZATION NAME AND ADDRESS

AFIT STUDENT AT: Stanford University

10. PROGRAM ELEMENT, PROJECT, TASK
AREA & WORK UNIT NUMBERS

11. CONTROLLING OFFICE NAME AND ADDRESS

AFIT/NR
WPAFB OH 45433

12. REPORT DATE

Jan 1985

13. NUMBER OF PAGES

235

14. MONITORING AGENCY NAME & ADDRESS (if different from Controlling Office)

15. SECURITY CLASS. (of this report)

UNCLASS

16. DECLASSIFICATION/DOWNGRADING
SCHEDULE

17. DISTRIBUTION STATEMENT (of this Report)

APPROVED FOR PUBLIC RELEASE; DISTRIBUTION UNLIMITED

18. DISTRIBUTION STATEMENT (of the abstract entered in Block 20, if different from Report)

19. SUPPLEMENTARY NOTES

APPROVED FOR PUBLIC RELEASE: IAW AFR 190-1

LYNN E. WOLAVER (dtd 8/85)
Dean for Research and
Professional Development
AFIT, Wright-Patterson AFB OH

20. KEY WORDS (Continue on reverse side if necessary and identify by block number)

ATTACHED

DTIC FILE COPY

DTIC
ELECTE
MAR 27 1985
S E D

FORM 1473 85 03 11 050

SECURITY CLASSIFICATION OF THIS PAGE (When Data Entered)

**A MODERN CONTROL DESIGN METHODOLOGY
WITH APPLICATION TO THE CH-47 HELICOPTER**

**A DISSERTATION
SUBMITTED TO THE DEPARTMENT OF AERONAUTICS AND
ASTRONAUTICS
AND THE COMMITTEE ON GRADUATE STUDIES
OF STANFORD UNIVERSITY
IN PARTIAL FULFILLMENT OF THE REQUIREMENTS
FOR THE DEGREE OF
DOCTOR OF PHILOSOPHY**

by
Richard D. Holdridge
January 1985

Accession For		
NTIS	GRA&I	<input checked="checked" type="checkbox"/>
DTIC	TAB	<input type="checkbox"/>
Unannounced		<input type="checkbox"/>
Justification		
By		
Distribution/		
Availability Codes		
Avail and/or		
Dist	Special	
A-1		



I certify that I have read this thesis and that in my opinion it is fully adequate, in scope and quality, as a dissertation for the degree of Doctor of Philosophy.

A. E. Bryson Jr.
(Principal Adviser)

I certify that I have read this thesis and that in my opinion it is fully adequate, in scope and quality, as a dissertation for the degree of Doctor of Philosophy.

R. Cannon

I certify that I have read this thesis and that in my opinion it is fully adequate, in scope and quality, as a dissertation for the degree of Doctor of Philosophy.

Samuel A. D. J.

Approved for the University Committee
on Graduate Studies:

Dean of Graduate Studies & Research

A MODERN CONTROL DESIGN METHODOLOGY WITH APPLICATION TO THE CH-47 HELICOPTER

Richard D. Holdridge, Ph.D.

Stanford University, 1985

A control system design methodology is developed which produces robust, low-order optimal controllers for multiple-input multiple-output systems. The methodology attempts to focus the strengths of recent "Modern Control" design algorithms on the problems associated with real control system designs. The methodology is a set of procedures which aids the engineer in creating a realizable controller in either digital or analog form.

To demonstrate the usefulness of the methodology, two control augmentation systems (CAS) were designed and flight tested on a CH-47 helicopter at NASA Ames Research Center. The first design was a longitudinal cruise CAS giving the pilot decoupled control of forward velocity and climb rate. This design task demonstrated the low-order controller and robustness features of the methodology. It also demonstrated the use of modern control techniques in designing integral-error controllers. Flight test results are presented. The second controller is a translational velocity command/ precision hover hold system. This two mode controller demonstrates the methodology as applied to a more complicated design task which includes control law switching and inner loop/ outer loop considerations. Flight test results are also presented.

Acknowledgements

I am grateful to my adviser, Prof. A. E. Bryson, for suggesting this research topic and then providing the enthusiastic support needed to bring it to a successful conclusion. I am equally grateful to Mr. Bill Hindson who was tireless in his efforts to make the flight test such a success. I suspect I learned as much engineering from Bill while working on the flight control system as I did in the many courses I took.

Thanks also to the many people at Ames who made the flight research possible. It was really a team effort: Dr. Vic Lebacqz, Dr. Bob Chen, Ms. Katy Hilbert who helped in the engineering and the flight test; Lt. Col. Grady Wilson and Mr. George Tucker, the project test pilots; Mr. Jim Jeske and Mr. Dave Guevara who provided the computer support. At Stanford, Doug Bernard, Peter Chu, Bruce Gardner, and Dan Rosenthal were very helpful by providing software which I incorporated into the various programs.

I'm also grateful to Prof. R. Cannon and Prof. D. Debra for reviewing this thesis and making helpful comments.

Finally, I can never adequately express the gratitude I feel to my parents, Mr. and Mrs. Kenneth B. Holdridge, whose love and support have sustained me far more than they can know.

CONTENTS

Abstract	iii
Acknowledgements	iv
Contents	v
Figures	ix
1. Introduction	1
1.1. Historical Background on Control System Design	1
1.2. A Modern Control Design Methodology	4
2. The Design Methodology	10
2.1. Model Derivation	10
2.2. Model Scaling	11
2.3. LQG Design	13
2.4. Compensator Order Reduction and Reoptimization	18
2.5. Command Inputs	23
2.6. Simulation and Test	25
2.7. Summary	30
3. Longitudinal CAS for the CH-47	31
3.1. Design Goals and Constraints	31
3.2. Linear Models and Basic Control Structure	34
3.3. Model Scaling	37

3.4.	LQG Design of the Full Order Compensator	40
3.4.1.	Redesign Using Arbitrary Measurement Spectral Densities	41
3.4.2.	Redesign Using an Inverse Optimal Controller	43
3.5.	Compensator Order Reduction	46
3.5.1.	Robust Longitudinal Third Order Compensator	49
3.5.2.	Longitudinal Output Feedback Controller	51
3.5.3.	Summary of Design Results	56
3.6.	Flight Test Implementation	59
3.7.	Flight Test Results	61
3.8.	Summary of Results for the Longitudinal CAS Design	63
4.	Hover Controller for the CH-47	71
4.1.	Design Goals and Constraints	71
4.2.	Linear Model and Basic Control Structure	73
4.3.	Model Scaling	74
4.4.	LQG Design and Compensator Order Reduction	78
4.5.	Outer Loop Design	80
4.5.1.	Transfer Function Analysis for X Axis Outer Loop	82
4.5.2.	Outer Loop Simulation	84
4.6.	Flight Test Implementation	85
4.6.1.	Inertial Velocity and Position Data	91
4.6.2.	Transient-Free Switching	93
4.7.	Flight Test Results	93
4.7.1.	Support Systems Development Flying	97
4.7.2.	Preliminary Closed Loop Flight Test in Hover	97

4.7.3. Hover Controller Redesign	98
4.7.4. Final Closed Loop Flight Test in Hover	107
4.8. Summary of Results of the Hover Controller Design	111
5. Conclusions	117
5.1. Methodology	117
5.2. Flight Tests	118
5.3. Lessons Learned	118
6. Recommendations for Further Research	120
References	122
A. Engineering Scaling	125
B. Optimal Compensator Design	129
C. Minimal Realizations	132
D. Set Point Design	136
E. Fixed Point Scaling	138
F. CH-47 Research Helicopter	141
G. CH-47 Linear Models	144
H. Bessel Filters	161
I. Flight Software	165

J. ROPTSYS Computer Program	201
K. RSANDY Computer Program	205
L. SETPNT Computer Program	209
M. SIMPLOT Computer Program	219
N. SCALEM1 and SCALEM2 Computer Programs	228

FIGURES

Figure 1.1. Classical Control	5
Figure 1.2. Modern Control	5
Figure 1.3. The Design Methodology	8
Figure 2.1. Navion Linear Model Before Scaling	12
Figure 2.2. Navion Linear Model After Scaling	14
Figure 2.3. Navion Full Order Compensator	19
Figure 2.4. Navion Full Order Compensator Performance	19
Figure 2.5. Navion Reduced Order Compensator Design Results	21
Figure 2.6. Commanding a Desired Output	24
Figure 2.7. Velocity Response for Full Order Compensator	26
Figure 2.8. Velocity Response for Reduced Order Compensator	26
Figure 2.9. Climb Rate Response for Full Order Compensator	27
Figure 2.10. Climb Rate Response for Reduced Order Compensator	28
Figure 2.11. Navion Full Order Compensator Performance in Turbulence	28
Figure 2.12. Navion Reduced Order Compensator Performance in Turbulence	29
Figure 3.1. Sensors Available on the NASA CH-47	33
Figure 3.2. CH-47 Longitudinal Model	34
Figure 3.3. Controller Structure for The Longitudinal Cruise Autopilot	36
Figure 3.4. CH-47 Longitudinal Linear Model at 60 knots	38
Figure 3.5. CH-47 Scaled Longitudinal Linear Model at 60 knots	39
Figure 3.6. CH-47 Longitudinal Full Order Compensator	42
Figure 3.7. Time Responses using Nomimal Noise	43

Figure 3.8. Time Responses with Commands to the Compensator	44
Figure 3.9. Longitudinal CAS using Arbitrary Measurement Spectral Density	45
Figure 3.10. Time Responses using Arbitrary Noise	46
Figure 3.11. Longitudinal Compensator based on Inverse Optimal Solution	47
Figure 3.12. Time Responses using Inverse Optimal Controller	48
Figure 3.13. Performance Comparison of Full Order Compensators	48
Figure 3.14. Longitudinal Reduced Order Compensator	50
Figure 3.15. Reduced Order Compensator Time Responses	51
Figure 3.16. Longitudinal Reduced Order Compensator with Integral Control	52
Figure 3.17. Reduced Order Integral Controller Time Responses	53
Figure 3.18. Longitudinal Full Order Compensator with Integral Control .	54
Figure 3.19. Longitudinal Full Order Integral Controller Time Responses .	55
Figure 3.20. Longitudinal Output Feedback Controller	55
Figure 3.21. Output Feedback Controller Time Responses	56
Figure 3.22. Longitudinal Output and Integral Feedback Controller	57
Figure 3.23. Output and Integral Feedback Controller Time Responses . .	58
Figure 3.24. Performance Comparison of All Compensators	58
Figure 3.25. Flight Test Implementation	60
Figure 3.26. Comparison of Analytical and Flight Test Designs	61
Figure 3.27. Full Order Flight Response to Velocity Command	64
Figure 3.28. Third Order Compensator Flight Response to Velocity Command	65
Figure 3.29. Output Feedback Flight Response to Velocity Command . . .	66
Figure 3.30. Full Order Flight Response to Climb Rate Command	67
Figure 3.31. Third Order Flight Response to Climb Rate Command . . .	68

Figure 3.32. Output Feedback Flight Response to Climb Rate Command	69
Figure 3.33. Third Order Climb Rate Flight Response, no Integral Control	70
Figure 4.1. Hover Control System Coordinate System	72
Figure 4.2. CH-47 Hover Model	73
Figure 4.3. Hover Control System	75
Figure 4.4. CH-47 Hover Linear Model	76
Figure 4.5. CH-47 Scaled Hover Linear Model	77
Figure 4.6. Hover Full Order Compensator Design Results	79
Figure 4.7. Reduced Order Hover Compensator	81
Figure 4.8. Transfer Function Analysis	84
Figure 4.9. Hover Forward Velocity Step Command in Simulation	86
Figure 4.10. Hover Side Velocity Step Command in Simulation	87
Figure 4.11. Hover Vertical Velocity Step Command in Simulation	88
Figure 4.12. Hover Forward Position Step Command in Simulation	89
Figure 4.13. Hover Lateral Position Step Command in Simulation	90
Figure 4.14. Second Order Complementary Filter	92
Figure 4.15. X Axis Transient-Free Switching Logic	94
Figure 4.16. Y Axis Transient-Free Switching Logic	95
Figure 4.17. Z Axis Transient-Free Switching Logic	96
Figure 4.18. Preliminary \dot{z} Flight Response with Pitch Oscillation	99
Figure 4.19. Preliminary \dot{z} Flight Response with Pitch Roll Coupling	100
Figure 4.20. Preliminary \dot{y} Flight Response	101
Figure 4.21. Preliminary \dot{z} Flight Response	102
Figure 4.22. Preliminary Forward Position Step Command in Flight	103

State Equations

$$\begin{bmatrix} \dot{u} \\ \dot{w} \\ \dot{q} \\ \dot{\theta} \end{bmatrix} = \begin{bmatrix} -.045 & .036 & 0 & -32.2 \\ -.37 & -2.02 & 176.0 & 0 \\ .00191 & -.0396 & -2.98 & 0 \\ 0 & 0 & 1.0 & 0 \end{bmatrix} \begin{bmatrix} u \\ w \\ q \\ \theta \end{bmatrix} + \begin{bmatrix} 0 & 1 \\ -28.2 & 0 \\ -11.0 & 0 \\ 0 & 0 \end{bmatrix} \begin{bmatrix} \delta_e \\ \delta_t \end{bmatrix} + \begin{bmatrix} .045 & -.036 \\ .37 & 2.02 \\ -.00191 & .0396 \\ 0 & 0 \end{bmatrix} \begin{bmatrix} u_w \\ w_w \end{bmatrix} \quad (2.2)$$

Measurements

$$\begin{bmatrix} u \\ h \\ \theta \end{bmatrix} = \begin{bmatrix} 1 & 0 & 0 & 0 \\ 0 & -1 & 0 & 176.0 \\ 0 & 0 & 0 & 1 \end{bmatrix} \begin{bmatrix} u \\ w \\ q \\ \theta \end{bmatrix} + \begin{bmatrix} 0 & 0 \\ 0 & 0 \\ 0 & 0 \end{bmatrix} \begin{bmatrix} \delta_e \\ \delta_t \end{bmatrix} + \begin{bmatrix} 0 & 0 \\ 0 & 0 \\ 0 & 0 \end{bmatrix} \begin{bmatrix} u_w \\ w_w \end{bmatrix} + \begin{bmatrix} v_u \\ v_h \\ v_\theta \end{bmatrix} \quad (2.3)$$

$$Q = \begin{bmatrix} 24.6 & 0 \\ 0 & 9.98 \end{bmatrix} \quad (2.4)$$

$$R = \begin{bmatrix} .318 & 0 & 0 \\ 0 & .318 & 0 \\ 0 & 0 & .00039 \end{bmatrix} \quad (2.5)$$

where:

- u - forward velocity, *ft/sec*
- w - vertical velocity, *ft/sec*
- q - pitch rate, *radians/sec*
- θ - pitch angle, *radians*
- δ_e - elevator, *radians*
- δ_t - throttle, *ft/sec²*
- u_w - longitudinal gusts, *ft/sec*
- w_w - vertical gusts, *ft/sec*
- v_u, v_h, v_θ - measurement noise, *ft/sec, ft/sec, radians*
- Q - disturbance spectral density [2]
- R - measurement noise spectral density (assumes standard deviations of 1 *ft/sec* for u and h and 2 deg for θ with .16 second correlation times(T_c)). The spectral densities come from the approximation $S.D. \approx 2\sigma^2 T_c$. [9])

Figure 2.1: Navion Linear Model Before Scaling. Nominal airspeed is 100 knots (100 *ft/sec*). Note the large order of magnitude differences in the elements of the system matrices. This is caused by the different units of the states.

needed is a linear system in state variable form:

$$\begin{aligned}\dot{x} &= Fx + Gu + \Gamma w \\ y &= Hx + Lu + Nw + v \\ \dot{z} &= Az + By \\ u &= Cz + Dy\end{aligned}\tag{2.1}$$

where:

x - system states, $n \times 1$

z - compensator states, $r \times 1$

u - controls, $m \times 1$

w - plant disturbances, $m' \times 1$

y - sensor measurements, $p \times 1$

v - sensor noise, $p \times 1$

Q - plant disturbance spectral density matrix, $m' \times m'$

R - sensor noise spectral density matrix, $p \times p$

This model is needed for all plant conditions for which the controller is expected to operate. Typically, the conditions include the nominal operating point and several off-nominal conditions for which the control system must also be stable and perform adequately. Figure 2.1 shows the Navion model at the sea level, 104 knot flight condition. No off-nominal flight conditions are included in the example. With the dynamic model now available, the methodology can continue with the scaling of the model.

2.2. Model Scaling

Model scaling is the systematic process of changing the units of the variables in the plant model. This process is described and used by Bryson(BR,sect 7.2) and is a necessary first step in the process of compensator order reduction. Since

Chapter 2.

The Design Methodology

From the discussion of Chapter 1, the need for a structured approach to using modern control methods to design control systems is apparent. This chapter describes a design methodology developed to take advantage of the strengths of the modern control techniques while eliminating or reducing their weaknesses. The methodology is a refinement and an expansion of design procedures described by Bryson and taught in the advanced flight control course at Stanford University.[1] Figure 1.3 shows a flow chart describing the methodology. This chapter describes each step and explains why it is necessary. To facilitate the description of the methodology, a simple design task is traced through the process, namely the design of a longitudinal autopilot for commanding aircraft airspeed and climb rate. The plant model represents the Navion general aviation aircraft at sea level and about 100 knots(176 ft/sec) airspeed. The objective is a dynamic compensator which could be implemented on a digital computer in the aircraft.

2.1. Model Derivation

The development of dynamic models for use in control system synthesis is an entire engineering discipline in itself. For this design methodology, the model

dures is the lack of experience in real world application, Chapters 3 and 4 present the results of applying these techniques to a real world problem. The "real world" problem is the design of a control system for a Boeing-Vertol CH-47 "Chinook" helicopter operated by the NASA Ames Research Center. Chapter 3 shows the application of the methodology to the design of a longitudinal cruise control augmentation system(CAS). Specifically, the CAS is designed to give the pilot a velocity/climb rate command capability for cruise flight. The controller is MIMO with 4 measurements and 2 controls. Chapter 4 applies the techniques to the more difficult task of designing a position hold/velocity command controller for the CH-47 during hover and low speed operations. For this task there are two modes of operation(velocity command and position hold), switching logic for going between the modes, 11 measurements, and 3 controls which must be considered in the design. For both these designs, simulation and flight test results are presented.

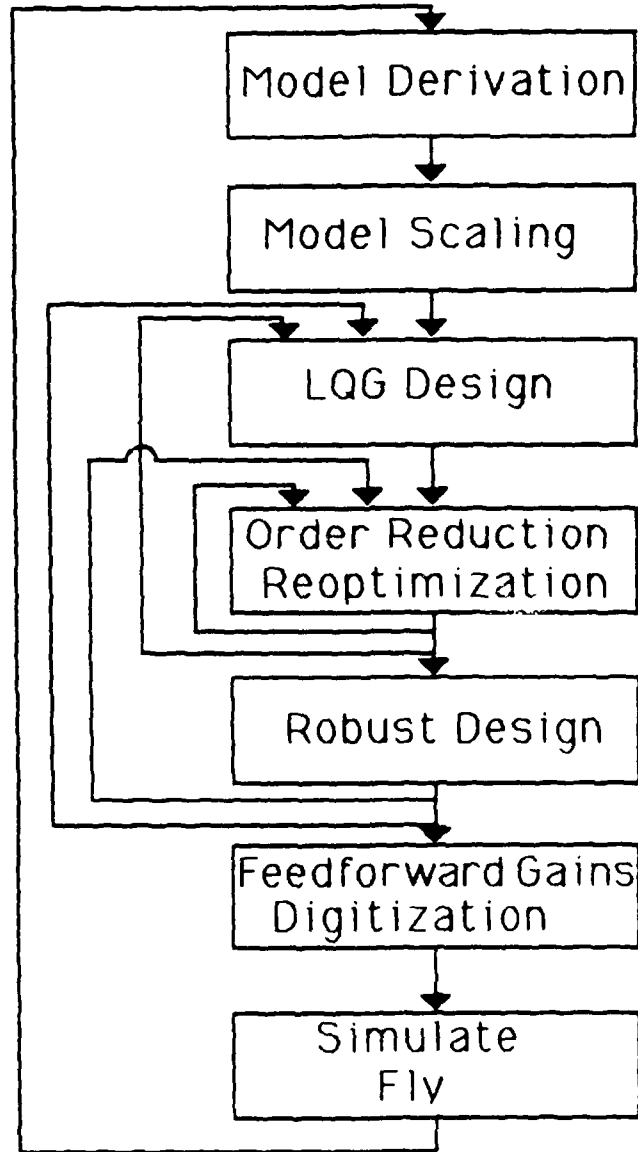


Figure 1.3: **The Design Methodology.** The many loops indicate the iterative nature of the process. The computer programs associated with each step are described in the appendices.

- The design and analysis tools for LQG techniques have only recently become easy to use in practical engineering applications.

These disadvantages provide a dilemma to the engineer faced with a difficult MIMO control design task. If he chooses to use LQG methods, he may be breaking new ground when he finally implements his system in actual operational hardware/software. On the other hand, if he uses classical techniques in his design procedure, he may end up with a design lacking in performance.

This report presents a control system design methodology which attempts to minimize the disadvantages of many modern control techniques, as described above, while taking advantage of the strengths of both modern and classical control techniques. Specifically, the methodology gives the engineer a structured approach to designing arbitrary order, robust, optimal controllers which can be implemented in digital or analog hardware. In this case, "arbitrary order" implies feedback compensation of any size, regardless of the plant model. This is an important consideration for high order plants. "Robust" is defined as insensitivity of the controller performance to changes in the plant. "Optimal" relates to the design methodology's attempt to minimize a quadratic performance index. This methodology is a refinement and expansion of techniques described by Bryson [2] and depends heavily on a robust-control design algorithm by Ly.[3] Figure 1.3 is a flow diagram showing the steps involved in the methodology. Chapter 2 of this report is a detailed description of this methodology. To clarify the description, a simple design is taken through all steps of the design procedures with explanations for design decisions made during the process.

Since one of the major disadvantages of using modern control design proce-

Modern (or LQG) design techniques are characterized by simultaneous closing of all loops from measurements to controls. Figure 1.2 shows the form of this type of controller. LQG design techniques offer several advantages to the designer of MIMO controllers:

- They ensure a stable design, if it exists, for the given measurements and controls.
- They result in coordinated, "graceful" controllers. In particular, the controls do not fight each other to satisfy the design requirements.
- For complicated systems, the design can be done fairly quickly.

Although these advantages make modern control design techniques very powerful, there are disadvantages which cannot be disregarded:

- The designs are often not robust to changes and uncertainties in the plant model, i.e. they are to "finely-tuned" to the plant model.
- For complex systems, the controller designs are complicated, making implementation difficult.
- Only a few designers have developed physical intuition for selecting performance indices.
- There is little physical intuition developed concerning the loops closed by the design process.
- There are relatively few examples of operational systems designed using these techniques. Practicing design engineers are therefore hesitant to use these techniques.

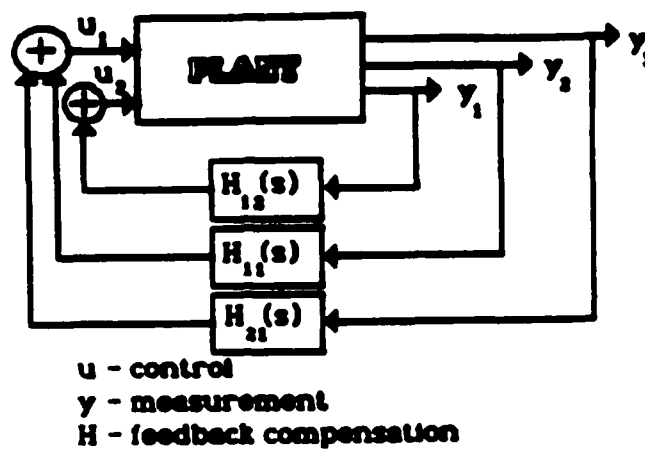


Figure 1.1: Classical Control. Characterized by incremental loop closures.

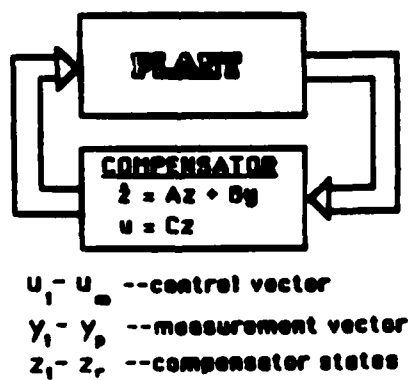


Figure 1.2: Modern Control. Characterized by simultaneous loop closures.

1.2. A Modern Control Design Methodology

Classical control techniques are routinely applied to the design of MIMO systems. The process is characterized by successive loop closing. (Figure 1.1) Some of the advantages of using this approach are:

- The designs are simple with clear physical intuition for each loop closed.
- For uncomplicated or open loop stable systems, the procedure is fairly fast.
- There is a large experience base for applying these methods.
- Numerous design and analysis tools exist.
- Operational hardware/software implementation is well understood and straightforward.

However, there are also some disadvantages to using classical design techniques for MIMO systems:

- For complicated or highly unstable systems, one loop may not stabilize the system.
- It may be difficult to decide what loops should be closed. This is especially true in complicated systems (large space structures for example), or in unfamiliar systems where little physical intuition has been developed.
- Different loops can "fight" each other resulting in using more control than is necessary or available.
- Many of the design techniques (Root locus, frequency response, etc.) are difficult to apply to MIMO systems.

- Better Numerical Methods(HQR, HQZ, SVD, etc.)- 1960-present
- Singular Value Techniques- Doyle and Stein and others,1970-present
- Gradient Design Methods- Ly and others,1980-present

These techniques are often labeled "modern control" where the previously mentioned methods(Root locus, Frequency Response, etc.) are often called "classical control" techniques. Perhaps the major difference between the two is that classical techniques are best suited to single input single output(SISO) dynamic systems where the modern control techniques are equally applicable to multiple input multiple output(MIMO) systems.

Virtually all control systems in operational use today, in numerous diverse applications, have been designed using classical control techniques. These techniques have been preferred over the modern control methods because most of the applications are fairly simple SISO systems. Even if the systems being controlled aren't truly SISO, acceptable SISO approximations can often be made. For instance, aircraft motions can be separated into longitudinal and lateral motions which can be approximated by fast and slow linear SISO systems. Design methodologies based on classical control use these SISO approximations for autopilot designs. As we might expect, this approach results in less performance than might be possible had we not made the simplifying assumptions (necessary to use the design techniques). This procedure is completely inappropriate if the system to be controlled cannot be adequately approximated by several uncoupled SISO systems.

engineers had the opportunity to build greatly improved control systems. However, the existing analytical tools were difficult to apply. More systematic analysis and design tools were needed to aid in developing control systems. Such techniques were developed in the early part of this century. A few of these techniques (applicable to linear systems) are listed below:

- Nyquist Stability Analysis— Nyquist, 1930's
- Frequency Response— Bode, 1940's
- Root Locus— Evans, 1940's

McRuer's Chapter 1 contains an excellent summary of these early analytical techniques and their applications.[1] All these techniques (plus others) provided the theory, and the signal processing devices existed to design sophisticated control systems which were installed in operational systems such as aircraft, missiles, rockets, ships, etc. The requirements of the military during World War II pushed the development and refinement of these techniques and of hardware capable of implementing the designs.

During the 1950's, the tools and hardware available to control engineers continued to expand. It was during this decade that the digital computer became a practical tool for designing and implementing control systems. With the digital computer, the control design engineer had much more signal processing capability. Analysis and design techniques soon developed which took advantage of the digital computer. A few of these techniques are:

- Kalman Filter— Kalman, 1960
- Linear Quadratic Gaussian (LQG) techniques— Bryson and others, 1960-present

Chapter 1.

Introduction

1.1. Historical Background on Control System Design

Control system design, as an engineering discipline, is relatively new. It has been coupled closely with the development of measurement devices(sensors), electronic signal processing capability(analog and digital hardware), and the development of mathematical techniques for the design and analysis of dynamic systems. Before electronic signal processing, ingenious mechanical devices were designed which incorporated simple feedback mechanisms. "Simple" here implies their analytical complexity; sometimes these devices could be quite complicated mechanically. Some simple examples of these mechanical feedback devices are:

- Water level control in a tank using float valves
- James Watts' centrifugal governor for steam engines

Conventional techniques for analyzing dynamic systems (Newtonian dynamics, Lagrangian dynamics, etc.) were adequate to study and design these mechanical devices.

With the development of electronic signal processing and electronic sensors,

Figure G.11. Linear Model, Airspeed 0 knots, Climb Rate 0 ft/min	155
Figure G.12. Linear Model, Airspeed 0 knots, Climb Rate 500 ft/min . . .	156
Figure G.13. Linear Model, Airspeed 0 knots, Climb Rate -500 ft/min . .	157
Figure G.14. Linear Model, Airspeed 20 knots, Climb Rate 0 ft/min . . .	158
Figure G.15. Linear Model, Airspeed 20 knots, Climb Rate 500 ft/min . .	159
Figure G.16. Linear Model, Airspeed 20 knots, Climb Rate -500 ft/min . .	160
Figure H.1. Bessel Filter Analog Flow Diagrams	163
Figure H.2. Comparison of Filtered and Unfiltered Data in Flight	164

Figure 4.23. Preliminary Lateral Position Step Command in Flight	104
Figure 4.24. Redesigned Hover Compensator	106
Figure 4.25. Hover Forward Velocity Step Command in Simulation	108
Figure 4.26. Hover Side Velocity Step Command in Simulation	109
Figure 4.27. Hover Vertical Velocity Step Command in Simulation	110
Figure 4.28. Final \dot{x} Flight Response	112
Figure 4.29. Final \dot{y} Flight Response	113
Figure 4.30. Final Hover Forward Position Step Command in Flight . . .	114
Figure 4.31. Hover Lateral Position Step Command in Flight	115
Figure B.1. Duality Between Regulators and Estimators	131
Figure F.1. Boeing-Vertol CH-47 Chinook Helicopter	142
Figure F.2. Cabin Layout	143
Figure F.3. Experimental Flight Systems	143
Figure G.1. Longitudinal and Lateral 4 th Order Models	145
Figure G.2. Coupled 8 th Order Model	146
Figure G.3. Linear Model, Airspeed 60 knots, Climb Rate 0 ft/min	147
Figure G.4. Linear Model, Airspeed 40 knots, Climb Rate 0 ft/min	148
Figure G.5. Linear Model, Airspeed 80 knots, Climb Rate 0 ft/min	149
Figure G.6. Linear Model, Airspeed 60 knots, Climb Rate 500 ft/min . . .	150
Figure G.7. Linear Model, Airspeed 60 knots, Climb Rate -500 ft/min . .	151
Figure G.8. Linear Model, Airspeed -20 knots, Climb Rate 0 ft/min . . .	152
Figure G.9. Linear Model, Airspeed -20 knots, Climb Rate 500 ft/min . .	153
Figure G.10. Linear Model, Airspeed -20 knots, Climb Rate -500 ft/min .	154

many dynamic systems, including the example here, have parameters with different units, it is often difficult to compare control gains or estimator gains for states or measurements with differing units. In the Navion example, to determine the relative importance of velocity to elevator and pitch angle to elevator gains would be difficult since velocity has units of *ft/sec* and pitch angle has units of radians. Model scaling allows the engineer to select a new set of units which result in the plant model having variables with units having a sort of "equivalent" importance to the designer. Of course, selection of such a set of units requires an understanding of the dynamics of the process being controlled. For the Navion, the angle variables are changed from *radians* to *.01 radians* while the linear variables remain in units of *ft/sec*. Such a selection is reasonable since *.01 radians* and *1 ft/sec* are similar in importance to a pilot flying the aircraft. For a supersonic aircraft, a suitable selection might be *.01 radians* and *10 ft/sec*.

Figure 2.2 shows the scaled dynamic model. This change of scaling is accomplished analytically using similarity transformations based on the changes in units. Appendix A presents the derivation of the transformations and the equations used to transform all matrices of the dynamic model into the new units. The computer program ROPTSYS, described in Appendix J, implements these equations as the first step in calculating an optimal full order compensator. The next step in the design methodology uses this scaled dynamic system as a starting point.

2.3. LQG Design

During this step in the design procedure, the optimal regulator and estimator gains are calculated for the scaled dynamic system. Appendix B shows the deriva-

State Equations

$$\begin{bmatrix} \dot{u} \\ \dot{w} \\ \dot{q} \\ \dot{\theta} \end{bmatrix}_{scaled} = \begin{bmatrix} -.045 & .036 & 0 & -.322 \\ -.37 & -2.02 & 1.76 & 0 \\ .191 & -3.96 & -2.98 & 0 \\ 0 & 0 & 1.0 & 0 \end{bmatrix} \begin{bmatrix} u \\ w \\ q \\ \theta \end{bmatrix}_{scaled} + \begin{bmatrix} 0 & 1 \\ -.282 & 0 \\ -11.0 & 0 \\ 0 & 0 \end{bmatrix} \begin{bmatrix} \delta_e \\ \delta_t \end{bmatrix}_{scaled} + \begin{bmatrix} .045 & -.036 \\ .37 & 2.02 \\ -.191 & 3.96 \\ 0 & 0 \end{bmatrix} \begin{bmatrix} u_w \\ w_w \end{bmatrix}_{scaled} \quad (2.6)$$

Measurements

$$\begin{bmatrix} u \\ h \\ \theta \end{bmatrix}_{scaled} = \begin{bmatrix} 1 & 0 & 0 & 0 \\ 0 & -1 & 0 & 1.76 \\ 0 & 0 & 0 & 1 \end{bmatrix} \begin{bmatrix} u \\ w \\ q \\ \theta \end{bmatrix}_{scaled} + \begin{bmatrix} 0 & 0 \\ 0 & 0 \\ 0 & 0 \end{bmatrix} \begin{bmatrix} \delta_e \\ \delta_t \end{bmatrix}_{scaled} + \begin{bmatrix} 0 & 0 \\ 0 & 0 \\ 0 & 0 \end{bmatrix} \begin{bmatrix} u_w \\ w_w \end{bmatrix}_{scaled} + \begin{bmatrix} v_u \\ v_h \\ v_\theta \end{bmatrix}_{scaled} \quad (2.7)$$

$$\begin{aligned} Q_{scaled} &= \begin{bmatrix} 24.6 & 0 \\ 0 & 9.98 \end{bmatrix} \\ R_{scaled} &= \begin{bmatrix} .318 & 0 & 0 \\ 0 & .318 & 0 \\ 0 & 0 & 3.9 \end{bmatrix} \end{aligned} \quad (2.8)$$

where:

- u - forward velocity, *ft/sec*
- w - vertical velocity, *ft/sec*
- q - pitch rate, *.01 radians/sec*
- θ - pitch angle, *.01 radians*
- δ_e - elevator, *.01 radians*
- δ_t - throttle, *ft/sec²*
- u_w - longitudinal gusts, *ft/sec*
- w_w - vertical gusts, *ft/sec*
- v_u, v_h, v_θ - measurement noise, *ft/sec, ft/sec, .01 radians*
- Q - disturbance spectral density, (From Bryson [2] sect 9.4)
- R - measurement noise spectral density (assumes standard deviations of 1 *ft/sec* for u and h and 2 *deg* for θ with .16 second correlation times(T_c). The spectral densities come from the approximation, $S.D. \approx 2\sigma^2 T_c$. [9])

Figure 2.2: Navion Linear Model After Scaling. The results of the scaling are most noticeable in the F , G , and R matrices.

tion of the technique used to calculate these gains. The optimal gain calculation of this appendix is based on the eigenvector decomposition of the Hamiltonian matrix as described in Hall and Bryson.[17] A modification to the technique is the capability to weight the linear combination of states and controls, $y_o = H_o x + Du$, in determining regulator gains, and, by duality, to include plant noise in the measurement, $y_m = H_m x + Lu + Nw + v$, in determining estimator gains.¹ This modification is essential for aerospace applications since it allows acceleration to be used as a measurement for estimator design, and weighted in regulator design. The ROPTSYS computer program, described in Appendix J, calculates these regulator and estimator gains. It also calculates the compensator dynamic system based on these gains. One item of note is that the A and B matrices, used in the quadratic performance index ($P.I. = \int_0^\infty (y_o^T A y_o + u^T B u) dt$), can start as the identity matrices since the system has been scaled in "equivalent" engineering units.

The compensator dynamic system is displayed in three formats:

Conventional Form

$$\begin{aligned}\dot{z} &= (F - GC - KH)z + Ky \\ u &= Cz\end{aligned}\tag{2.9}$$

where:

z - compensator states, $n \times 1$

y - sensor measurements, $p \times 1$

u - controls, $m \times 1$

K - steady state Kalman filter gains, $n \times p$

C - optimal regualtor gains, $m \times n$

¹Franklin and Powell show this derivation for the direct digital design case.[6]

Modal Form

$$\begin{aligned}\dot{z} &= F_{mod} z + K_{mod} y \\ u &= C_{mod} z\end{aligned}\tag{2.10}$$

where:

F_{mod} - modal form of $(F - GC - KH)$

K_{mod} - modal form of K

C_{mod} - modal form of C

$$\begin{aligned}F_{mod} &= \begin{bmatrix} \sigma_1 & \omega_1 & 0 & \dots \\ -\omega_1 & \sigma_1 & & \\ 0 & & \sigma_2 & \omega_2 & \dots \\ & & -\omega_2 & \sigma_2 & \dots \\ \vdots & & \vdots & & \ddots \end{bmatrix}, n \times n \\ K_{mod} &= \begin{bmatrix} \star & \star & \dots \\ \star & \star & \dots \\ \vdots & \vdots & \ddots \end{bmatrix}, n \times p \\ C_{mod} &= \begin{bmatrix} \star & \star & \dots \\ \star & \star & \dots \\ \vdots & \vdots & \ddots \end{bmatrix}, m \times n\end{aligned}\tag{2.11}$$

Block Minimal Form

$$\begin{aligned}\dot{z} &= F_{min} z + K_{min} y \\ u &= C_{min} z\end{aligned}\tag{2.12}$$

where:

F_{min} - minimal form of $(F - GC - KH)$

K_{min} - minimal form of K

C_{min} - minimal form of C

$$\begin{aligned}
 F_{min} &= \begin{bmatrix} 0 & 1 & 0 & \dots \\ a_1 & a_2 & 0 & \dots \\ 0 & 0 & a_1 & a_2 & \dots \\ \vdots & \vdots & \vdots & \ddots \end{bmatrix}, n \times n \\
 K_{min} &= \begin{bmatrix} \star & \star & \dots \\ \star & \star & \dots \\ \vdots & \vdots & \ddots \end{bmatrix}, n \times p \\
 C_{min} &= \begin{bmatrix} \star & \star & 0 & 1 & \dots \\ 0 & 1 & \star & \star & \dots \\ \star & \star & \star & \star & \dots \\ \vdots & \vdots & \vdots & \vdots & \ddots \end{bmatrix}, m \times n
 \end{aligned} \tag{2.13}$$

The modal form is calculated using the eigenvector matrix as a similarity transformation. Appendix C shows the equations needed to do this. The transformation to minimal form is derived in Appendix C. The modal and minimal realizations are important since they are unique realizations of the dynamic system. From the block minimal realization of the compensator, the designer can assess the relative importance of the different modes. To aid in this determination of modal importance, the ROPTSYS program also calculates two input/output measures, both based on work done by Bernard.[7] One measure is the singular value of the residue matrix associated with that mode. It is defined as:

$$M_1 = \bar{\sigma}(R_i) = \sqrt{g_1 g_1^T + g_2 g_2^T} \sqrt{h_1^T h_1 + h_2^T h_2} \tag{2.14}$$

where:

g_1, g_2 - the two rows of K_{min} associated with the mode being analyzed

h_1, h_2 - the two columns of C_{min} associated with the mode being analyzed

$\bar{\sigma}(R_i)$ - the singular value of the residue matrix for the i^{th} mode

The second measure of merit, M_2 , is just the first weighted by the real part of the mode being evaluated:

$$M_2 = \frac{\bar{\sigma}(R_i)}{|\sigma_i|} \tag{2.15}$$

The larger these measures are, the more important that mode is to the overall input/output characteristics of the compensator. In the case of unstable compensator modes, these should not be eliminated since they are usually required for stabilization of unstable plant modes. Figure 2.3 shows the results for the Navion control, which came from ROPTSYS. The input data required to get these results are shown in Appendix J.

From these results, we note that the open loop Navion has a well damped short period (the fast open loop mode) but the phugoid (the slow open loop mode) is only lightly damped. The regulator design improves these dynamics by forcing the two phugoid roots onto the real axis and speeding them up. The resulting compensator is fairly fast (as fast as the aircraft response itself) and well damped. This design was also analyzed using the RSANDY program, described in Appendix K, to evaluate the compensator performance in the presence of plant disturbances (vertical and longitudinal wind gusts) and measurement noise. The wind gust data come from a turbulence model described by Bryson.[1] The performance is tabulated in Figure 2.4.

Using these data, Figures 2.3 and 2.4, we can proceed to the next step of the design, simplification of the full-order compensator.

2.4. Compensator Order Reduction and Reoptimization

As with each step in this methodology, the subject of compensator order reduction and simplification is an engineering discipline in itself. For this methodology, the compensator mode measures, M_1 and M_2 , are the criteria for deciding which

System	Eigenvalues	Damping
Open Loop(F)	$-2.51 \pm j2.59, -0.17 \pm j.21$.7, .08
Regulator(F-GC)	$-2.43 \pm j3.05, -1.03, -2.43$.62, 1, 1
Estimator(F-KH)	$-11.3, -2.98, -.84 \pm j.43$	1, 1, .89
Compensator(F-GC-KH)	$-11.3, -3.04 \pm j2.34, -1.82$	1, .8, 1

Mode	Real	Imag	M_1	M_2
1	-11.34	0	2.62	.23
2	-3.04	2.34	1.86	.61
3	-3.04	-2.34	-	-
4	-1.82	0	.83	.46

Compensator Dynamic System Matrices

$$\begin{aligned}
 F_{min} &= \begin{bmatrix} -11.342 & 0 & 0 & 0 \\ 0 & 0 & 1 & 0 \\ 0 & -14.686 & -6.0721 & 0 \\ 0 & 0 & 0 & -1.8155 \end{bmatrix} \\
 K_{min}(scaled) &= \begin{bmatrix} -.0133 & -2.6218 & .0244 \\ -.278 & -.0886 & .0652 \\ 1.49 & .872 & -.337 \\ .771 & -.0464 & -.101 \end{bmatrix} \\
 K_{min}(unscaled) &= \begin{bmatrix} -.0133 & -2.6218 & 2.44 \\ -.278 & -.0886 & 6.52 \\ 1.49 & .872 & -33.7 \\ .771 & -.0464 & -10.1 \end{bmatrix} \\
 C_{min}(scaled) &= \begin{bmatrix} 1.0 & 0 & 1.0 & -.36 \\ -.0344 & .198 & .0216 & 1.0 \end{bmatrix} \\
 C_{min}(unscaled) &= \begin{bmatrix} -.01 & 0 & -.01 & .0036 \\ .0344 & -.198 & -.0216 & -1.0 \end{bmatrix}
 \end{aligned} \tag{2.16}$$

Figure 2.3: Navion Full Order Compensator. The unscaled matrices are in units of the physical system.

Standard Deviations						
Controls		States				
δ_e (deg)	δ_t (deg/sec ²)	u (ft/sec)	w (ft/sec)	q (deg/sec)	θ (deg)	h (ft/sec)
.153	.284	.5	2.25	.66	.47	1.32

Figure 2.4: Navion Full Order Compensator Performance. This statistical performance is based on the noise characteristics described in Figure 2.1.

modes of a compensator can be eliminated. The M_2 term seems to be most useful in the work here on flight vehicles. A mode can probably be eliminated with little performance impact if its value of $M_2/M_{2largest}$ is .1 or less. When this ratio is greater than .1, that mode may still be neglectable but the decision must rest on reduced order analysis results. In addition to eliminating modes, a compensator can also be simplified by eliminating unimportant measurements. This is desirable since it would lower the cost of the control system. The scaled K_{min} matrix provides the data which are used to decide if a specific measurement is necessary. If the magnitudes of the elements of a specific column of K_{min} are smaller than the other column elements, the measurement associated with that column may be neglectable. Of course, the final decision must be based on the simplified compensator analysis results.

Applying these design guidelines to the Navion example, Figure 2.3, we note the two real modes have an M_2 smaller than the single complex mode so we eliminate these modes and the associated rows of K_{min} and columns of C_{min} . Examining the values of scaled K_{min} , we note the column associated with the θ (pitch angle) measurement is smaller than the other so we try eliminating this measurement. The importance of the scaling process is evident here since the θ column elements in the unscaled K_{min} matrix have large magnitudes due to the radian units. Thus, without scaling, the θ measurement would have seemed more important than it was. The compensator is now second order, 2 input, and 2 output, a significant simplification from the fourth order, 3 input, and 2 output full order compensator.

The next step is to analyze and reoptimize the reduced order compensator

Simplified Compensator before Reoptimisation

$$\begin{aligned} \begin{bmatrix} \dot{z}_1 \\ \dot{z}_2 \end{bmatrix} &= \begin{bmatrix} 0 & 1 \\ -14.69 & -6.072 \end{bmatrix} \begin{bmatrix} z_1 \\ z_2 \end{bmatrix} + \begin{bmatrix} -.278 & -.0886 \\ 1.485 & .873 \end{bmatrix} \begin{bmatrix} u \\ \dot{h} \end{bmatrix} \\ \begin{bmatrix} \delta_e \\ \delta_t \end{bmatrix} &= \begin{bmatrix} 0 & -.01 \\ -.1978 & -.0216 \end{bmatrix} \begin{bmatrix} z_1 \\ z_2 \end{bmatrix} \end{aligned} \quad (2.17)$$

Simplified Compensator after Reoptimisation

$$\begin{aligned} \begin{bmatrix} \dot{z}_1 \\ \dot{z}_2 \end{bmatrix} &= \begin{bmatrix} 0 & 1 \\ -13.59 & -16.93 \end{bmatrix} \begin{bmatrix} z_1 \\ z_2 \end{bmatrix} + \begin{bmatrix} -.1366 & .2124 \\ 2.676 & -3.241 \end{bmatrix} \begin{bmatrix} u \\ \dot{h} \end{bmatrix} \\ \begin{bmatrix} \delta_e \\ \delta_t \end{bmatrix} &= \begin{bmatrix} 0 & -.01 \\ -13.14 & -1.228 \end{bmatrix} \begin{bmatrix} z_1 \\ z_2 \end{bmatrix} \end{aligned} \quad (2.18)$$

Full Order vs Reduced Order Performance

System	Standard Deviation						
	δ_e (deg)	δ_t (deg/sec ²)	u (ft/sec)	w (ft/sec)	q (deg/sec)	θ (deg)	\dot{h} (ft/sec)
Full Order	.153	.284	.5	2.25	.66	.47	1.32
Reduced Order	.2	.31	.57	2.39	.77	.58	1.23

Figure 2.5: Navion Reduced Order Compensator Design Results. The reduced order compensator was unstable before the reoptimization. The performance is based on the disturbance and noise properties of Figure 2.1

using the RSANDY computer program. The RSANDY program, described in Appendix K, is a modified version of a design and analysis code written by Ly.[8] The program designs robust, low order compensators using a gradient search technique based on a quadratic performance index. The results of using this code on the Navion simplified compensator are shown in Figure 2.5.

The reduced order compensator resulted in an unstable closed loop system. This points to the necessity of the reoptimization step after compensator simplification. The utility of Ly's code is also evident here since it allows unstable initial guesses when reoptimizing the compensator. Another important feature,

not used in this example, is the capability of including several plant conditions in the optimization to ensure compensator stability robustness to changes in plant parameters. The selection of weighting matrices in the quadratic performance index, used by the RSANDY program, was based on "Bryson's Rule" as applied to the scaling parameters. Briefly, "Bryson's Rule" suggests that the outputs and controls be weighted by the inverse square of their scale factors. For this example, the outputs were u (velocity) and \dot{h} (climb rate), and the controls were δ_e (elevator) and δ_t (throttle), with units of ft/sec , ft/sec , $radians$, and ft/sec^2 , respectively. The scaled units were ft/sec , ft/sec , $.01 radians$, and ft/sec^2 . The performance index is then:

$$P.I. = \int_0^{t_f} (y^T Q y + u^T R u) dt \quad (2.19)$$

where:

$$\begin{aligned} y &= \begin{bmatrix} u \\ \dot{h} \end{bmatrix} \\ u &= \begin{bmatrix} \delta_e \\ \delta_t \end{bmatrix} \\ Q &= \begin{bmatrix} \frac{1}{1^2} & 0 \\ 0 & \frac{1}{1^2} \end{bmatrix} \text{ or } \begin{bmatrix} 1 & 0 \\ 0 & 1 \end{bmatrix} \\ R &= \begin{bmatrix} \frac{1}{(.01)^2} & 0 \\ 0 & \frac{1}{1^2} \end{bmatrix} \text{ or } \begin{bmatrix} 10000 & 0 \\ 0 & 1 \end{bmatrix} \end{aligned} \quad (2.20)$$

For more complicated problems, these weighting terms may need to be adjusted to get the desired performance. The input file for RSANDY used to get the results of Figure 2.5 is listed in Appendix K.

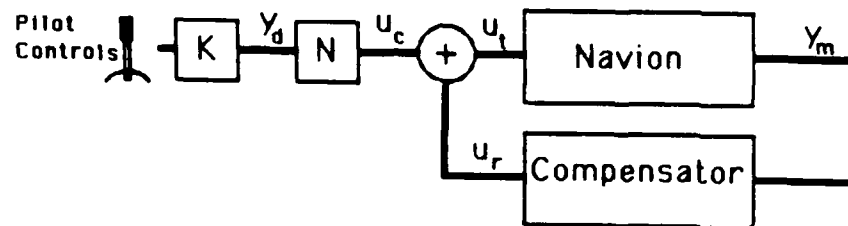
The results of Figure 2.5 show what might be expected. The simplified compensator has slightly degraded performance in that both the aircraft motion and control activity is slightly larger than the full order compensator. These statistical

performance parameters are important since they indicate the disturbance rejection properties of the design but we recall the design objective was a velocity and climb rate *command* system for the Navion. Since the designs thus far are only regulators, we still need to design the command capability for the controller.

2.5. Command Inputs

Generally, control systems are expected to do more than regulate the outputs of a process to some nominal value. We need the ability to change the output of the compensated system to any selected realizable value. To accomplish this end, the desired outputs are used to determine actuator commands which are the steady state controls for the desired outputs. Figure 2.6 shows this concept. The maximum number of outputs which can be commanded is the same as the number of independent controls in the system. This means that the feedforward matrix is square. An additional constraint is that the desired outputs must be physically realizable. For instance, velocity and position cannot be decoupled, i.e. you cannot command a steady velocity while holding position. Appendix D derives the algorithm which calculates this decoupling feedforward matrix for the case of equal numbers of controls and desired outputs. This algorithm is implemented in the SETPNT computer program described in Appendix L.

To complete the Navion autopilot design, we need to include the climb rate and forward velocity command capabilities required by the specifications. For this aircraft, these two outputs can be decoupled (controlled independently) with the two controls, elevator and throttle. Using the SETPNT program with the Navion data (shown in Appendix L), the feedforward matrix for the full order compensator



y_d -- Desired Output = $\begin{bmatrix} \text{velocity} \\ \text{climb rate} \end{bmatrix}$

y_m -- Measurements = $\begin{bmatrix} \text{velocity} \\ \text{climb rate} \end{bmatrix}$

u_c -- Command Control = $\begin{bmatrix} \text{elevator} \\ \text{throttle} \end{bmatrix}$

u_r -- Regulator Control = $\begin{bmatrix} \text{elevator} \\ \text{throttle} \end{bmatrix}$

u_t -- Total Control = $\begin{bmatrix} \text{elevator} \\ \text{throttle} \end{bmatrix}$

K -- Control Sensitivities

N -- Feedforward Gains

Figure 2.6: **Commanding a Desired Output.** The K matrix is diagonal and based on human factor considerations. The N matrix comes from an analysis of the system in steady state; the derivation is described in Appendix D.

is:

$$N = \begin{bmatrix} .002165 & -.001578 \\ .4505 & .1398 \end{bmatrix} \quad (2.21)$$

For the reduced order controller, the result is:

$$N = \begin{bmatrix} .002243 & -.002124 \\ .5354 & .2653 \end{bmatrix} \quad (2.22)$$

where:

$$\begin{bmatrix} \delta_c(\text{radians}) \\ \delta_t(\text{ft/sec}^2) \end{bmatrix} = N \begin{bmatrix} u_{desired}(\text{ft/sec}) \\ \dot{h}_{desired}(\text{ft/sec}) \end{bmatrix} \quad (2.23)$$

One item to note here is the fact that the feedforward matrices are dependent on both the plant and the controller. The correctness of these decoupling feedforward matrices becomes clear when the Navion designs are evaluated in simulation.

2.6. Simulation and Test

The final step of any design methodology is the demonstration of performance. The first step in such a demonstration is the use of a simple linear simulation. Once the design is validated in linear simulation, the simulation might be expanded to model some of the important nonlinearities in the physical system. In this methodology, the RSANDY program, described in Appendix K, includes the option of creating a linear simulation model. This model is then used by the SIMPLOT program (described in Appendix M) to simulate the closed or open loop system with or without the random disturbances. Using these RSANDY and SIMPLOT programs the Navion full and reduced order compensators can be compared.

The results of step commands in velocity and climb rate are shown in the following figures. Comparing Figures 2.7 and 2.8 we note the performance is

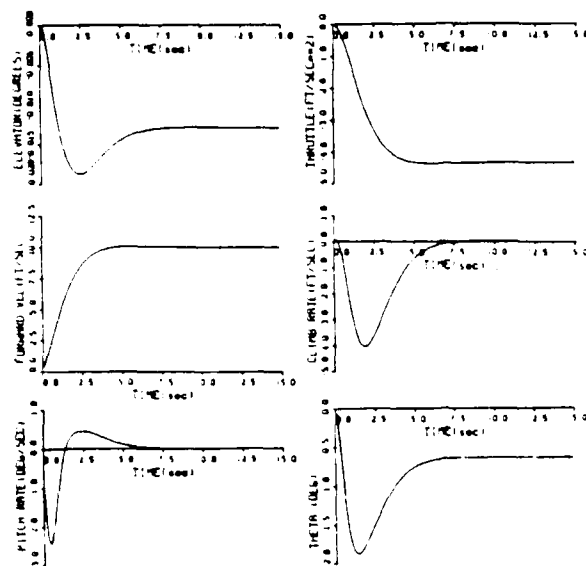


Figure 2.7: **Velocity Response for Full Order Compensator.** The system has a rise time of about 2.5 seconds and near critical damping.

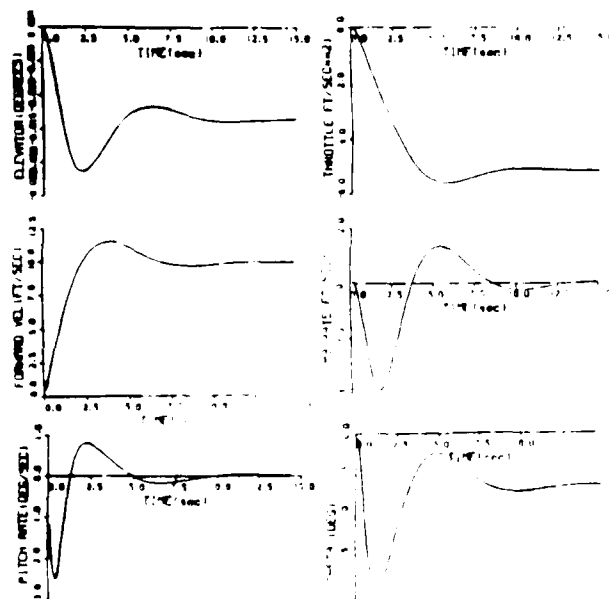


Figure 2.8: **Velocity Response for Reduced Order Compensator.** The rise time is about 2.5 seconds but the damping is only about .5.

unscaled model q and θ appear much less noisy than the u and \dot{h} measurements indicating the possibility that u and \dot{h} may not even be necessary. After scaling, the spectral densities are closer in magnitude but θ is still more accurate. With the scaling accomplished, the methodology continued with the design of the full order compensator using the ROPTSYS program.

3.4. LQG Design of the Full Order Compensator

The design of the full order compensator is straightforward since we have all the data necessary to run the design program ROPTSYS. Since we have the system scaled, the first choices for output and control weighting matrices in the regulator design are identity matrices. With this selection, the compensator is calculated and shown in Figure 3.6. Examining the closed loop roots (the estimator and regulator roots) we note the very slow estimator pole at $-.0088$. The slow estimator pole results from having a very accurate measurement of θ (low noise spectral density) but relatively noisy measurements of u and \dot{h} . The fast filter roots estimate mostly θ and q while the slow mode estimates mainly u . If we had introduced \dot{h} and u commands into the compensator (Equation 3.9), the slow estimator mode would not have affected the response to commands, since the estimator would have been "tracking" closely before the commands. For perfect tracking, the estimator modes are not excited at all. This need to include the command in the compensator was not recognized until later so the responses of Figure 3.7 show the poor performance when commands are *not* properly fed forward to the compensator. Figure 3.8 shows

State Equations

$$\begin{bmatrix} \dot{u} \\ \dot{w} \\ \dot{q} \\ \dot{\theta} \\ \dot{\delta_e} \\ \dot{\delta_c} \end{bmatrix} = \begin{bmatrix} -.0204 & .0377 & .0236 & -.3217 & .0127 & .0426 \\ -.0663 & -.551 & .9902 & -.0186 & .0467 & -.936 \\ -.42 & 1.76 & -1.682 & 0 & 3.91 & 1.53 \\ 0 & 0 & 1.0 & 0 & 0 & 0 \\ 0 & 0 & 0 & 0 & -40.0 & 0 \\ 0 & 0 & 0 & 0 & 0 & -40.0 \end{bmatrix} \begin{bmatrix} u \\ w \\ q \\ \theta \\ \delta_e \\ \delta_c \end{bmatrix} + \begin{bmatrix} 0 & 0 \\ 0 & 0 \\ 0 & 0 \\ 0 & 0 \\ 40.0 & 0 \\ 0 & 40.0 \end{bmatrix} \begin{bmatrix} \delta_e \\ \delta_c \end{bmatrix} + \begin{bmatrix} .0205 & -.037 \\ .0663 & .5512 \\ .42 & -1.76 \\ 0 & 0 \\ 0 & 0 \\ 0 & 0 \end{bmatrix} \begin{bmatrix} u_w \\ w_w \end{bmatrix} \quad (3.6)$$

Measurements

$$\begin{bmatrix} q \\ \theta \\ h \\ u \end{bmatrix} = \begin{bmatrix} 0 & 0 & 1 & 0 & 0 & 0 \\ 0 & 0 & 0 & 1 & 0 & 0 \\ 0 & -1 & 0 & 100.0 & 0 & 0 \\ 1 & 0 & 0 & 0 & 0 & 0 \end{bmatrix} \begin{bmatrix} u \\ w \\ q \\ \theta \\ \delta_e \\ \delta_c \end{bmatrix} + \begin{bmatrix} 0 & 0 \\ 0 & 0 \\ 0 & 0 \\ 0 & 0 \end{bmatrix} \begin{bmatrix} \delta_e \\ \delta_c \end{bmatrix} + \begin{bmatrix} 0 & 0 \\ 0 & 0 \\ 0 & 0 \\ 0 & 0 \end{bmatrix} \begin{bmatrix} u_w \\ w_w \end{bmatrix} + \begin{bmatrix} v_q \\ v_\theta \\ v_h \\ v_u \end{bmatrix} \quad (3.7)$$

$$Q = \begin{bmatrix} 24.6 & 0 \\ 0 & 9.98 \end{bmatrix}$$

$$R = \begin{bmatrix} .323 & 0 & 0 & 0 \\ 0 & 8.1 \times 10^{-4} & 0 & 0 \\ 0 & 0 & 16.0 & 0 \\ 0 & 0 & 0 & 1.1 \end{bmatrix} \quad (3.8)$$

where:

- u forward velocity, *ft/sec*
- w vertical velocity, *ft/sec*
- q pitch rate, *.01 radians/sec*
- θ pitch angle, *.01 radians*
- δ_e pitch control, *.1 inches*
- δ_c collective lever, *.1 inches*
- u_w longitudinal gusts, *ft/sec*
- w_w vertical gusts, *ft/sec*
- v_q, v_θ, v_h, v_u measurement noise, *.01 radians/sec, .01 radians, ft/sec, ft/sec*
- Q disturbance spectral density, [1]
- R measurement noise spectral density (assumes standard deviations shown in Figure 3.1 with 3 Hz bandwidth) The spectral densities come from the approximation $S.D. \approx 2\sigma^2 T_c$. [9]

Figure 3.5: **CH-47 Scaled Longitudinal Linear Model at 60 knots.** Even after scaling, the θ measurement is much more accurate than the others.

State Equations

$$\begin{bmatrix} \dot{u} \\ \dot{w} \\ \dot{q} \\ \dot{\theta} \\ \dot{\delta_e} \\ \dot{\delta_c} \end{bmatrix} = \begin{bmatrix} -.0204 & .0377 & 2.36 & -32.17 & .127 & .426 \\ -.0663 & -.551 & 99.02 & -1.86 & .467 & -9.36 \\ -.0042 & .0176 & -1.652 & 0 & .391 & .153 \\ 0 & 0 & 1.0 & 0 & 0 & 0 \\ 0 & 0 & 0 & 0 & -40.0 & 0 \\ 0 & 0 & 0 & 0 & 0 & -40.0 \end{bmatrix} \begin{bmatrix} u \\ w \\ q \\ \theta \\ \delta_e \\ \delta_c \end{bmatrix} + \begin{bmatrix} 0 & 0 \\ 0 & 0 \\ 0 & 0 \\ 0 & 0 \\ 40.0 & 0 \\ 0 & 40.0 \end{bmatrix} \begin{bmatrix} \delta_e \\ \delta_c \end{bmatrix} + \begin{bmatrix} .0205 & -.037 \\ .0663 & .5512 \\ .42 & -1.76 \\ 0 & 0 \\ 0 & 0 \\ 0 & 0 \end{bmatrix} \begin{bmatrix} u_w \\ w_w \end{bmatrix} \quad (3.3)$$

Measurements

$$\begin{bmatrix} q \\ \theta \\ h \\ u \end{bmatrix} = \begin{bmatrix} 0 & 0 & 1 & 0 & 0 & 0 \\ 0 & 0 & 0 & 1 & 0 & 0 \\ 0 & -1 & 0 & 100.0 & 0 & 0 \\ 1 & 0 & 0 & 0 & 0 & 0 \end{bmatrix} \begin{bmatrix} u \\ w \\ q \\ \theta \\ \delta_e \\ \delta_c \end{bmatrix} + \begin{bmatrix} 0 & 0 \\ 0 & 0 \\ 0 & 0 \\ 0 & 0 \end{bmatrix} \begin{bmatrix} \delta_e \\ \delta_c \end{bmatrix} + \begin{bmatrix} 0 & 0 \\ 0 & 0 \\ 0 & 0 \\ 0 & 0 \end{bmatrix} \begin{bmatrix} u_w \\ w_w \end{bmatrix} + \begin{bmatrix} v_q \\ v_\theta \\ v_h \\ v_u \end{bmatrix} \quad (3.4)$$

$$Q = \begin{bmatrix} 24.6 & 0 \\ 0 & 9.98 \end{bmatrix}$$

$$R = \begin{bmatrix} 3.23 \times 10^{-5} & 0 & 0 & 0 \\ 0 & 8.1 \times 10^{-8} & 0 & 0 \\ 0 & 0 & 16.0 & 0 \\ 0 & 0 & 0 & 1.1 \end{bmatrix} \quad (3.5)$$

where:

u	forward velocity, <i>ft/sec</i>
w	vertical velocity, <i>ft/sec</i>
q	pitch rate, <i>radians/sec</i>
θ	pitch angle, <i>radians</i>
δ_e	pitch control, <i>inches</i>
δ_c	collective lever, <i>inches</i>
u_w	longitudinal gusts, <i>ft/sec</i>
w_w	vertical gusts, <i>ft/sec</i>
v_q, v_θ, v_h, v_u	measurement noise, <i>radians/sec, radians, ft/sec, ft/sec</i>
Q	disturbance spectral density, [1]
R	measurement noise spectral density (assumes standard deviations shown in Figure 3.1 with 3 Hz bandwidth) The spectral densities come from the approximation $S.D. \approx 2\sigma^2 T_c$. [9]

Figure 3.4: CH-47 Longitudinal Linear Model at 60 knots. The highly accurate θ measurement comes from the inertial navigation system(INS), the pitch rate from a body mounted rate gyro, the velocity from the pitot-static system, and the climb rate from an instantaneous vertical speed indicator (IVSI).

other consideration in the development of a linear model for this design is the need to avoid "nuisance disengages" of the experimental control system in the CH-47. These automatic disengages are a safety feature of the modified control system which cause the experimental control system to be tripped off when the control rates exceed a known rate. The approach used to eliminate the possibility of these problems was to include simple first order actuator models:

$$\dot{u}_{actual} = -40 u_{actual} + 40 u_{desired} \quad (3.2)$$

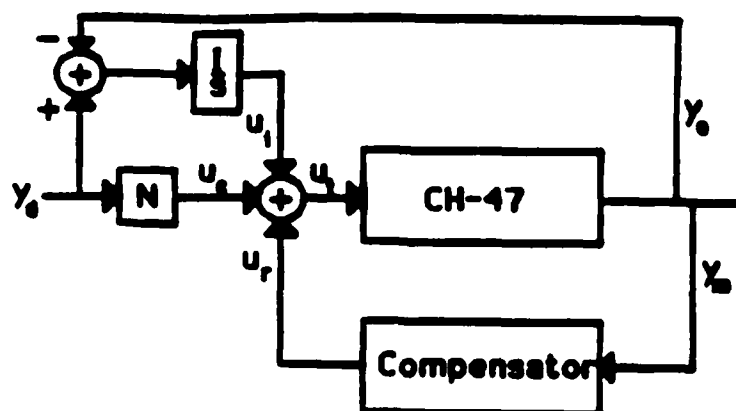
By weighting \dot{u}_{actual} in the performance index, the control rates should not get large, hence eliminating the nuisance disengages.¹ Before starting the control design, the linear model was scaled to help in compensator order reduction.

3.3. Model Scaling

The selection of units for the CH-47 at a 60 knot flight condition is dependent on our understanding of the aircraft dynamics. In this case, 1 *ft/sec* of velocity or climb rate is about as important to the pilot as .01 *radian* of pitch angle or .01 *radian/sec* of pitch rate. Similarly, the pilot would feel comfortable using .1 *inch* of either control to command the 1 *ft/sec* of velocity. Another way of looking at this scaling is to note that a .01 *radian* pitch angle would result in a 1 *ft/sec* climb rate at the nominal airspeed of 60 knots ($\approx 100 \text{ ft/sec}$). Figures 3.4 and 3.5 show the linear model at 60 knots both before and after scaling the system into the units above.

The usefulness of the scaling step is again evident if we look at the measurement noise spectral density matrix for the scaled and unscaled models. In the

¹Flight test later confirmed that the experimental system seldom had these type disengages.



y_o -- Actual Outputs (Subset of Measurements)

y_d -- Desired Outputs

y_m -- Measurements

u_e -- Command Control

u_i -- Integral Control

u_r -- Regulator Control

u_t -- Total Control

Figure 3.3: Controller Structure for The Longitudinal Cruise Autopilot. Flexibility comes from making the controls, outputs, and measurements vectors rather than scalars.

The form of the controller to be used for the design depends on its function. For this design, the controller must give the pilot a command capability. From Section 2.4, we recall that the command capability comes from the feedforward matrix which decouples the desired outputs. Appendix D shows that this matrix results from inverting the steady-state dynamic system. In flight, this matrix would exactly decouple the two desired outputs only if the helicopter were actually linear and had the same parameters as the model. Of course, this can never happen for several reasons:

- The helicopter dynamics are not linear.
- The helicopter has dynamics which were not modeled.
- The atmosphere is never "standard".
- The helicopter burns off fuel during flight, changing its inertia properties.
- The sensors have biases and scale factor errors.

The list could go on but it is clear we need to correct for differences between the model and the actual aircraft. One obvious solution is to use integral-error control. Figure 3.3 shows a form of the controller which includes this capability.

An interesting difference between this type of controller and more conventional flight control systems is the presence of off-diagonal terms in the integral-error feedback. Normally, the integral feedback is from desired output to the primary actuator for that output. For instance, a classically designed integral controller would use integral of velocity error for pitch control and integral of h error for collective. These off diagonal gains would be difficult to find using classical techniques since four transfer functions would be used to calculate the four integral gains. Finding these gains is straightforward using the RSANDY program. An-

$$\begin{bmatrix} \dot{u}(\text{ft/sec}) \\ \dot{w}(\text{ft/sec}) \\ \dot{q}(\text{radians/sec}) \\ \dot{\theta}(\text{radians}) \end{bmatrix} = F \begin{bmatrix} u \\ w \\ q \\ \theta \end{bmatrix} + G \begin{bmatrix} \delta_e(\text{inches of longitudinal stick}) \\ \delta_c(\text{inches of collective lever}) \end{bmatrix} \quad (3.1)$$

$$y_m(\text{measurements}) = \begin{bmatrix} q \\ \theta \\ h \\ u \end{bmatrix} = \begin{bmatrix} 0 & 0 & 1 & 0 \\ 0 & 0 & 0 & 1 \\ 0 & -1.0 & 0 & 100.0 \\ 1 & 0 & 0 & 0 \end{bmatrix} \begin{bmatrix} u \\ w \\ q \\ \theta \end{bmatrix}$$

Figure 3.2: **CH-47 Longitudinal Model.** This is a conventional longitudinal model found in most textbooks. The climb rate measurement is based on the approximation, $\dot{h} = -w + u_{\text{nominal}}\theta$.

the need for a fairly rigid control structure. This was necessary since the controller was to be programmed in fixed point assembly language on the aircraft's Sperry 1819A flight control computer. Since major controller structural changes would be difficult and time consuming, the baseline controller had to have a broad control structure which would allow design flexibility to come from changes in the compensator order or in the matrices themselves. With these goals and constraints in mind, the application of the methodology began.

3.2. Linear Models and Basic Control Structure

The models used for these designs come from Reference 11. This reference gives the aerodynamic coefficients at several different flight conditions and a general form of the "F" and "G" matrices based on these coefficients, the inertia properties of the aircraft, and the nominal airspeed. Appendix G shows this general form as well as the resulting linear models used for this research. Figure 3.2 shows the parameters of the longitudinal model.

Measurement	Units	Approx. Noise Standard Deviation	Approx. Correlation Time in Seconds	Spectral Density $S.D. \approx 2(\sigma^2)T_c$
$\theta_{\text{vertical gyro}}$	degrees	.1	.053	1.061×10^{-3}
$\phi_{\text{vertical gyro}}$	degrees	.1	.053	1.061×10^{-3}
$\psi_{\text{directional gyro}}$	degrees	1.0	.053	.1061
θ_{INS}	degrees	.05	.053	2.653×10^{-4}
ϕ_{INS}	degrees	.05	.053	2.653×10^{-4}
ψ_{INS}	degrees	.1	.053	1.061×10^{-3}
p	degrees/sec	2.0	.053	.424
q	degrees/sec	1.0	.053	.106
r	degrees/sec	.5	.053	2.653×10^{-2}
a_x	ft/sec ²	3.22	.053	1.1
a_y	ft/sec ²	3.22	.053	1.1
a_z	ft/sec ²	3.22	.053	1.1
$h_{\text{barometric}}$	ft	2.0	.318	2.546
h_{radar}	ft	.5	.053	2.653×10^{-2}
$vel_{\text{pitot static}}$	ft/sec	3.0	.318	5.73
$\alpha_{\text{boom vane}}$	degrees	2.0	.053	.424
$\beta_{\text{boom vane}}$	degrees	2.0	.053	.424

Figure 3.1: **Sensors Available on the NASA CH-47.** The standard deviations are estimates based on flight test data from the CH-47 instrumentation system. The .053 second correlation times corresponds to a 3 hz bandwidth.

Similarly, to establish a constant speed climb, the pilot must add collective thrust to begin climbing but simultaneously adjust pitch attitude to hold airspeed. In a sense, the pilot (through his extensive training) becomes an inner-loop decoupling controller, needed to give good speed and climb rate performance, the ultimate goal in cruising flight. The design goal, in terms of human factors, can be restated as reducing the pilot's workload in cruise flight by taking him out of the aircraft inner loops and giving him a direct velocity command system.

With the design goal stated, the physical hardware and flight software constraints must also be considered. Appendix F briefly describes the highly modified CH-47B flight research helicopter flown and maintained at the NASA Ames Research Center. The Langley Report gives a more detailed description of this particular helicopter, which has been modified to include a full authority fly-by-wire flight control system and extensive instrumentation.[10] Figure 3.1 shows the list of sensors available on the aircraft. Unfortunately, many of these sensors were quite noisy in the sense that they contained frequencies associated with the rotor motion. Rather than attempt to use the noisy measurements directly in the digital compensator, the TR-48 analog computer on the aircraft was programmed to filter several of the important aircraft motion sensor outputs. Specifically, fourth order Bessel filters were used on the longitudinal, lateral, and vertical accelerometers; a third order Bessel filter was used on the roll rate gyro; and second order Bessel filters on pitch rate, yaw rate, altitude, and pitot-static airspeed measurements. The filters were designed with 5 Hertz breakpoints to eliminate the "3 per rev" and "6 per rev" main rotor harmonics at 11 and 22 Hz. A brief description of these filters is included in Appendix H. A further constraint on the design process was

Chapter 3.

Longitudinal CAS for the CH-47

3.1. Design Goals and Constraints

The first example of an application of the methodology in Chapter 2 is the design of a longitudinal cruise autopilot for the CH-47. The goal was to synthesize a controller which gave the pilot independent control of airspeed and climb rate using separate pilot controls. For this design, the pilot longitudinal stick was used for the airspeed control and his collective lever was used for climb rate control. This implementation is unconventional since most helicopter control systems, even the highly augmented ones, give the pilot either pitch rate or pitch angle command from longitudinal stick and direct collective thrust command from the collective lever. Some of the more modern helicopters (CH-47D, HH60, CH-53) do close outer loops such as altitude or speed-hold around the collective thrust and pitch rate inner loops, but these are usually implemented as additional pilot-selectable autopilot modes. One trouble with pitch-angle, collective-thrust controllers is the coupling between the two. To increase speed in level flight, the pilot must pitch down, add collective thrust to maintain altitude and accelerate, then pitch up and reduce to a thrust slightly higher than the original to hold the new airspeed.

the compensator and then further simplifies the discrete compensator by putting it back into block minimal form. The SETPNT program uses an algorithm which finds the exact digital representation of a 2×2 compensator subsystem. One advantage of having the digital compensator in block minimal form is the reduction of arithmetic operations required by the computer. Specifically, the minimal form reduces the number of multiplies and adds, required by the compensator, by $r(r-1)$ where r is the order of the compensator. For large order compensators, such as required by systems controlling structural modes, the reduction can be important. The SETPNT program calculates this digital compensator in a form immediately usable in a floating point digital controller.

2.7. Summary

This chapter has shown an approach to designing control systems based on "modern control" methodologies. The approach is especially useful for MIMO systems of large order where compensator order reduction is essential. The Navion autopilot design was a simple example chosen to illustrate the design methodology. In applying this methodology to real control systems, problems will surface requiring the designer to modify and iterate the design to achieve the desired performance specifications. The next two chapters show this methodology applied to a real design problem. They illustrate the usefulness of the approach applied to a fairly complicated design task. They also show the type of problems which surface in real design applications.

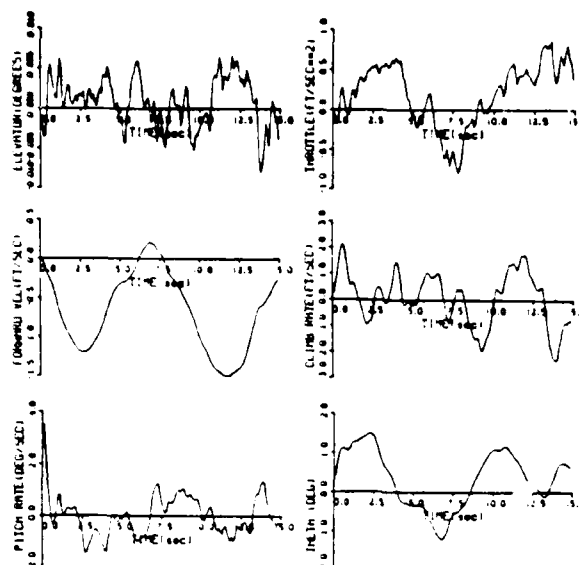


Figure 2.12: Navion Reduced Order Compensator Performance in Turbulence. The performance is nearly identical to the full order compensator (Figure 2.11) and is shown numerically in Figure 2.5

could be "tuned" by changing the weighting matrices and disturbance properties in the RSANDY program.

Eventually, the control system may be put into the physical system and tested. Since these compensator designs can be computationally intensive, it is unlikely to see any analog or continuous implementations for anything other than the simplest designs. Since the entire design process has been in the continuous domain, the final compensator must therefore be discretized to be useful in a digital computer based control system. The process of discretization is simple since the compensator is in a block minimal form. If the control is assumed to be a zero order hold (ZOH), i.e. step commands over the cycle time, then the discrete form can be solved exactly for the 2×2 and 1×1 blocks which make up the compensator dynamic system. The SETPNT program does this exact ZOH discretization for

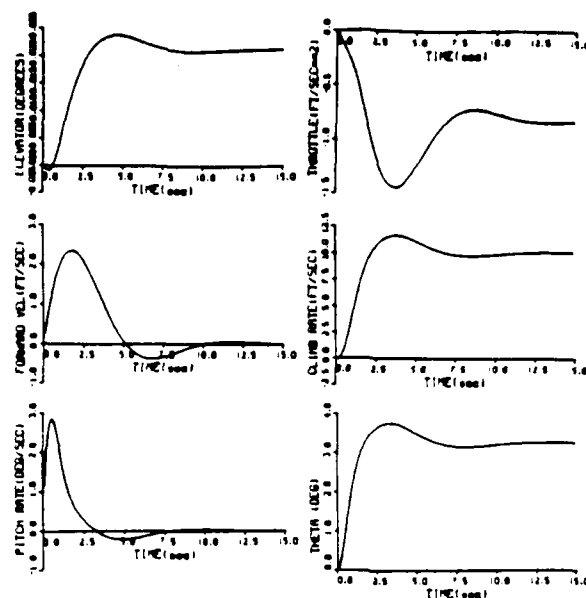


Figure 2.10: Climb Rate Response for Reduced Order Compensator. As with the velocity responses of Figures 2.7 and 2.8, the reduced order compensator has slightly reduced stability with a damping of about .6.

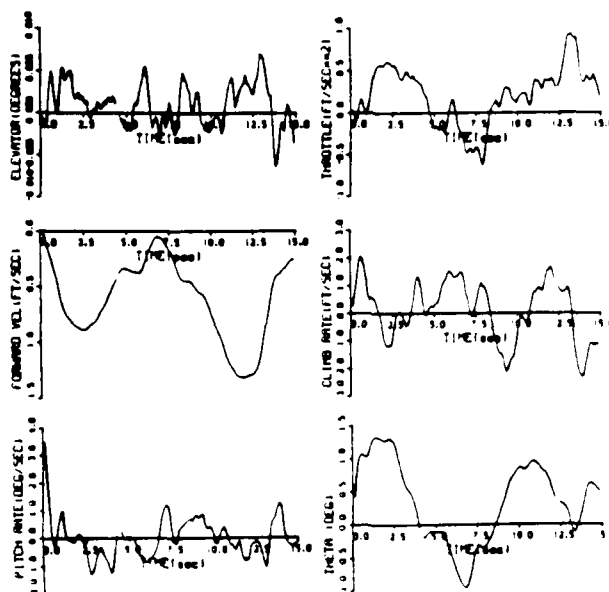


Figure 2.11: Navion Full Order Compensator Performance in Turbulence. The primary difference between the full order performance and reduced order performance (this figure and Figure 2.12) is in the control response which is smoother here.

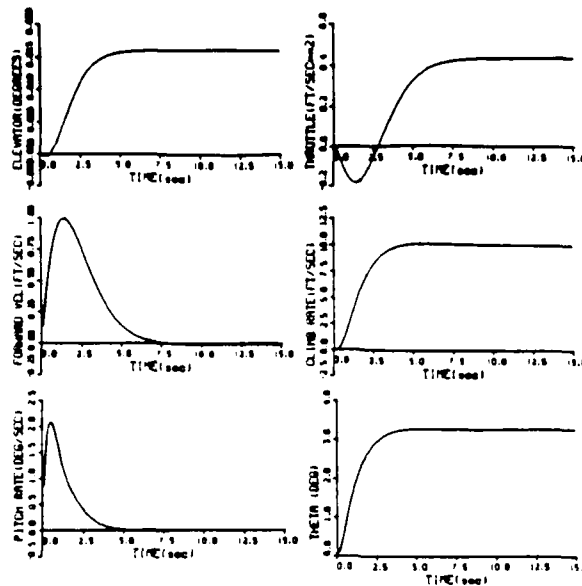


Figure 2.9: **Climb Rate Response for Full Order Compensator.** The rise time is 2 seconds with critical damping.

as we might expect. The velocity is better damped and faster using the full order compensator. Also, with the elimination of the θ measurement, we note the reduced order compensator has greater pitch angle excursions due to the velocity command. Comparing the climb rate responses of Figures 2.9 and 2.10, we note similar performance between the full and reduced order compensators. To compare the disturbance rejection characteristics of the two designs, we use the SIMPLOT program with plant disturbances and measurement noise. Figures 2.11 and 2.12 show the system performance in response to an initial pitch rate of 5 degrees in the presence of identical disturbances. As expected the full order compensator does a better job, as seen earlier in Figure 2.5. At this point, the design could be iterated by eliminating more modes or measurements, or by adding modes or measurements to improve performance. Alternately, the reduced order design

the responses when the commands *are* correctly accounted for in the compensator.

$$\begin{aligned}\dot{z} &= A z + B y_m + T_{min}^{-1} T_{mod}^{-1} G u_{command} \\ u_{regulator} &= C z\end{aligned}\tag{3.9}$$

where:

- A: the block minimal form of the compensator dynamics matrix($F - GC - KH$) which already includes the regulator control effects (the GC term)
- B: The minimal form of the Kalman gain matrix from ROPTSYS
- C: The minimal form of the optimal regulator gain matrix from ROPTSYS
- G: the control distribution matrix for the physical system
- T_{min}^{-1} : the similarity transformation from the modal form to the block minimal form described in Appendix C
- T_{mod}^{-1} : the similarity transformation from the nominal form to the modal form, composed of the eigenvectors of $F - GC - KH$

At this point in the process, alternative approaches to the design were used.(Still before we realized how to implement Equation 3.9 above.) Two such alternatives are shown below:

- Pick noise spectral density matrices independent of the actual noise but which give good time responses.
- Use an inverse optimal solution as described by Bernard to establish the performance index weighting matrices and noise spectral density matrices.[7]

3.4.1. Redesign Using Arbitrary Measurement Spectral Densities

The first intermediate approach to improving the poor time response in the velocity channel required selecting noise spectral densities which give an adequate time response. This approach violates the assumptions of the LQG estimator design procedure where the Kalman filter gains are calculated to minimize the estimate errors in the presence of the given noise. However, the noise properties are

$$F_{min} = \begin{bmatrix} 0 & 1 & 0 & 0 & 0 & 0 \\ -260.43 & -20.31 & 0 & 0 & 0 & 0 \\ 0 & 0 & -14.5 & 0 & 0 & 0 \\ 0 & 0 & 0 & 0 & 1 & 0 \\ 0 & 0 & 0 & -27.3 & -6.8 & 0 \\ 0 & 0 & 0 & 0 & 0 & -4.86 \end{bmatrix} \quad (3.10)$$

$$K_{min}(scaled) = \begin{bmatrix} -.58 & -12.1 & -.011 & .0078 \\ 6.98 & 226.5 & .0411 & .058 \\ -.72 & -100.7 & -.154 & .233 \\ -1.99 & -8.5 & .355 & -.75 \\ 9.12 & -3.78 & -2.36 & 4.35 \\ -11.34 & -49.3 & 2.44 & -4.44 \end{bmatrix} \quad (3.11)$$

$$K_{min}(unscaled) = \begin{bmatrix} -.58 & -121 & -.011 & .0078 \\ 69.8 & 22649 & .0411 & .058 \\ -.72 & -10070 & -.154 & .233 \\ -199 & -850 & .355 & -.75 \\ 912 & -378 & -2.36 & 4.35 \\ -1134 & -4930 & 2.44 & -4.44 \end{bmatrix} \quad (3.12)$$

$$C_{min}(scaled) = \begin{bmatrix} 4.05 & .74 & .75 & -.506 & -.46 & -.25 \\ 0 & 1 & 1 & 0 & 1 & 1 \end{bmatrix} \quad (3.13)$$

$$C_{min}(unscaled) = \begin{bmatrix} .405 & .074 & .075 & -.0506 & -.046 & -.025 \\ 0 & -.1 & -.1 & 0 & -.1 & -.1 \end{bmatrix} \quad (3.14)$$

System	Eigenvalues	Damping
Open Loop(F)	-40.0, -40.0, -2.54, .503, $-1.05 \pm j.276$	1, 1, 1, <i>unstable</i> , .35
Regulator(F-GC)	$-4.64 \pm 5.82j$, $-5.04 \pm 1.2j$, $-2.94 \pm 4.01j$.62, .98, .59
Estimator(F-KH)	-40.0, -40.0, $-11.55 \pm 8.69j$, $-3.74 \pm .0088j$	1, 1, .79, 1, 1
Compensator(F-GC-KH)	$-10.15 \pm 12.54j$, -14.5 , $-3.39 \pm 3.97j$, -4.86	.63, 1, .65, 1

Mode	Real	Imag	M_1	M_2
1	-10.15	12.54	277.9	27.4
2	-10.15	-12.54	-	-
3	-14.54	0	126	8.66
4	-3.4	3.97	68	20
5	-3.4	-3.97	-	-
6	-4.87	0	52	10.8

Figure 3.6: **CH-47 Longitudinal Full Order Compensator.** Notice the highly unstable open loop mode at $s = .503$. According to the test pilots, the 60 knot flight condition is the most unstable in the envelope.

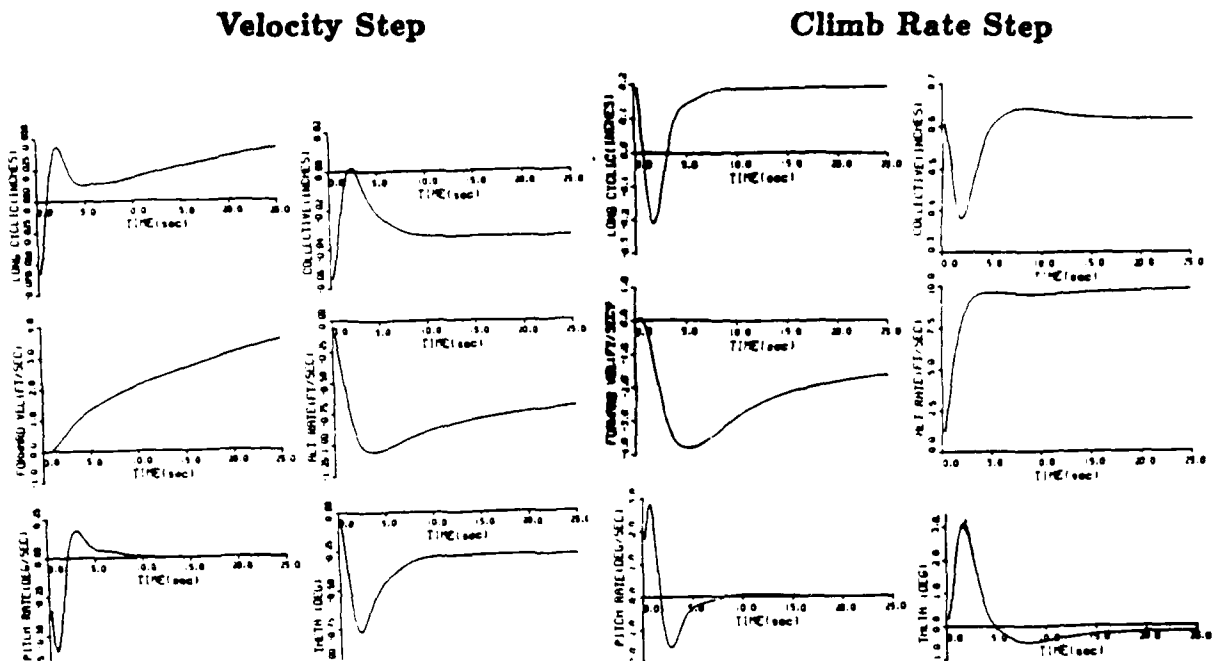


Figure 3.7: Longitudinal CAS Time Responses using Nominal Noise. The poor velocity command response is dominated by the slow estimator mode ($s = -.0088$).

fairly uncertain and furthermore, the goal of this design was not a good estimator, but a good compensator. The selection of Q and R matrices which give "good" performance is an iterative process. Figure 3.9 shows the compensator when the spectral densities of all the measurements are set to .2. The very slow estimator pole is eliminated. Figure 3.10 shows the improved velocity response and the unchanged climb rate response.

3.4.2. Redesign Using an Inverse Optimal Controller

The second intermediate approach uses Bernard's "inverse optimal controller" technique.[7] This technique computes A , B , Q and R matrices which, if used in an LQG design, give a closed loop system with desired poles. Figure 3.11 shows this compensator including the A , B , Q and R provided by Bernard. The time

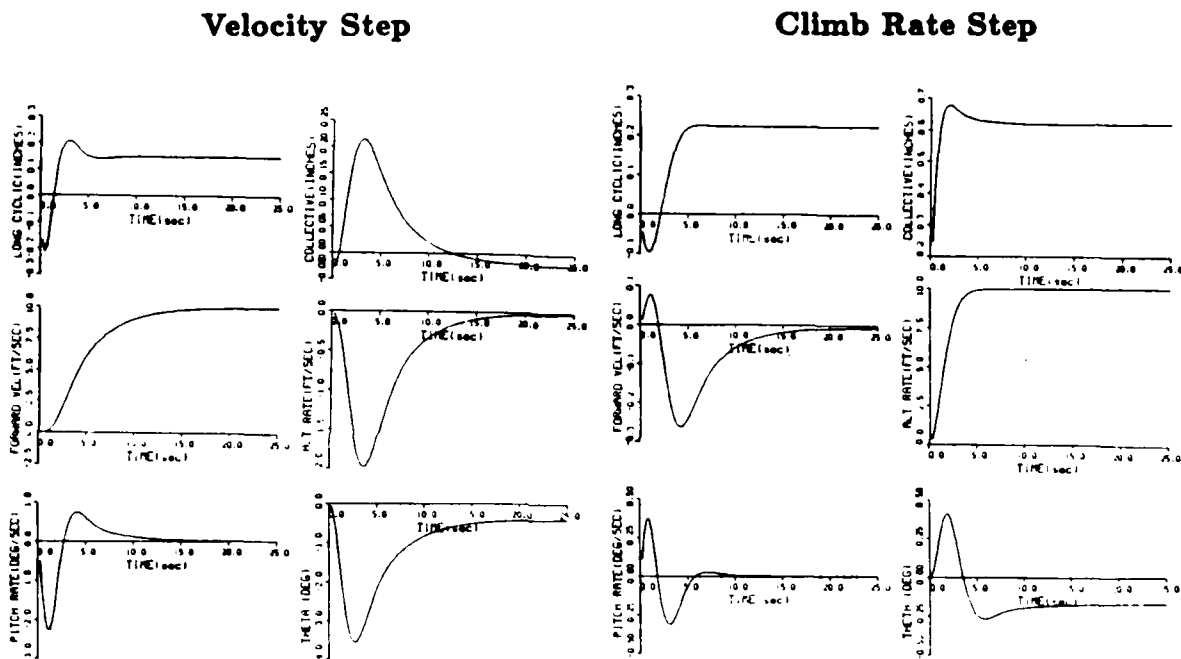


Figure 3.8: Longitudinal CAS Time Responses with Commands to the Compensator. With the command correctly fed to the compensator, the response is identical to a full-state feedback controller. The climb rate response is unchanged from Figure 3.7.

$$F_{min} = \begin{bmatrix} 0 & 1 & 0 & 0 & 0 & 0 \\ -14.715 & -7.43 & 0 & 0 & 0 & 0 \\ 0 & 0 & 0 & 1 & 0 & 0 \\ 0 & 0 & -4.27 & -1.61 & 0 & 0 \\ 0 & 0 & 0 & 0 & 0 & 1 \\ 0 & 0 & 0 & 0 & -2.7 & -3.16 \end{bmatrix} \quad (3.15)$$

$$K_{min}(scaled) = \begin{bmatrix} .00014 & .00048 & -.009 & -1.12 \\ -.001 & -.0018 & -2.40 & 3.99 \\ -.0076 & -.00093 & -.18 & .99 \\ .0012 & .0018 & 3.11 & -3.66 \\ -.000093 & 1.1 \times 10^{-4} & -.15 & -.24 \\ .00015 & .0018 & -.026 & -.20 \end{bmatrix} \quad (3.16)$$

$$K_{min}(unscaled) = \begin{bmatrix} .014 & .048 & -.009 & -1.12 \\ -.10 & -.18 & -2.40 & 3.99 \\ -.076 & -.093 & -.18 & .99 \\ .12 & .18 & 3.11 & -3.66 \\ -.0093 & .00011 & -.15 & -.24 \\ .015 & .018 & -.026 & -.20 \end{bmatrix} \quad (3.17)$$

$$C_{min}(scaled) = \begin{bmatrix} 0.0 & 1.0 & 0.0 & 1.0 & 1.65 & 1.17 \\ .26 & .40 & .23 & .38 & 0.0 & 1.0 \end{bmatrix} \quad (3.18)$$

$$C_{min}(unscaled) = \begin{bmatrix} 0.0 & -.1 & 0.0 & -.1 & -.165 & -.117 \\ -.026 & -.040 & -.023 & -.038 & 0.0 & -.1 \end{bmatrix} \quad (3.19)$$

System	Eigenvalues	Damping
Open Loop(F)	-40.0, -40.0, -2.54, .503, $-.105 \pm j.276$	1, 1, 1, <i>unstable</i> , .35
Regulator(F-GC)	-2.62, $-.866 \pm j.913$, $-1.035 \pm .384$, $-.281$	1, .69, .94, 1
Estimator(F-KH)	-40.0, -40.0, -4.45, $-1.0 \pm j.721$, -1.31	1, 1, 1, .81, 1
Compensator(F-GC-KH)	$-3.72 \pm j.947$, $-.803 \pm j1.90$, $-1.58 \pm j.445$.97, .39, .96

Mode	Real	Imag	M_1	M_2
1	-3.72	.947	11.33	3.05
2	-3.72	-.947	-	-
3	-.803	1.90	5.24	6.53
4	-.803	-1.90	-	-
5	-1.58	.45	.254	1.61
6	-1.58	-.45	-	-

Figure 3.9: Longitudinal CAS using Arbitrary Measurement Spectral Density. The slow estimator mode of Figure 3.6 is eliminated.

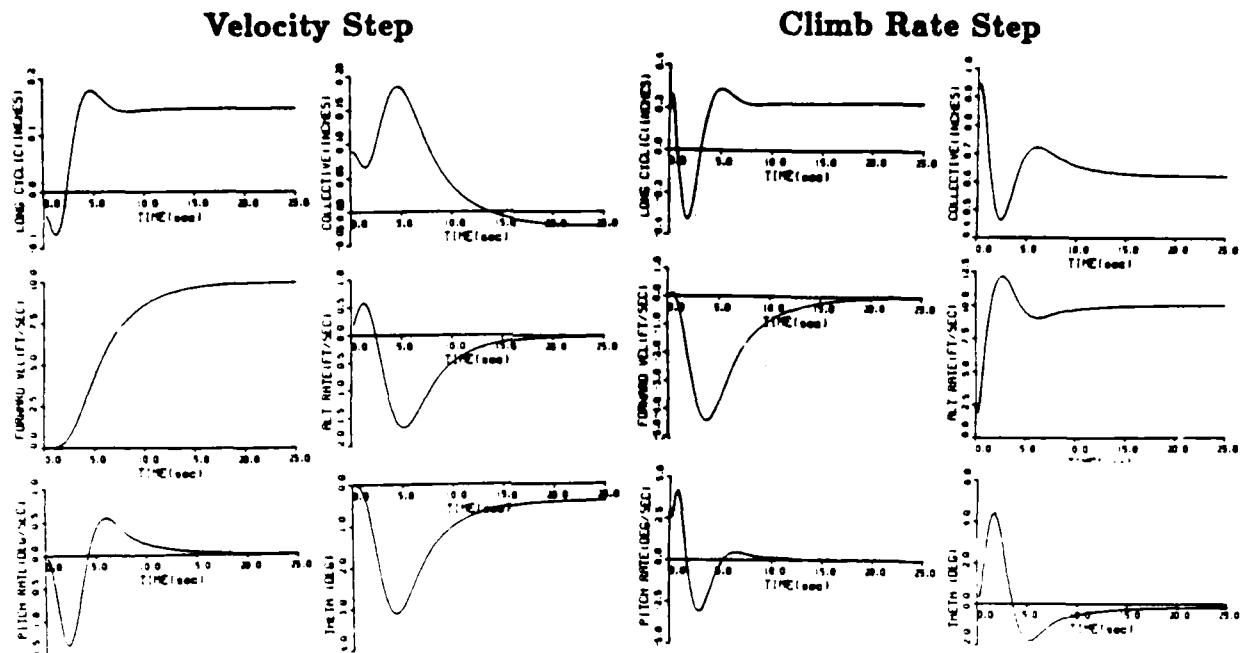


Figure 3.10: Longitudinal CAS Time Responses using Arbitrary Noise. The poor velocity response of Figure 3.7 is eliminated.

responses of Figure 3.12 confirm the improved performance.

Figure 3.13 shows the statistical performance of the original design and the two alternate designs. As expected, the nominal design has the lowest errors. The inverse optimal controller is nearly as good but the other is clearly the worst. Based on the combination of statistical performance and the time responses, the inverse optimal design was the best of the full order compensators. With the full order compensator in hand, the process of order reduction began.

3.5. Compensator Order Reduction

Using the M_2 criterion of section 2.3, both the nominal and the inverse optimal compensators indicate reduction to third order is feasible. From a more practical

$$F_{min} = \begin{bmatrix} 0 & 1 & 0 & 0 & 0 & 0 \\ -205.73 & -22.68 & 0 & 0 & 0 & 0 \\ 0 & 0 & -3.73 & 0 & 0 & 0 \\ 0 & 0 & 0 & 0 & 1 & 0 \\ 0 & 0 & 0 & -1.55 & -2.33 & 0 \\ 0 & 0 & 0 & 0 & 0 & -.68 \end{bmatrix} \quad (3.20)$$

$$K_{min}(scaled) = \begin{bmatrix} -.013 & -.87 & -.34 & -.0015 \\ -.17 & 4.95 & .17 & -1.03 \\ .37 & -.84 & .01 & 1.84 \\ -.011 & -.43 & -.12 & .88 \\ .022 & .34 & .069 & -.57 \\ .014 & .63 & .16 & -1.40 \end{bmatrix} \quad (3.21)$$

$$K_{min}(unscaled) = \begin{bmatrix} -1.29 & -86.68 & -.033 & -.0015 \\ -16.62 & 494.75 & .17 & -1.03 \\ 37.28 & -84.30 & .01 & 1.84 \\ -1.132 & -42.52 & -.12 & .88 \\ 2.16 & 33.85 & .069 & -.57 \\ 1.44 & 63.12 & .16 & -1.40 \end{bmatrix} \quad (3.22)$$

$$C_{min}(scaled) = \begin{bmatrix} 0.0 & 1.0 & 1.0 & 1.61 & .33 & 1.0 \\ .10 & .25 & .21 & 0.0 & 1.0 & -.42 \end{bmatrix} \quad (3.23)$$

$$C_{min}(unscaled) = \begin{bmatrix} 0.0 & -0.1 & -.1 & -.16 & -.033 & -.1 \\ -.01 & -.025 & -.021 & 0.0 & -.1 & .042 \end{bmatrix} \quad (3.24)$$

System	Eigenvalues	Damping
Open Loop(F)	-40.0, -40.0, -2.54, .503, $-.105 \pm j.276$	1, 1, 1, <i>unstable</i> , .35
Regulator(F-GC)	$-2.13 \pm j.78$, $-.56 \pm j.23$, $-.82 \pm j.33$.94, .93, .93
Estimator(F-KH)	-40.0, -40.0, $-11.54 \pm j8.70$, -1.01, -.52	1, 1, .80, 1, 1
Compensator(F-GC-KH)	$-11.34 \pm j8.78$, -3.73, $-1.17 \pm j.44$, -.68	.79, 1, .94, 1

Mode	Real	Imag	M_1	M_2
1	-11.34	8.78	15.33	1.35
2	-11.34	-8.78	-	-
3	-3.73	0.0	2.11	.56
4	-1.17	.44	2.59	2.22
5	-1.17	-.44	-	-
6	-.68	0.0	1.67	2.46

Figure 3.11: Longitudinal Compensator based on Inverse Optimal Solution. The slow estimator mode of the nominal design, Figure 3.6, is gone.

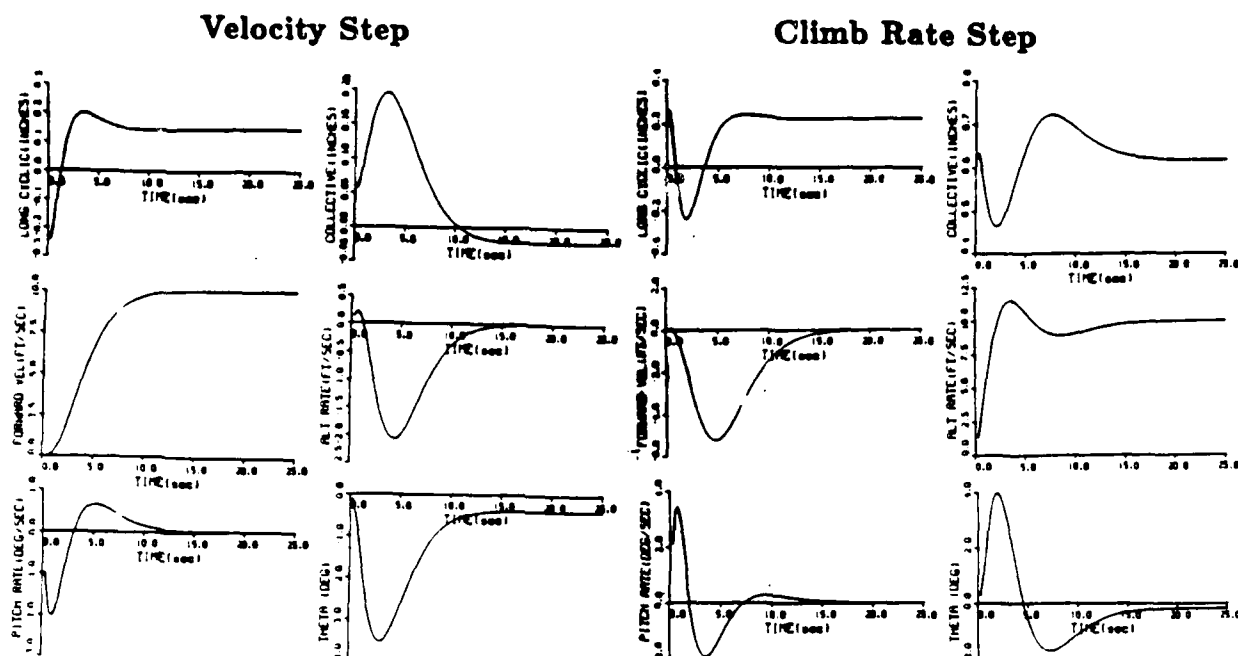


Figure 3.12: Longitudinal CAS Time Responses using Inverse Optimal Controller. The velocity response is much improved from Figure 3.7.

System	Standard Deviation						
	δ_c (inches)	δ_c (inches)	u (ft/sec)	w (ft/sec)	q (deg/sec)	θ (deg)	h (ft/sec)
Nominal	.12	.06	1.01	1.51	0.84	0.78	1.49
Arbitrary Noise	.39	.21	4.24	3.96	3.46	3.34	2.65
Inverse Optimal	.16	.07	1.43	2.90	1.24	1.29	1.72

Figure 3.13: Performance Comparison of Full Order Compensators. These data are based on the measurement noise shown in Figure 3.1 and disturbance noise of Figure 3.4.

standpoint, using output feedback of the measurements is also a possibility. This is appropriate if we recall from section 3.1 that all the measurements were being analog filtered before entering the flight control computer. The next two sections show these two designs.

3.5.1. Robust Longitudinal Third Order Compensator

Using the nominal compensator reduced to third order as a starting guess, the RSANDY program was used to optimize the low order compensator using its robust design feature. The following flight conditions were used with the weightings shown.

Condition	Airspeed(knots)	Climb Rate(ft/min)	Weighting
Nominal	60	0	.8
Off Nominal 1	60	500	.05
Off Nominal 2	60	-500	.05
Off Nominal 3	40	0	.05
Off Nominal 4	80	0	.05

Stability is ensured by the RSANDY program for each of these flight conditions. Figure 3.14 shows the results including the closed loop roots at the nominal flight condition. There is still a slow mode ($s = -.059$) which is shown in the time responses of Figure 3.15 indicating the need for integral control.

When the integral control loop is added to the third order controller, the RSANDY program was again used to set the four gains in the K_I matrix of Figure 3.3. The program did not converge with only the four gains of K_I allowed to vary in the optimization. By releasing both the K_I and the compensator gains, the compensator of Figure 3.16 emerged. Figure 3.17 shows the associated time responses. The same approach was used to set the integral gains for the full-order compensator when the integral control loop was added. Figures 3.18 and 3.19

$$F_{min} = \begin{bmatrix} 0.0 & 1.0 & 0.0 \\ -226.3 & -78.49 & 0.0 \\ 0.0 & 0.0 & -1.397 \end{bmatrix} \quad (3.25)$$

$$K_{min} = \begin{bmatrix} -22.17 & -121.7 & -.35 & -.11 \\ 53.14 & 3527. & .87 & .24 \\ -31.38 & -84.46 & -.90 & -.38 \end{bmatrix} \quad (3.26)$$

$$C_{min} = \begin{bmatrix} 0.0 & -.10 & -.10 \\ -.11 & -.056 & .012 \end{bmatrix} \quad (3.27)$$

Real Part	Imag Part	Damping	Freq(rad/sec)	Freq(Hz)
-75.45	0.0	1.0	75.45	12.01
-40.00	0.0	1.0	40.00	6.37
-40.18	0.0	1.0	40.18	6.40
-3.12	0.0	1.0	3.12	.50
-.96	1.36	.58	1.67	.27
-.96	-1.36	.58	1.67	.27
-.059	0.0	1.0	.059	.0094
-.42	0.0	1.0	.42	.068
-.96	0.0	1.0	.96	.15

Figure 3.14: **Longitudinal Reduced Order Compensator.** Reducing from 6th to 3rd order decreases the number of independent gains in the compensator from 36 to 18.

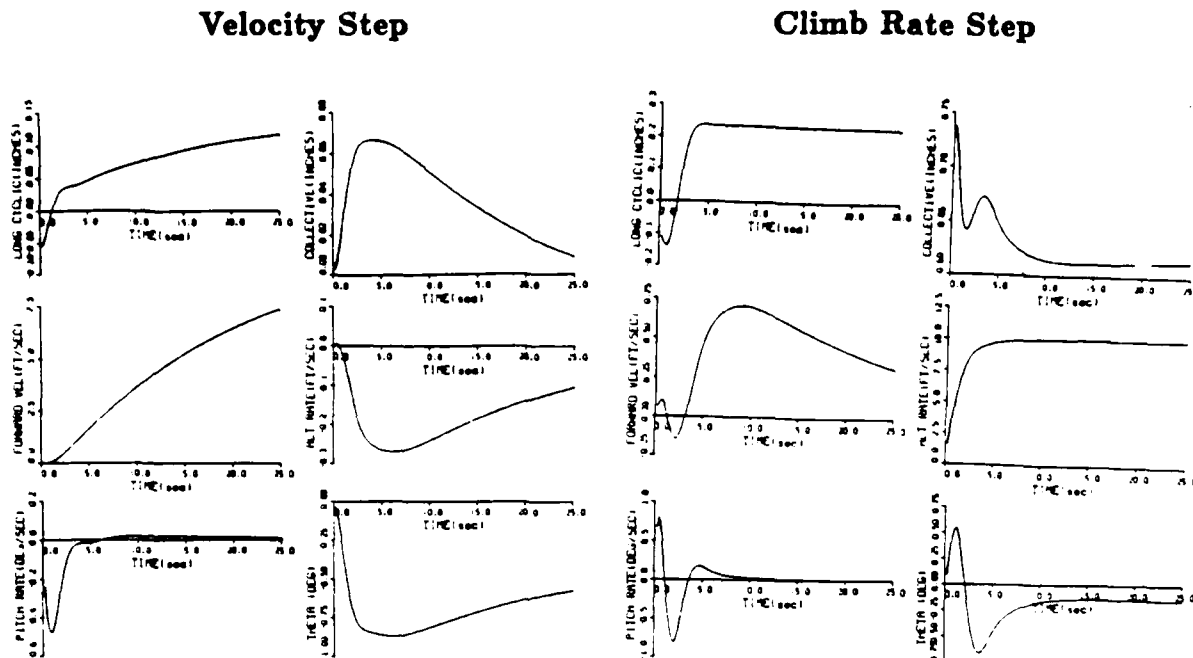


Figure 3.15: **Longitudinal Reduced Order Compensator Time Responses.**
The velocity response is still quite slow but climb rate is adequate.

show the resulting compensator and time responses.

3.5.2. Longitudinal Output Feedback Controller

Since the measurements available ($q\theta u\dot{h}$) are nearly the same ² as the states of a fourth order model, the gains of a regulator design are a good starting point in using RSANDY to compute output feedback gains. In fact, using these gains with no further optimization gave quite impressive performance as shown in Figures 3.20 and 3.21.

As with the reduced order compensator, an integral control loop is necessary to ensure that the actual commands are achieved in flight. Using the K_I gains from the reduced order design (Figure 3.16) and the output feedback controller of

²The fourth order model has states ($uwq\theta$) and $\dot{h} \approx u_{nominal}\theta - w$.

$$A_{min} = \begin{bmatrix} 0.0 & 1.0 & 0.0 \\ -229.5 & -16.82 & 0.0 \\ 0.0 & 0.0 & -2.48 \end{bmatrix} \quad (3.28)$$

$$K_{min} = \begin{bmatrix} -22.83 & -190.9 & -.07 & .059 \\ 57.00 & 3528. & .044 & -.33 \\ -18.57 & -59.93 & -1.37 & -.67 \end{bmatrix} \quad (3.29)$$

$$C_{min} = \begin{bmatrix} 0.0 & -.1 & -.1 \\ .45 & -.071 & .041 \end{bmatrix} \quad (3.30)$$

$$I = \begin{bmatrix} -.0054 & .0098 \\ -.00823 & .047 \end{bmatrix} \quad (3.31)$$

Closed Loop Eigenvalues

Real Part	Imag Part	Damping	Freq(rad/sec)	Freq(Hz)
-39.75	0.0	1.0	39.75	6.32
-40.03	0.0	1.0	40.03	6.37
-7.61	11.46	.55	13.75	2.19
-7.61	-11.46	.55	13.75	2.19
-1.81	2.17	.64	2.83	.45
-1.81	-2.17	.64	2.83	.45
-1.77	0.0	1.0	1.77	.28
-.044	.092	.44	.10	.016
-.044	-.092	.44	.10	.016
-.53	.37	.82	.65	.10
-.53	-.37	.82	.65	.10

Figure 3.16: Longitudinal Reduced Order Compensator with Integral Control. The A_{min} , K_{min} , and C_{min} matrices are not the same as in Figure 3.14.

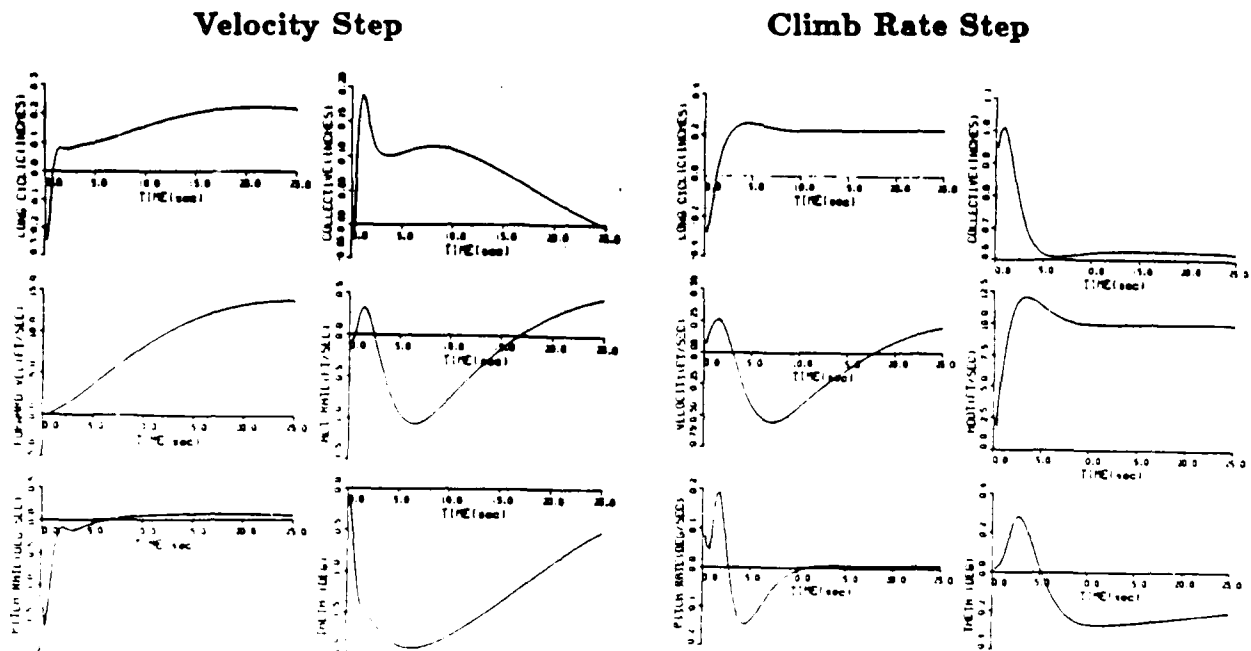


Figure 3.17: Longitudinal Reduced Order Integral Controller Time Responses. Although the velocity response is still fairly slow, this design was selected for evaluation in flight.

$$F_{min} = \begin{bmatrix} 0 & 1 & 0 & 0 & 0 & 0 \\ -205.7 & -22.67 & 0 & 0 & 0 & 0 \\ 0 & 0 & 0 & 1 & 0 & 0 \\ 0 & 0 & -1.781 & -2.661 & 0 & 0 \\ 0 & 0 & 0 & 0 & -4.279 & 0 \\ 0 & 0 & 0 & 0 & 0 & -2.63 \end{bmatrix} \quad (3.32)$$

$$K = \begin{bmatrix} -1.96 & -86.7 & -.148 & -.0213 \\ -16.62 & 494.8 & .166 & -.81 \\ -1.11 & -42.6 & -.437 & .475 \\ 2.171 & 33.8 & .727 & -.174 \\ 37.3 & -84.3 & .148 & 1.09 \\ 1.33 & 63.1 & .0823 & -.395 \end{bmatrix} \quad (3.33)$$

$$C = \begin{bmatrix} 4.932 & .122 & .477 & 1.01 & -.068 & -.44 \\ -.0105 & -.025 & 0 & -.1 & -.021 & .042 \end{bmatrix} \quad (3.34)$$

$$I = \begin{bmatrix} -.00003 & -.01 \\ .000157 & .053 \end{bmatrix} \quad (3.35)$$

Closed Loop Eigenvalues

Real Part	Imag Part	Damping	Freq(rad/sec)	Freq(Hz)
-40.01	.0022	1.0	40.01	6.37
-40.01	-.0022	1.0	40.01	6.37
-11.43	8.21	.81	14.07	2.239
-11.43	-8.21	.81	14.07	2.239
-.543	2.87	.185	2.93	.466
-.543	-2.87	.185	2.93	.466
-3.38	0.0	1.0	3.38	.537
-2.86	0.0	1.0	2.86	.455
-.299	.90	.315	.947	.151
-.299	-.90	.315	.947	.151
-.561	.334	.86	.65	.104
-.561	-.334	.86	.65	.104
-.206	0.0	1.0	.206	.0329
-4.24×10^{-5}	0.0	1.0	4.24×10^{-5}	6.75×10^{-6}

Figure 3.18: **Longitudinal Full Order Compensator with Integral Control.**
As with the third order design, the A, K, and C matrices are different from the full order design without integral control (Figure 3.11).

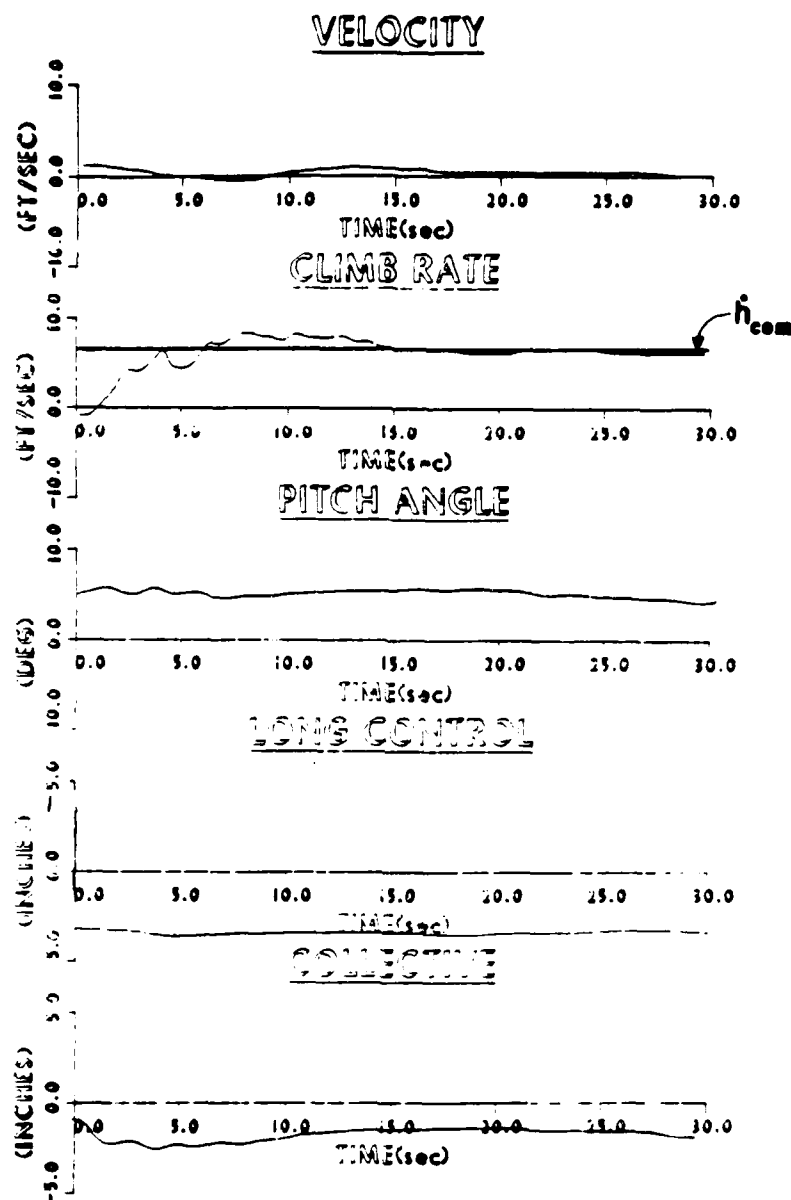


Figure 3.31: **Third Order Compensator Flight Response to Climb Rate Command.** Atmospheric turbulence masked the transient portion of the response but steady state was achieved in about 10 seconds, similar to the simulation of Figure 3.17.

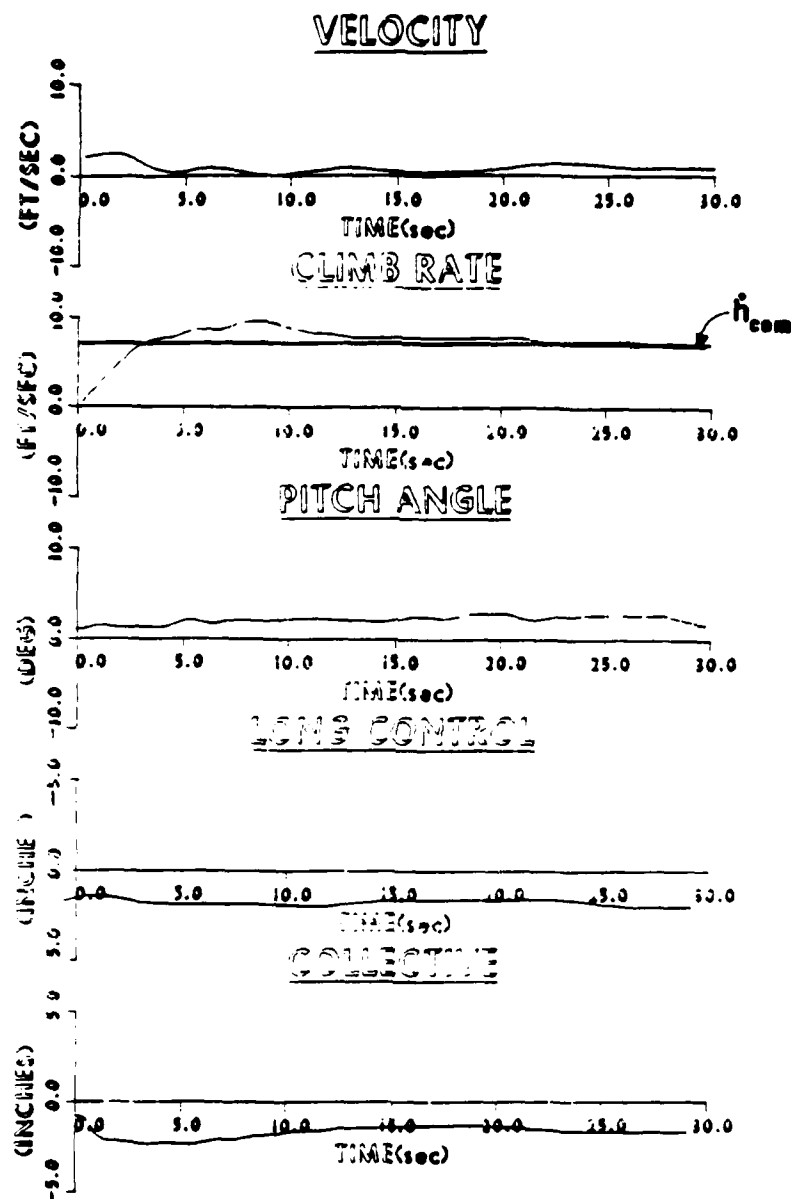


Figure 3.30: Full Order Compensator Flight Response to Climb Rate Command. As in the velocity response of Figure 3.27, the h command response was well predicted by the simulation results of Figure 3.19. This response also shows the decoupling between velocity and climb rate.

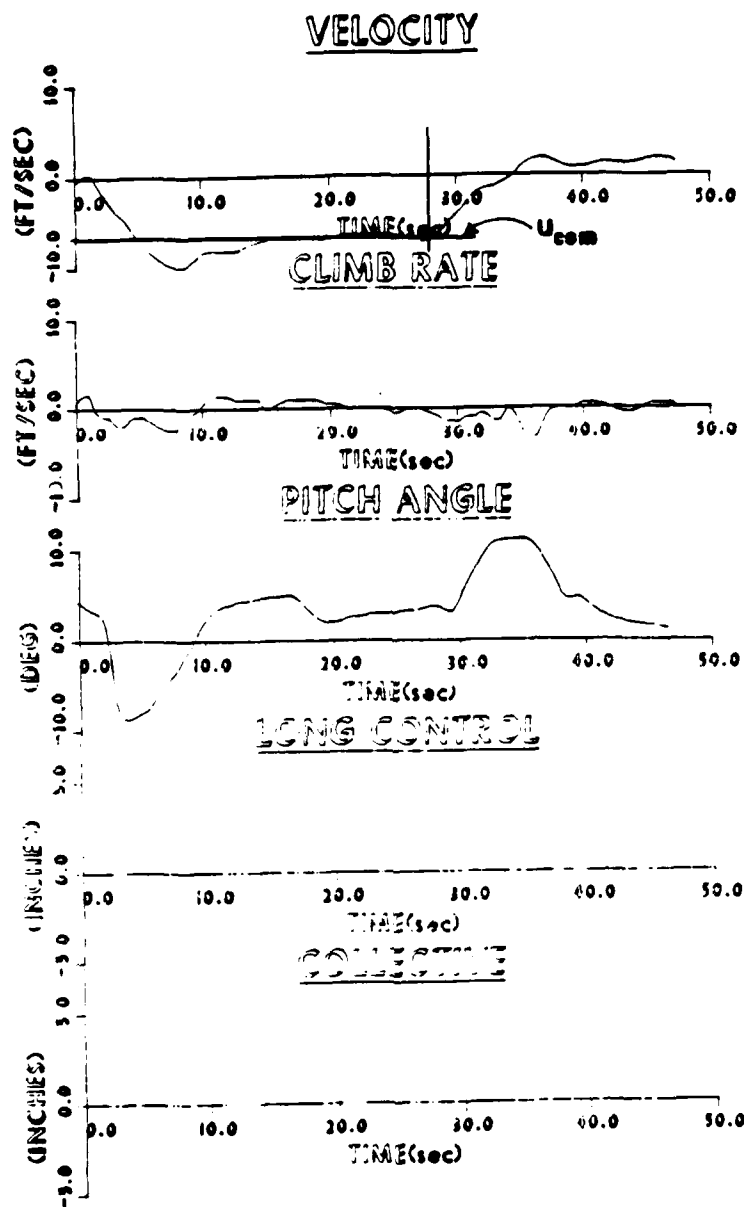


Figure 3.29: Output Feedback Compensator Flight Response to Velocity Command. As in the responses of Figures 3.27 and 3.28, this flight response agrees with the simulation predictions. In this case, however, the overall loop gain (final gain to the actuator) was reduced by half.

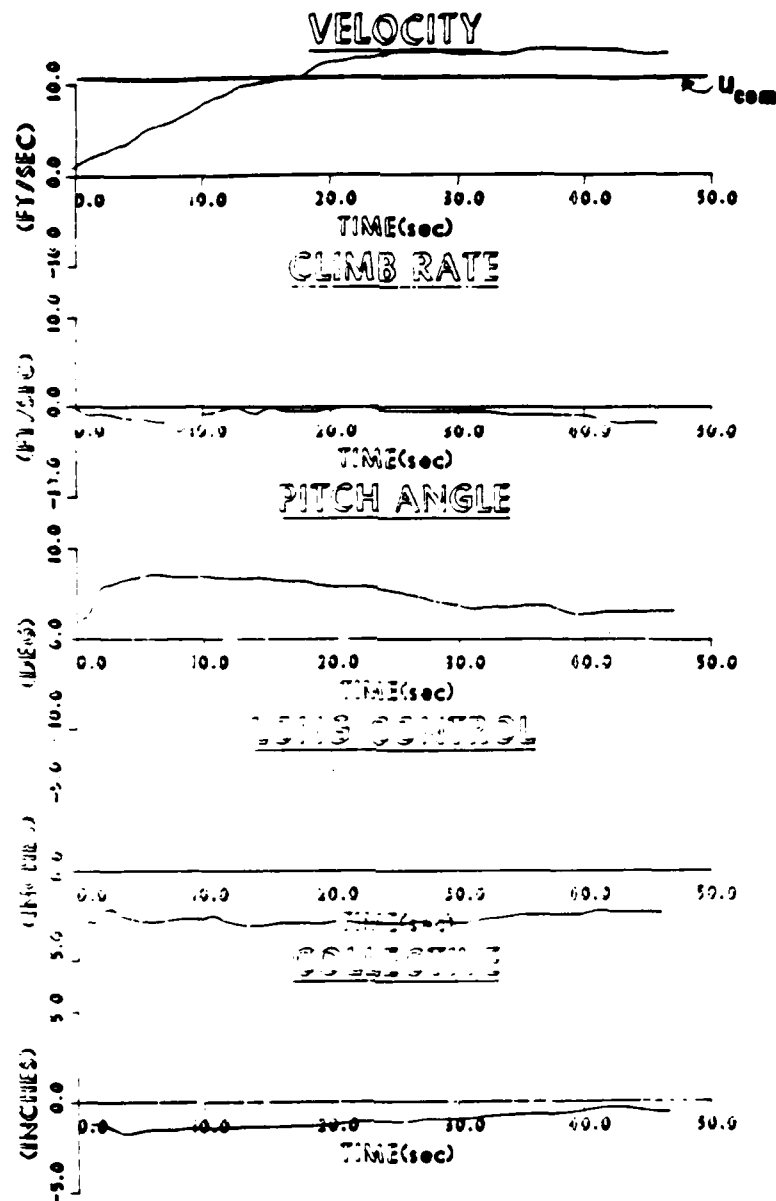


Figure 3.28: **Third Order Flight Response to Velocity Command.** This response to a command of approximately 10 ft/sec follows closely the simulation results of Figure 3.17.

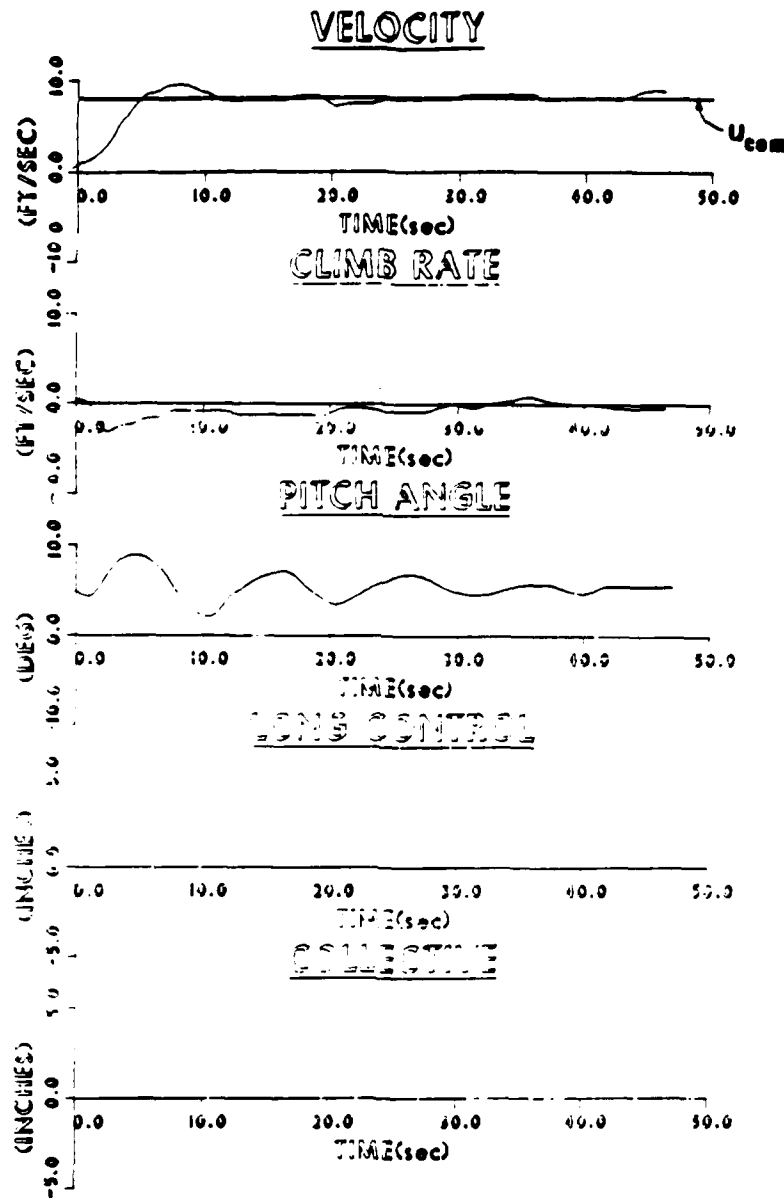


Figure 3.27: **Full Order Compensator Flight Response to Velocity Command.** The rapid velocity response and poorly damped pitch angle were also evident in the simulation response of Figure 3.19.

in a realistic task such as flying a precision approach.

3.8. Summary of Results for the Longitudinal CAS Design

The results of this section can be separated into two categories:

- the design task
- the flight test results

The design task was important because it established an experience base for use of the design methodology. This task showed that use of integral-error feedback in a state variable based controller eliminates the effects of an inaccurate plant model in achieving commanded outputs. It also showed the difficulty encountered when using LQG design techniques with specified time domain properties. In this example, three methods of setting weighting matrices and spectral density matrices were compared. From a practical standpoint, this first design task was very important since an accurate way of scaling the analytical design for use in the fixed point flight computer was developed. An equally important result of this task was the coding and testing of a general form of a modern controller for the Sperry 1819 flight computer.

The flight test results showed the technical feasibility of decoupled control using a "modern" controller. The test system had adequate handling qualities but, due to time constraints, no attempt was made to iterate the designs for "good" handling qualities. Also, the disturbance rejection capabilities were not thoroughly investigated.

took place at the Crows Landing test facility (in the San Joaquin valley) to avoid the heavy traffic of the South San Francisco Bay Area near Ames Research Center. The purpose of the flight test was to validate the performance of the different controllers rather than "tune" the system for maximum pilot acceptance. Step commands from the computer or the pilot were used to evaluate the different systems. The nominal airspeed was 60 knots but stability and performance were checked from 40 to 80 knots. Figures 3.27, 3.28 and 3.29 show the responses of the full-order, third-order, and direct feedback compensators to velocity step commands of about 10 ft/sec. All three of these systems show good decoupling between velocity and climb rate. Their velocity responses are similar to the simulation results of figures 3.12, 3.17, and 3.23 but the pitch angle behavior is less damped than the simulation results. Chen has shown that unmodeled dynamics, especially rotor dynamics, are the probable cause for the lower achievable control bandwidth in flight.[12] In fact, the output feedback flight implementation had the overall pitch and collective loop gains reduced by half to achieve an acceptable response. Figures 3.30, 3.31 and 3.32 show similar results for climb rate commands. The importance of integral control is demonstrated in figure 3.33 which shows the response to a climb rate command for the third order controller without integral control. Although a steady climb rate is achieved, an unwanted velocity change of similar magnitude is also present.

Pilot opinion was mixed concerning the system. They were impressed at how well it held airspeed and climb rate but the transient behavior was not totally acceptable and the system was "sloppy" in response to gusts. This is valid criticism based on the pitch angle responses. Unfortunately the system was not evaluated

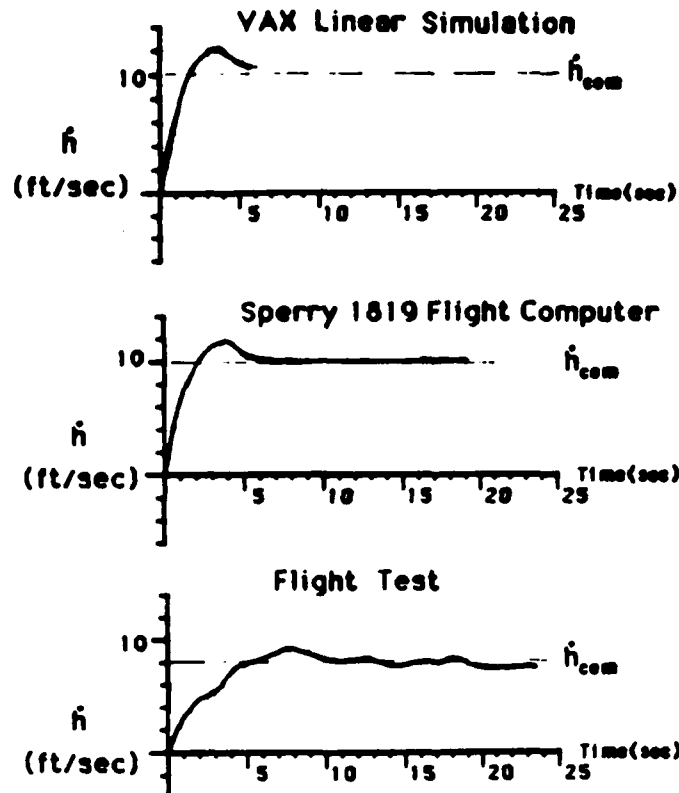


Figure 3.26: Comparison of Analytical Design and Flight Test Implementation of the Controller. This figure confirms the correctness of the steps needed to go from the analytical design to flight. These responses are for the 3rd order compensator with integral control.

tinuous designs were digitized and scaled correctly. The OBS was also useful in preliminary pilot evaluation of the control laws and in initial setting of the stick sensitivities and other pilot-related items. Figure 3.26 shows a comparison of the time responses for a climb rate command for the third order system. This confirmed the accurate digitization and scaling of the analytical design. All flight controllers were similarly checked prior to each flight.

3.7. Flight Test Results

Once the designs had been implemented and checked out in the flight hardware, the flight testing began. Since the controller was designed for cruise, the testing

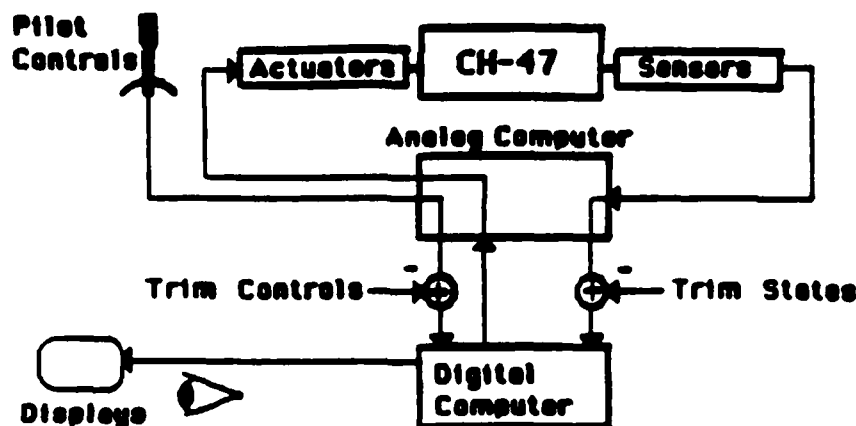


Figure 3.25: **Flight Test Implementation.** Sensor outputs and actuator commands were filtered in the analog computer while the control laws were executed in the digital computer.

pose matrix multiply routine was programmed to take advantage of the minimal form of the compensator dynamics matrix.

- The existing instrumentation output subroutines were modified to send internal compensator data to the ground support station.
- Since the Sperry 1819A flight computer is an 18 bit fixed point machine, the matrices from the previous section were scaled to avoid numerical overflow during program execution. Appendix E describes this "fixed point scaling" technique and lists the SCALEM computer programs which accomplish this.

The actual assembly code implementing the controller is shown in Appendix I.

One important capability of the research system was onboard simulation(OBS). The OBS allowed the real-time flight software to be checked in the closed-loop system prior to actual flight. It was especially useful in confirming that the con-

could work without integral assistance. This would determine how well the design models compared with the real aircraft. Using the SETPNT program, the digital block minimal forms of each of these compensators were computed for flight implementation.

3.6. Flight Test Implementation

Once the analytical designs were complete, the tedious task of actual flight implementation began. Figure 3.25 shows a block diagram of the control structure on the research vehicle. The TR-48 analog computer was used to filter the sensor outputs and the digital actuator commands from the Sperry computer. The digital commands from the computer were filtered to avoid possible actuator wear caused by the 20 Hz chatter. The control laws were implemented in the Sperry 1819A digital flight control computer. Before the designs of the previous sections could be tested, the flight control computer software had to be modified to use them. In order to implement design changes more quickly, the flight software was set up to use the compensator matrices directly. Some of the considerations involved in programming the general form of the compensator in assembly language (shown in Figure 3.3) are listed below:

- Since the design was based on a linear perturbation model, the measurement and control trim values were approximated as the values at engage time; these were subtracted from their sensed values for use by the controller. This had the added advantage of eliminating engage transients.
- The compensator states were initialized to zero before system engage.
- To minimize time required for the compensator calculations, a special pur-

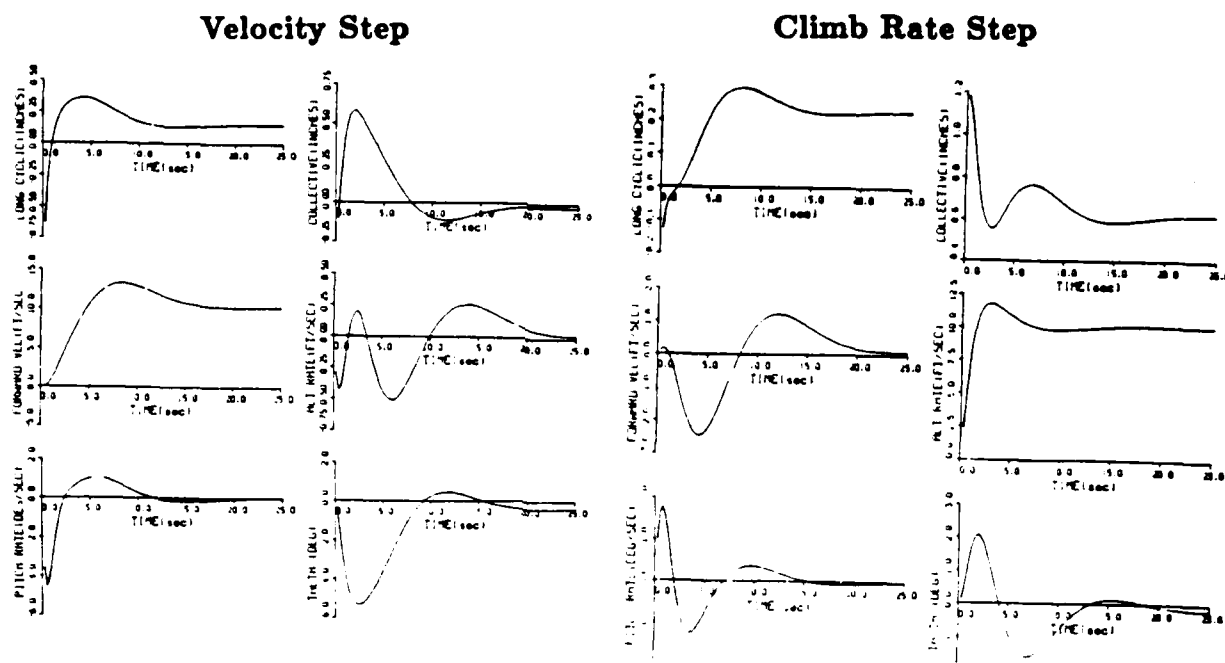


Figure 3.23: Longitudinal Output and Integral Feedback Controller Time Responses. This design was selected for flight evaluation.

System	Standard Deviation						
	δ_z (inches)	δ_c (inches)	u (ft/sec)	w (ft/sec)	q (deg/sec)	θ (deg)	h (ft/sec)
Nominal	.12	.06	1.01	1.51	0.84	0.78	1.49
Arbitrary Noise	.39	.21	4.24	3.96	3.46	3.34	2.65
Inverse Optimal	.16	.07	1.43	2.90	1.24	1.29	1.72
Inv Opt w/Int Cntrl	.34	.18	.82	1.53	2.0	1.1	1.64
3rd Order	.08	.08	2.83	0.83	0.67	0.78	1.39
3rd Order w/ Int Cntrl	.10	.14	0.72	0.83	0.55	0.38	0.86
Output Feedback	.32	.19	.82	1.58	1.29	0.80	0.80
Output Feedback w/Int Cntrl	.32	.21	.93	1.54	1.30	0.84	0.81

Figure 3.24: Performance Comparison of All Compensators. The boldfaced systems were selected for flight evaluation.

$$D = \begin{bmatrix} -5.74 & -12.51 & .041 & .103 \\ -1.23 & -10.44 & -.057 & .013 \end{bmatrix} \quad (3.37)$$

$$I = \begin{bmatrix} -.017 & .054 \\ -.013 & .084 \end{bmatrix} \quad (3.38)$$

Closed Loop Eigenvalues

Real Part	Imag Part	Damping	Freq(rad/sec)	Freq(Hz)
-37.52	0.0	1.0	37.52	5.97
-39.42	0.0	1.0	39.42	6.27
-2.39	0.0	1.0	2.39	.38
-1.17	.58	.89	1.30	.21
-1.17	-.58	.89	1.30	.21
-.13	0.0	1.0	.13	.021
-.23	.36	.54	.43	.068
-.23	-.36	.54	.42	.068

Figure 3.22: **Longitudinal Output and Integral Feedback Controller.** As with the full order and 3rd order designs, the use of integral control reduces damping slightly.

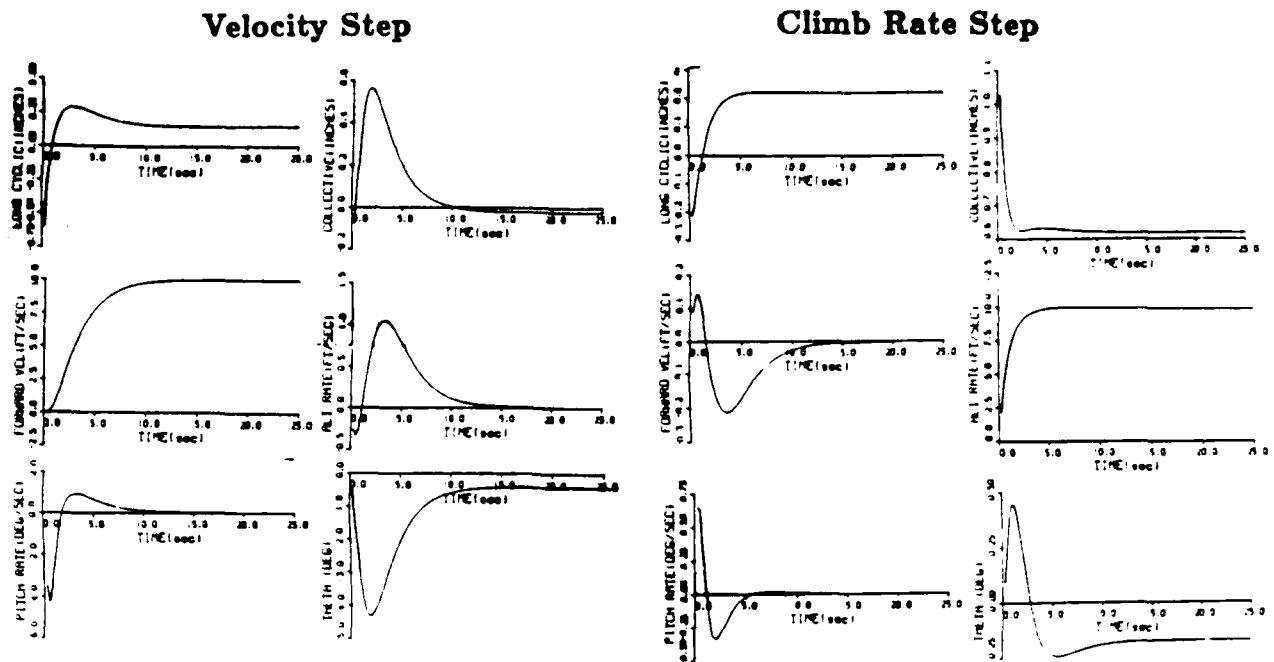


Figure 3.21: Longitudinal Output Feedback Controller Time Responses. These responses are critically damped and typical of full-state feedback designs.

Figure 3.20, good results were achieved with no further optimization. Figures 3.22 and 3.23 show these results.

3.5.3. Summary of Design Results

A number of controllers have been presented to show the iterative nature of the design methodology and to show an application of several methods to meeting the requirements. Selecting designs for flight test implementation required a review of these results. Figure 3.24 shows a comparison of all the designs. The controllers shown in boldface in Figure 3.24 were selected as candidates for flight. The three designs with integral-error control show a comparison of three sizes of compensators (full-order, reduced order and output feedback). The 3rd order controller without integral control was included to see if the decoupling matrix

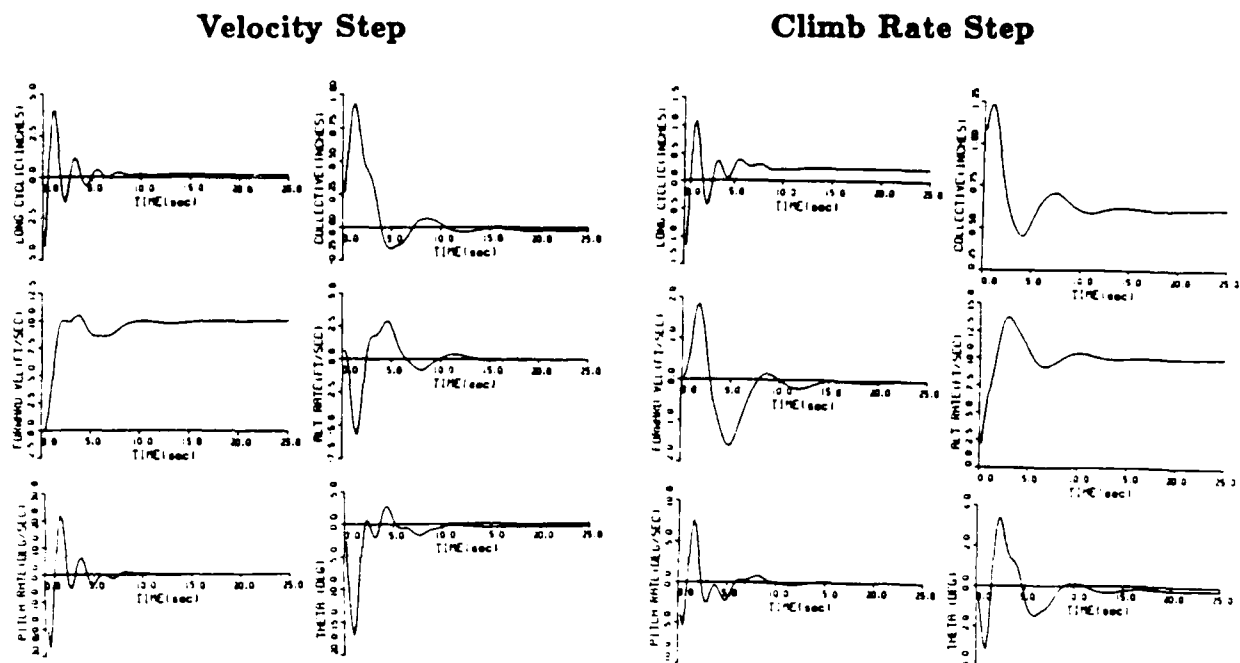


Figure 3.19: Longitudinal Full Order Integral Controller Time Responses. This design was also selected for flight evaluation.

$$D = \begin{bmatrix} -5.74 & -12.51 & .041 & .103 \\ -1.23 & -10.44 & -.057 & .013 \end{bmatrix} \quad (3.36)$$

System	Eigenvalues	Damping
Open Loop(F)	-40.0, -40.0, -2.54, .503, $-.105 \pm j.276$	1, 1, 1, <i>unstable</i> , .35
Closed Loop($F - G D H_m$)	-39.4, -37.52, $-2.07 \pm j.213$, $-.72$, $-.47$	1, 1, .99, 1, 1

Figure 3.20: Longitudinal Output Feedback Controller. Since the measurements (q , θ , h , and u) are almost the same as the states of a 4th order aircraft model (u , w , q , and θ), the output gains were set to the full-state feedback gains from a 4th order regulator design.

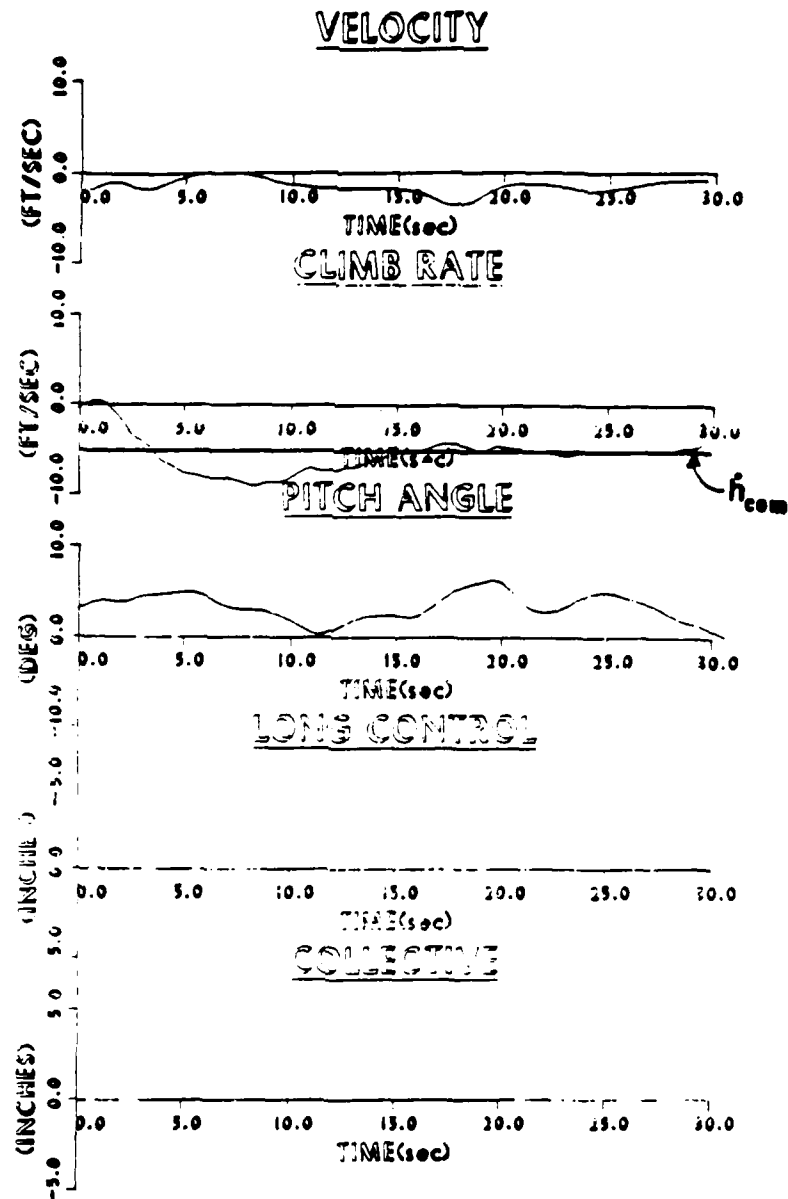


Figure 3.32: Output Feedback Compensator Flight Response to Climb Rate Command. As in Figure 3.29, the overall loop gains to the actuators were decreased by half from the analytical design.

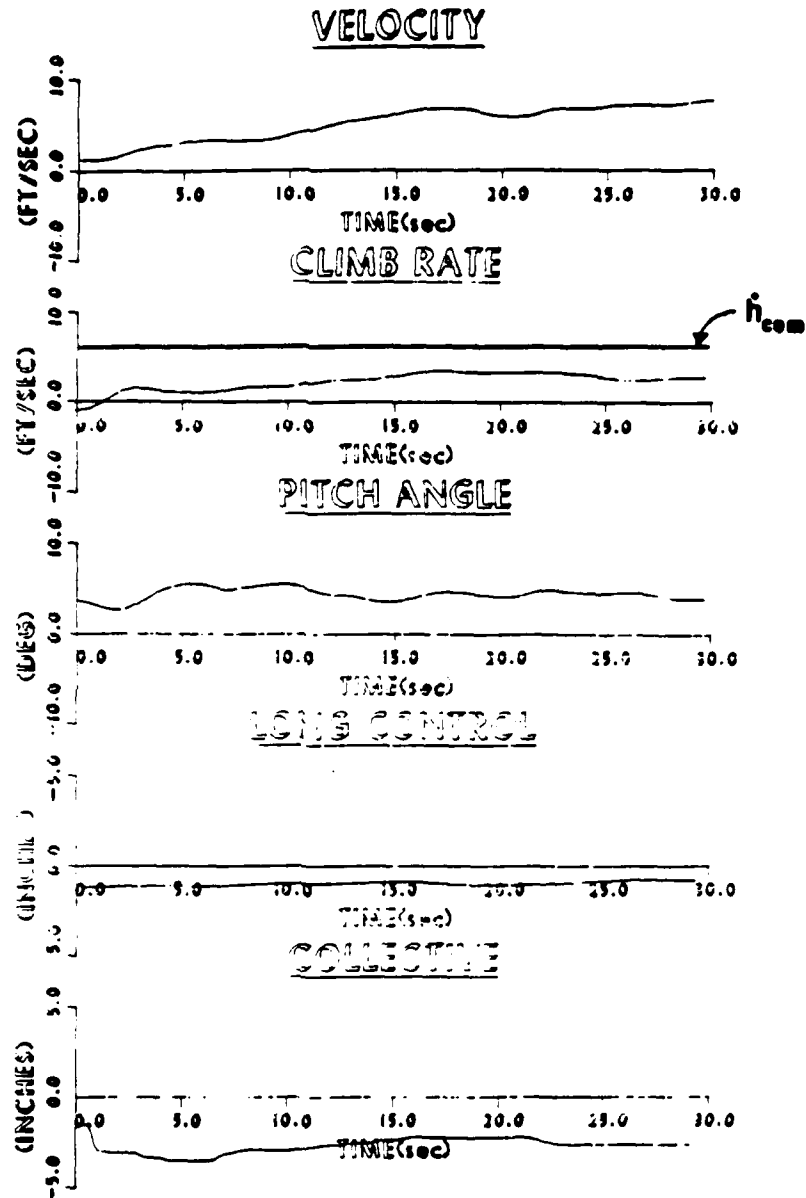


Figure 3.33: **Third Order Flight Response to Climb Rate Command without Integral Control.** This figure documents the effectiveness of the integral control loops. It also emphasizes the need for better models of the CH-47.

Chapter 4.

Hover Controller for the CH-47

4.1. Design Goals and Constraints

With the experience gained in the design of the longitudinal CAS, a more difficult task was selected for the next flight experiment. The second application of the methodology was the design of a translational velocity command, precision hover hold control system for the CH-47. This system was to provide the pilot with "split-axis" control of translational velocity in an heading-oriented inertial coordinate frame. "Split-axis" here means the pilot could select either a velocity command or position-hold control mode in each of the three translational degrees of freedom of the aircraft. As in Chapter 3, this design required decoupling of the three axes of interest. Figure 4.1 shows the coordinate system used for the design. As in Chapter 3, this control law is somewhat unconventional since the pilot's workload is reduced by removing him from inner loop attitude control tasks. For this system, forward velocity is controlled by longitudinal stick displacement, side velocity by lateral stick, and vertical velocity by the collective lever. If a particular pilot control is within a small distance of the neutral position (the detent), then the system enters a position-hold mode for that axis. Yaw rate control, using the

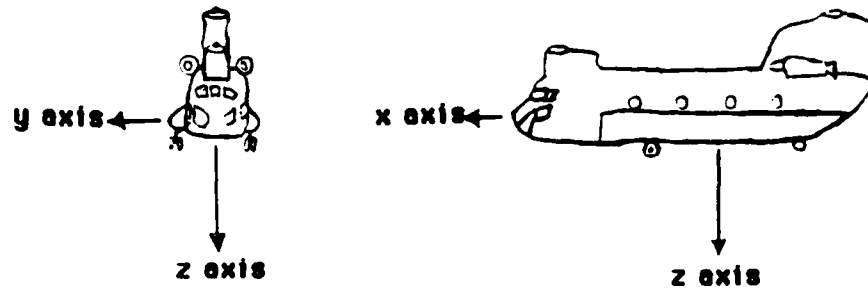


Figure 4.1: **Hover Control System Coordinate System.** The x , y , and z coordinates are in a heading-oriented inertial system.

standard CH-47 SAS, comes from the pedals. No operational helicopter control systems have this type of capability although the concept was tried on a modified CH-47 helicopter during early work on the Army's Heavy Lift Helicopter(HLH) concept.[13] This type of control law has numerous advantages with potential applications such as:

- Search and rescue
- Shipboard operations
- Slung load operations

Before proceeding with the description of how the design methodology was applied, the design constraints must be mentioned. As in the longitudinal CAS design, the TR-48 was used to filter the aircraft motion sensor data. The inertial velocity and position measurements came from either a laser or radar tracker on the ground. This was necessary since the onboard inertial navigation system(INS) had a drift of several knots ($\approx 5ft/sec$) and provided only position data (no velocities). To avoid major changes in the flight software, a general form of the controller was programmed in the flight computer which provided for a flexible control structure.

$$\begin{bmatrix} \dot{u} \text{ (ft/sec)} \\ \dot{v} \text{ (ft/sec)} \\ \dot{w} \text{ (ft/sec)} \\ \dot{p} \text{ (radians/sec)} \\ \dot{q} \text{ (radians/sec)} \\ \dot{r} \text{ (radians/sec)} \\ \dot{\theta} \text{ (radians)} \\ \dot{\phi} \text{ (radians)} \\ \dot{\delta}_{e\text{actual}} \text{ (inches)} \\ \dot{\delta}_{c\text{actual}} \text{ (inches)} \\ \dot{\delta}_{a\text{actual}} \text{ (inches)} \end{bmatrix} = F \begin{bmatrix} u \\ v \\ w \\ p \\ q \\ r \\ \theta \\ \phi \\ \delta_{e\text{actual}} \\ \delta_{c\text{actual}} \\ \delta_{a\text{actual}} \end{bmatrix} + G \begin{bmatrix} \delta_{e\text{desired}} \text{ (inches of longitudinal stick)} \\ \delta_{c\text{desired}} \text{ (inches of collective lever)} \\ \delta_{a\text{desired}} \text{ (inches of lateral stick)} \end{bmatrix}$$

$$y_m(\text{measurements}) = \begin{bmatrix} \dot{x} \\ \dot{y} \\ \dot{z} \\ p \\ q \\ r \\ \theta \\ \phi \end{bmatrix}$$

(4.1)

Figure 4.2: **CH-47 Hover Model.** This is the conventional 8th order model described in Appendix G.

4.2. Linear Model and Basic Control Structure

The 8th order basic airframe model is described in Appendix G. This model was augmented with three actuator states as shown in Equation 3.2. These actuator states allow the the designer to penalize control rate, a necessary step to avoid nuisance disengages of the research control system during flight. Figure 4.2 shows this model as it was used for the control law synthesis. One item to note is that there is no yaw control in the model. The yaw SAS was approximated by adding -1 to the N_{δ_r} element of the "F" matrix of Figure 4.2 and Appendix G.

Since the longitudinal CAS showed the necessity of integral-error control, the hover control structure had to accommodate this capability. Figure 4.3 shows the hover controller. Unlike the longitudinal CAS, integral control decoupling is not done in the inner loop. Instead, *PID* (Proportional Integral Derivative) outer loops are closed separately to $\dot{x}_{command}$, $\dot{y}_{command}$, and $\dot{z}_{command}$, which act as controls for these outer loops. The velocity command system is the inner loop. Setting up the control structure in this way had several advantages:

- The inner loop and outer loop designs, both fairly complicated, could be separated.
- By using the desired outputs as controls, the magnitude of the outer loop gains became physically meaningful. This proved to be important later when these gains were adjusted during flight to achieve good performance.
- Keeping the inner loop separate made the mode switching between pilot velocity command and *PID* control easier.

Before the full-order design began, the system was scaled in equivalent units.

4.3. Model Scaling

The hover model was scaled into the same units as used in the longitudinal CAS design. *Ft/sec* remained *ft/sec*; *radians* and *radian/sec* became .01 *radians* and .01 *radians/sec*; and *inches* of control became .1 *inches* of control. Figures 4.4 and 4.5 show the model before and after scaling. The ROPTSYS computer program did this scaling.

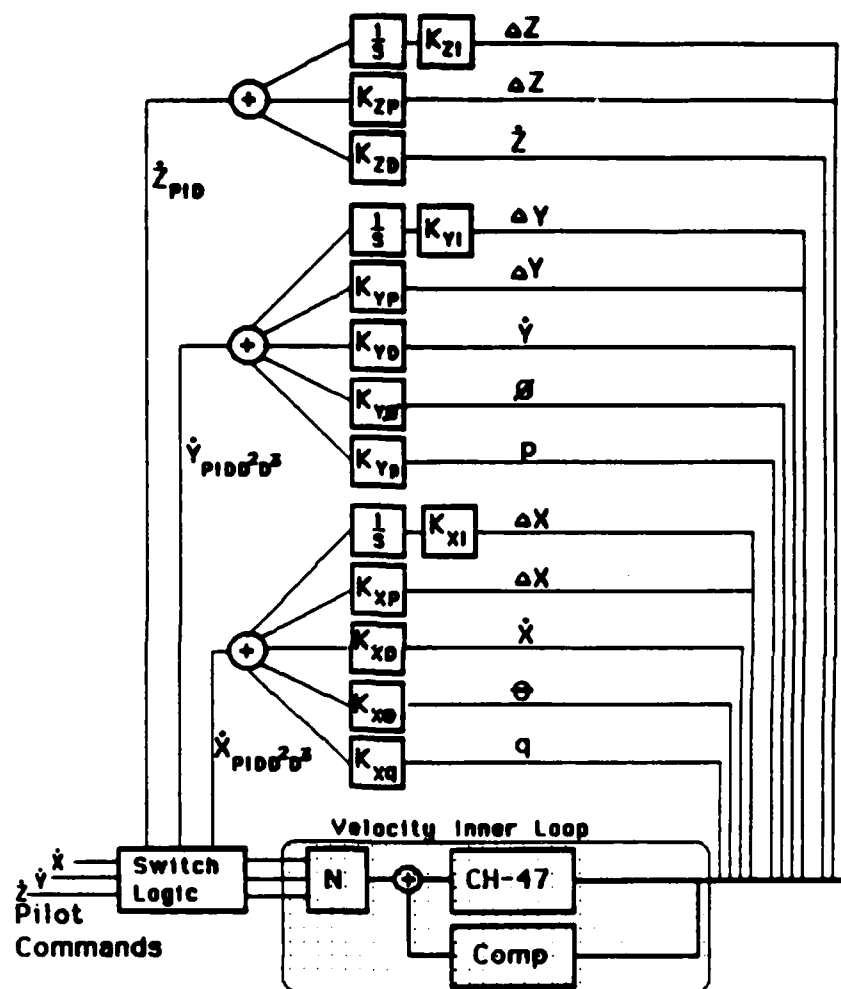


Figure 4.3: **Hover Control System.** The control system is divided into a distinct inner loop (velocity command) and outer loops which provide position hold using *PID* control.

State Equations

$$\dot{x} = F x + G u$$

$$F = \begin{bmatrix} -0.021 & -0.00085 & 0.0326 & 0.0205 & 2.585 & -0.106 & -31.986 & 0.0 & 0.114 & 0.939 & 0.0 \\ -0.00019 & -0.137 & 0.00265 & -1.494 & 0.00414 & -0.165 & 0.0292 & 31.99 & 0.0118 & 0.0635 & 1.159 \\ 0.0248 & 0.00374 & -0.296 & 0.0419 & 0.435 & 0.362 & -3.71 & 0.0 & 0.303 & -8.062 & .00002 \\ -0.00013 & -0.00652 & 0.00058 & -0.716 & 0.0382 & -0.0708 & 0.0 & 0.0 & -0.00596 & -0.0142 & .432 \\ 0.00925 & 0.00017 & 0.00234 & 0.0427 & -1.23 & -0.00433 & 0.0 & 0.0 & 0.329 & 0.019 & 0.0 \\ 0.00039 & -0.00112 & 0.00027 & -0.0544 & -0.158 & -1.0 & 0.0 & 0.0 & 0.0461 & -0.00037 & .0425 \\ 0.0 & 0.0 & 0.0 & 0.0 & 1.0 & 0.00788 & 0.0 & 0.0 & 0.0 & 0.0 & 0.0 \\ 0.0 & 0.0 & 0.0 & 1.0 & 0.00091 & 0.116 & 0.0 & 0.0 & 0.0 & 0.0 & 0.0 \\ 0.0 & 0.0 & 0.0 & 0.0 & 0.0 & 0.0 & 0.0 & 0.0 & -40.0 & 0.0 & 0.0 \\ 0.0 & 0.0 & 0.0 & 0.0 & 0.0 & 0.0 & 0.0 & 0.0 & 0.0 & -40.0 & 0.0 \\ 0.0 & 0.0 & 0.0 & 0.0 & 0.0 & 0.0 & 0.0 & 0.0 & 0.0 & 0.0 & -40.0 \end{bmatrix}$$

$$G = \begin{bmatrix} 0.0 & 0.0 & 0.0 \\ 0.0 & 0.0 & 0.0 \\ 0.0 & 0.0 & 0.0 \\ 0.0 & 0.0 & 0.0 \\ 0.0 & 0.0 & 0.0 \\ 0.0 & 0.0 & 0.0 \\ 0.0 & 0.0 & 0.0 \\ 0.0 & 0.0 & 0.0 \\ 40.0 & 0.0 & 0.0 \\ 0.0 & 40.0 & 0.0 \\ 0.0 & 0.0 & 40.0 \end{bmatrix}$$

$$Q = \begin{bmatrix} 24.6 & 0 & 0 \\ 0 & 24.6 & 0 \\ 0 & 0 & 9.98 \end{bmatrix}$$

$$R = \begin{bmatrix} 2.6 \times 10^{-2} & 0 & 0 & 0 & 0 & 0 & 0 & 0 & 0 & 0 \\ 0 & 2.6 \times 10^{-2} & 0 & 0 & 0 & 0 & 0 & 0 & 0 & 0 \\ 0 & 0 & 2.6 \times 10^{-2} & 0 & 0 & 0 & 0 & 0 & 0 & 0 \\ 0 & 0 & 0 & 1.293 \times 10^{-4} & 0 & 0 & 0 & 0 & 0 & 0 \\ 0 & 0 & 0 & 0 & 3.232 \times 10^{-5} & 0 & 0 & 0 & 0 & 0 \\ 0 & 0 & 0 & 0 & 0 & 8.079 \times 10^{-6} & 0 & 0 & 0 & 0 \\ 0 & 0 & 0 & 0 & 0 & 0 & 3.232 \times 10^{-7} & 0 & 0 & 0 \\ 0 & 0 & 0 & 0 & 0 & 0 & 0 & 3.232 \times 10^{-7} & 0 & 0 \\ 0 & 0 & 0 & 0 & 0 & 0 & 0 & 0 & 3.232 \times 10^{-7} & 0 \end{bmatrix}$$

Figure 4.4: CH-47 Hover Linear Model. The last 3 states are 40 radian actuator models.

State Equations

$$\dot{x}_{scaled} = F_{scaled}x_{scaled} + G_{scaled}u_{scaled}$$

$$F_{scaled} = \begin{bmatrix} -0.021 & -0.00085 & 0.0326 & 0.000205 & .02585 & -0.00106 & -.31986 & 0.0 & 0.0114 & 0.0939 & 0.0 \\ -0.00019 & -0.137 & 0.00265 & -.1494 & 0.0000414 & -0.00165 & 0.000292 & .3199 & 0.00118 & 0.00635 & .1159 \\ 0.0248 & 0.00374 & -0.296 & 0.000419 & 0.00435 & 0.00362 & -.0371 & 0.0 & 0.0303 & -.8062 & .000002 \\ -0.013 & -0.652 & 0.058 & -0.716 & 0.0382 & -0.0708 & 0.0 & 0.0 & -0.0596 & -0.142 & 4.32 \\ 0.925 & 0.017 & 0.234 & 0.0427 & -1.23 & -0.00433 & 0.0 & 0.0 & 3.29 & 0.19 & 0.0 \\ 0.039 & -0.112 & 0.027 & -0.0544 & -0.158 & -1.0 & 0.0 & 0.0 & 0.461 & -0.0037 & .425 \\ 0.0 & 0.0 & 0.0 & 0.0 & 1.0 & 0.00788 & 0.0 & 0.0 & 0.0 & 0.0 & 0.0 \\ 0.0 & 0.0 & 0.0 & 1.0 & 0.00091 & 0.116 & 0.0 & 0.0 & 0.0 & 0.0 & 0.0 \\ 0.0 & 0.0 & 0.0 & 0.0 & 0.0 & 0.0 & 0.0 & 0.0 & -40.0 & 0.0 & 0.0 \\ 0.0 & 0.0 & 0.0 & 0.0 & 0.0 & 0.0 & 0.0 & 0.0 & 0.0 & -40.0 & 0.0 \\ 0.0 & 0.0 & 0.0 & 0.0 & 0.0 & 0.0 & 0.0 & 0.0 & 0.0 & 0.0 & -40.0 \end{bmatrix}$$

$$G_{scaled} = \begin{bmatrix} 0.0 & 0.0 & 0.0 \\ 0.0 & 0.0 & 0.0 \\ 0.0 & 0.0 & 0.0 \\ 0.0 & 0.0 & 0.0 \\ 0.0 & 0.0 & 0.0 \\ 0.0 & 0.0 & 0.0 \\ 0.0 & 0.0 & 0.0 \\ 0.0 & 0.0 & 0.0 \\ 40.0 & 0.0 & 0.0 \\ 0.0 & 40.0 & 0.0 \\ 0.0 & 0.0 & 40.0 \end{bmatrix}$$

$$Q_{scaled} = \begin{bmatrix} 24.6 & 0 & 0 \\ 0 & 24.6 & 0 \\ 0 & 0 & 9.98 \end{bmatrix}$$

$$R_{scaled} = \begin{bmatrix} 2.6 \times 10^{-2} & 0 & 0 & 0 & 0 & 0 & 0 & 0 & 0 & 0 \\ 0 & 2.6 \times 10^{-2} & 0 & 0 & 0 & 0 & 0 & 0 & 0 & 0 \\ 0 & 0 & 2.6 \times 10^{-2} & 0 & 0 & 0 & 0 & 0 & 0 & 0 \\ 0 & 0 & 0 & 1.293 & 0 & 0 & 0 & 0 & 0 & 0 \\ 0 & 0 & 0 & 0 & 3.232 \times 10^{-1} & 0 & 0 & 0 & 0 & 0 \\ 0 & 0 & 0 & 0 & 0 & 8.079 \times 10^{-2} & 0 & 0 & 0 & 0 \\ 0 & 0 & 0 & 0 & 0 & 0 & 3.232 \times 10^{-2} & 0 & 0 & 0 \\ 0 & 0 & 0 & 0 & 0 & 0 & 0 & 3.232 \times 10^{-2} & 0 & 0 \\ 0 & 0 & 0 & 0 & 0 & 0 & 0 & 0 & 3.232 \times 10^{-2} & 0 \end{bmatrix}$$

Figure 4.5: CH-47 Scaled Hover Linear Model. After scaling, the weak coupling terms in the F matrix become very obvious.

4.4. LQG Design and Compensator Order Reduction

The scaled 11th order model shown in Figure 4.5 was used by the ROPTSYS program to calculate the full-order compensator. At this point, an important simplification should be emphasized. The system was to control \dot{x} , \dot{y} , and \dot{z} which are inertial velocities. The model as used included u , v , and w which are body axis airmass velocities. The implicit assumption, needed to facilitate the design, was that the two sets of velocities were equal:

$$\begin{aligned}\dot{x} &= u \\ \dot{y} &= v \\ \dot{z} &= w\end{aligned}\tag{4.2}$$

This assumption is reasonable only if θ and ϕ remain small, which they must for safe hover in a large helicopter such as the CH-47. The outputs, y_o , weighted in the performance index:

$$P.I. = \int_0^\infty (y_o^T A y_o + u^T B u) dt\tag{4.3}$$

were the three velocities (u , v , and w) and the three control rates. Since the system had been scaled, the weighting matrices, A and B , were just 6×6 and 3×3 identity matrices. Using these assumptions and criterion, the resulting full-order compensator is shown in Figure 4.6.

Based on these data, especially the modal cost M_2 , the 11th order compensator was reduced to 5th order. This represents a significant reduction of complexity in the resulting compensator. The 11th order design had 121 independent gains while the 5th order compensator had only 55. After the order reduction, the compensator

$$F_{min} = \begin{bmatrix} 0 & 1 & 0 & 0 & 0 & 0 & 0 & 0 & 0 & 0 & 0 \\ -80.615 & -15.033 & 0 & 0 & 0 & 0 & 0 & 0 & 0 & 0 & 0 \\ 0 & 0 & 0 & 1 & 0 & 0 & 0 & 0 & 0 & 0 & 0 \\ 0 & 0 & -55.126 & -11.587 & 0 & 0 & 0 & 0 & 0 & 0 & 0 \\ 0 & 0 & 0 & 0 & -5.78 & 0 & 0 & 0 & 0 & 0 & 0 \\ 0 & 0 & 0 & 0 & 0 & -2.74 & 0 & 0 & 0 & 0 & 0 \\ 0 & 0 & 0 & 0 & 0 & 0 & -2.33 & 0 & 0 & 0 & 0 \\ 0 & 0 & 0 & 0 & 0 & 0 & 0 & -1.48 & 0 & 0 & 0 \\ 0 & 0 & 0 & 0 & 0 & 0 & 0 & 0 & -1.01 & 0 & 0 \\ 0 & 0 & 0 & 0 & 0 & 0 & 0 & 0 & 0 & -2.03 & 0 \\ 0 & 0 & 0 & 0 & 0 & 0 & 0 & 0 & 0 & 0 & -1.04 \end{bmatrix}$$

$$K_{min}(unscaled) = \begin{bmatrix} .0032 & -.00096 & .0024 & -.0112 & -.63 & .023 & -32.4 & .097 \\ .0294 & .0183 & -.00274 & .21 & -17.3 & -2.76 & 59.8 & 4.3 \\ -.002 & -.06 & .0127 & -.442 & .166 & -.99 & .587 & -61.4 \\ .0072 & -.32 & -.023 & -3.6 & -1.64 & -10.62 & -17.3 & 170.1 \\ -.077 & .0115 & .616 & -.074 & -.079 & -.56 & -1.45 & -6.74 \\ -.028 & .56 & .17 & 5.56 & 4.24 & 16.2 & 1.34 & -100.8 \\ -.054 & -.0134 & .136 & -.233 & 25.4 & 3.66 & 3.78 & .33 \\ .087 & -.0084 & -.69 & .146 & .00085 & .81 & .50 & .053 \\ -.0003 & -.02 & .0033 & -.18 & .83 & -.34 & -.48 & -2.19 \\ .000054 & -.034 & -.0022 & -.21 & -.023 & -.56 & .018 & 5.16 \\ -.014 & -.00012 & -.00117 & -.00145 & .125 & .0133 & 4.37 & -.028 \end{bmatrix}$$

$$C_{min}(unscaled) = \begin{bmatrix} 0.0 & -.1 & -.0128 & -.00328 & .0226 & -.00356 & -.1 & .00119 & -.024 & .00067 & -.1 \\ .0011 & -.0036 & .0089 & .00294 & -.1 & .0044 & -.0041 & -.1 & -.012 & .012 & -.0108 \\ .065 & .0056 & 0.0 & -.1 & .0146 & -.1 & .0166 & -.0058 & -.1 & -.1 & -.00247 \end{bmatrix}$$

System Eigenvalues										
Mode	Open Loop(F)		Regulator(F-GC)		Estimator(F-KH)		Compensator(F-GC-KH)		Compensator Measures	
	Real	Imag	Real	Imag	Real	Imag	Real	Imag	M_1	M_2
1	-1.41	0	-.406	.085	-7.63	4.85	-7.52	4.91	4.47	.59
2	-1.07	0	-.406	-.085	-7.63	-4.85	-7.52	-4.91	-	-
3	-.902	0	-.382	.072	-6.04	4.6	-5.79	4.64	5.58	.96
4	-.297	0	-.382	-.072	-6.04	-4.6	-5.79	4.64	-	-
5	.079	.46	-.839	.4	-5.88	0	-5.78	0	.65	.11
6	.079	-.46	-.839	-.4	-.975	0	-2.73	0	1.18	.43
7	.062	.46	-1.2	.33	-.11	0	-2.32	0	.3	.13
8	.062	-.46	-1.2	-.33	-.12	0	-1.48	0	.69	.47
9	-40.0	0	-1.3	.11	-40.0	0	-1.01	0	.032	.032
10	-40.0	0	-1.3	-.11	-40.0	0	-.20	0	.063	.31
11	-40.0	0	-.98	0	-40.0	0	-.10	0	.046	.45

Figure 4.6: Hover Full Order Compensator Design Results. The open loop has two unstable modes which are divergent pitch and roll oscillations. Figure 4.7 is the reduced and reoptimized compensator based on this full order design. Order reduction was based on the M_2 terms shown here.

was optimized using the RSANDY program. Figure 4.7 shows the optimal reduced order compensator including the closed loop roots. This optimization step was difficult since the initial guess (the original 11th order compensator reduced to 5th) was quite unstable. This caused numerical overflows on the VAX computer used to run the RSANDY program. Convergence to a stable 5th order compensator was finally achieved after numerous iterations of the outputs and the output weightings of Equation 4.3. Figure 4.7 shows these outputs, y_o , and the elements of the diagonal A and B matrices. This figure also shows another aspect of the difficulty of this optimization. The entire C matrix was allowed to vary which meant that there were 60 gains being adjusted by the RSANDY program, 5 more than the 55 independent gains of a minimal realization.

The simulation step responses are shown in Figures 4.9, 4.10, and 4.11. All three velocity responses look good but the pitch angle damping has several overshoots. A modal analysis later confirmed this by showing the mode at $-.50 \pm j2.03$ of Figure 4.7 to be strongest in θ . With the velocity inner loop regulator designed, the feedforward matrix was calculated for direct command of \dot{x} , \dot{y} , and \dot{z} . The PID outer loop gains could now be designed.

4.5. Outer Loop Design

As discussed in Section 4.2, the velocity command inner loop and the PID outer loop were separate. With the inner loop velocity controller set, the outer loop design began. This approach (inner loop first then outer loop) is common in the development of operational aircraft autopilots except that the inner loops are normally designed classically using incremental loop closure. Initially, these PID

$$F_{min} = \begin{bmatrix} 0 & 1 & 0 & 0 & 0 \\ -17.93 & -4.90 & 0 & 0 & 0 \\ 0 & 0 & -1.98 & 0 & 0 \\ 0 & 0 & 0 & -8.15 & 0 \\ 0 & 0 & 0 & 0 & -6.31 \end{bmatrix}$$

$$K_{min} = \begin{bmatrix} -.035 & -.050 & -.040 & -.56 & 1.96 & .216 & 3.22 & -74.7 \\ -.037 & -.74 & .071 & -.28 & -1.6 & -7.63 & -19.7 & 169.0 \\ -.58 & .140 & -.23 & .19 & 28.9 & 16.05 & 1.35 & -100.3 \\ -.45 & .0079 & 1.45 & .068 & 6.5 & 1.20 & 2.64 & 7.16 \\ .018 & -.0058 & -.003 & -.029 & -.36 & -.66 & 13.7 & 8.32 \end{bmatrix}$$

$$C_{min} = \begin{bmatrix} -.092 & .0080 & -.13 & -.020 & -5.14 \\ .026 & -.0045 & -.029 & .022 & -.52 \\ .44 & -.021 & -.062 & .00078 & -.42 \end{bmatrix}$$

$$N = \begin{bmatrix} -.071 & -.0061 & .013 \\ .0070 & .0021 & -.079 \\ -.012 & .059 & -.0034 \end{bmatrix}$$

Closed Loop Eigenvalues				
Real Part	Imag Part	Damping	Freq(rad/sec)	Freq(Hz)
-39.99	.0085	1.0	39.99	6.37
-39.99	-.0085	1.0	39.99	6.37
-40.01	0.0	1.0	40.01	6.37
-7.14	0.0	1.0	7.14	1.14
-2.37	2.77	.65	3.65	.58
-2.37	-2.77	.65	3.65	.58
-.50	2.03	.24	2.09	.33
-.50	-2.03	.24	2.09	.33
-.54	1.59	.32	1.68	.27
-.54	-1.59	.32	1.68	.27
-.55	.50	.74	.74	.12
-.55	-.50	.74	.74	.12
-.61	.43	.82	.75	.12
-.61	-.43	.82	.75	.12
-.90	0.0	1.0	.90	.14
-.22	0.0	1.0	.22	.0035

Performance Index Data		
Outputs or Controls	Units	Weighting
u	ft/sec	5×10^3
v	ft/sec	5×10^3
w	ft/sec	5×10^3
p	rad/sec	1×10^5
q	rad/sec	1×10^5
r	rad/sec	1×10^5
δ_e	inches/sec	1×10^5
δ_c	inches/sec	1×10^5
δ_a	inches/sec	1×10^5
\dot{u}	ft/sec ²	5×10^3
\dot{v}	ft/sec ²	5×10^3
\dot{w}	ft/sec ²	5×10^3
δ_e	inches	1×10^3
δ_c	inches	1×10^3
δ_a	inches	1×10^3

Figure 4.7: **Reduced Order Hover Compensator.** The poorly damped modes ($s = -.5 \pm j2.03$) dominate the pitch angle response as Figure 4.9 shows.

outer loop gains were set using the RSANDY program. This approach did not work well as the convergence was very slow. The alternative was to set the gains intuitively. This approach was actually quite reasonable if one recalls the control structure of Figure 4.3. The gains were set by determining how much velocity would be reasonable to use to correct a given position error. For instance, if the aircraft were 10 feet from the desired hover point and a pilot would be willing to use 5 *ft/sec* of \dot{y} then $K_{\dot{y}\delta y}$ would be $.5 \frac{ft/sec}{ft\ error}$. This approach worked well for the *y* and *z* axes but failed for the *x* axis. For this axis, a conventional transfer function analysis was used to set the 5 outer loop gains which were then adjusted in simulation.

4.5.1. Transfer Function Analysis for X Axis Outer Loop

The first step in the process required a transfer function from $u_{command}$ to u_{actual} for the helicopter with velocity inner controller. This came from use of Bernard's code for calculating the matrix of transfer functions for any MIMO linear dynamic system.[7] These transfer functions were 11th order so to make the process tractable, the NAVFIT program at NASA Ames simplified them to 3rd order. The following transfer function resulted:

$$\frac{u_{actual}}{u_{command}} = \frac{.94}{(s + .24) [(s + .5)^2 + 1.87^2]} \quad (4.4)$$

To justify the use of θ and q as second and third derivatives of *x*, consider the longitudinal equation of motion from Etkin: [14]

$$F_x - mg \sin\theta = m [\dot{u} + (q_B^E + q) w - (r_B^E + r) v] \quad (4.5)$$

where if the following assumptions are made:

AD-A151 946

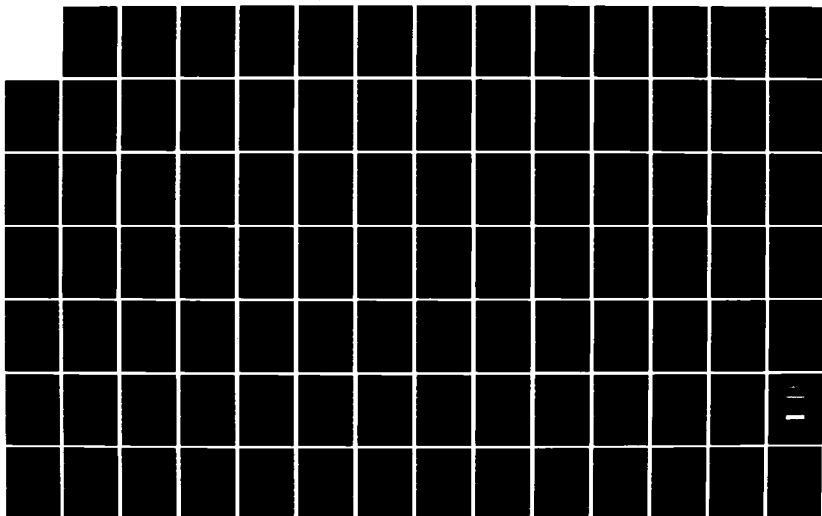
A MODERN CONTROL DESIGN METHODOLOGY WITH APPLICATION TO 2/3
THE CH-47 HELICOPTER(U) AIR FORCE INST OF TECH
WRIGHT-PATTERSON AFB OH R D HOLDRIDGE JAN 85

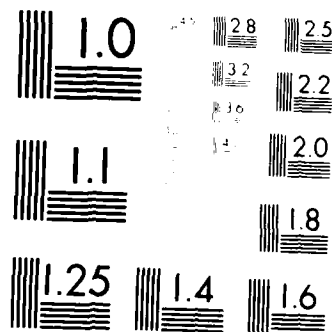
UNCLASSIFIED

AFIT/CI/NR-85-33D

F/G 1/4

NL





MICROCOPY RESOLUTION TEST CHART
NATIONAL BUREAU OF STANDARDS-1963-A

$q_B^E \approx 0$ Earth rotation negligible

$r_B^E \approx 0$ Earth rotation negligible

$qw \approx 0$ Second order effect

$rv \approx 0$ Second order effect

$\sin \theta \approx \theta$ Small angle assumption

$F_z \approx 0$ Reasonable for a helicopter in hover

$\dot{u} \approx \ddot{x}$ Small angle assumption(θ)

then these simplifications result:

$$\begin{aligned}\ddot{x} &\approx -g\theta \\ \ddot{u} &\approx -g\dot{\theta} \approx -gq\end{aligned}\tag{4.6}$$

The actual gain setting is done by including the following for the $PIDD^2D^3$ controller in Figure 4.8.

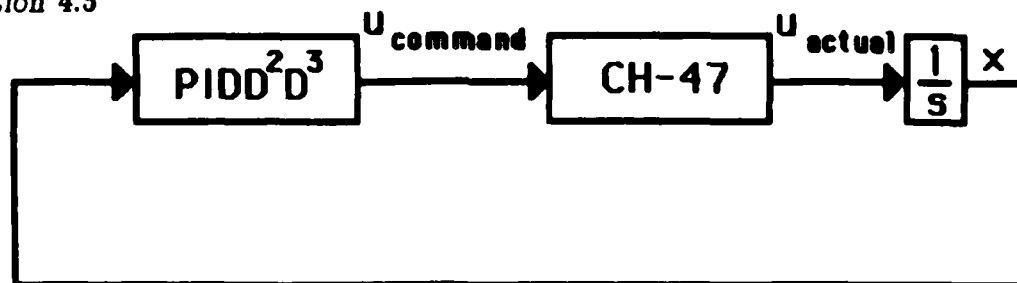
$$PIDD^2D^3 = K_P x + K_I \frac{x}{s} + K_D x s + K_{D^2} x s^2 + K_{D^3} x s^3\tag{4.7}$$

where

$$\begin{aligned}K_P &= K_{\ddot{x} \delta z} \\ K_I &= K_{\dot{x} \int z} \\ K_D &= K_{\dot{x} \dot{z}} \\ K_{D^2} &= K_{\dot{x} \ddot{\theta}} \\ K_{D^3} &= K_{\dot{x} q}\end{aligned}\tag{4.8}$$

Rewriting Equation 4.7 as:

$$PIDD^2D^3 = K_{D^3} \left(s^4 + \frac{K_{D^2}}{K_{D^3}} s^3 + \frac{K_D}{K_{D^3}} s^2 + \frac{K_P}{K_{D^3}} s + \frac{K_I}{K_{D^3}} \right) \frac{1}{s}\tag{4.9}$$



u- forward velocity

Figure 4.8: **Transfer Function Analysis.** The $PIDD^2D^3$ compensation was calculated to cancel the two lightly damped poles of Equation 4.4 and move the two poles at the origin to the left.

then the four numerator zeros of the $PIDD^2D^3$ controller were selected to cancel the lightly damped poles of Equation 4.4 and to draw the two poles at the origin to the left. The gain K_D^3 was selected for good speed of response. Following are the gains calculated:

$$\begin{aligned}
 K_P &= K_{XP} = -1.085 \frac{fps}{(ft \text{ error})} \\
 K_I &= K_{XI} = -.131 \frac{fps}{(ft \text{ sec error})} \\
 K_D &= K_{XD} = -2.94 \frac{fps}{fps} \\
 K_{D^2} &= K_{X\theta} = .551 \frac{fps}{deg} \\
 K_{D^3} &= K_{XQ} = .393 \frac{fps}{(deg/sec)}
 \end{aligned} \tag{4.10}$$

4.5.2. Outer Loop Simulation

With these gains as a starting point, the time responses were improved using the onboard simulation in the flight computer. Although this approach ("tweek-ing" the gains) may seem somewhat unscientific, it was appropriate for several reasons:

- Extensive use of the onboard simulation had the added advantage of helping discover many errors in the flight software before actual flight.
- Pilot comments concerning the performance and response characteristics could be better incorporated into the design.
- Working directly with the fixed point digital computer avoided the additional time and effort required to digitize and scale the continuous design.
- The transient-free switching between the velocity command and position hold modes could be developed. This is discussed in the next section.

The *PID* gains coming from this simulation are shown below:

$$\begin{aligned}
 K_{XP} &= -0.75 \frac{\text{ft/sec}}{(\text{ft error})} & K_{YP} &= -1.0 \frac{\text{ft/sec}}{(\text{ft error})} & K_{ZP} &= -2.0 \frac{\text{ft/sec}}{(\text{ft error})} \\
 K_{XI} &= -3.8 \times 10^{-4} \frac{\text{ft/sec}}{(\text{ft sec error})} & K_{YI} &= -7.6 \times 10^{-4} \frac{\text{ft/sec}}{(\text{ft sec error})} & K_{ZI} &= -1.9 \times 10^{-3} \frac{\text{ft/sec}}{(\text{ft sec error})} \\
 K_{XD} &= -3.0 \frac{\text{ft/sec}}{\text{ft/sec}} & K_{YD} &= -0.18 \frac{\text{ft/sec}}{\text{ft/sec}} & K_{ZD} &= -4.5 \frac{\text{ft/sec}}{\text{ft/sec}} \\
 K_{X\theta} &= 0.2 \frac{\text{ft/sec}}{\text{deg}} & K_{Y\phi} &= 0.0 \frac{\text{ft/sec}}{\text{deg}} & & \\
 K_{XQ} &= 2.0 \frac{\text{ft/sec}}{(\text{deg/sec})} & K_{Y\dot{P}} &= 0.0 \frac{\text{ft/sec}}{(\text{deg/sec})} & &
 \end{aligned} \tag{4.11}$$

Time responses from simulation are shown in Figures 4.9 to 4.13. These figures show the results of both the inner and outer loop designs.

4.6. Flight Test Implementation

The flight implementation of the hover control system was based on the software and flight procedures developed for the longitudinal CAS flight test. As before, the sensor data were filtered by the TR-48 analog computer before being digitized and sent to the Sperry digital computer. There were two areas where the hover controller was quite different from the longitudinal system and required new flight capabilities. The first was the inertial position and velocity data and the second was the transient-free switching required to make the transition from

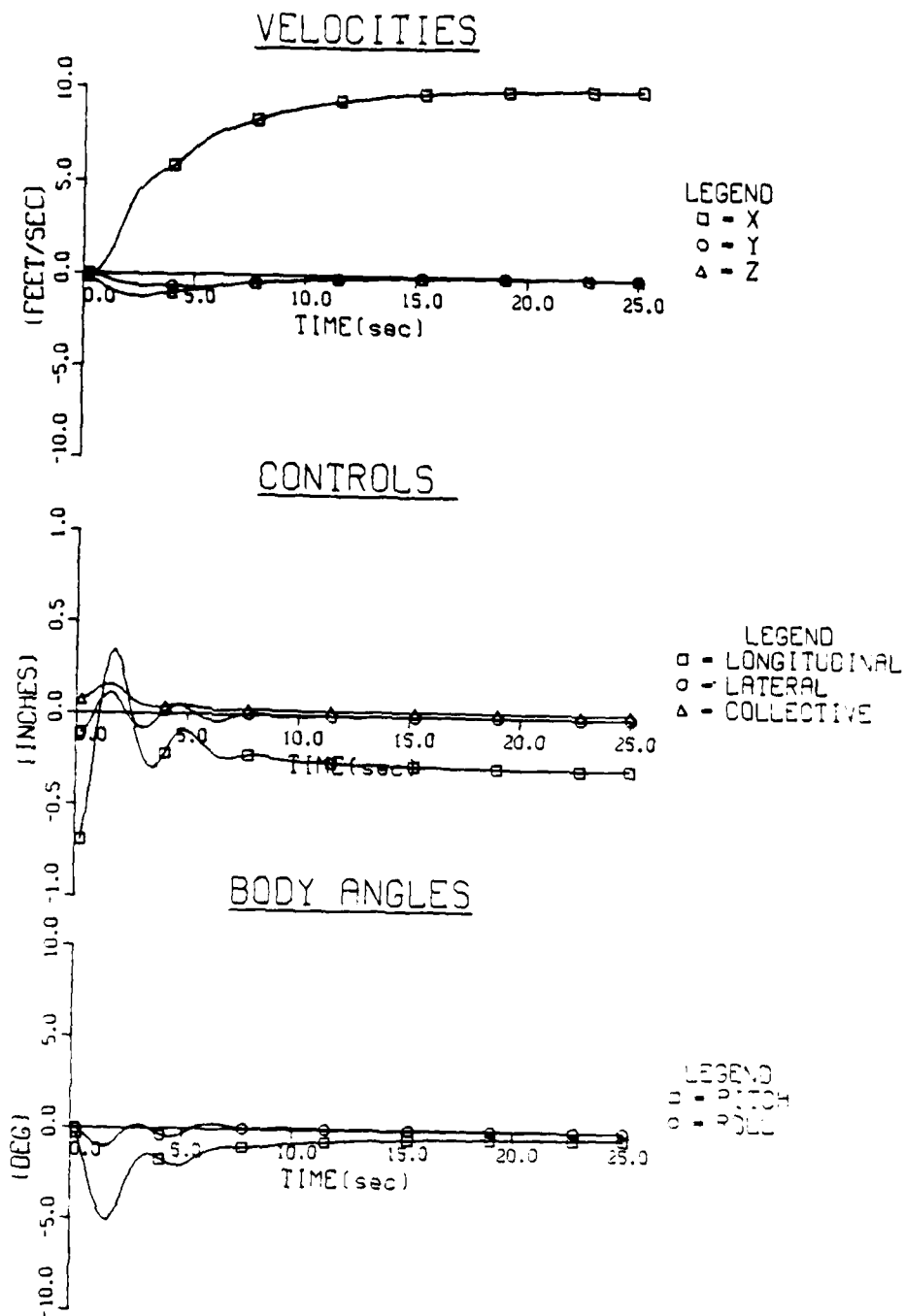


Figure 4.9: **Hover Forward Velocity Step Command in Simulation.** The poor damping is evident in the pitch angle response.

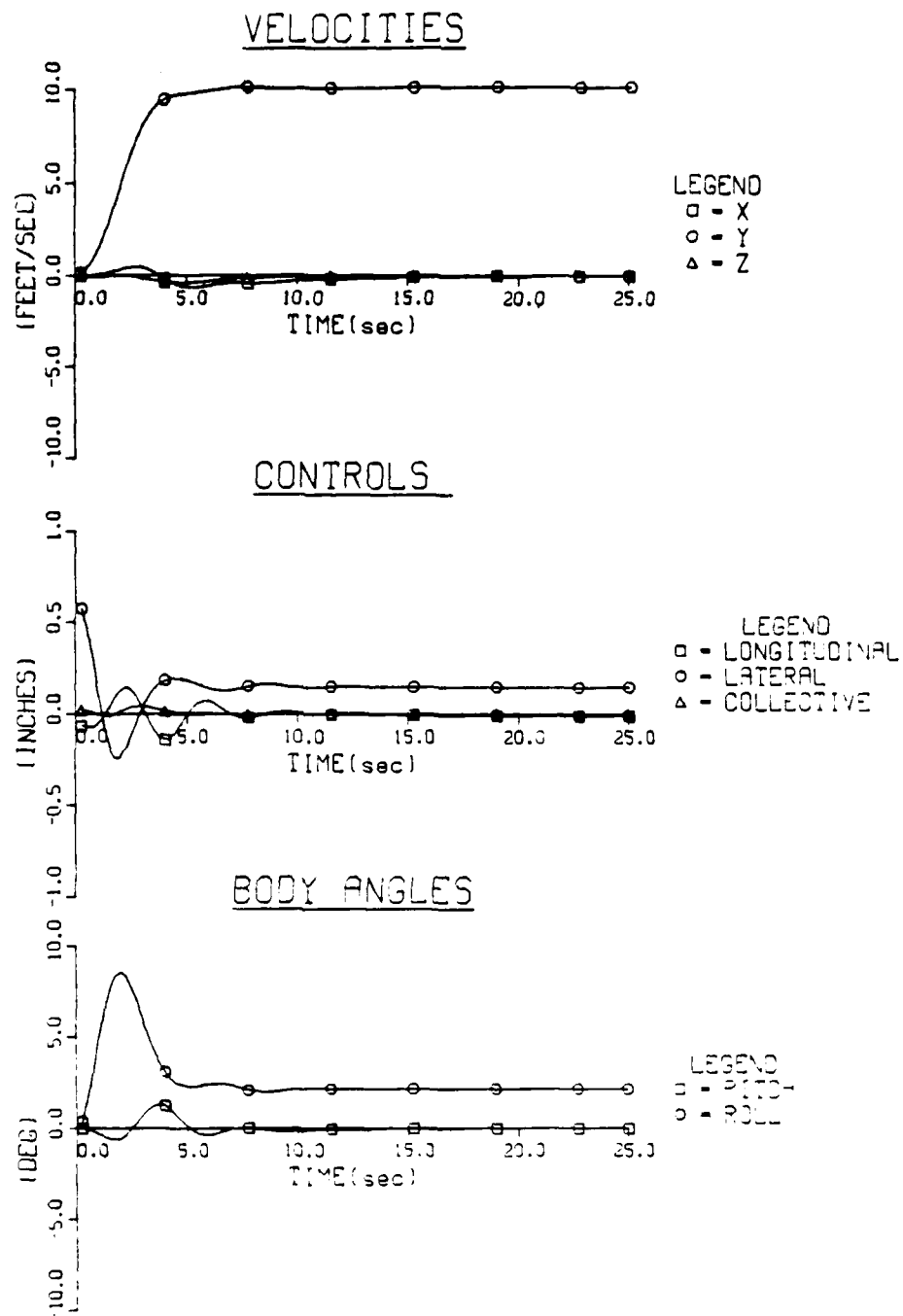


Figure 4.10: **Hover Side Velocity Step Command in Simulation.** Side velocity performance is adequate but the poorly damped pitch mode is also excited.

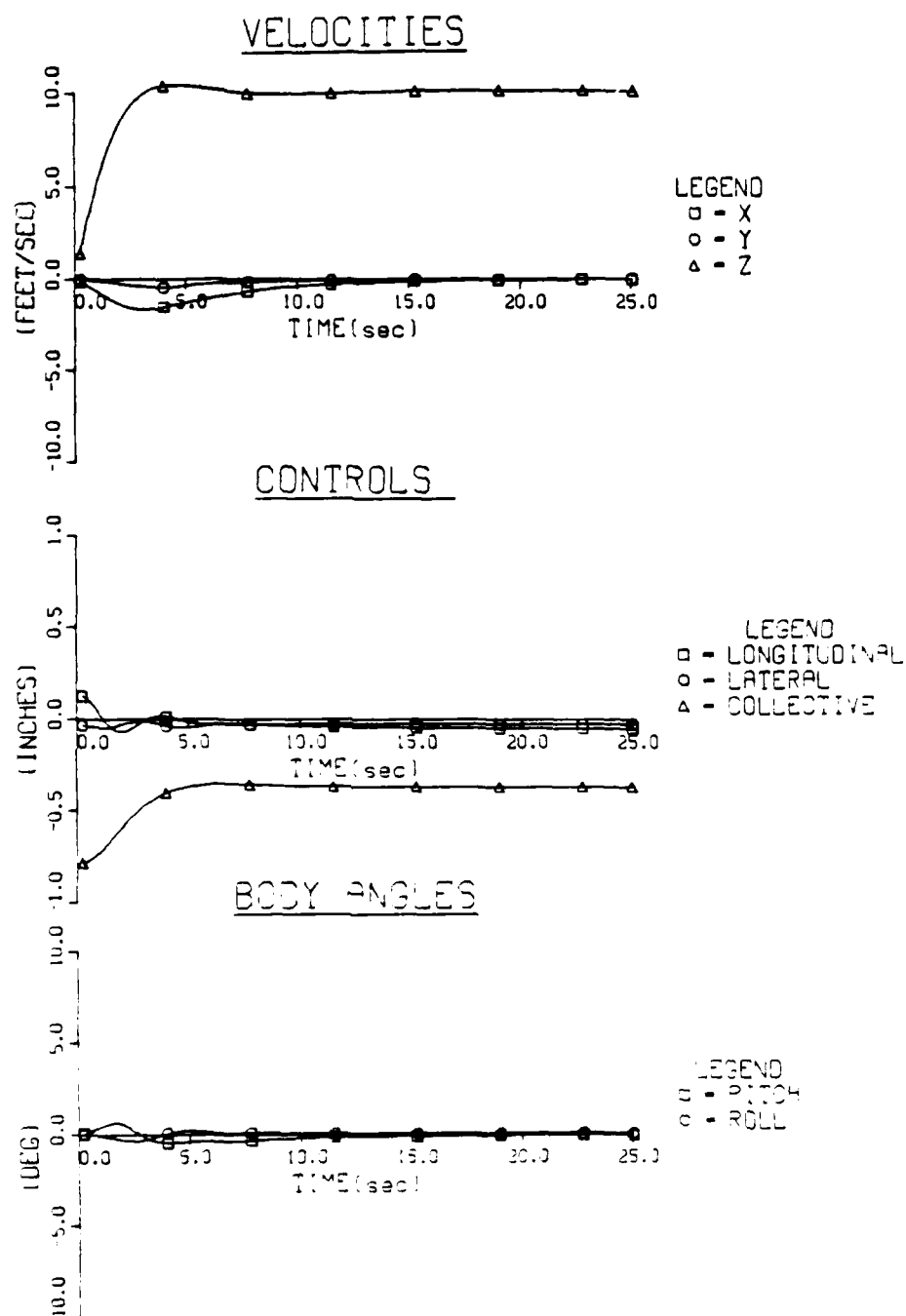


Figure 4.11: **Hover Vertical Velocity Step Command in Simulation.** The heave response is adequate and does not excite the pitch modes as strongly as the lateral velocity response of Figure 4.10

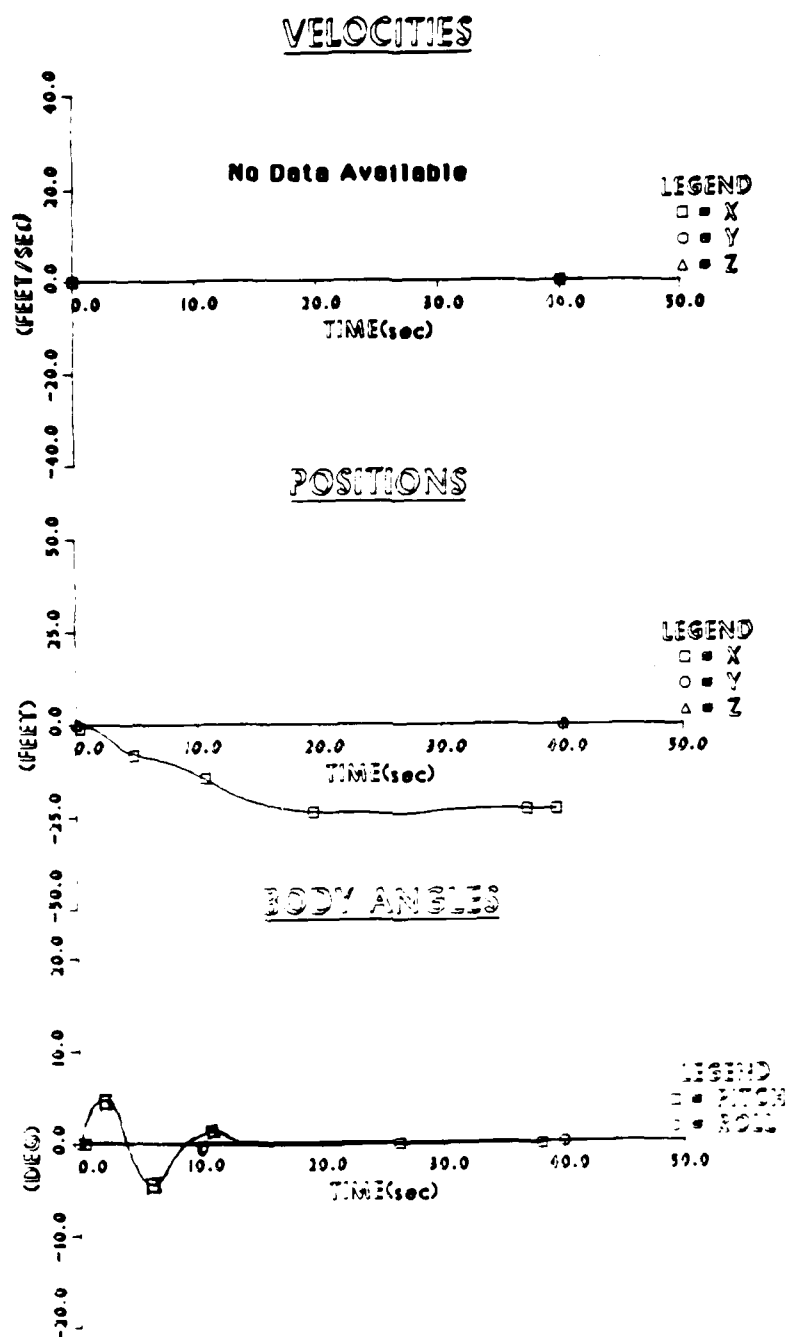


Figure 4.12: **Hover Forward Position Step Command in Simulation.** This response came from the onboard simulation and shows the the outer loop performance using the flight software.

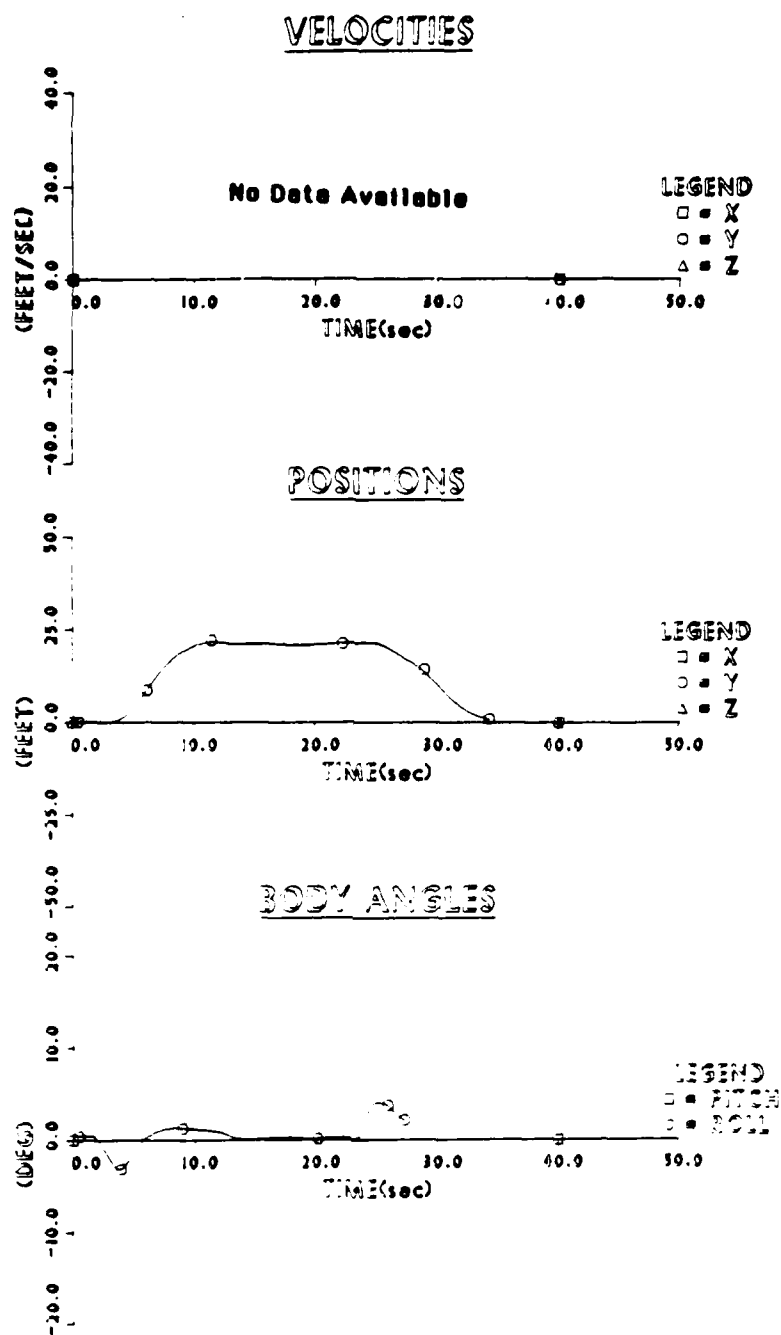


Figure 4.13: Hover Lateral Position Step Command in Simulation. Again, the flight software shows good outer loop performance.

pilot velocity command to automatic position hold.

4.6.1. Inertial Velocity and Position Data

Although the hover controller uses the inertial data (x , \dot{x} , y , \dot{y} , z , and \dot{z}) as it does the other measurements, a considerable effort was required to get these data.¹ Since the INS positions drifted so quickly and there were no inertial velocities available from the INS, an alternative source for these data was needed. The ground based tracker at Crows Landing was able to provide these data using a ground-to-air telemetry link that was specially developed for this program. The steps required to make these ground based position measurements usable by the control laws are described below:

- The laser or radar tracker measured position of the aircraft in a runway based polar coordinate system.
- These measurements of azimuth angle (Az), elevation angle (El), and range (r) were telemetered from the ground tracking station to the helicopter.
- These data, as well as tracker status information, were decoded and scaled into units common to the rest of the flight software.
- The Az , El , and range data were converted to a runway based rectangular coordinate system with a new origin located over the runway.
- These data were used with aircraft accelerometer data (rotated into the runway coordinate frame) in a second order complementary filter to estimate x , \dot{x} , y , \dot{y} , z , and \dot{z} . Figure 4.14 shows the block diagram of this complementary filter.

¹ This work was done primarily by Bill Hindson of NASA Ames

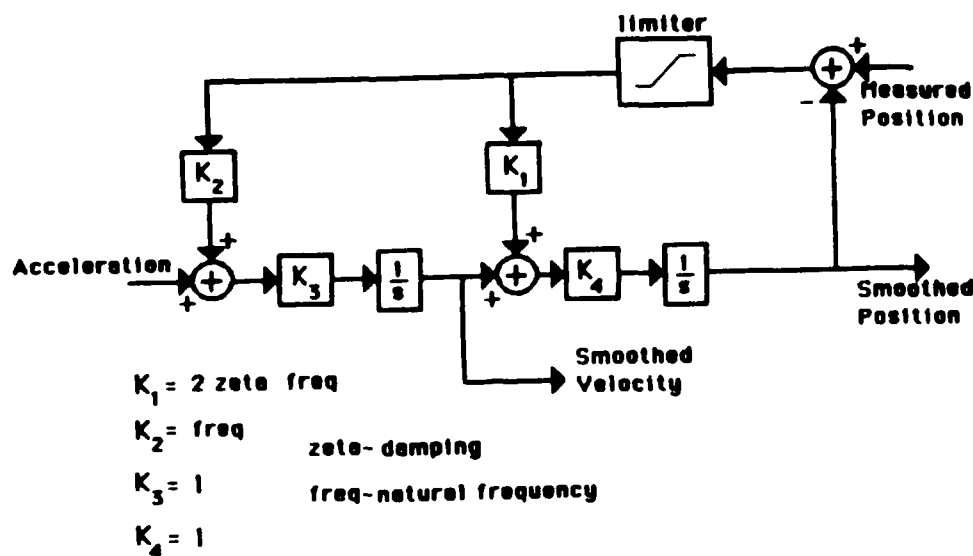


Figure 4.14: **Second Order Complementary Filter.** The filter uses acceleration and position to determine the smoothed position and velocity needed by the control law.

- These smoothed values of x , \dot{x} , y , \dot{y} , z , and \dot{z} were then rotated through the aircraft heading angle to the heading-oriented inertial frame required by the control system.
- Based on the tracker status information coming from the ground and based on data reasonableness checks, an algorithm kept the inertial data consistent during short term tracker breaklocks. For longer term breaklocks, the experimental control system was disengaged to avoid the large control motions caused by trying to follow bad data. Initially, the laser tacker was used since it provided more precise range information (1 - 2 foot accuracy). Unfortunately, the laser had frequent and unpredictable breaklocks which made the data essentially unusable in the control loop. Because of this inability to hold lock, the radar tracker was used for the flight test although its accuracy was only 5 - 10 feet.

4.6.2. Transient-Free Switching

Since this control system had both manual and automatic capability in the three body axes, a way was needed to transition smoothly among these different control modes. This task was complicated by the following characteristics of the control system:

- The pilot had the freedom to change heading at any time.
- The x coordinate of the desired hover point had to follow the x coordinate of the actual position when the pilot was commanding \dot{x} velocity. At the same time, the helicopter had to hold both y and z position in the heading inertial frame.
- Same as above in the y and z directions.
- A detent on the pilot controls was needed. If the pilot's control was less than the detent value, that axis was in position hold mode; else, the pilot was commanding a velocity.

Figures 4.15, 4.16, and 4.17 show the switching logic for the three axes. The assembly code, shown in Appendix I, implements this logic.

4.7. Flight Test Results

The hover flight testing was done at the Crows Landing test facility. The testing was limited to this location since the system required the use of the radar tracker at Crows. Unlike the longitudinal CAS control system, the hover controller was very difficult to debug and make operational. The flight testing was divided into three phases to accommodate these difficulties. The first phase developed the

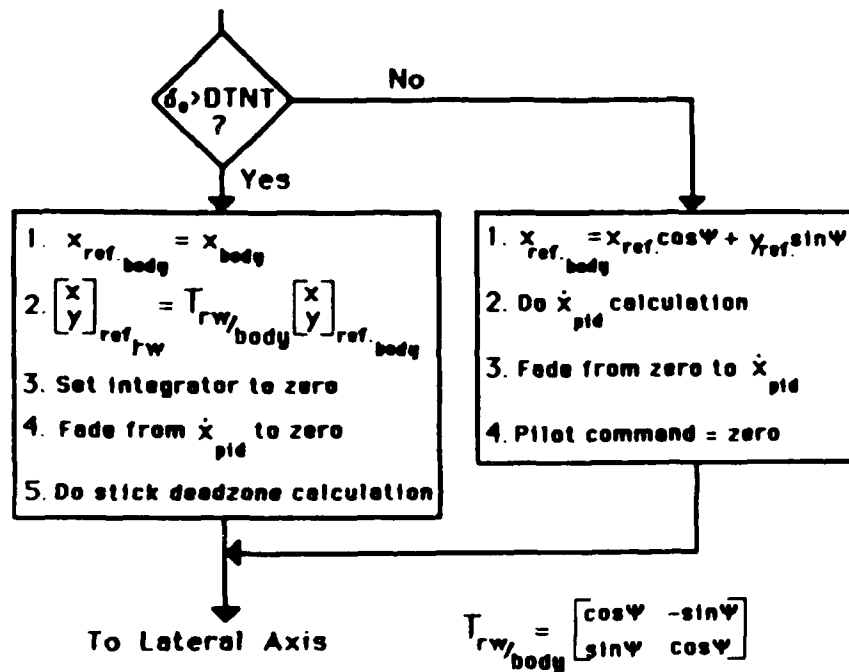


Figure 4.15: **X Axis Transient-Free Switching Logic.** The transformation from body to runway uses heading angle from the INS. The best deadzone or detent value was about .25 inches.

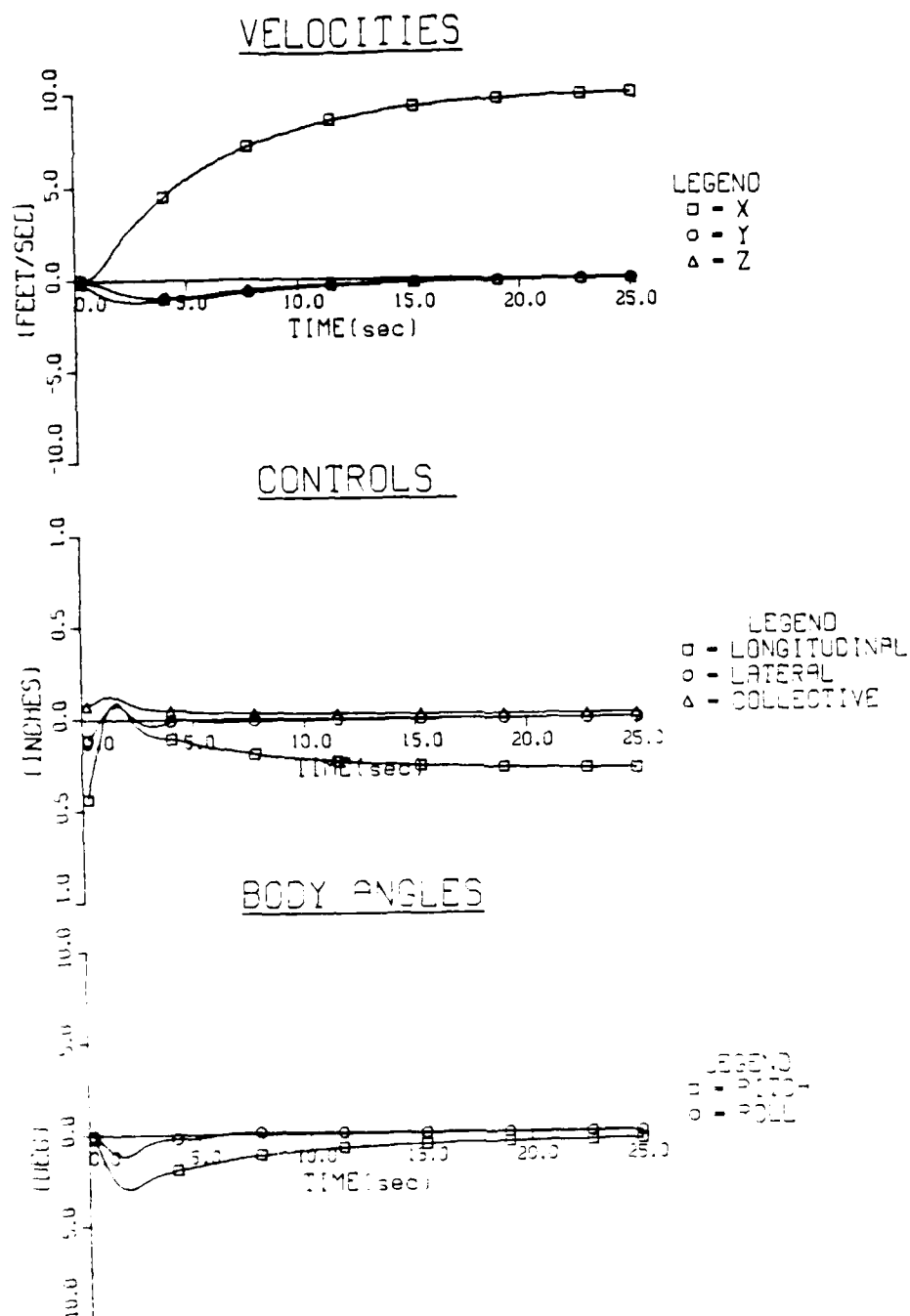


Figure 4.25: **Hover Forward Velocity Step Command in Simulation.** The pitch angle response is improved from the original design of Figure 4.9.

quicken the lateral response while in hold mode hence reducing any coupling due to action in the longitudinal axis. With these two changes to reduce the coupling, and the redesigned inner loop velocity system, the final flight testing began.

4.7.4. Final Closed Loop Flight Test in Hover

With the redesigned controller, the velocity performance was significantly improved. Figure 4.28 shows the response to a command in \dot{x} . The poor pitch damping has been eliminated and the coupling to bank angle is gone. The y axis velocity performance remains good as shown in Figure 4.29. The z velocity response remained almost identical to the original design shown in Figure 4.21. The position hold performance is also evident in these figures when the velocity commands are removed and the system reenters the position hold mode. Figures 4.30 and 4.31 confirm the good hold performance in the y and z axes but the poor damping in position hold in x . The x axis position hold dynamics are dominated by a slow, poorly damped mode ($\zeta \approx .4$ and $\omega \approx 50 \text{ sec}$). A significant amount of flight time was spent adjusting gains in the *PID* outer loops to improve this x hold performance. Shown below are the final set of outer loop gains which resulted from these efforts. Later flight tests used the integrator in the x axis *PIDD²D³* controller only when the error was less than 40 feet. This improved the damping slightly to about .5.

$$\begin{aligned}
 K_{XP} &= -20 \frac{\text{fps}}{(\text{ft error})} & K_{YP} &= -1.0 \frac{\text{fps}}{(\text{ft error})} & K_{ZP} &= -2.0 \frac{\text{fps}}{(\text{ft error})} \\
 K_{XI} &= -7.6 \times 10^{-4} \frac{\text{fps}}{(\text{ft sec error})} & K_{YI} &= -7.6 \times 10^{-3} \frac{\text{fps}}{(\text{ft sec error})} & K_{ZI} &= -1.9 \times 10^{-3} \frac{\text{fps}}{(\text{ft sec error})} \\
 K_{XD} &= -2.0 \frac{\text{fps}}{\text{fps}} & K_{YD} &= -1.0 \frac{\text{fps}}{\text{fps}} & K_{ZD} &= -4.5 \frac{\text{fps}}{\text{fps}} \\
 K_{X\theta} &= 1.0 \frac{\text{fps}}{\text{deg}} & K_{Y\phi} &= -.5 \frac{\text{fps}}{\text{deg}} & & \\
 K_{XQ} &= 3.0 \frac{\text{fps}}{(\text{deg/sec})} & K_{YP} &= -.5 \frac{\text{fps}}{(\text{deg/sec})} & &
 \end{aligned}
 \tag{4.12}$$

$$F_{min} = \begin{bmatrix} 0 & 1 & 0 & 0 & 0 & 0 \\ -17.93 & -4.90 & 0 & 0 & 0 & 0 \\ 0 & 0 & -1.98 & 0 & 0 & 0 \\ 0 & 0 & 0 & -8.15 & 0 & 0 \\ 0 & 0 & 0 & 0 & 0 & -6.31 \end{bmatrix}$$

$$K_{min} = \begin{bmatrix} -.035 & -.050 & -.040 & -.56 & 2.18 & .216 & 3.23 & -74.7 \\ -.037 & -.74 & .071 & -.28 & -1.57 & -7.63 & -19.7 & 169.0 \\ -.58 & .140 & -.23 & .19 & 29.2 & 16.05 & 1.30 & -100.3 \\ -.45 & .0079 & 1.45 & .068 & 6.52 & 1.20 & 2.57 & 7.16 \\ .018 & -.0058 & -.003 & -.029 & 3.4 & -.66 & 14.03 & 8.32 \end{bmatrix}$$

$$C_{min} = \begin{bmatrix} .07 & .054 & -.0776 & -.0036 & -4.61 \\ .026 & -.0045 & -.029 & .022 & -.52 \\ .44 & -.021 & -.062 & .00078 & -.42 \end{bmatrix}$$

$$N = \begin{bmatrix} -.048 & -.0098 & -.0024 \\ .007 & -.0079 & .0021 \\ 0.0 & -.0034 & .0059 \end{bmatrix}$$

Closed Loop Eigenvalues				
Real Part	Imag Part	Damping	Freq(rad/sec)	Freq(Hz)
-40.2	0.0	1.0	40.2	6.39
-40.01	0.0	1.0	40.01	6.367
-39.99	0.0	1.0	39.99	6.365
-6.007	0.0	1.0	6.007	.956
-2.37	2.70	.66	3.59	.57
-2.37	-2.70	.66	3.59	.57
-.94	2.13	.40	2.33	.37
-.94	-2.13	.40	2.33	.37
-.60	1.51	.37	1.62	.26
-.60	-1.51	.37	1.62	.26
-.55	.48	.75	.73	.116
-.55	-.48	.75	.73	.116
-.62	.402	.84	.74	.117
-.62	-.402	.84	.74	.117
-.90	0.0	1.0	.90	.14
-.17	0.0	1.0	.17	.027

Performance Index Data		
Outputs or Controls	Units	Weighting
u	ft/sec	5×10^3
v	ft/sec	5×10^3
w	ft/sec	5×10^3
p	rad/sec	1×10^5
q	rad/sec	1×10^5
r	rad/sec	1×10^5
δ_e	inches/sec	1×10^5
δ_c	inches/sec	1×10^5
δ_a	inches/sec	1×10^5
\dot{u}	ft/sec ²	5×10^3
\dot{v}	ft/sec ²	5×10^3
\dot{w}	ft/sec ²	5×10^3
δ_e	inches	1×10^3
δ_c	inches	1×10^3
δ_a	inches	1×10^3

Figure 4.24: **Redesigned Hover Compensator.** Only the columns of K associated q and θ and the row of C corresponding to longitudinal control (δ_e) are changed from the initial design of Figure 4.7.

good time responses. In this case, the measurement noise characteristics were left unchanged and an unrealistically high value of the vertical velocity disturbance was used. Specifically, the vertical gust root mean square (rms) was increased from 2.3 ft/sec to 10 ft/sec. Vertical gust was selected since it affects the pitch angle more strongly than the other disturbances. With this one change, the RSANDY program was used to find a new compensator. To speed up the convergence in the RSANDY program, only the columns of the K_{min} matrix associated with measurements of q and θ , and the row of C_{min} associated with the longitudinal control were allowed to vary. This approach was also logical since we wished to keep the vertical and lateral axes unchanged from the first design. The redesigned compensator is shown in Figure 4.24 and can be compared to the initial design in Figure 4.7. Figure 4.25 shows the simulation response of the redesigned velocity command inner loop with the improvement in pitch damping compared to the initial design shown in Figure 4.9. Figures 4.26 and 4.27 show that the y and z responses were essentially unchanged by the redesign.

Since there was nothing in the simulation to suggest that there would be coupling from \dot{z} command to ϕ , the approach to solving this problem was based on the experience gained thus far. Two changes were made to the controller which would have to wait for flight to be evaluated. The first change was the zeroing of the feedforward gain from \dot{z} command to δ_a in the N matrix of Figure 4.3. This was a logical approach to solving the problem since the N matrix was highly dependent on accurate modeling and the longitudinal flight test had already shown the model to be lacking. The other change made to solve this coupling was to include nonzero values for $K_{Y\phi}$ and K_{YP} in the lateral PID outer loop. This change was made to

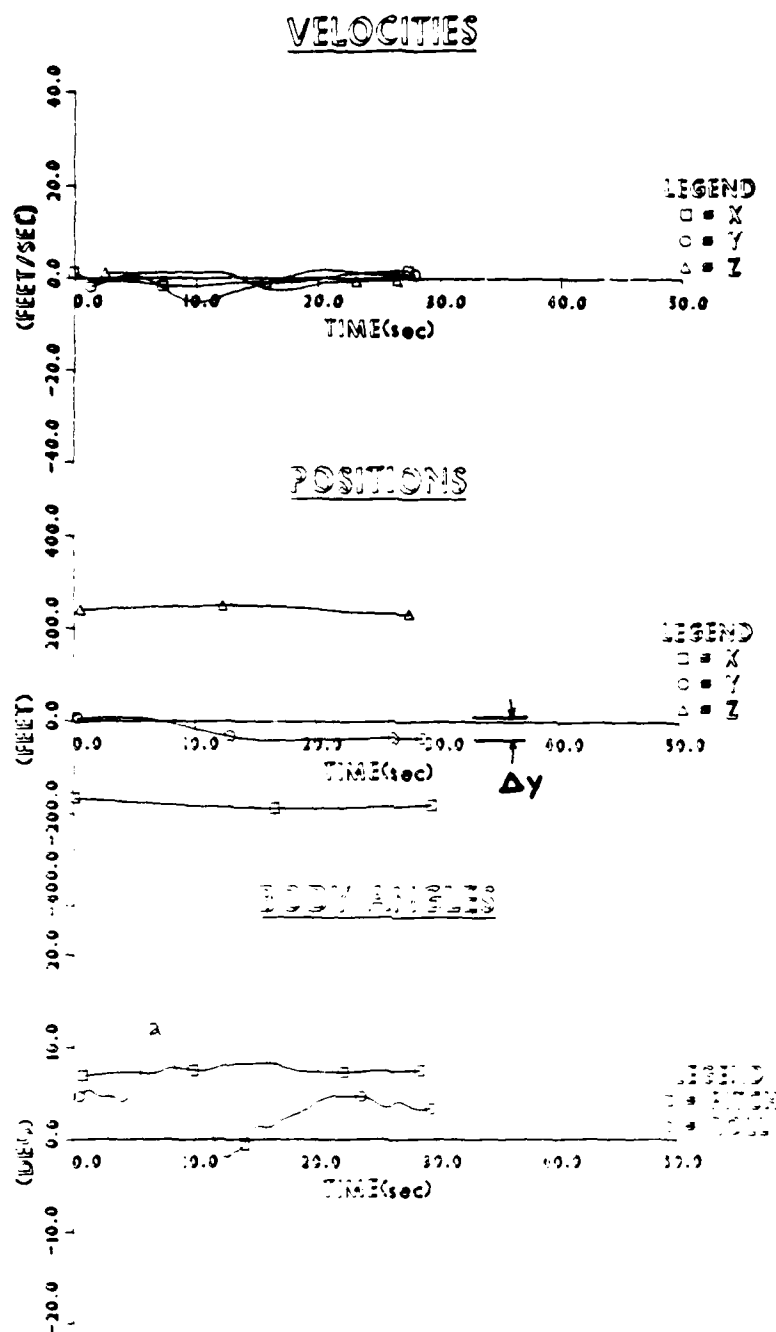


Figure 4.23: Preliminary Lateral Position Step Command in Flight. The y position hold performance is well damped and similar to the simulation of Figure 4.13.

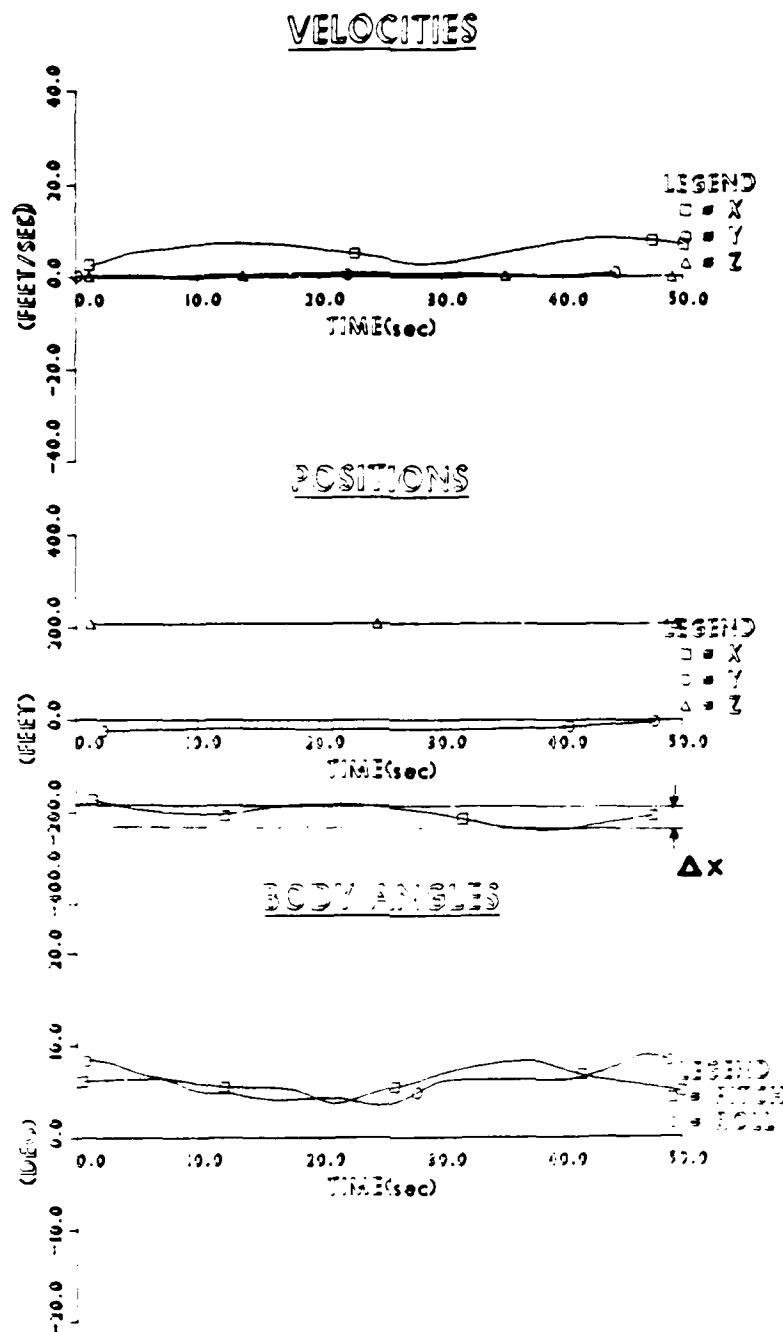


Figure 4.22: Preliminary Forward Position Step Command in Flight. The x position damping is very poor ($\zeta \approx .1$), unlike the near critical damping of the simulation shown in Figure 4.12.

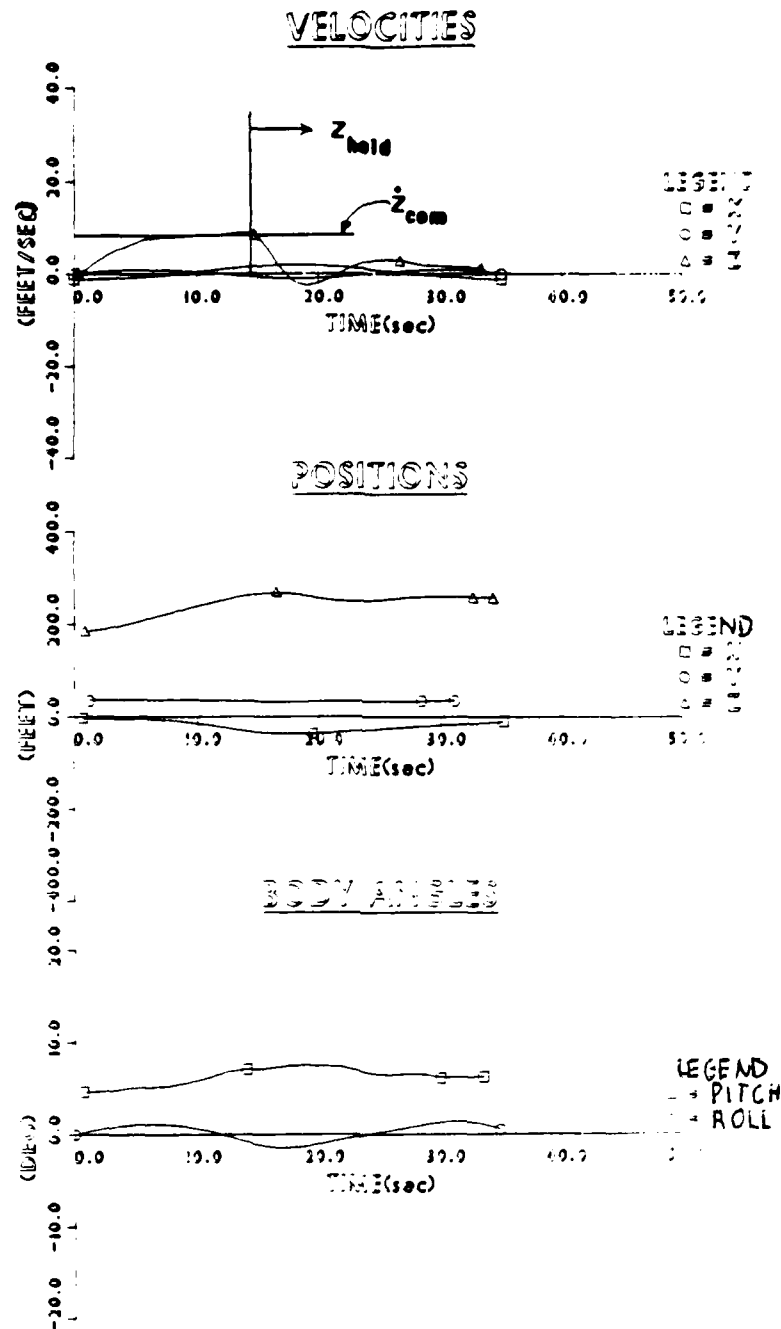


Figure 4.21: **Preliminary \dot{z} Flight Response.** The 5 second time to steady state matches the simulation shown in Figure 4.11.

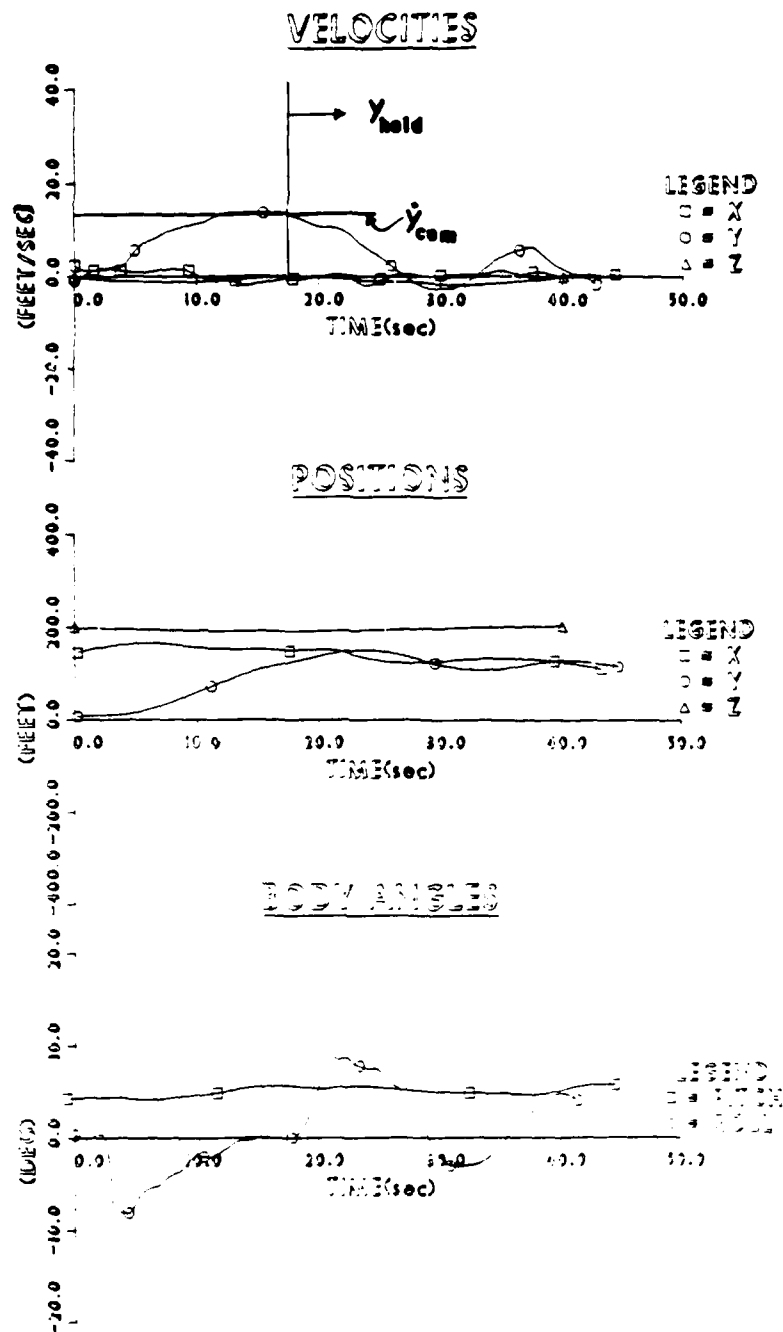


Figure 4.20: **Preliminary \dot{y} Flight Response.** The \dot{y} response is well behaved and similar to the simulation results of Figure 4.10. The peak roll angle is about 8 degrees for both responses to a command of about 10 ft/sec.

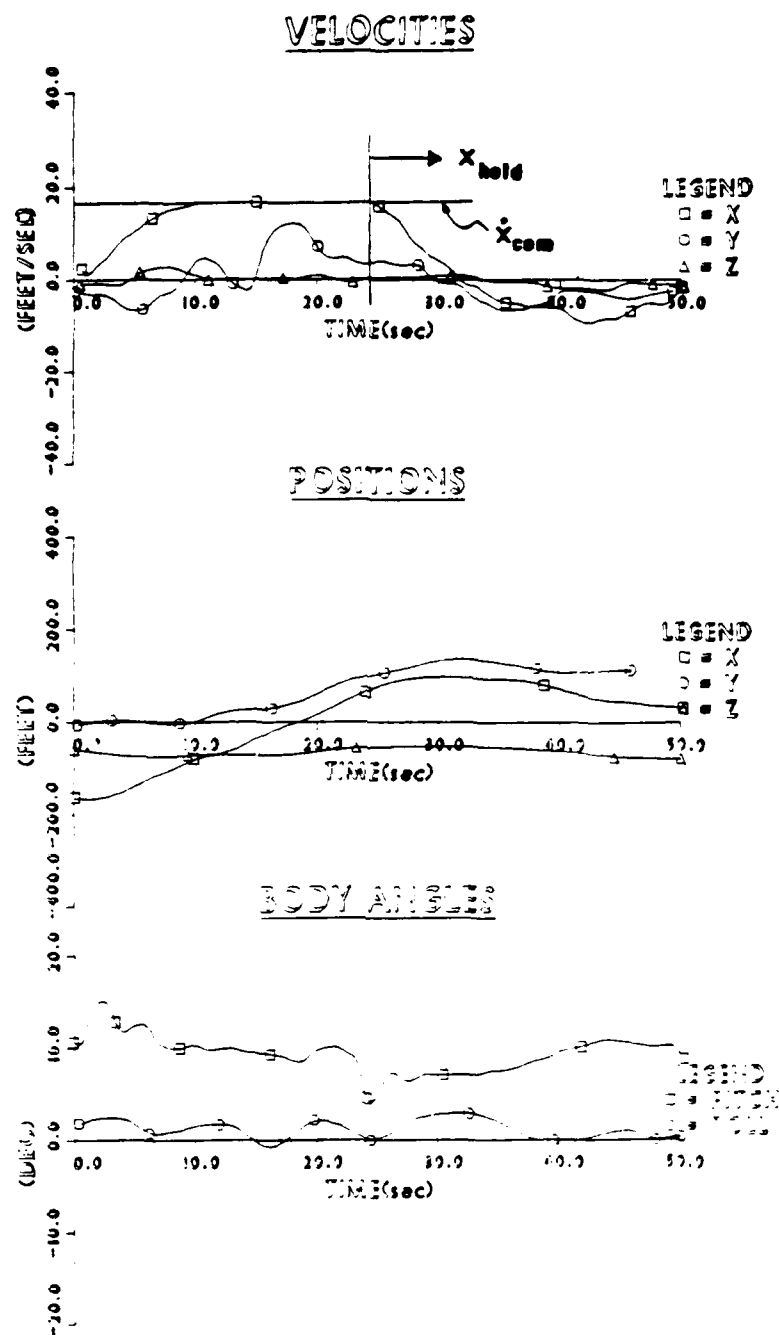


Figure 4.19: Preliminary \dot{x} Flight Response with Pitch Roll Coupling. With the instability of Figure 4.18 corrected, the roll coupling, shown here, was discovered.

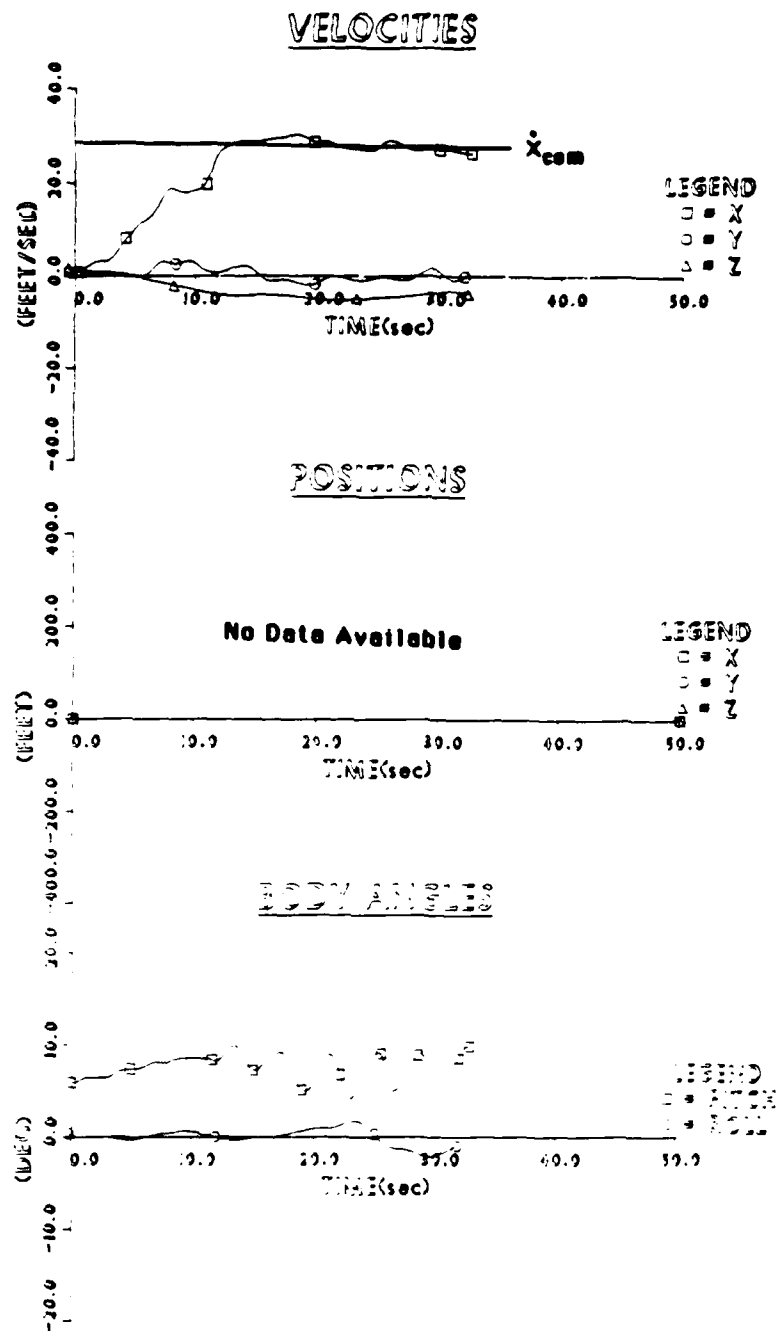


Figure 4.18: Preliminary \dot{x} Flight Response with Pitch Oscillation. The poorly damped simulation response of Figure 4.9 became unstable in flight as the pitch angle shows. The decoupling using the outer loops worked well.

system in flight. Figure 4.18 shows the flight results with the extremely poor x axis performance. After a redesign of the velocity inner loop system, described in the next section, another problem was found. There was unacceptable coupling between the x and y axes. The coupling, evident in Figure 4.19, was manifested as roll oscillations resulting from the \dot{x} command. The next section also describes the approach taken to solve this pitch to roll coupling problem. The coupling was one way, however, as seen in Figure 4.20 where the response to a step in \dot{y} is quite acceptable and similar to the simulation results of Figure 4.10. The \dot{z} command capability is also quite good as Figure 4.21 shows. The x position hold performance of Figure 4.22 was very poor due to the low damping ($\approx .1$). y position (Figure 4.22) was much better damped and faster than x . The z position hold performance was very good with vertical position changes of less than 10 feet during the velocity commands of Figures 4.19, 4.20, and 4.21. Use of the radar tracker data in the inner loops, which was considered risky due to its complexity, worked well throughout the flight test.

4.7.3. Hover Controller Redesign

The redesign of the system was necessitated by bad performance in two modes. First, the x velocity response was slightly unstable in flight. The other problem was the coupling from x velocity command to roll angle. The first problem was handled by redesigning the inner loop velocity control system in order to slow the longitudinal response. This redesign was first attempted by changing the weighting matrices in the RSANDY program to get a better damped longitudinal response. This approach did not work so the technique of Section 3.4.1 was used. Section 3.4.1 described using an arbitrary set of measurement spectral densities to achieve

new capabilities needed by the hover controller including data uplink capability and complementary filtering to get smooth inertial data. The second phase included preliminary flight test which discovered poor velocity performance which necessitated a redesign of the velocity inner loop. The final phase of the flying evaluated the redesigned control system.

4.7.1. Support Systems Development Flying

The complexity of the hover controller required that essentially all the aircraft systems and all the ground support equipment be working in order to exercise the system. A number of flights was required just to ensure that the uplink system and the associated complementary filters were producing good inertial data. Once these systems were operating correctly, the flight testing continued with checks of the mode switching and transient suppression logic while using the real data coming from the complementary filters. It was while doing this work that the laser tracker's poor ability to hold lock was discovered and the decision was made to go with the less accurate radar tracker.

4.7.2. Preliminary Closed Loop Flight Test in Hover

Preliminary closed loop testing included velocity step commands in the three axes and changes in desired position while remaining in the hover hold mode. These closed loop tests confirmed what the longitudinal CAS tests had already shown. The flight responses were less damped than the simulations had predicted. In other words, we couldn't achieve as high a bandwidth in flight as in simulation. This was most evident in the x axis where the well damped velocity response in the simulation (Figure 4.9) turned into a neutrally stable or slightly unstable

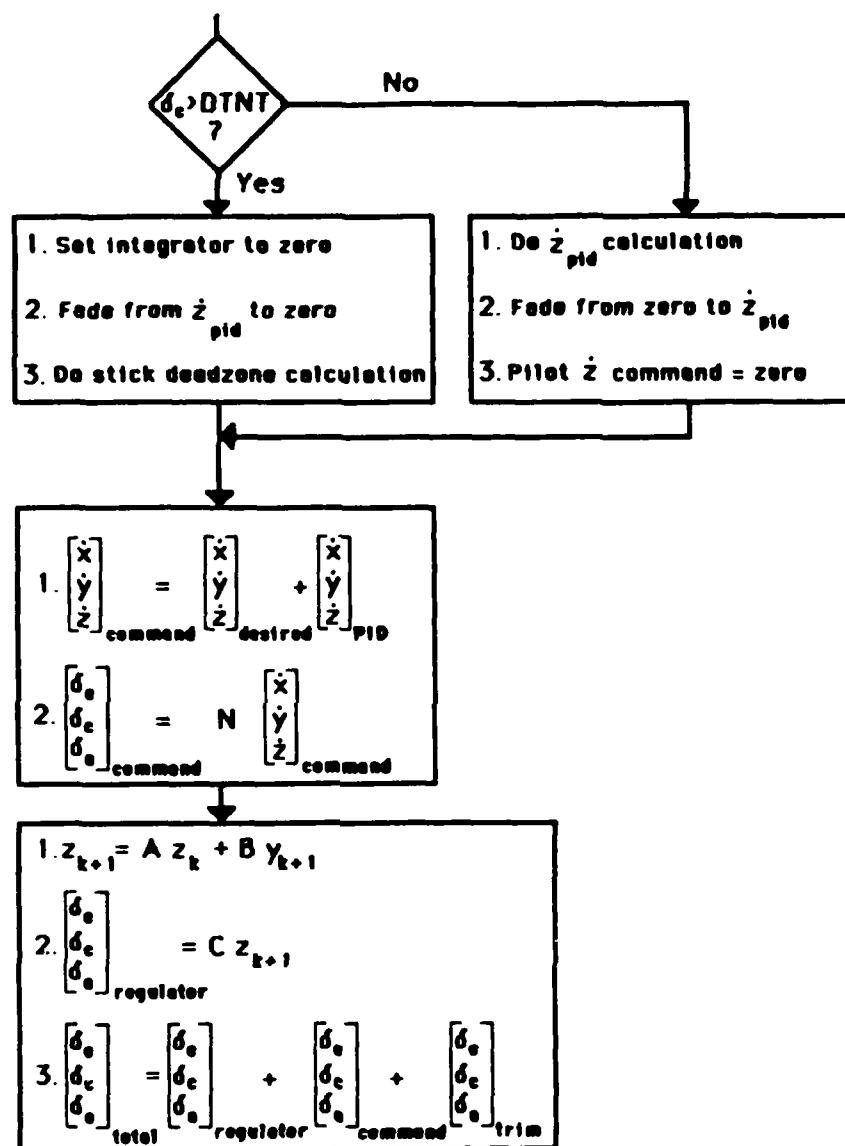


Figure 4.17: **Z Axis Transient-Free Switching Logic.** This figure also shows the rest of the hover controller which was shown in Figure 4.3.

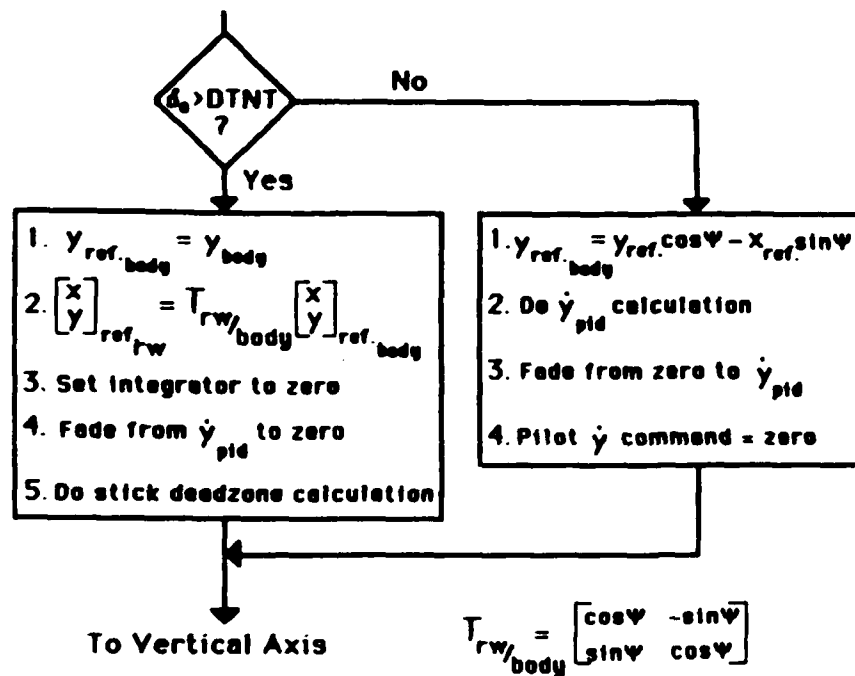


Figure 4.16: **Y Axis Transient-Free Switching Logic.** The switching logic for the x and y axes was identical. The best detent was .25 inches.

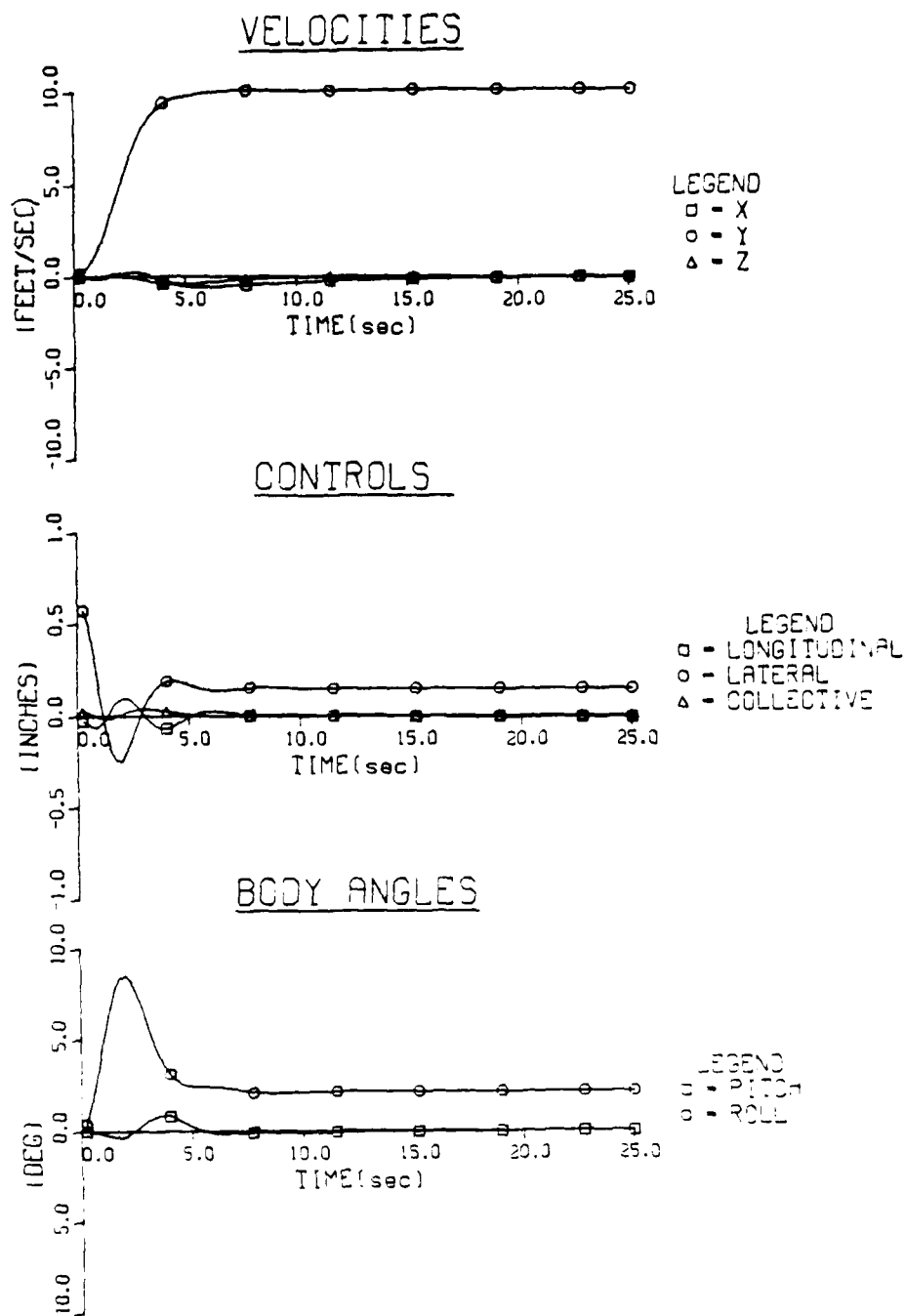


Figure 4.26: **Hover Side Velocity Step Command in Simulation.** The response is nearly identical to the original design of Figure 4.10.

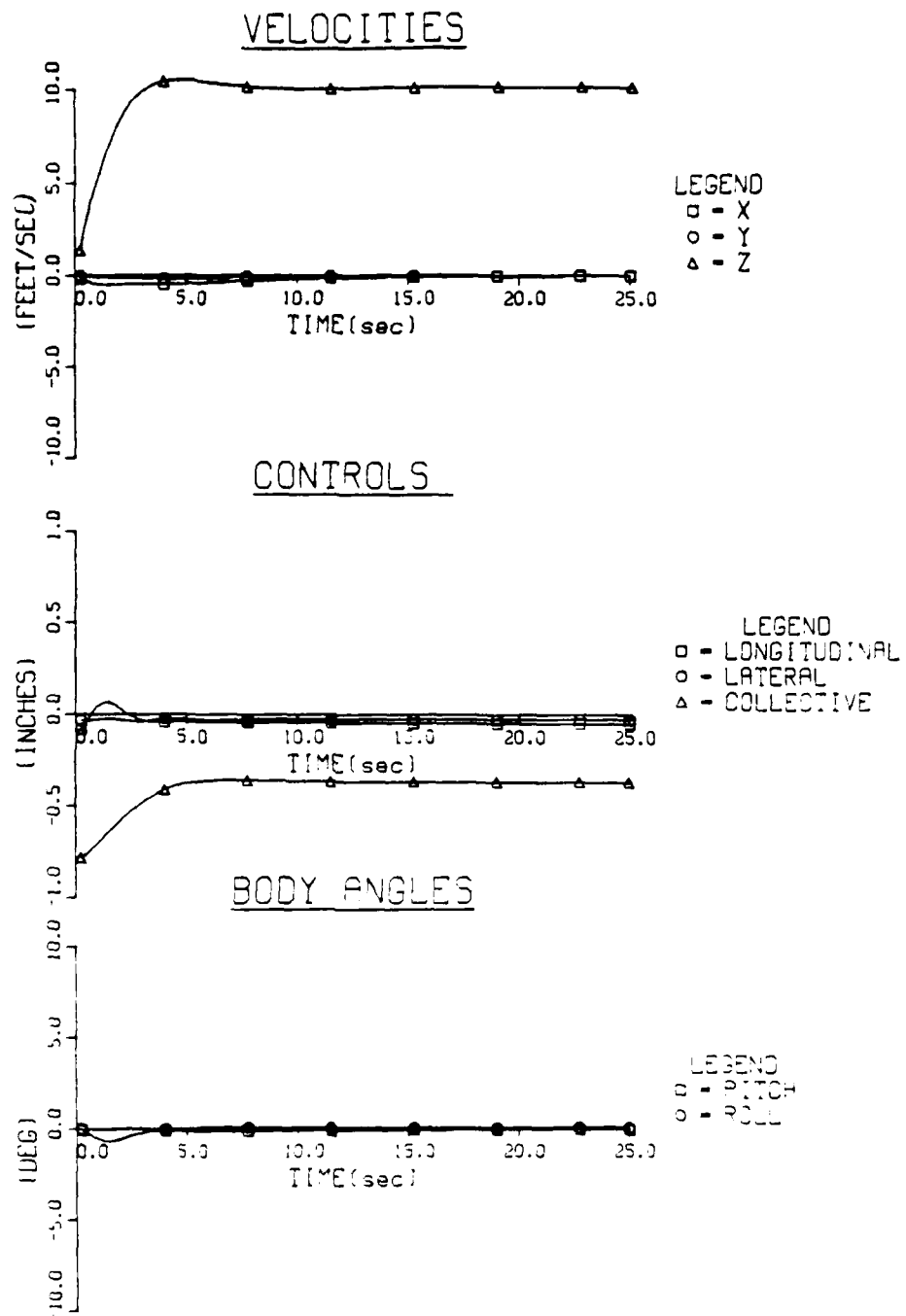


Figure 4.27: **Hover Vertical Velocity Step Command in Simulation.** The response is nearly identical to the original design of Figure 4.11.

4.8. Summary of Results of the Hover Controller Design

As with the longitudinal CAS, the discussion of results is separated into two groups:

- the effectiveness of the methodology
- the flight test results

The hover controller emphasized the usefulness of the design methodology for a more complicated control system. To have used classical incremental loop closures to do this design would probably have taken longer or would have required more specific experience in helicopter control systems than I had. This task also showed the advantage of using a modern control inner loop to modify the open loop plant in such a way as to increase the physical intuition for the design engineer. The increased physical intuition made classically designed outer loops simpler. In this case, the plant was changed from control motion in, measurement out to desired output in, actual output out. This change simplified the selection of the outer loop control structure and made the outer loop gains more intuitive. Figure 4.3 showed these advantages. This task also emphasized the relative speed and ease with which design iterations can be made on MIMO systems. When the first design of the hover controller was found unacceptable in flight, the redesign described in Section 4.7.3 was done in only 2 - 3 days which avoided delays in the flight testing. As with the longitudinal CAS design, the analysis tools developed to use the methodology (described in the various appendices) were sufficient but their

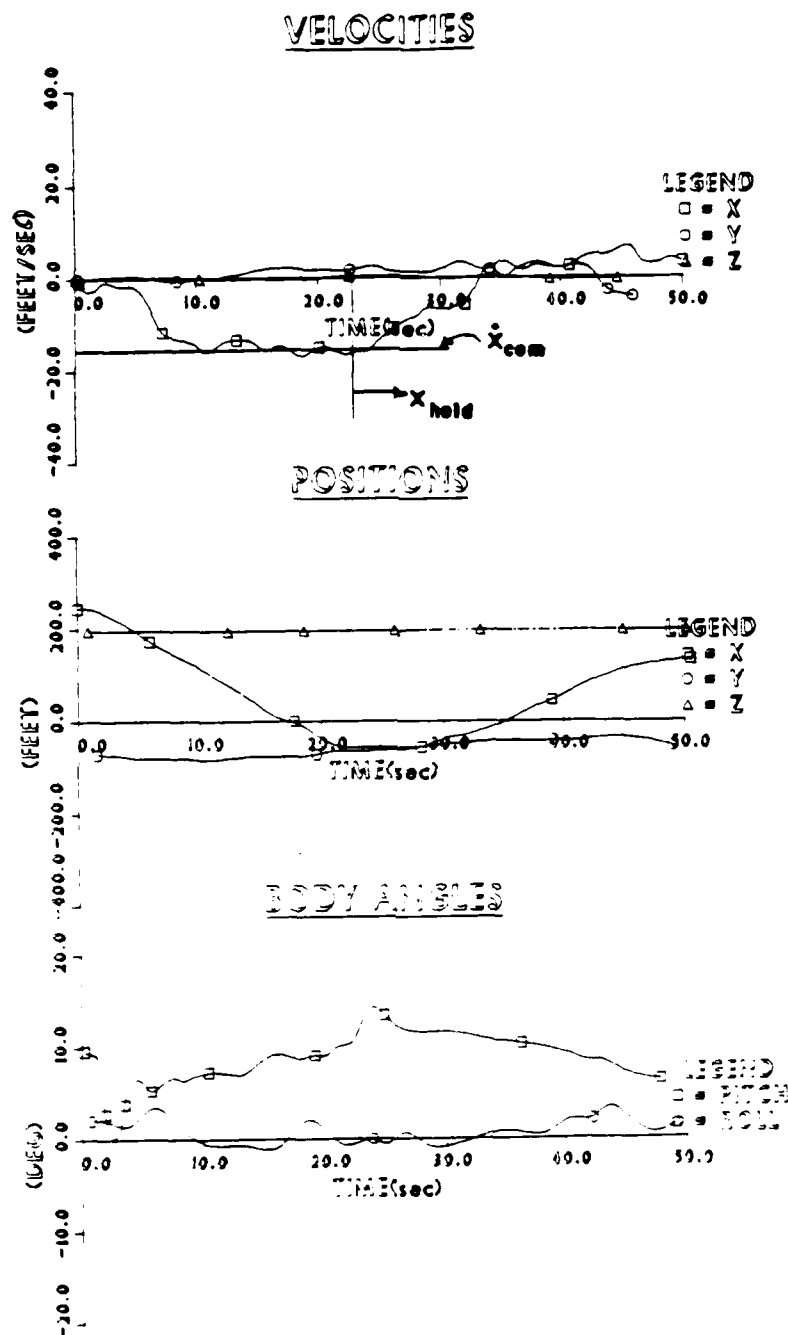


Figure 4.28: **Final \pm Flight Response.** The instability in pitch (Figure 4.18) and the pitch roll coupling (Figure 4.19) are gone but the pitch angle damping is still less than the simulation response of Figure 4.25.

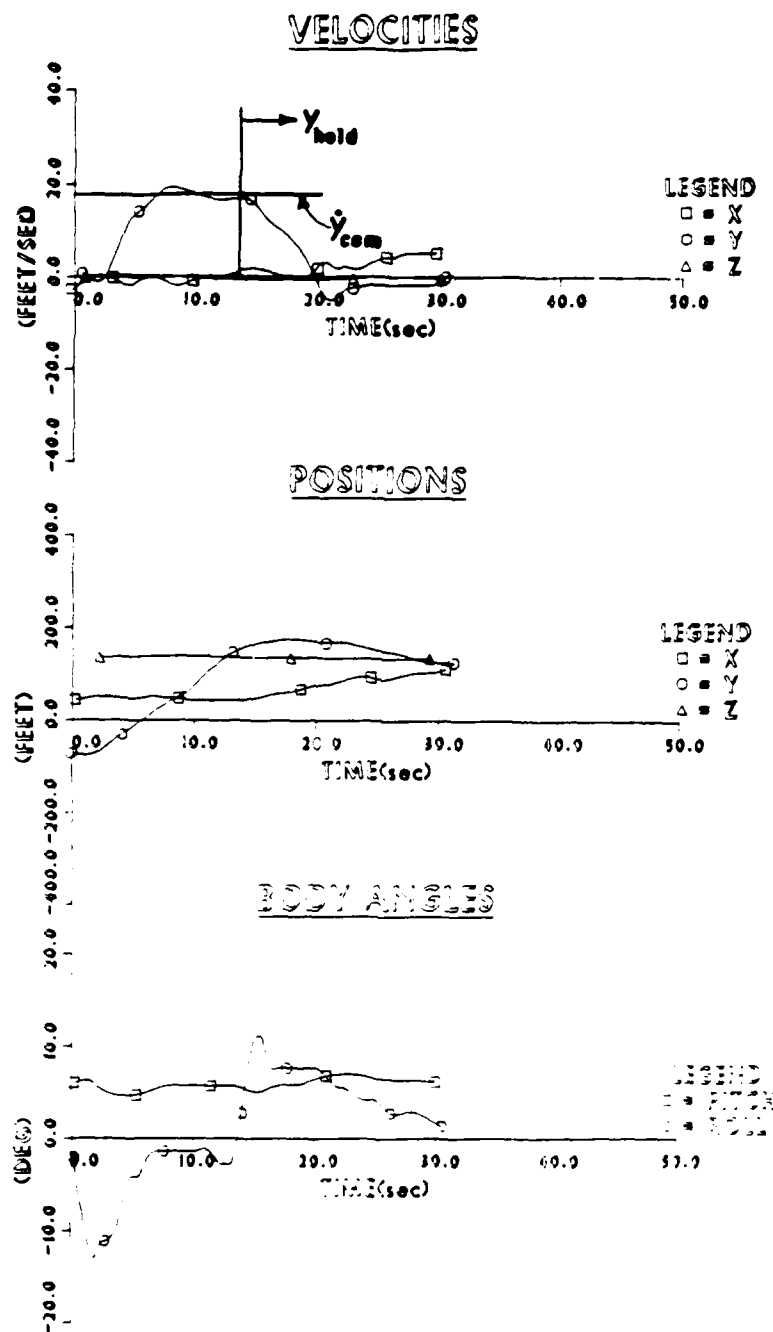


Figure 4.29: **Final y Flight Response.** The y response is little changed from the first flight test results of Figure 4.20.

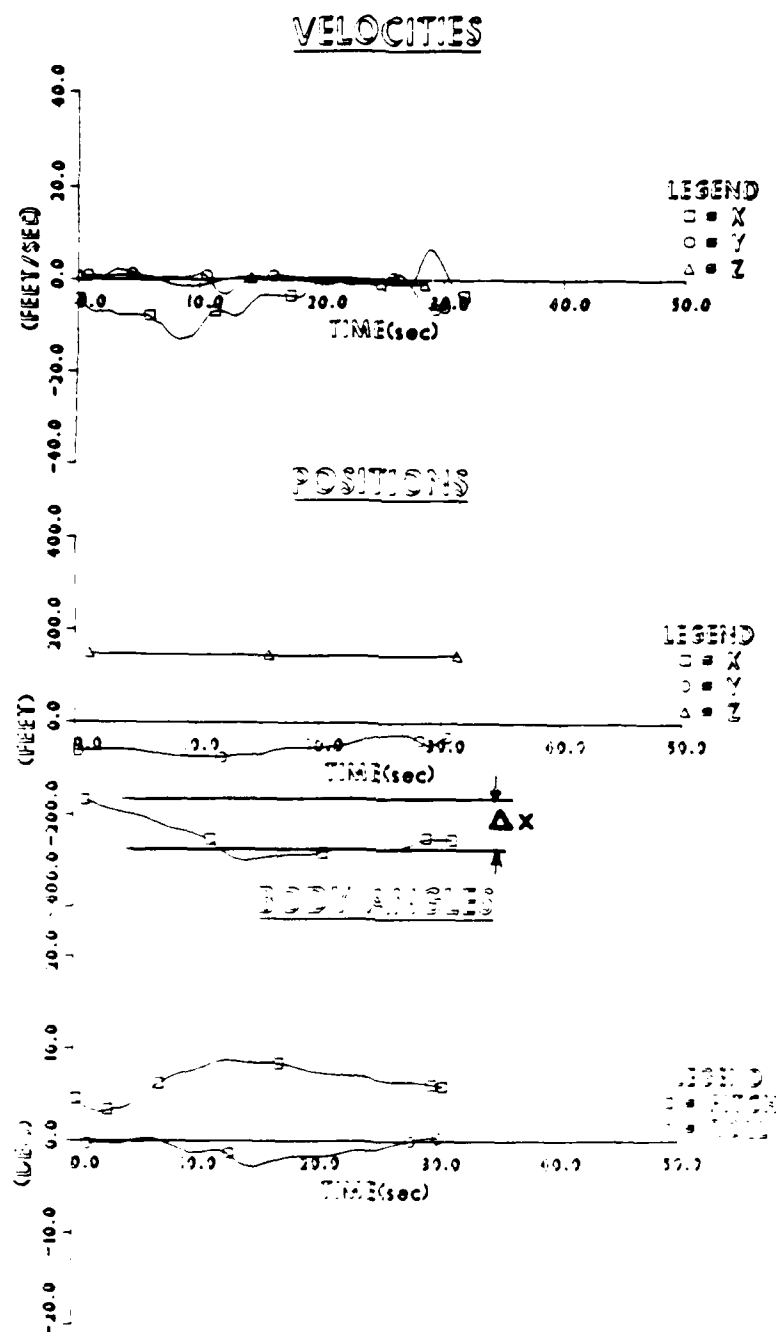


Figure 4.30: **Final Hover Forward Position Step Command in Flight.** The performance is much improved from Figure 4.22 but the damping of $\approx .4$ is still not good enough for operational use.

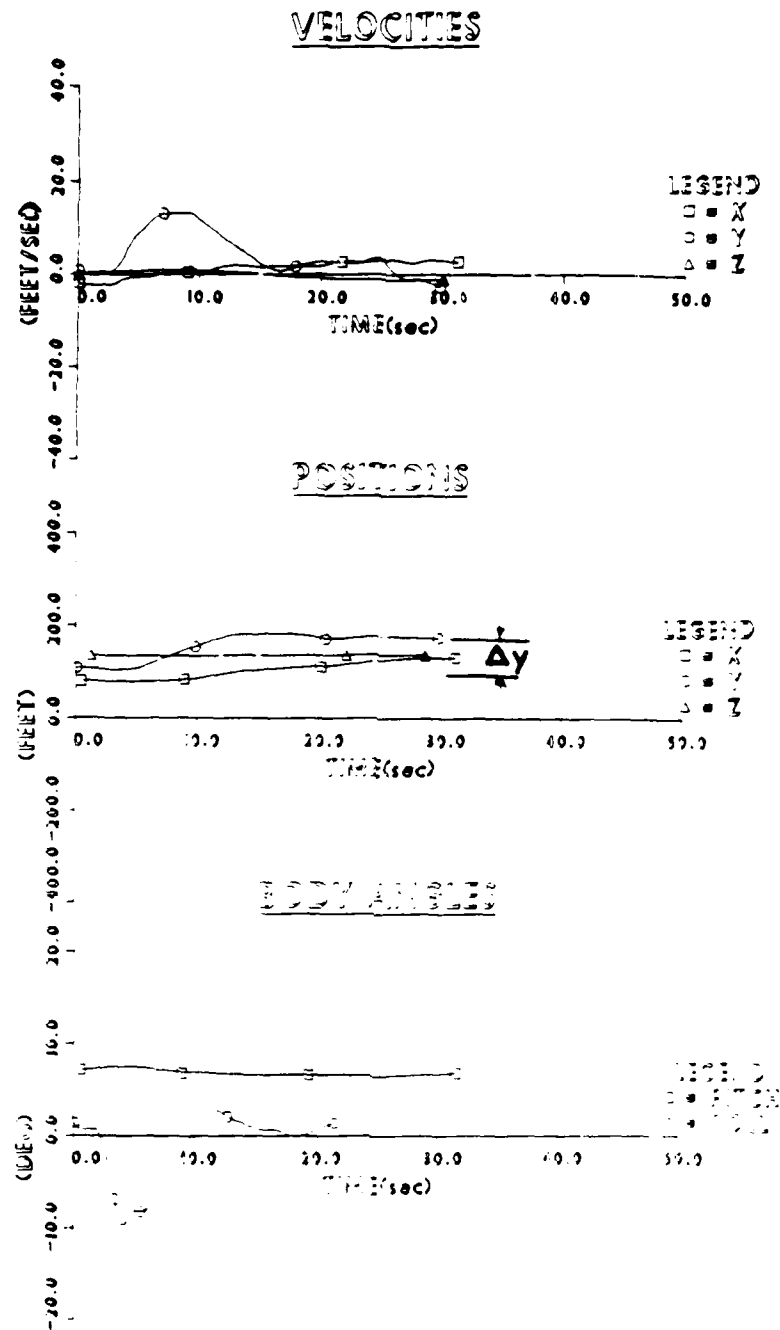


Figure 4.31: **Hover Lateral Position Step Command in Flight.** The lateral position response is adequate and little changed from the first tests of Figure 4.23.

"user friendliness" needed improvement.

In flight test, the hover controller was fairly successful. Many advanced helicopter or VTOL airplane designs call for a translational velocity control(TVC) system such as was tested here. Normally the evaluations of these concepts seldom leave the simulators to address the hardware and software difficulties of flight implementation. This test reemphasized two of the important difficulties of TVC systems, the inertial position/velocity sensor and the human factors involved. The primary contribution of this work was the development of a flexible TVC system where these type issues can be studied. Specifically, this system showed good velocity command performance in all three axes, excellent hold performance in the lateral and vertical axes, and marginally acceptable hold performance longitudinally. The switching logic worked well from a control viewpoint but the pilots who flew the system commented on the need for a better indication of switching from hold mode to velocity command mode in each axis.

Chapter 5.

Conclusions

The conclusions are separated into those applicable to the design methodology and those associated with the flight tests.

5.1. Methodology

- The process of scaling and using the modal input/output measures is an effective way to reduce the order of the compensator.
- The scaled block minimal realization of the compensator is useful in identifying unimportant measurements and controls.
- The decoupling feedforward matrix depends heavily on an accurate model so practical designs will usually require some sort of integral control. For very poor models, integral control alone should be used for implementing output commands.
- The software tools were adequate for application of the methodology.
- Both "modern" and "classical" control techniques are important for MIMO control system design. The specific application determines the appropriate techniques to use. In this research, the use of a modern control inner loop

with classically designed outer loops was a useful approach for the hover controller.

5.2. Flight Tests

- Although requiring some change of pilot technique (retraining), the decoupled velocity and climb rate controller was well received by the pilots who flew it.
- The hover controller performed adequately as a translational velocity command system, had good position hold capability in the vertical and lateral axes, but its hold performance in the longitudinal direction was marginal.
- Integral control was crucial to achieve decoupled control for both the cruise and hover control systems.

5.3. Lessons Learned

Finally, two "lessons learned" (or relearned) during this research should be emphasized, even though they may seem obvious. First, there is no substitute for experience. For this methodology, experience was important in:

- selecting the correct units for scaling the dynamic system
- determining which gains are "small" for compensator simplification
- selecting outputs and their weightings in the optimization using the ROPT-SYS and RSANDY computer programs
- selecting scale factors for fixed-point scaling, Appendix E

- selecting stick and collective lever gains for the pilot
- determining the structure of the integral control loops

Also, experience in use of the methodology itself, especially the design tools, was critical. The hover controller, though much more complicated, took about as much time to design as the longitudinal CAS. The other lesson is that the design of the control logic is often the easiest and fastest step in building an operational control system. Most of the work is spent on:

- software design, coding, and testing
- hardware modifications and testing
- ground based closed loop testing

Chapter 6.

Recommendations for Further Research

The CH-47 research helicopter at Ames is a very flexible test vehicle and is being improved by the addition of a floating point digital computer programmable in a higher order language. With this improvement, a number of potential research projects should be considered:

- Parameter identification to improve the existing models used for design and simulation
- Refinement of the two designs presented here and pilot evaluation in a more realistic setting such as instrument landing
- Outer loop guidance work (Microwave Landing System, 4-dimensional navigation, etc.) using these inner loops
- Application of singular value LQG-LTR (Linear Quadratic Gaussian - Loop Transfer Recovery) to account for unmodeled rotor dynamics

One difficulty in applying the methodology was the poor convergence characteristics of the first order gradient algorithm in the RSANDY program. A second order technique to speed convergence would be an important improvement to the program. Another possibility for research is finding a way of commanding a system without exciting all the closed-loop modes similar to the method described in

Chapter 3 for the case of the full-order compensator.

Saberi has shown a technique for calculating helicopter stability derivatives during low speed flight near the ground.[18] This research vehicle is an excellent testbed for validating these derivatives.

References

1. McRuer,D., Ashkenas, I., and Graham, D., *Aircraft Dynamics and Automatic Control*, Princeton University Press, Princeton, New Jersey, 1973.
2. Bryson,A.E., Notes from the "Advanced Stability and Control of Flight Vehicles" course at Stanford(AA271b), 1983.
3. Ly,U.L., "A Design Algorithm for Robust Low-Order Controllers", Stanford University, SUDAAR 536, November 1982.
4. Bryson,A.E. and Ho,Y., *Applied Optimal Control*, Hemishpere Publishing Corporation, New York, 1975.
5. Kailath,T., *Linear Systems*, Prentice-Hall,Inc., Englewood Cliffs, New Jersey, 1980.
6. Franklin,G.F. and Powell,J.D., *Digital Control of Dynamic Systems*, Addison-Wesley Publishing Company, Menlo Park, California, 1981.
7. Bernard,D., "Control System Design for Lightly Coupled Space Structures", PhD Dissertation, Stanford University, September 1984.
8. Ly,U.L., "Optimal Robust Low-Order Controller Design, User Guide for the Program SANDY", Stanford University, 1982.

Appendix D.

Set Point Design

This appendix derives the feedforward matrix which commands a dynamic system, including compensator, to a new equilibrium. This matrix turns desired outputs into the steady-state controls needed to achieve the outputs. The restrictions are that these outputs (or new operating point) be physically realizable and that the number of controls be equal to the number of outputs.

Consider the following dynamic system:

$$\begin{aligned}\dot{x} &= Fx + Gu \\ y_s &= H_s x + D_{su} u \\ \dot{z} &= Az + By_s + G_z u_c \\ u &= Cz + Dy_s + u_c\end{aligned}\tag{D.1}$$

where:

x - plant states

y_s - measurements

z - compensator states

u - controls

The general form of the transformation is:

$$T = \begin{bmatrix} T_1 & 0 & \dots & 0 \\ 0 & T_2 & 0 & 0 \\ \vdots & 0 & \ddots & 0 \\ 0 & 0 & 0 & \frac{1}{c_l} \end{bmatrix} \quad (C.11)$$

$$T^{-1} = \begin{bmatrix} T_1^{-1} & 0 & \dots & 0 \\ 0 & T_2^{-1} & 0 & 0 \\ \vdots & 0 & \ddots & 0 \\ 0 & 0 & 0 & c_l \end{bmatrix}$$

where:

$$T_i = \frac{\begin{bmatrix} c_{l,2i}(f_i g_i - e_i h_i) & e_i c_{l,2i} - b_i c_{l,2i-1} \\ -c_{l,2i-1}(f_i g_i - e_i h_i) & g_i c_{l,2i-1} - h_i c_{l,2i-1} \end{bmatrix}}{-f_i c_{l,2i-1}^2 + (e_i - h_i) c_{l,2i-1} c_{l,2i} + g_i c_{l,2i}^2} \quad (C.12)$$

i - the i^{th} complex mode

l - row index corresponding to the largest value of $c_1^2 + c_2^2$ for that mode's double column, or the largest value of c_1^2 for the a real mode

A listing of a FORTRAN subroutine, MINCOM, which does this transformation is shown in Appendix L.

The "0 1" in the C_{min} matrix results from scaling the system by the largest values in the C double columns.

Consider a second order system in general form:

$$\begin{aligned} \begin{bmatrix} \dot{z}_1 \\ \dot{z}_2 \end{bmatrix} &= \begin{bmatrix} e & f \\ g & h \end{bmatrix} \begin{bmatrix} z_1 \\ z_2 \end{bmatrix} + \begin{bmatrix} b_1 \\ b_2 \end{bmatrix} y \\ u &= [c_1 \quad c_2] \begin{bmatrix} z_1 \\ z_2 \end{bmatrix} \end{aligned} \quad (C.6)$$

The desired transformation will put this system into the following form:

$$\begin{aligned} \begin{bmatrix} \dot{z}'_1 \\ \dot{z}'_2 \end{bmatrix} &= \begin{bmatrix} 0 & 1 \\ a_1 & a_2 \end{bmatrix} \begin{bmatrix} z'_1 \\ z'_2 \end{bmatrix} + \begin{bmatrix} b'_1 \\ b'_2 \end{bmatrix} y \\ u &= [0 \quad 1] \begin{bmatrix} z'_1 \\ z'_2 \end{bmatrix} \end{aligned} \quad (C.7)$$

The similarity transformation requires the two systems to have identical eigenvalues, that is:

$$\begin{aligned} |sI - A| &= |sI - A_{min}| \\ \Downarrow \end{aligned} \quad (C.8)$$

$$a_1 = fg - eh$$

$$a_2 = e + h$$

Introducing the transformation matrix and expanding:

$$TA_{min} = AT$$

$$C_{min} = CT$$

$$\begin{aligned} \begin{bmatrix} T_{11} & T_{12} \\ T_{21} & T_{22} \end{bmatrix} \begin{bmatrix} 0 & 1 \\ fg - eh & e + h \end{bmatrix} &= \begin{bmatrix} e & f \\ g & h \end{bmatrix} \begin{bmatrix} T_{11} & T_{12} \\ T_{21} & T_{22} \end{bmatrix} \\ [0 \quad 1] &= [c_1 \quad c_2] \begin{bmatrix} T_{11} & T_{12} \\ T_{21} & T_{22} \end{bmatrix} \end{aligned} \quad (C.9)$$

where $c_1^2 + c_2^2$ has the largest magnitude of any row pair in double column associated with the mode being made minimal. Solving the equations above we have the desired transformation:

$$T = \frac{\begin{bmatrix} c_2(fg - eh) & ec_2 - bc_1 \\ -c_1(fg - eh) & gc_2 - hc_1 \end{bmatrix}}{-fc_1^2 + (e - h)c_1c_2 + gc_2^2} \quad (C.10)$$

where:

$$A = \begin{bmatrix} \star & \star & 0 & 0 & \dots \\ \star & \star & & & \\ & 0 & \star & \star & 0 & 0 \\ & & \star & \star & & \\ 0 & & 0 & & \ddots & 0 \\ \vdots & & 0 & 0 & & \star \end{bmatrix}, r \times r \quad (C.2)$$

$$B = [Full], r \times p$$

$$C = [Full], m \times r$$

We want a transformation to a new form:

$$\dot{z}' = A_{min} z' + B_{min} y \quad (C.3)$$

$$u = C_{min} z'$$

where:

A_{min} - minimal form of A

B_{min} - minimal form of B

C_{min} - minimal form of C

$$A_{min} = \begin{bmatrix} 0 & 1 & & 0 & \dots \\ a_1 & a_2 & & & \\ & 0 & & 0 & 1 & \dots \\ & & a_1 & a_2 & & \\ \vdots & & \vdots & & \ddots & \end{bmatrix}, n \times n$$

$$B_{min} = \begin{bmatrix} \star & \star & \dots \\ \star & \star & \dots \\ \vdots & \vdots & \ddots \end{bmatrix}, n \times p \quad (C.4)$$

$$C_{min} = \begin{bmatrix} \star & \star & 0 & 1 & \dots \\ 0 & 1 & \star & \star & \dots \\ \star & \star & \star & \star & \dots \\ \vdots & \vdots & \vdots & \vdots & \ddots \end{bmatrix}, m \times n$$

$$z = T z'$$

$$A_{min} = T^{-1} A T \quad (C.5)$$

$$B_{min} = T^{-1} B$$

$$C_{min} = C T$$

Appendix C.

Minimal Realizations

The design methodology described in Chapter 2 used minimal realizations in two places. The first was when the ROPTSYS computer program displayed the compensator in minimal form to be better suited for the optimization in the RSANDY program. This eliminated redundant parameters which could cause trouble in the RSANDY gradient search procedures. The second use of a minimal realization came when the discrete compensator was transformed to minimal form for computational efficiency. In the first case, the transformation was from arbitrary form to block modal form then to block minimal form. The second was from an arbitrary 2×2 block form to the block minimal form. The derivation is shown for an arbitrary 2×2 system then expanded for any order.

Given the following form of the dynamic system:

$$\begin{aligned}\dot{z} &= Az + By \\ u &= Cz\end{aligned}\tag{C.1}$$

By the duality property of regulators and estimators (Figure B.1), these gains, $K^T = (R + NQN^T)^{-1}(NQ\Gamma^T + H_mP)$, are determined using the randomly disturbed equations of motion:

$$\begin{aligned}\dot{x} &= Fx + \Gamma w \\ y_m &= H_m x + Nw + v\end{aligned}\tag{B.12}$$

where

Q — noise spectral density matrix of plant disturbances, w

R — noise spectral density matrix of measurement noise, v

Regulator	F	G	H	L	A	B	S	C
Estimator	F^T	H_m^T	Γ^T	N^T	Q	R	P	K^T

Figure B.1: **Duality Between Regulators and Estimators.** This shows the property of duality which allows the use of the regulator results for design of an optimal estimator (a steady-state Kalman filter).

Adjoining the constraints (the equations of motion) to form the Hamiltonian:

$$H = \mathcal{L} + \lambda^T(Fx + Gu) \quad (B.5)$$

Recalling the optimality conditions:

$$\dot{\lambda}^T = \frac{\partial H}{\partial x} \quad (B.6)$$

$$0 = \frac{\partial H}{\partial u} \quad (B.7)$$

Introducing the system equations, $\dot{x} = Fx + Gu$, and expanding the optimality equations, we have the Euler-Lagrange equations (here in matrix form):

$$\begin{bmatrix} \dot{x} \\ \dot{\lambda} \end{bmatrix} = \begin{bmatrix} F - G(B + L^T AL)^{-1} L^T AM & -G(B + L^T AL)^{-1} G^T \\ -M^T AM - M^T AL(B + L^T AL)^{-1} L^T AM & -F - M^T AL(B + L^T AL)^{-1} G^T \end{bmatrix} \begin{bmatrix} x \\ \lambda \end{bmatrix} \quad (B.8)$$

As shown in *Bryson and Ho* [4] or *Franklin and Powell* [6], the solution to these equations is $\lambda = Sx$ where $S = \Lambda_- \chi_-^{-1}$. Λ_- and χ_- are the submatrices of the eigenvector matrix of the Hamiltonian matrix associated with eigenvalues having negative real values, i.e.

$$\begin{bmatrix} x \\ \lambda \end{bmatrix} = \begin{bmatrix} \chi_- & \chi_+ \\ \Lambda_- & \Lambda_+ \end{bmatrix} \begin{bmatrix} \xi_- \\ \xi_+ \end{bmatrix} \quad (B.9)$$

With this solution for λ , the optimal steady state control, u , can be expressed as a linear combination of the state variables, x :

$$u = Cx \quad (B.10)$$

$$C = (B + L^T AL)^{-1} (L^T AM + G^T S)$$

The same approach applies to finding the estimator gains, K , of the equation:

$$\dot{\hat{x}} = F\hat{x} + Gu + K(y_m - H_m \hat{x}) \quad (B.11)$$

Appendix B.

Optimal Compensator Design

The design methodology described in Chapter 2 uses an optimal full order compensator as the starting point. This appendix summarizes the derivation of the optimal compensator. From Hall and Bryson, we see that to design a set of regulator gains which minimize a quadratic performance index, we minimize the Hamiltonian with respect to the control.[17] In this case, the performance index includes the control in the output, thus enabling the weighting of state rates (accelerations). This is essential in aerospace applications where vehicle acceleration is an important parameter in the design and analysis of the control system. Starting with the modified performance index:

$$J = \int_0^{\infty} \mathcal{L} dt = \int_0^{\infty} \frac{1}{2} (y^T A y + u^T B u) dt \quad (B.1)$$

where:

$$y = Mx + Lu \quad (B.2)$$

$$y^T = x^T M^T + u^T L^T \quad (B.3)$$

Expanding the integrand of J :

$$\mathcal{L} = \frac{1}{2} [x^T M^T A M x + x^T M^T A L u + u^T L^T A M x + u^T (L^T A L + B) u] \quad (B.4)$$

σ - standard deviation of the noise variable

T_c - correlation time of the noise

With these transformations, the resulting compensator will use scaled measurements to calculate a scaled control signal. If we want to use the compensator in the physical system, we need only unscale the gain matrices. The compensator based on the scaled variables is:

$$\begin{aligned}\dot{z} &= \bar{A}z + \bar{B}\bar{y}_s \\ \bar{u} &= \bar{C}z + \bar{D}\bar{y}_s\end{aligned}\tag{A.8}$$

We unscale the system by replacing scaled vectors \bar{u} and \bar{y}_s with their unscaled equivalents $\bar{u} = T_c^{-1}u$ and $\bar{y}_s = T_m^{-1}y_s$:

$$\begin{aligned}\dot{z} &= \bar{A}z + \bar{B}T_m^{-1}y_s \\ \bar{u} &= T_c\bar{C}z + \bar{D}T_m^{-1}y_s\end{aligned}\tag{A.9}$$

Now the compensator uses actual (unscaled) measurements and gives unscaled control signals as outputs.

To make the scaling process consistent, I've listed some rules of thumb below:

- Scale the matrices consistently; for example, if a measurement is also a state, use the same units.
- Scale intermediate state variables in an actuator model the same as the control itself. For example, if we have a first order actuator model, $\dot{u}_a = -au_a + au_c$, then scale the actuator position state(u_a), its rate(\dot{u}_a), and the command(u_c) identically.
- Similarly, if sensor noise filters are included in the plant model, then these noise filter states should be scaled the same as the measurements they filter.

turbances:

$$\begin{aligned}
 y_s &= T_m \bar{y}_s \\
 y_c &= T_p \bar{y}_c \\
 w &= T_d \bar{w} \\
 v &= T_m \bar{v}
 \end{aligned} \tag{A.4}$$

With these transformations, the scaled dynamic system is:

$$\begin{aligned}
 \dot{\bar{x}} &= \bar{F} \bar{x} + \bar{G} \bar{u} + \bar{\Gamma} \bar{w} \\
 \bar{y}_s &= \bar{H}_s \bar{x} + \bar{D}_{su} \bar{u} + \bar{N} \bar{w} + \bar{v} \\
 \bar{y}_c &= \bar{H}_c \bar{x} + \bar{D}_{cu} \bar{u}
 \end{aligned} \tag{A.5}$$

where:

$$\begin{aligned}
 \bar{F} &= T_s^{-1} F T_s \\
 \bar{G} &= T_s^{-1} G T_c \\
 \bar{\Gamma} &= T_s^{-1} \Gamma T_d \\
 \bar{H}_s &= T_m^{-1} H_s T_s \\
 \bar{D}_{su} &= T_m^{-1} D_{su} T_c \\
 \bar{N} &= T_m^{-1} N T_d \\
 \bar{H}_c &= T_p^{-1} H_c T_s \\
 \bar{D}_{cu} &= T_p^{-1} D_{cu} T_c \\
 \bar{Q} &= T_d^{-1} Q T_d^{-1} \\
 \bar{R} &= T_m^{-1} R T_m^{-1}
 \end{aligned} \tag{A.6}$$

The scaled power spectral density matrices were derived using the approximation:

$$PSD \approx 2\sigma^2 T_c \tag{A.7}$$

where:

- F - plant dynamics matrix, $n \times n$
 G - control distribution matrix, $n \times m$
 Γ - plant disturbance distribution matrix, $n \times m'$
 H_s - state to measurement distribution matrix, $p \times n$
 D_{su} - control to measurement distribution matrix, $p \times m$
 N - plant disturbance to measurement distribution matrix, $p \times m'$
 H_c - state to output distribution matrix, $p' \times n$
 D_{cu} - control to output distribution matrix, $p' \times m$
 Q - plant disturbance spectral density matrix, $m' \times m'$
 R - sensor noise spectral density matrix, $p \times p$

The scaling process continues by describing the changes of units on the states, controls, etc. as simple transformations. For instance, if we want new states, \bar{x} , and new controls, \bar{u} , to be $s_{x_1}x_1, s_{x_2}x_2, \dots, s_{x_n}x_n$ and $s_{u_1}u_1, s_{u_2}u_2, \dots, s_{u_n}u_n$, then we can define scaling (also similarity) transformations:

$$\begin{aligned} x &= T_s \bar{x} \\ u &= T_c \bar{u} \end{aligned} \tag{A.2}$$

where:

$$\begin{aligned} T_s &= \begin{bmatrix} \frac{1}{s_{x_1}} & & & \\ & \frac{1}{s_{x_2}} & & \\ & & \ddots & \\ & & & \frac{1}{s_{x_n}} \end{bmatrix} \\ T_c &= \begin{bmatrix} \frac{1}{s_{u_1}} & & & \\ & \frac{1}{s_{u_2}} & & \\ & & \ddots & \\ & & & \frac{1}{s_{u_n}} \end{bmatrix} \end{aligned} \tag{A.3}$$

Using an identical procedure, we scale the outputs, measurements, and plant dis-

Appendix A.

Engineering Scaling

This appendix derives engineering scaling equations used in the ROPTSYS computer program. This process transforms the model of the physical system into a "similar" model where the units of the variables have changed. Similar means the eigenvalues of the system are not changed by the transformation to the new coordinates. As described in section 2.2, the new units are chosen to make the new variables of the dynamic system of equal importance to the design engineer. The process begins with the linear model shown below:

$$\begin{aligned}\dot{x} &= Fx + Gu + \Gamma w \\ y_s &= H_s x + D_{su} u + Nw + v \\ y_c &= H_c x + D_{cu} u \\ J &= \int_0^\infty (y_c^T A y_c + u^T B u) dt\end{aligned}\tag{A.1}$$

where:

- x - system states, $n \times 1$
- z - compensator states, $r \times 1$
- u - controls, $m \times 1$
- w - plant disturbances, $m' \times 1$
- y_s - sensor measurements, $p \times 1$
- y_c - weighted outputs, $p' \times 1$
- v - sensor noise, $p \times 1$

ber, 1971.

18. Saberi, H.A., "Ground Effect on Helicopter Aerodynamics and Stability", PhD Dissertation, Stanford University, October 1984.

9. Bryson, A.E., Notes from the "Optimal Estimation and Control Logic in the Presence of Noise" course at Stanford(AA278b), 1984.
10. Kelly, J.R., Niessen, F.R., Garren, J.F., and Abbott, T.S., "Description of the VTOL Approach and Landing Technology(VALT) CH-47 Research System", NASA TP 1436, August 1979.
11. Ostroff, A.J., Downing, D.R., and Rood, W.J., "A Technique Using a Non-linear Helicopter Model for Determining Trims and Derivatives", NASA TN D-8159, May 1976.
12. Chen, R.T.N. and Hindson, W.S., "Influence of Rotor and Other High-Order Dynamics on Helicopter Flight Control System Bandwidth", a paper to be presented at the International Conference on Rotorcraft Basic Research, Research Triangle Park, NC, February 1985.
13. Hutto, A.J., "Flight Test Report on the Heavy-Lift Helicopter Flight Control System", 31st Annual National Forum of the American Helicopter Society, May 1975.
14. Etkin, B., *Dynamics of Atmospheric Flight*, John Wiley and Sons, Inc., Toronto, 1972.
15. Valkenburg, M.E., *Introduction to Modern Network Synthesis*, John Wiley and Sons, Inc., New York, 1964.
16. Gardner, B.E., "Feedforward/Feedback Control Logic for Robust Target Tracking", PhD Dissertation, Stanford University, December 1984.
17. Hall, W.E. and Bryson, A.E., "Optimal Control and Filter Synthesis by Eigenvector Decomposition", SUDAAR No. 436, Stanford University, Novem-

If $DD_{uu} = 0$, then these equations can be rewritten as:

$$\begin{bmatrix} \dot{x} \\ \dot{z} \end{bmatrix} = \begin{bmatrix} F + GDH_s & GC \\ B(I + D_{uu}D)H_s & A + BD_{uu}C \end{bmatrix} \begin{bmatrix} x \\ z \end{bmatrix} + \begin{bmatrix} G \\ BD_{uu} + G_z \end{bmatrix} u_c \quad (D.2)$$

Defining $x_T = \begin{bmatrix} x \\ z \end{bmatrix}$, we can rewrite the equations above as:

$$\dot{x}_T = F_T x_T + G_T u_c \quad (D.3)$$

Expressing the desired outputs, y_D , as a linear combination of x_T and u_c we have:

$$y_D = H_D x_T + L_D u_c \quad (D.4)$$

At steady state, $\dot{x}_T = 0$, and the two previous equations become:

$$\begin{bmatrix} F_T & G_T \\ H_D & L_D \end{bmatrix} \begin{bmatrix} x_T \\ u_c \end{bmatrix}_{ss} = \begin{bmatrix} 0 \\ y_D \end{bmatrix} \quad (D.5)$$

inverting:

$$\begin{aligned} \begin{bmatrix} x_T \\ u_c \end{bmatrix}_{ss} &= \begin{bmatrix} F_T & G_T \\ H_D & L_D \end{bmatrix}^{-1} \begin{bmatrix} 0 \\ y_D \end{bmatrix} \\ &= \begin{bmatrix} \star & M \\ \star & N \end{bmatrix} \begin{bmatrix} 0 \\ y_D \end{bmatrix} \end{aligned} \quad (D.6)$$

The steady-state controls are $u_c = N y_D$ and new equilibrium state vector is $x_T = M y_D$ where:

$$\begin{bmatrix} \star & M \\ \star & N \end{bmatrix} = \begin{bmatrix} F + GDH_s & GC & G \\ B(I + D_{uu}D)H_s & A + BD_{uu}C & BD_{uu} + G_z \\ H_D & L_D & \end{bmatrix}^{-1} \quad (D.7)$$

This last equation is used by the SETPNT program, Appendix L, to calculate the N matrix.

Appendix E.

Fixed Point Scaling

This appendix describes the technique of scaling the analytical designs to run on the Sperry 1819A flight computer. The process is similar in principle to scaling engineering problems for an analog computer. This computer is an 18 bit fixed-point digital computer. There are two problems which must be considered when doing this scaling. The first is avoiding overflows (exceeding $2^{17} - 1$ during calculations) and the second is maintaining precision in the results. The procedure which follows handles both these potential problems.

Consider the compensator dynamic system:

$$\begin{aligned}\dot{z} &= Az + By \\ u &= Cz\end{aligned}\tag{E.1}$$

where y and u are in engineering units (not yet computer scaled). In the computer, these variable have computer scaling factors, K , such that $\dot{z}K_z$, zK_z , yK_y , and uK_u have units of bits. For example, if $K_\theta = 500 \frac{\text{bits}}{\text{deg}}$, then then 5 deg of θ is 2500 bits in the computer. In these computer scaled variables, the compensator appears:

$$\begin{aligned}[\dot{z}] K_z &= K_A [A] \frac{K_z}{K_z K_A} [z] K_z + K_B [B] \frac{K_z}{K_y K_B} [y] K_y \\ [u] K_u &= K_C [C] \frac{K_u}{K_z K_C} [z] K_z\end{aligned}\tag{E.2}$$

where A , B , and C are in engineering units. The scale factors, K , for y and u are part of the computer environment (set up by the programmers of the original flight program) but we need to calculate K_z and K_x . This is simplified by the digital implementation; we have z_{k+1} and z_k rather than \dot{z} and z . This means only one scale factor, K_z , is needed. To find this factor, first estimate the largest value that any z_{k+1} or z_k can achieve by finding the maximum single product in the matrix multiply, $[B][y]_{max}$. For controls, measurements, and desired outputs, the maximum values can be set using engineering judgement and intuition. Since we also want precision in the z term, we select K_z so that z_{max} uses all of the 18 bits available:

$$K_z = \frac{2^{17}}{z_{max}} \quad (E.3)$$

where z_{max} is rounded up to the next power of 2. 2^{17} is used since the largest negative number expressed in 18 bits is -2^{17} .

With the K_z term, the problem of overflow is solved. Now we need only ensure that precision is maintained in the calculations by choosing the additional scale factors, K_A , K_B , and K_C that scale the elements of the A , B , and C matrices. Making use of all 18 bits, we can find these scale factors in the same way as the K_z term above was calculated:

$$\begin{aligned} K_A &= \frac{2^{17}}{a_{max} \frac{K_z}{K_x}} \\ K_B &= \frac{2^{17}}{b_{max} \frac{K_z}{K_y}} \\ K_C &= \frac{2^{17}}{c_{max} \frac{K_z}{K_u}} \end{aligned} \quad (E.4)$$

where a_{max} , b_{max} , and c_{max} are the maximum elements of the A , B , and C matrices which have been rounded up to the nearest power of 2.

One product from the matrix multiplies is:

$$(b_{ij} \frac{K_z}{K_v}) K_B (y_j K_v) \quad (E.5)$$

This number is included in the double precision (36 bits) A register in the 1819A and is always less than $2^{35} - 1$. We want to accumulate these double precision elements to get one element of By . Finally, we divide by K_A (or equivalently shift the A register) to regain the single precision inner product. This is done for each of the matrix multiplies.

The same approach is used to scale the feedforward matrix and the integral gain matrix used in the longitudinal CAS. The two BASIC computer programs, which do this scaling for the longitudinal CAS and for the hover controller, are listed in Appendix N along with example data files.

Appendix F.

CH-47 Research Helicopter

The helicopter used for this research is a highly modified version of the Boeing-Vertol CH-47 "Chinook" used by the U.S Army for cargo and troop transport. Figure F.1 shows the tandem rotor helicopter, which is operated by the NASA Ames Research Center. Reference 10 is a more complete description of this particular helicopter including the many modifications made to the basic CH-47. Below are listed some of the modifications and improved capabilities:

- Full authority, variable stability, fly-by-wire flight control system in all four axes.
- Programmable analog and digital computers capable of executing the control laws.
- Programmable force-feel system on the experimental pilot's stick.
- Flight instrumentation system capable of recording over 100 variables at 100 times per second.
- Operator's console for control of the experimental systems.
- Additional sensors: INS, radar altimeter, body-mounted accelerometers, improved air data sensors, numerous control position sensors, boom-mounted angle of attack and sideslip vanes, rate gyros
- Digital ground to air uplink capability

Figures F.2 and F.3, from reference 10, show the cabin layout in this experimental vehicle and a block diagram of the experimental control system.

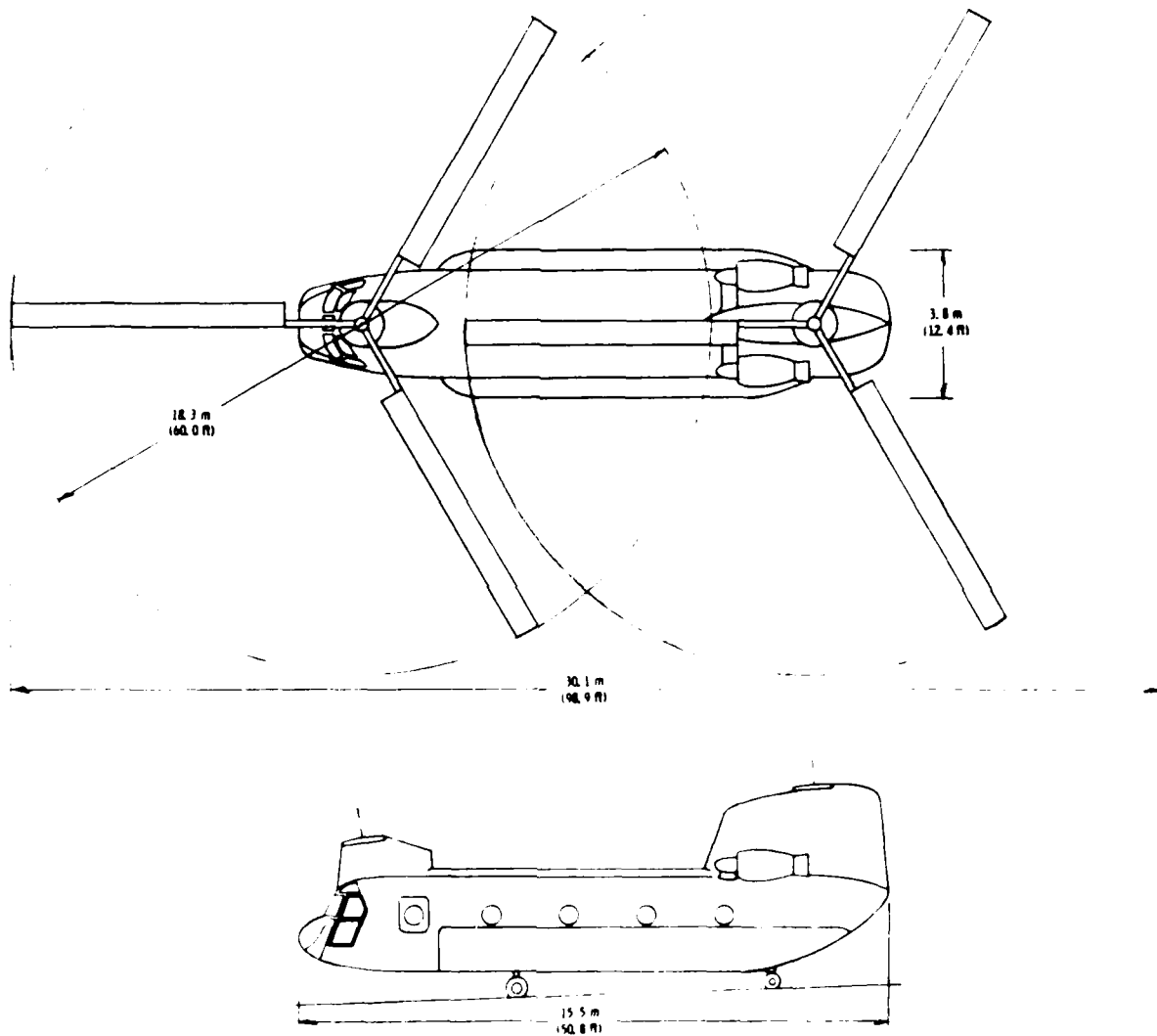


Figure F.1: Boeing-Vertol CH-47 Chinook Helicopter. The large tandem rotor helicopter is used operationally by the U.S. Army for cargo and troop transport. Maximum gross weight is 38000 pounds with typical operating wieght of 30000 pounds.

Appendix G.

CH-47 Linear Models

The models described in this appendix were calculated using the information from reference 11. The general forms for the decoupled 4th order models and for the coupled 8th order are shown in Figures G.1 and G.2. The linear models for the flight conditions related to this research are shown in Figures G.3 to G.16.

$$\begin{bmatrix} \dot{U}_P \\ \dot{W}_P \\ \dot{Q}_P \\ \dot{\theta}_P \end{bmatrix} = \begin{bmatrix} \frac{X_U}{m} & \frac{X_W}{m} & \left(\frac{X_Q}{m} - W_N \right) & -g \cos \theta_N \\ \frac{Z_U}{m} & \frac{Z_W}{m} & \left(U_N + \frac{ZQ}{m} \right) & -g \sin \theta_N \\ \frac{M_U}{I_{YY}} & \frac{M_W}{I_{YY}} & \frac{M_Q}{I_{YY}} & 0 \\ 0 & 0 & 1 & 0 \end{bmatrix} \begin{bmatrix} U_P \\ W_P \\ Q_P \\ \theta_P \end{bmatrix} + \begin{bmatrix} \frac{X_{\delta_B}}{m} & \frac{X_{\delta_C}}{m} \\ \frac{Z_{\delta_B}}{m} & \frac{Z_{\delta_C}}{m} \\ \frac{M_{\delta_B}}{I_{YY}} & \frac{M_{\delta_C}}{I_{YY}} \\ 0 & 0 \end{bmatrix} \begin{bmatrix} \delta_{B,P} \\ \delta_{C,P} \end{bmatrix}$$

$$\begin{bmatrix} \dot{P}_P \\ \dot{\phi}_P \\ \dot{R}_P \\ \dot{V}_P \end{bmatrix} = \begin{bmatrix} \left(\frac{I_1 L_P}{I_{XX}} + \frac{I_3 N_P}{I_{ZZ}} \right) & 0 & \left(\frac{I_1 L_R}{I_{XX}} + \frac{I_3 N_R}{I_{ZZ}} \right) & \left(\frac{I_1 L_V}{I_{XX}} + \frac{I_3 N_V}{I_{ZZ}} \right) \\ 1 & 0 & \tan \theta_N & 0 \\ \left(\frac{I_2 L_P}{I_{XX}} + \frac{I_1 N_P}{I_{ZZ}} \right) & 0 & \left(\frac{I_2 L_R}{I_{XX}} + \frac{I_1 N_R}{I_{ZZ}} \right) & \left(\frac{I_2 L_V}{I_{XX}} + \frac{I_1 N_V}{I_{ZZ}} \right) \\ \left(W_N + \frac{Y_P}{m} \right) & g \cos \theta_N & \left(\frac{Y_R}{m} - U_N \right) & \frac{Y_V}{m} \end{bmatrix} \begin{bmatrix} P_P \\ \phi_P \\ R_P \\ V_P \end{bmatrix}$$

$$+ \begin{bmatrix} \left(\frac{I_1 L_{\delta_S}}{I_{XX}} + \frac{I_3 N_{\delta_S}}{I_{ZZ}} \right) & \left(\frac{I_1 L_{\delta_R}}{I_{XX}} + \frac{I_3 N_{\delta_R}}{I_{ZZ}} \right) \\ 0 & 0 \\ \left(\frac{I_2 L_{\delta_S}}{I_{XX}} + \frac{I_1 N_{\delta_S}}{I_{ZZ}} \right) & \left(\frac{I_2 L_{\delta_R}}{I_{XX}} + \frac{I_1 N_{\delta_R}}{I_{ZZ}} \right) \\ \frac{Y_{\delta_S}}{m} & \frac{Y_{\delta_R}}{m} \end{bmatrix} \begin{bmatrix} \delta_{S,P} \\ \delta_{R,P} \end{bmatrix}$$

Figure G.1: **Longitudinal and Lateral 4th Order Models.** The longitudinal model above was used in the design of the longitudinal CAS (Chapter 3).

$$\begin{bmatrix} \dot{U}_p \\ \dot{V}_p \\ \dot{W}_p \\ \dot{P}_p \\ \dot{Q}_p \\ \dot{R}_p \\ \dot{\delta}_p \\ \dot{\phi}_p \end{bmatrix} = \begin{bmatrix} \frac{X_U}{m} & \frac{X_V}{m} & \frac{X_W}{m} & \frac{X_P}{m} & \left(\frac{X_Q}{m} + W_N\right) & \left(\frac{X_R}{m} + V_N\right) & -g \cos \theta_N & 0 \\ \frac{Y_U}{m} & \frac{Y_V}{m} & \frac{Y_W}{m} & \left(\frac{Y_P}{m} + W_N\right) & \frac{Y_Q}{m} & \left(\frac{Y_R}{m} + U_N\right) & -g \sin \theta_N \sin \phi_N & g \cos \theta_N \cos \phi_N \\ \frac{Z_U}{m} & \frac{Z_V}{m} & \frac{Z_W}{m} & \frac{Z_P}{m} & \left(\frac{Z_Q}{m} + U_N\right) & \frac{Z_R}{m} & -g \cos \theta_N & 0 \\ \left(\frac{I_1 L_U}{I_{XX}} + \frac{I_3 N_U}{I_{ZZ}}\right) & \left(\frac{I_1 L_V}{I_{XX}} + \frac{I_3 N_V}{I_{ZZ}}\right) & \left(\frac{I_1 L_W}{I_{XX}} + \frac{I_3 N_W}{I_{ZZ}}\right) & \left(\frac{I_1 L_P}{I_{XX}} + \frac{I_3 N_P}{I_{ZZ}}\right) & \left(\frac{I_1 L_Q}{I_{XX}} + \frac{I_3 N_Q}{I_{ZZ}}\right) & \left(\frac{I_1 L_R}{I_{XX}} + \frac{I_3 N_R}{I_{ZZ}}\right) & 0 & 0 \\ \frac{M_U}{I_{YY}} & \frac{M_V}{I_{YY}} & \frac{M_W}{I_{YY}} & \frac{M_P}{I_{YY}} & \frac{M_Q}{I_{YY}} & \frac{M_R}{I_{YY}} & 0 & 0 \\ \left(\frac{I_2 L_U}{I_{XX}} + \frac{I_1 N_U}{I_{ZZ}}\right) & \left(\frac{I_2 L_V}{I_{XX}} + \frac{I_1 N_V}{I_{ZZ}}\right) & \left(\frac{I_2 L_W}{I_{XX}} + \frac{I_1 N_W}{I_{ZZ}}\right) & \left(\frac{I_2 L_P}{I_{XX}} + \frac{I_1 N_P}{I_{ZZ}}\right) & \left(\frac{I_2 L_Q}{I_{XX}} + \frac{I_1 N_Q}{I_{ZZ}}\right) & \left(\frac{I_2 L_R}{I_{XX}} + \frac{I_1 N_R}{I_{ZZ}}\right) & 0 & 0 \\ 0 & 0 & 0 & 0 & \cos \phi_N & -\sin \phi_N & 0 & 0 \\ 0 & 0 & 0 & 1 & -\sin \phi_N \tan \theta_N & \cos \phi_N \tan \theta_N & 0 & 0 \end{bmatrix} \begin{bmatrix} U_p \\ V_p \\ W_p \\ P_p \\ Q_p \\ R_p \\ \delta_p \\ \phi_p \end{bmatrix}$$

$$+ \begin{bmatrix} \frac{X_{\delta_B}}{m} & \frac{X_{\delta_C}}{m} & \frac{X_{\delta_g}}{m} & \frac{X_{\delta_R}}{m} \\ \frac{Y_{\delta_B}}{m} & \frac{Y_{\delta_C}}{m} & \frac{Y_{\delta_g}}{m} & \frac{Y_{\delta_R}}{m} \\ \frac{Z_{\delta_B}}{m} & \frac{Z_{\delta_C}}{m} & \frac{Z_{\delta_g}}{m} & \frac{Z_{\delta_R}}{m} \\ \left(\frac{I_1 L_{\delta_B}}{I_{XX}} + \frac{I_3 N_{\delta_B}}{I_{ZZ}}\right) & \left(\frac{I_1 L_{\delta_C}}{I_{XX}} + \frac{I_3 N_{\delta_C}}{I_{ZZ}}\right) & \left(\frac{I_1 L_{\delta_g}}{I_{XX}} + \frac{I_3 N_{\delta_g}}{I_{ZZ}}\right) & \left(\frac{I_1 L_{\delta_R}}{I_{XX}} + \frac{I_3 N_{\delta_R}}{I_{ZZ}}\right) \\ \frac{M_{\delta_B}}{I_{YY}} & \frac{M_{\delta_C}}{I_{YY}} & \frac{M_{\delta_g}}{I_{YY}} & \frac{M_{\delta_R}}{I_{YY}} \\ \left(\frac{I_2 L_{\delta_B}}{I_{XX}} + \frac{I_1 N_{\delta_B}}{I_{ZZ}}\right) & \left(\frac{I_2 L_{\delta_C}}{I_{XX}} + \frac{I_1 N_{\delta_C}}{I_{ZZ}}\right) & \left(\frac{I_2 L_{\delta_g}}{I_{XX}} + \frac{I_1 N_{\delta_g}}{I_{ZZ}}\right) & \left(\frac{I_2 L_{\delta_R}}{I_{XX}} + \frac{I_1 N_{\delta_R}}{I_{ZZ}}\right) \\ 0 & 0 & 0 & 0 \\ 0 & 0 & 0 & 0 \end{bmatrix} \begin{bmatrix} \delta_{B,p} \\ \delta_{C,p} \\ \delta_{g,p} \\ \delta_{R,p} \end{bmatrix}$$

$$I_{XX} = 50\,386.3 \text{ kg-m}^2 \text{ (37\,163 slug-ft}^2\text{)}$$

$$I_{YY} = 273\,536 \text{ kg-m}^2 \text{ (201\,750 slug-ft}^2\text{)}$$

$$I_{ZZ} = 257\,685 \text{ kg-m}^2 \text{ (190\,059 slug-ft}^2\text{)}$$

$$I_{XZ} = 19\,338.3 \text{ kg-m}^2 \text{ (14\,632 slug-ft}^2\text{)}$$

$$m = 14\,968.6 \text{ kg (1\,025.67 slug)}$$

where

$$I_1 = \frac{I_{XX} I_{ZZ}}{I_{XX} I_{ZZ} - I_{XZ}^2}$$

$$I_2 = \frac{I_{XX} I_{XZ}}{I_{XX} I_{ZZ} - I_{XZ}^2}$$

$$I_3 = \frac{I_{ZZ} I_{XZ}}{I_{XX} I_{ZZ} - I_{XZ}^2}$$

Figure G.2: Coupled 8th Order Model. This model was used in the design of the hover controller, described in Chapter 4.

THIS IS DATA FOR ZDOT= 0 FT/MIN AND XDOT OR AIRSPEED= 60 KNOTS

	X	Y	Z	L	M	N
U	-0.002046	-0.000017	-0.06631	-0.00024	-0.00420	0.00030
V	0.000014	-0.07404	0.00487	-0.00548	-0.00006	-0.00009
W	0.003764	0.00330	-0.55118	0.00156	0.01764	-0.00036
DB	0.12688	0.51850	0.46734	0.00376	0.39113	0.02811
DC	0.42640	0.04854	-9.35989	-0.00864	0.15286	0.00552
DS	0.00003	1.11989	-0.00044	0.40554	0.00000	0.00887
DR	0.00004	-0.05298	0.00008	-0.13452	0.00011	0.19699
P	0.00380	-2.03591	0.21481	-0.81835	0.02270	-0.01663
Q	2.35790	0.00340	-1.17918	0.00117	-1.68183	-0.07923
R	-0.04676	-0.22199	0.29535	-0.06732	0.00267	-0.03912

LONGITUDINAL F-MATRIX IS:

	1	2	3	4
1	-0.002046	0.003764	2.35790	-12.14647
2	-0.06631	-0.55118	99.02081	-1.85603
3	-0.00420	0.01764	-1.68183	0.00000
4	0.00000	0.00000	1.00000	0.00000

LONGITUDINAL G-MATRIX IS:

	1	2
1	0.12688	0.42640
2	0.46734	-9.35989
3	0.39113	0.15286
4	0.00000	0.00000

LATERAL F-MATRIX IS:

	1	2	3	4
1	-0.85072	0.00000	-0.08531	-0.00569
2	1.00000	0.00000	0.05774	0.00000
3	-0.08221	0.00000	-0.04570	-0.00053
4	-2.03591	12.14647	-100.42200	-0.07404

LATERAL G-MATRIX IS:

	1	2
1	0.42183	-0.05975
2	0.00000	0.00000
3	0.04139	0.19246
4	1.11989	-0.05298

THE 8TH ORDER F-MATRIX IS:

	1	2	3	4	5	6	7	8
1	-0.002046	0.000014	0.003764	0.00380	2.35790	-0.04676	-12.14647	0.00000
2	-0.06631	-0.07404	0.00330	-2.03591	0.00340	-100.42200	0.00902	12.14647
3	-0.06631	0.00487	-0.55118	0.21481	99.02081	0.29535	-1.85603	0.00000
4	-0.00017	0.00589	0.00157	-0.85072	-0.00096	-0.18531	0.00000	0.00000
5	0.00420	-0.00006	0.01764	0.02270	-1.68183	0.00267	0.00000	0.00000
6	0.12688	0.00003	-0.00024	-0.08221	-0.08183	0.04570	0.00000	0.00000
7	0.42640	0.00000	0.00000	0.00000	0.39999	0.0436	0.00000	0.00000
8	0.39113	0.00000	0.00000	1.00000	0.00023	0.05774	0.00000	0.00000

THE 8TH ORDER G-MATRIX IS:

	1	2	3	4
1	0.11588	0.42640	0.00003	0.00004
2	0.46734	0.04854	1.11989	-0.05298
3	0.46734	9.35989	-0.00044	0.00008
4	0.15286	-0.00867	0.42183	-0.05375
5	0.00000	0.00000	0.00000	0.00011
6	0.04139	-0.00591	0.04139	-0.01069
7	0.00000	0.00000	0.00000	0.00000
8	0.00000	0.00000	0.00000	0.00000

Figure G.3: Linear Model for Airspeed of 60 knots, Climb Rate 0 ft/min.

ATTENTION - ALL PERSONS IN THE AREA

[illegible]

CONSTITUTIONAL COURT

1970	1971	1972	1973	1974	1975
1.141355	1.141355	1.141355	1.141355	1.141355	1.141355
1.141355	1.141355	1.141355	1.141355	1.141355	1.141355
1.141355	1.141355	1.141355	1.141355	1.141355	1.141355
1.141355	1.141355	1.141355	1.141355	1.141355	1.141355
1.141355	1.141355	1.141355	1.141355	1.141355	1.141355

1947-1948

[illegible]

148

THE UNIVERSITY OF CHICAGO

[illegible]

SECRET - 14-00000

CONFIDENTIAL - SECURITY INFORMATION

Year	1983	1984	1985	1986	1987	1988
1	1.1000	1.1000	1.1000	1.1000	1.1000	1.1000
2	1.1000	1.1000	1.1000	1.1000	1.1000	1.1000
3	1.1000	1.1000	1.1000	1.1000	1.1000	1.1000
4	1.1000	1.1000	1.1000	1.1000	1.1000	1.1000
5	1.1000	1.1000	1.1000	1.1000	1.1000	1.1000
6	1.1000	1.1000	1.1000	1.1000	1.1000	1.1000
7	1.1000	1.1000	1.1000	1.1000	1.1000	1.1000
8	1.1000	1.1000	1.1000	1.1000	1.1000	1.1000
9	1.1000	1.1000	1.1000	1.1000	1.1000	1.1000
10	1.1000	1.1000	1.1000	1.1000	1.1000	1.1000

1998, 1999, 2000, 2001, 2002, 2003, 2004, 2005, 2006, 2007, 2008, 2009, 2010, 2011, 2012, 2013, 2014, 2015, 2016, 2017, 2018, 2019, 2020, 2021, 2022, 2023, 2024, 2025, 2026, 2027, 2028, 2029, 2030, 2031, 2032, 2033, 2034, 2035, 2036, 2037, 2038, 2039, 2040, 2041, 2042, 2043, 2044, 2045, 2046, 2047, 2048, 2049, 2050, 2051, 2052, 2053, 2054, 2055, 2056, 2057, 2058, 2059, 2060, 2061, 2062, 2063, 2064, 2065, 2066, 2067, 2068, 2069, 2070, 2071, 2072, 2073, 2074, 2075, 2076, 2077, 2078, 2079, 2080, 2081, 2082, 2083, 2084, 2085, 2086, 2087, 2088, 2089, 2090, 2091, 2092, 2093, 2094, 2095, 2096, 2097, 2098, 2099, 2100, 2101, 2102, 2103, 2104, 2105, 2106, 2107, 2108, 2109, 2110, 2111, 2112, 2113, 2114, 2115, 2116, 2117, 2118, 2119, 2120, 2121, 2122, 2123, 2124, 2125, 2126, 2127, 2128, 2129, 2130, 2131, 2132, 2133, 2134, 2135, 2136, 2137, 2138, 2139, 2140, 2141, 2142, 2143, 2144, 2145, 2146, 2147, 2148, 2149, 2150, 2151, 2152, 2153, 2154, 2155, 2156, 2157, 2158, 2159, 2160, 2161, 2162, 2163, 2164, 2165, 2166, 2167, 2168, 2169, 2170, 2171, 2172, 2173, 2174, 2175, 2176, 2177, 2178, 2179, 2180, 2181, 2182, 2183, 2184, 2185, 2186, 2187, 2188, 2189, 2190, 2191, 2192, 2193, 2194, 2195, 2196, 2197, 2198, 2199, 2200, 2201, 2202, 2203, 2204, 2205, 2206, 2207, 2208, 2209, 2210, 2211, 2212, 2213, 2214, 2215, 2216, 2217, 2218, 2219, 2220, 2221, 2222, 2223, 2224, 2225, 2226, 2227, 2228, 2229, 2230, 2231, 2232, 2233, 2234, 2235, 2236, 2237, 2238, 2239, 2240, 2241, 2242, 2243, 2244, 2245, 2246, 2247, 2248, 2249, 2250, 2251, 2252, 2253, 2254, 2255, 2256, 2257, 2258, 2259, 2260, 2261, 2262, 2263, 2264, 2265, 2266, 2267, 2268, 2269, 2270, 2271, 2272, 2273, 2274, 2275, 2276, 2277, 2278, 2279, 2280, 2281, 2282, 2283, 2284, 2285, 2286, 2287, 2288, 2289, 2290, 2291, 2292, 2293, 2294, 2295, 2296, 2297, 2298, 2299, 2300, 2301, 2302, 2303, 2304, 2305, 2306, 2307, 2308, 2309, 2310, 2311, 2312, 2313, 2314, 2315, 2316, 2317, 2318, 2319, 2320, 2321, 2322, 2323, 2324, 2325, 2326, 2327, 2328, 2329, 2330, 2331, 2332, 2333, 2334, 2335, 2336, 2337, 2338, 2339, 2340, 2341, 2342, 2343, 2344, 2345, 2346, 2347, 2348, 2349, 2350, 2351, 2352, 2353, 2354, 2355, 2356, 2357, 2358, 2359, 2360, 2361, 2362, 2363, 2364, 2365, 2366, 2367, 2368, 2369, 2370, 2371, 2372, 2373, 2374, 2375, 2376, 2377, 2378, 2379, 2380, 2381, 2382, 2383, 2384, 2385, 2386, 2387, 2388, 2389, 2390, 2391, 2392, 2393, 2394, 2395, 2396, 2397, 2398, 2399, 2400, 2401, 2402, 2403, 2404, 2405, 2406, 2407, 2408, 2409, 2410, 2411, 2412, 2413, 2414, 2415, 2416, 2417, 2418, 2419, 2420, 2421, 2422, 2423, 2424, 2425, 2426, 2427, 2428, 2429, 2430, 2431, 2432, 2433, 2434, 2435, 2436, 2437, 2438, 2439, 2440, 2441, 2442, 2443, 2444, 2445, 2446, 2447, 2448, 2449, 2450, 2451, 2452, 2453, 2454, 2455, 2456, 2457, 2458, 2459, 2460, 2461, 2462, 2463, 2464, 2465, 2466, 2467, 2468, 2469, 2470, 2471, 2472, 2473, 2474, 2475, 2476, 2477, 2478, 2479, 2480, 2481, 2482, 2483, 2484, 2485, 2486, 2487, 2488, 2489, 2490, 2491, 2492, 2493, 2494, 2495, 2496, 2497, 2498, 2499, 2500, 2501, 2502, 2503, 2504, 2505, 2506, 2507, 2508, 2509, 2510, 2511, 2512, 2513, 2514, 2515, 2516, 2517, 2518, 2519, 2520, 2521, 2522, 2523, 2524, 2525, 2526, 2527, 2528, 2529, 2530, 2531, 2532, 2533, 2534, 2535, 2536, 2537, 2538, 2539, 2540, 2541, 2542, 2543, 2544, 2545, 2546, 2547, 2548, 2549, 2550, 2551, 2552, 2553, 2554, 2555, 2556, 2557, 2558, 2559, 2560, 2561, 2562, 2563, 2564, 2565, 2566, 2567, 2568, 2569, 2570, 2571, 2572, 2573, 2574, 2575, 2576, 2577, 2578, 2579, 2580, 2581, 2582, 2583, 2584, 2585, 2586, 2587, 2588, 2589, 2590, 2591, 2592, 2593, 2594, 2595, 2596, 2597, 2598, 2599, 2600, 2601, 2602, 2603, 2604, 2605, 2606, 2607, 2608, 2609, 2610, 2611, 2612, 2613, 2614, 2615, 2616, 2617, 2618, 2619, 2620, 2621, 2622, 2623, 2624, 2625, 2626, 2627, 2628, 2629, 2630, 2631, 2632, 2633, 2634, 2635, 2636, 2637, 2638, 2639, 2640, 2641, 2642, 2643, 2644, 2645, 2646, 2647, 2648, 2649, 2650, 2651, 2652, 2653, 2654, 2655, 2656, 2657, 2658, 2659, 2660, 2661, 2662, 2663, 2664, 2665, 2666, 2667, 2668, 2669, 2670, 2671, 2672, 2673, 2674, 2675, 2676, 2677, 2678, 2679, 26

DATE: 1941.12.15

1. *Journal of Management Studies*, 1996, 33, 1, 1-14.

149

THIS IS DATA FOR IDOT= 500 FT/MIN AND IDOT OF AIR SPEED=

	1	2	3	4	5	6
1	-0.01924	-0.00039	-0.00155	-0.00075	-0.000519	-0.00019
2	-0.00012	-0.00041	-0.00050	-0.000511	-0.000002	-0.00014
3	-0.01901	-0.0001	-0.00448	-0.00149	-0.00190	-0.00015
4	-0.01495	-0.00059	-0.00490	-0.00059	-0.00148	-0.000107
5	-0.00052	-0.00051	-0.00001	-0.000432	-0.00001	-0.000181
6	-0.00007	-0.00003	-0.00012	-0.00007	-0.00001	-0.00002
7	-0.00007	-0.00001	-0.00049	-0.00021	-0.00001	-0.00002
8	-0.00043	-0.00038	-0.00049	-0.00049	-0.00049	-0.00049
9	-0.00194	-0.00019	-0.00049	-0.00019	-0.00019	-0.00049
10	-0.00019	-0.00019	-0.00019	-0.00019	-0.00019	-0.00019

LONGITUDINAL MATRIX 13:

LONGITUDINAL MATRIX 14:

	1	2	3	4	5	6
1	-0.01924	-0.00039	-0.00155	-0.00075	-0.000519	-0.00019
2	-0.00012	-0.00041	-0.00050	-0.000511	-0.000002	-0.00014
3	-0.01901	-0.0001	-0.00448	-0.00149	-0.00190	-0.00015
4	-0.01495	-0.00059	-0.00490	-0.00059	-0.00148	-0.000107

LONGITUDINAL MATRIX 15:

LONGITUDINAL MATRIX 16:

	1	2	3	4	5	6
1	-0.01924	-0.00039	-0.00155	-0.00075	-0.000519	-0.00019
2	-0.00012	-0.00041	-0.00050	-0.000511	-0.000002	-0.00014
3	-0.01901	-0.0001	-0.00448	-0.00149	-0.00190	-0.00015
4	-0.01495	-0.00059	-0.00490	-0.00059	-0.00148	-0.000107

LONGITUDINAL MATRIX 17:

LONGITUDINAL MATRIX 18:

	1	2	3	4	5	6
1	-0.01924	-0.00039	-0.00155	-0.00075	-0.000519	-0.00019
2	-0.00012	-0.00041	-0.00050	-0.000511	-0.000002	-0.00014
3	-0.01901	-0.0001	-0.00448	-0.00149	-0.00190	-0.00015
4	-0.01495	-0.00059	-0.00490	-0.00059	-0.00148	-0.000107
5	-0.00052	-0.00051	-0.00001	-0.000432	-0.00001	-0.000181
6	-0.00007	-0.00003	-0.00012	-0.00007	-0.00001	-0.00002

LONGITUDINAL MATRIX 19:

LONGITUDINAL MATRIX 20:

	1	2	3	4	5	6
1	-0.01924	-0.00039	-0.00155	-0.00075	-0.000519	-0.00019
2	-0.00012	-0.00041	-0.00050	-0.000511	-0.000002	-0.00014
3	-0.01901	-0.0001	-0.00448	-0.00149	-0.00190	-0.00015
4	-0.01495	-0.00059	-0.00490	-0.00059	-0.00148	-0.000107
5	-0.00052	-0.00051	-0.00001	-0.000432	-0.00001	-0.000181
6	-0.00007	-0.00003	-0.00012	-0.00007	-0.00001	-0.00002

Figure G.6: Linear Model for Airspeed of 60 knots, Climb Rate 500 ft/min.

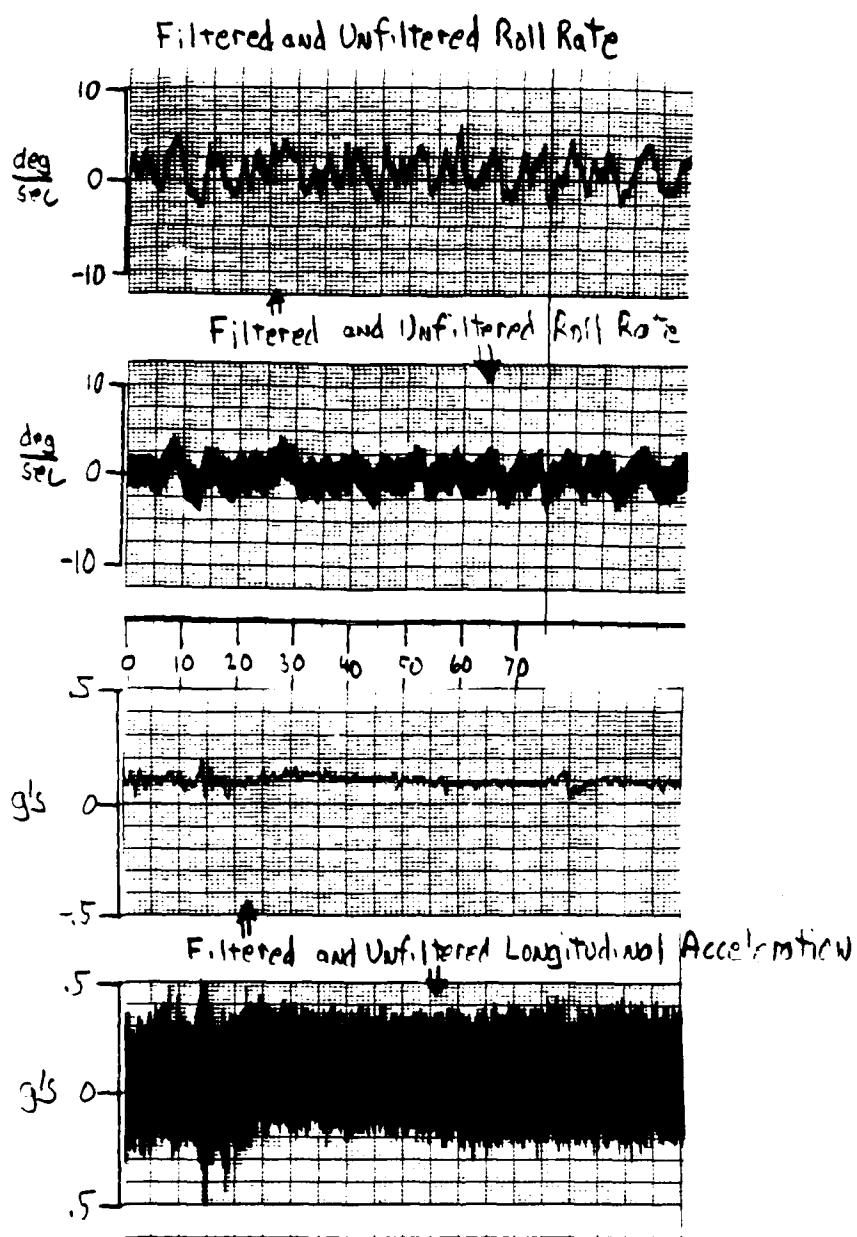


Figure H.2: Comparison of Filtered and Unfiltered Data in Flight. The importance of the filters is evident here where -data- is shown before and after the filter.

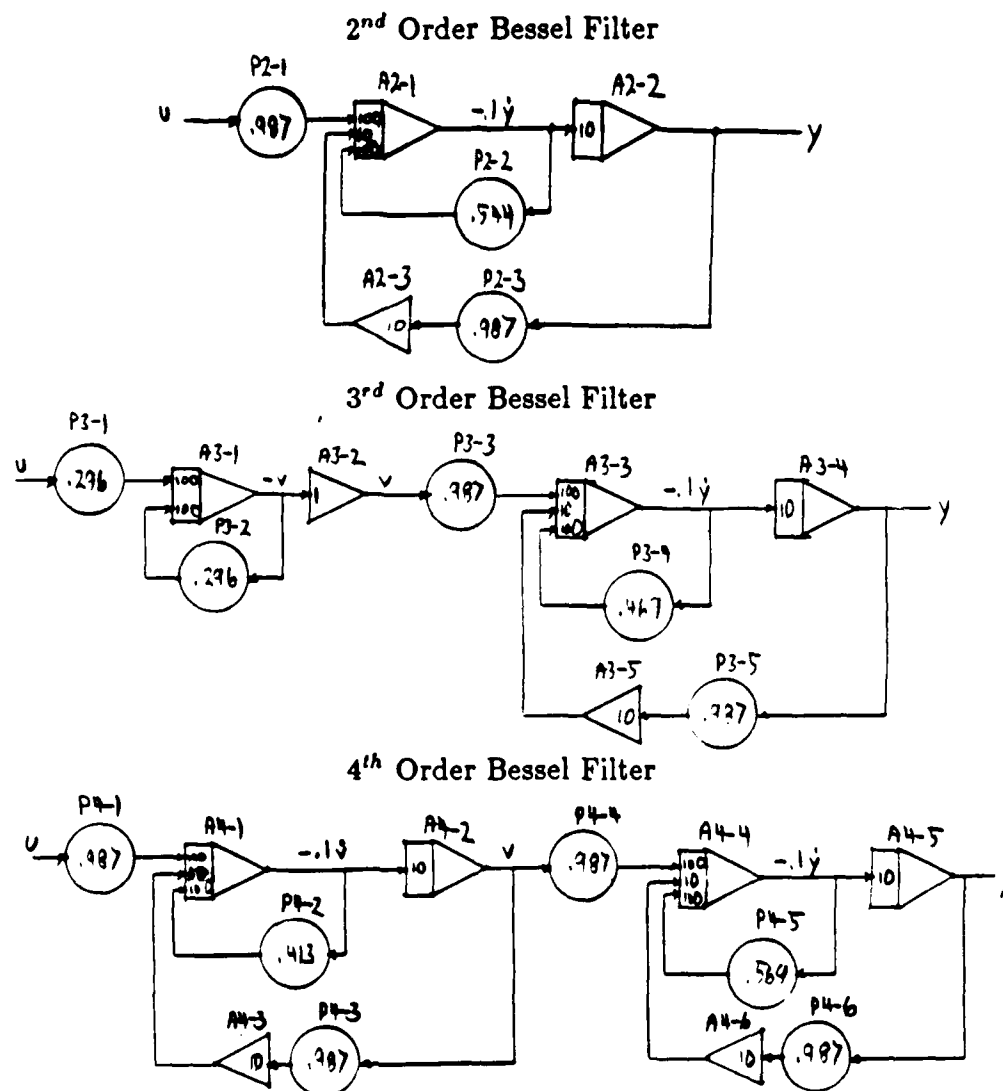


Figure H.1: Bessel Filter Analog Flow Diagrams. These filters were programmed on the airborne TR-48 analog computer.

shown in Figure H.2 where the unfiltered and filtered measurements are compared. By the end of flight test, all these filters were replaced by hardwired 3rd order Bessel filters located in a signal conditioning box.

Appendix H.

Bessel Filters

The Bessel filters described here were designed to eliminate the "3 per rev" and "6 per rev" harmonics at 11 Hz and 22 Hz due to the 225 rpm rotor. The break frequency was chosen at 5 Hz as a compromise between noise attenuation and measurement bandwidth. The actual filter designs came from reference 15. Nine filters were patched on the airborne TR-48 analog computer:

4th order- Body axis accelerations (A_x , A_y , A_z)

3rd order- Roll rate (p)

2nd order- Pitch rate (q), Yaw rate (r), Velocity (u), Altitude (h)

The transfer functions for these filters are shown below:

$$\begin{aligned} & \frac{974603}{s^4 + 98s^3 + 4323s^2 + 96906s + 974603} \\ & \frac{29220}{s^3 + 76s^2 + 2374s + 29220} \\ & \frac{987}{s^2 + 54s + 987} \end{aligned} \tag{H.1}$$

Figure H.1 shows the analog patch diagrams for these filters. Their effectiveness is

THIS IS DATA FOR ZDOT= -500 FT/MIN AND XDOT OR AIRSPEED= 20 KNOTS

	X	Y	Z	L	M	N
U	-0.00641	0.00087	-0.11816	-0.00012	0.00468	0.00050
V	0.00053	-0.11666	0.00208	-0.00619	-0.00088	0.00135
W	0.03589	0.00354	-0.37819	0.00067	0.00836	0.00028
DB	0.11223	0.03487	0.15524	-0.01678	0.34191	0.04829
DC	0.70594	0.06762	-8.31674	-0.01528	0.03169	0.00386
DS	-0.00007	1.15112	0.00073	0.41279	0.00000	0.01026
DR	-0.00005	-0.03522	-0.00002	-0.13336	-0.00015	0.20260
P	-0.00190	-1.40184	-0.09404	-0.66455	-0.05462	-0.01072
Q	2.52291	-0.02457	0.38001	0.07991	-1.31713	-0.16680
R	-0.02995	-0.15189	-0.44359	-0.04845	-0.00624	-0.04239

LONGITUDINAL F-MATRIX IS:

	1	2	3	4
1	-0.00641	0.03589	10.85624	-32.05505
2	-0.11816	-0.37819	33.78001	-3.05181
3	0.00468	0.00836	-1.31713	0.00000
4	0.00000	0.00000	1.00000	0.00000

LONGITUDINAL G-MATRIX IS:

	1	2
1	0.11223	0.70594
2	0.15524	-8.31674
3	0.34191	0.03169
4	0.00000	0.00000

LATERAL F-MATRIX IS:

	1	2	3	4
1	-0.68970	0.00000	-0.06718	-0.00584
2	1.00000	0.00000	0.09521	0.00000
3	-0.06389	0.00000	-0.04757	0.00090
4	-9.73517	32.05505	-33.55189	-0.11666

LATERAL G-MATRIX IS:

	1	2
1	0.42988	-0.05528
2	0.00000	0.00000
3	0.04340	0.19834
4	1.15112	-0.03522

THE 8TH ORDER F-MATRIX IS:

	1	2	3	4	5	6	7	8
1	-0.00641	0.00053	0.03589	-0.00190	10.85624	-0.02995	-32.05505	0.00000
2	0.00087	-0.11666	0.00354	-9.73517	-0.02457	-33.55189	0.02449	32.05403
3	-0.11816	0.00208	-0.37819	-0.09404	33.78001	-0.44359	-3.05181	0.00000
4	0.00008	-0.00584	0.00080	-0.68970	0.01469	-0.06718	0.00000	0.00000
5	0.00468	-0.00088	0.00836	-0.05462	-1.31713	-0.00624	0.00000	0.00000
6	0.00051	0.00090	0.00034	-0.06389	-0.16567	-0.04757	0.00000	0.00000
7	0.00000	0.00000	0.00000	0.00000	0.99997	0.00802	0.00000	0.00000
8	0.00000	0.00000	0.00000	1.00000	0.00076	0.09520	0.00000	0.00000

THE 8TH ORDER G-MATRIX IS:

	1	2	3	4
1	0.11223	0.70594	-0.00007	-0.00005
2	0.03487	0.06762	1.15112	-0.03522
3	0.15524	-8.31674	0.00073	-0.00002
4	0.00270	-0.01419	0.42988	-0.05528
5	0.34191	0.03169	0.00000	-0.00015
6	0.04847	0.00277	0.04740	-0.01060
7	0.00000	0.00000	0.00000	0.00000
8	0.00000	0.00000	0.00000	0.00000

Figure G.16: Linear Model for Airspeed of 20 knots, Climb Rate -500 ft/min.

THIS IS DATA FOR ZDOT= 500 FT/MIN AND XDOT OR AIRSPEED= 20 KNOTS

	X	Y	Z	L	M	N
U	0.00129	0.00122	-0.16248	0.00027	0.00965	0.00031
V	-0.00143	-0.10831	0.01176	-0.00563	0.00097	0.00131
W	0.03219	0.00341	-0.31546	0.00096	0.01226	0.00010
DB	0.10490	0.04843	0.16602	-0.00798	0.32750	0.03966
DC	0.69235	0.05507	-8.15329	-0.01434	0.00333	0.00324
DS	0.00013	1.14249	-0.00136	0.41067	0.00000	0.01006
DR	0.00008	-0.03710	0.00018	-0.13291	0.00027	0.20108
P	0.01602	-1.73729	0.31697	-0.74894	0.08761	-0.00977
Q	2.52136	-0.06817	-0.09012	0.04674	-1.34224	-0.13206
R	-0.17655	-0.19694	1.42350	-0.06014	0.01388	-0.04086

LONGITUDINAL F-MATRIX IS:

	1	2	3	4
1	0.00129	0.03219	-5.81197	-32.05065
2	-0.16248	-0.31546	33.30988	-3.09780
3	0.00965	0.01226	-1.34224	0.00000
4	0.00000	0.00000	1.00000	0.00000

LONGITUDINAL G-MATRIX IS:

	1	2
1	0.10490	0.69235
2	0.16602	-8.15329
3	0.32750	0.00333
4	0.00000	0.00000

LATERAL F-MATRIX IS:

	1	2	3	4
1	-0.77635	0.00000	-0.07861	-0.00527
2	1.00000	0.00000	0.09665	0.00000
3	-0.06962	0.00000	-0.04692	0.00090
4	6.59604	32.05065	-33.59694	-0.10831

LATERAL G-MATRIX IS:

	1	2
1	0.42761	-0.05543
2	0.00000	0.00000
3	0.04302	0.19681
4	1.14249	-0.03710

THE 8TH ORDER F-MATRIX IS:

	1	2	3	4	5	6	7	8
1	0.00129	-0.00143	0.03219	0.01602	-5.81197	-0.17655	-32.05065	0.00000
2	0.00122	-0.10831	0.00341	6.59604	-0.06817	-33.59694	0.02086	32.04992
3	-0.16248	0.01176	-0.31546	0.31697	33.30988	1.42350	-3.09780	0.00000
4	0.00965	-0.00527	0.00103	-0.77635	-0.00541	-0.07361	0.00000	0.00000
5	0.00965	0.00097	0.01226	0.08761	-1.34224	0.01388	0.00000	0.00000
6	0.00014	0.00090	0.00018	-0.06962	-0.13291	-0.04692	0.00000	0.00000
7	0.00000	0.00000	0.00000	0.00000	0.99998	0.00000	0.00000	0.00000
8	0.00000	0.00000	0.00000	1.00000	0.00000	0.00000	0.00000	0.00000

THE 8TH ORDER G-MATRIX IS:

	1	2	3	4
1	0.10490	0.69235	0.00013	0.00008
2	0.04843	0.05507	1.14249	-0.03710
3	0.16602	-8.15329	-0.00136	0.00018
4	0.00798	-0.01434	0.42761	-0.05543
5	0.32750	0.00333	0.00000	0.00027
6	0.00027	0.00020	0.04302	-0.01057
7	0.00000	0.00000	0.00000	0.00000
8	0.00000	0.00000	0.00000	0.00000

Figure G.15: Linear Model for Airspeed of 20 knots, Climb Rate 500 ft/min.

THIS IS DATA FOR ZDOT= 0 FT/MIN AND XDOT OR AIRSPEED= 20 KNOTS

	X	Y	Z	L	M	N
U	-0.00259	0.00095	-0.14099	0.00004	0.00679	0.00042
V	-0.00046	-0.11155	0.00524	-0.00591	-0.00006	0.00132
W	0.03412	0.00334	-0.34885	0.00077	0.00992	0.00021
DB	0.10849	0.04076	0.16269	-0.01247	0.33528	0.04371
DC	0.69883	0.06166	-8.21477	-0.01453	0.02107	0.00344
DS	0.00004	1.14599	-0.00040	0.41153	0.00000	0.01014
DR	0.00002	-0.03632	0.00012	-0.13309	0.00009	0.20170
P	0.00784	-1.57519	0.18709	-0.70862	0.03618	-0.00921
Q	2.51853	-0.04279	0.21293	0.06396	-1.31598	-0.14872
R	-0.09582	-0.17614	0.39539	-0.05466	-0.00294	-0.04145

LONGITUDINAL F-MATRIX IS:

	1	2	3	4
1	-0.00259	0.03412	2.51853	-32.05281
2	-0.14099	-0.34885	33.61293	-3.07534
3	0.00679	0.00992	-1.31598	0.00000
4	0.00000	0.00000	1.00000	0.00000

LONGITUDINAL G-MATRIX IS:

	1	2
1	0.10849	0.69883
2	0.16269	-8.21477
3	0.33528	0.02107
4	0.00000	0.00000

LATERAL F-MATRIX IS:

	1	2	3	4
1	-0.73454	0.00000	-0.07320	-0.00556
2	1.00000	0.00000	0.09595	0.00000
3	-0.06583	0.00000	-0.04709	0.00089
4	-1.57519	32.05281	-33.57614	-0.11155

LATERAL G-MATRIX IS:

	1	2
1	0.42853	-0.05537
2	0.00000	0.00000
3	0.04317	0.19743
4	1.14599	-0.03632

THE 8TH ORDER F-MATRIX IS:

	1	2	3	4	5	6	7	8
1	-0.00259	-0.00046	0.03412	0.00784	2.51853	-0.09582	-32.05281	0.00000
2	0.00095	-0.11155	0.00334	-1.57519	-0.04279	-33.57614	0.02265	32.05194
3	-0.14099	0.00524	-0.34885	0.18709	33.61293	0.39539	-3.07534	0.00000
4	0.00021	-0.00556	0.00088	-0.73454	-0.00558	-0.07320	0.00000	0.00000
5	0.00679	-0.00006	0.00992	0.03618	-1.31598	-0.00294	0.00000	0.00000
6	0.00044	0.00089	0.00028	-0.06583	-0.14872	-0.04709	0.00000	0.00000
7	0.00000	0.00000	0.00000	0.00000	0.99997	0.00735	0.00000	0.00000
8	0.00000	0.00000	0.00000	1.00000	0.00071	0.09594	0.00000	0.00000

THE 8TH ORDER G-MATRIX IS:

	1	2	3	4
1	0.10849	0.69883	0.00004	0.00002
2	0.04076	0.06166	1.14599	-0.03632
3	0.16269	-8.21477	-0.00040	0.00012
4	0.00489	-0.01359	0.42853	-0.05537
5	0.33528	0.02107	0.00000	0.00009
6	0.04409	-0.00279	0.04317	-0.01058
7	0.00000	0.00000	0.00000	0.00000
8	0.00000	0.00000	0.00000	0.00000

Figure G.14: Linear Model for Airspeed of 20 knots, Climb Rate 0 ft/min.

THIS IS DATA FOR ZDOT= -500 FT/MIN AND XDOT OR AIRSPEED=

	KNOTS					
	X	Y	Z	L	M	N
U	-0.02325	-0.00038	0.02826	-0.00037	0.00623	0.00050
V	-0.00097	-0.14525	0.00135	-0.00635	0.00008	-0.00070
W	0.03589	0.00301	-0.32741	0.00047	0.00203	0.00026
DB	0.11831	0.01249	0.02908	-0.02638	0.33695	0.05075
DC	0.94701	0.06887	-8.13578	-0.01448	0.02009	0.00098
DS	-0.00015	1.16274	0.00125	0.41643	0.00000	0.00924
DR	-0.00008	-0.05288	-0.00009	-0.13909	-0.00026	0.20448
P	0.03242	-1.32917	-0.17822	-0.65429	0.00108	0.00184
Q	2.59202	0.00144	0.46157	0.10871	-1.24188	-0.17600
R	-0.12040	-0.14595	0.31169	-0.04691	-0.00288	-0.04263

LONGITUDINAL F-MATRIX IS:

	1	2	3	4
1	-0.02325	0.03589	10.92535	-31.98588
2	0.02826	-0.32741	0.46157	-3.70723
3	0.00623	0.00203	-1.24188	0.00000
4	0.00000	0.00000	1.00000	0.00000

LONGITUDINAL G-MATRIX IS:

	1	2
1	0.11831	0.94701
2	0.02908	-8.13578
3	0.33695	0.02009
4	0.00000	0.00000

LATERAL F-MATRIX IS:

	1	2	3	4
1	-0.67402	0.00000	-0.06569	-0.00683
2	1.00000	0.00000	0.11590	0.00000
3	-0.05012	0.00000	-0.04769	-0.00123
4	-9.66250	31.98588	-0.14595	-0.14525

LATERAL G-MATRIX IS:

	1	2
1	0.43322	-0.06042
2	0.00000	0.00000
3	0.04264	0.19982
4	1.16274	-0.05288

THE 8TH ORDER F-MATRIX IS:

	1	2	3	4	5	6	7	8
1	-0.02325	-0.00097	0.03589	0.03242	10.92535	-0.12040	-31.98588	0.00000
2	-0.00038	-0.14525	0.00301	-9.58250	0.00144	-0.14595	0.03116	31.98475
3	0.02826	0.00135	-0.32741	-0.17822	0.46157	0.31169	-3.70723	0.00000
4	-0.00018	-0.00683	0.00059	-0.67402	0.04068	-0.06569	0.00000	0.00000
5	0.00623	0.00008	0.00203	0.00108	-1.24188	-0.00288	0.00000	0.00000
6	0.00047	-0.00123	0.00031	-0.05012	-0.17287	-0.04769	0.00000	0.00000
7	0.00000	0.00000	0.00000	0.00000	0.99996	0.00840	0.00000	0.00000
8	0.00000	0.00000	0.00000	1.00000	0.00097	0.11590	0.00000	0.00000

THE 8TH ORDER G-MATRIX IS:

	1	2	3	4
1	0.11831	0.94701	-0.00015	-0.00008
2	0.01249	0.06887	1.16274	-0.05288
3	0.02908	-8.13578	0.00125	-0.00009
4	-0.00660	-0.01454	0.43322	-0.06042
5	0.33695	0.02009	0.00000	-0.00026
6	0.05024	-0.00014	0.04264	-0.01106
7	0.00000	0.00000	0.00000	0.00000
8	0.00000	0.00000	0.00000	0.00000

Figure G.13: Linear Model for Airspeed of 0 knots, Climb Rate -500 ft/min.

THIS IS DATA FOR ZDOT= 500 FT/MIN AND XDQT OR AIRSPEED=

	0	KNOTS				
	X	Y	Z	L	M	N
U	-0.01857	-0.00001	0.02097	-0.00014	0.01356	0.00023
V	-0.00127	-0.13179	0.00975	-0.00583	0.00027	-0.00055
W	0.02894	0.00244	-0.25982	0.00052	0.00285	0.00018
DB	0.10910	0.01113	0.03148	-0.02213	0.31958	0.04294
DC	0.93710	0.05696	-8.05096	-0.01419	0.01764	0.00052
DS	0.00012	1.15717	-0.00110	0.41509	0.00000	0.00906
DR	0.00007	-0.05506	0.00005	-0.13905	0.00021	0.20349
P	-0.02869	-1.64496	0.35800	-0.73128	0.01003	-0.00148
Q	2.57072	0.00500	0.40010	0.09244	-1.24855	-0.14708
R	-0.08620	-0.18117	0.43277	-0.05704	0.01044	-0.04078

LONGITUDINAL F-MATRIX IS:

	1	2	3	4
1	-0.01857	0.02894	-5.76261	-31.98550
2	0.02097	-0.25982	0.40010	-3.71050
3	0.01356	0.00285	-1.24855	0.00000
4	0.00000	0.00000	1.00000	0.00000

LONGITUDINAL G-MATRIX IS:

	1	2
1	0.10910	0.93710
2	0.03148	-8.05096
3	0.31958	0.01764
4	0.00000	0.00000

LATERAL F-MATRIX IS:

	1	2	3	4
1	-0.75477	0.00000	-0.07538	-0.00624
2	1.00000	0.00000	0.11601	0.00000
3	-0.05966	0.00000	-0.04659	-0.00103
4	6.68837	31.98550	-0.18117	-0.13179

LATERAL G-MATRIX IS:

	1	2
1	0.43176	-0.06079
2	0.00000	0.00000
3	0.04234	0.19880
4	1.15717	-0.05506

THE 8TH ORDER F-MATRIX IS:

	1	2	3	4	5	6	7	8
1	-0.01857	-0.00127	0.02894	-0.02869	-5.76261	-0.08620	-31.98550	0.00000
2	-0.00001	-0.13179	0.00244	6.68837	0.00500	-0.18117	0.02737	31.98464
3	0.02097	0.00975	-0.25982	0.35800	0.40010	0.43277	-3.71050	0.00000
4	-0.00005	-0.00624	0.00061	-0.75477	0.03562	-0.07538	0.00000	0.00000
5	0.01356	0.00027	0.00285	0.01003	-1.24855	0.01044	0.00000	0.00000
6	0.00023	-0.00103	0.00023	-0.05966	-0.14433	-0.04659	0.00000	0.00000
7	0.00000	0.00000	0.00000	0.00000	0.99997	0.00778	0.00000	0.00000
8	0.00000	0.00000	0.00000	1.00000	0.00086	0.11600	0.00000	0.00000

THE 8TH ORDER G-MATRIX IS:

	1	2	3	4
1	0.10910	0.93710	0.00012	0.00007
2	0.01113	0.05696	1.15717	-0.05506
3	0.03148	-8.05096	-0.00110	0.00005
4	-0.00539	-0.01442	0.43176	-0.06079
5	0.31958	0.01764	0.00000	0.00021
6	0.04234	-0.00059	0.04234	-0.01105
7	0.00000	0.00000	0.00000	0.00000
8	0.00000	0.00000	0.00000	0.00000

Figure G.12: Linear Model for Airspeed of 0 knots, Climb Rate 500 ft/min.

THIS IS DATA FOR ZDOT= 0 FT/MIN AND XDOT OR AIRSPEED=

	KNOTS					
	X	Y	Z	L	M	N
U	-0.02114	-0.00019	0.02484	-0.00028	0.00925	0.00040
V	-0.00085	-0.13712	0.00374	-0.00608	0.00017	-0.00062
W	0.03259	0.00265	-0.29557	0.00048	0.00234	0.00022
DB	0.11408	0.01175	0.30310	-0.02410	0.32921	0.04655
DC	0.93867	0.06353	-8.06188	-0.01403	0.01905	0.00072
DS	0.00000	1.15902	-0.00002	0.41552	0.00000	0.00914
DR	-0.00001	-0.05395	0.00011	-0.13896	0.00000	0.20382
P	0.02051	1.49383	0.04190	-0.69495	0.04267	0.00080
Q	2.58521	0.00414	0.43507	0.10020	-1.22925	-0.16052
R	-0.10552	-0.16450	0.36222	-0.05220	-0.00433	-0.04172

LONGITUDINAL F-MATRIX IS:

	1	2	3	4
1	-0.02114	0.03259	2.58521	-31.98577
2	0.02484	-0.29557	0.43507	-3.70815
3	0.00925	0.00234	-1.22925	0.00000
4	0.00000	0.00000	1.00000	0.00000

LONGITUDINAL G-MATRIX IS:

	1	2
1	0.11408	0.93867
2	0.30310	-8.06188
3	0.32921	0.01905
4	0.00000	0.00000

LATERAL F-MATRIX IS:

	1	2	3	4
1	-0.71638	0.00000	-0.07077	-0.00652
2	1.00000	0.00000	0.11593	0.00000
3	-0.05442	0.00000	-0.04718	-0.00112
4	-1.49383	31.98577	-0.16450	-0.13712

LATERAL G-MATRIX IS:

	1	2
1	0.43224	-0.06056
2	0.00000	0.00000
3	0.04246	0.19915
4	1.15902	-0.05395

THE 8TH ORDER F-MATRIX IS:

	1	2	3	4	5	6	7	8
1	-0.02114	-0.00085	0.03259	0.02051	2.58521	-0.10552	-31.98577	0.00000
2	-0.00019	-0.13712	0.00265	-1.49383	0.00414	-0.16450	0.02922	31.98478
3	0.02484	0.00374	-0.29557	0.04190	0.43507	0.36222	-3.70815	0.00000
4	-0.00028	-0.00652	0.00048	-0.71638	0.07817	-0.07077	0.00000	0.00000
5	0.00925	0.00017	0.00234	0.04267	-1.22925	-0.00433	0.00000	0.00000
6	0.00039	-0.00112	0.00027	-0.05442	-0.15758	-0.04718	0.00000	0.00000
7	0.00000	0.00000	0.00000	0.00000	0.99997	0.00788	0.00000	0.00000
8	0.00000	0.00000	0.00000	1.00000	0.00091	0.11593	0.00000	0.00000

THE 8TH ORDER G-MATRIX IS:

	1	2	3	4
1	0.11408	0.93867	0.00000	-0.00001
2	0.01175	0.06353	1.15902	-0.05395
3	0.30310	-8.06188	-0.00002	0.00011
4	-0.00596	-0.01418	0.43224	-0.06056
5	0.32921	0.01905	0.00000	0.00000
6	0.04609	-0.00017	0.04246	-0.01105
7	0.00000	0.00000	0.00000	0.00000
8	0.00000	0.00000	0.00000	0.00000

Figure G.11: Linear Model for Airspeed of 0 knots, Climb Rate 0 ft/min.

IS IS DATA FOR ZDOT=				-500		FT/MIN AND XDOT OR AIRSPEED=	
-20		KNOTS					
X	Y	Z	L	M	N		
U	-0.04431	-0.00170	0.18208	-0.00058	0.00498	0.00033	
V	-0.00184	-0.14266	-0.00104	-0.00631	0.00121	-0.00271	
W	0.04284	0.00272	-0.34017	0.00049	-0.00447	0.00025	
DB	0.13510	-0.01042	-0.09822	-0.03337	0.34340	0.04849	
DC	1.22694	0.06576	-8.22802	-0.01187	0.01087	-0.00194	
DS	-0.00025	1.16691	0.00182	0.41832	0.00000	0.00791	
DR	-0.00013	-0.07451	-0.00001	-0.14503	-0.00037	0.20502	
P	0.07629	-1.41972	-0.31843	-0.68419	0.06421	0.01341	
Q	2.54761	0.02677	0.57144	0.12586	-1.31840	-0.16553	
R	-0.21772	-0.15751	1.17901	-0.05023	-0.00735	-0.04199	

LONGITUDINAL F-MATRIX IS:				LONGITUDINAL G-MATRIX IS:		
1	2	3	4	1	2	
1	-0.04431	0.04284	10.88094	-31.90117	0.13510	1.22694
2	0.18208	-0.34017	-32.82856	-4.37670	-0.09822	-8.22802
3	0.00498	-0.00447	-1.31840	0.00000	0.34340	0.01087
4	0.00000	0.00000	1.00000	0.00000	0.00000	0.00000

LATERAL F-MATRIX IS:				LATERAL G-MATRIX IS:		
1	2	3	4	1	2	
1	-0.70016	0.00000	-0.06885	-0.00761	0.43462	-0.06633
2	1.00000	0.00000	0.13720	0.00000	0.00000	0.00000
3	-0.04049	0.00000	-0.04729	-0.00330	0.04137	0.17992
4	-9.75305	31.90117	32.24249	-0.14266	1.16691	-0.07451

THE 8TH ORDER F-MATRIX IS:								
1	2	3	4	5	6	7	8	
1	-0.04431	-0.00184	0.04284	0.07629	10.88094	-0.21772	-31.90117	0.00000
2	-0.00170	-0.14266	0.00272	-9.75305	0.02677	32.24249	0.03467	31.90117
3	0.18208	-0.00104	-0.34017	-0.31843	-32.82856	1.17901	-4.37670	0.00000
4	-0.00048	-0.00761	0.00061	-0.70016	0.06259	-0.06885	0.00000	0.00000
5	0.00498	0.00121	-0.00447	0.06421	-1.31840	-0.00735	0.00000	0.13510
6	0.00029	-0.00330	0.00030	-0.04049	-0.15072	-0.04729	0.00000	0.00000
7	0.00000	0.00000	0.00000	0.00000	0.99997	0.00792	0.00000	0.00000
8	0.00000	0.00000	0.00000	1.00000	0.00109	0.13719	0.00000	0.00000

THE 8TH ORDER G-MATRIX IS:				
1	2	3	4	
1	0.13510	1.22694	-0.00025	-0.00013
2	-0.01042	0.06576	1.16691	-0.07451
3	-0.09822	-8.22802	0.00182	-0.00001
4	-0.01473	-0.01303	0.41462	-0.06633
5	0.34340	0.01087	0.00000	-0.00037
6	0.04736	-0.00194	0.04137	-0.01152
7	0.00000	0.00000	0.00000	0.00000
8	0.00000	0.00000	0.00000	0.00000

Figure G.10: Linear Model for Airspeed of -20 knots, Climb Rate -500 ft/min.

THIS IS DATA FOR ZDOT= 500 FT/MIN AND XDOT OR AIRSPEED=

	-20 KNOTS					
	X	Y	Z	L	M	N
U	-0.04422	-0.00151	0.21206	-0.00063	0.01045	0.00008
V	-0.00058	-0.12523	0.00570	-0.00574	-0.00033	-0.00242
W	0.03283	0.00221	-0.27064	0.00530	-0.00731	0.00030
DB	0.12940	-0.02766	-0.10331	-0.03274	0.32931	0.03949
DC	1.20437	0.05345	-8.06621	-0.01071	0.03615	-0.00256
DS	0.00007	1.15921	-0.00050	0.41645	0.00001	0.00772
DR	0.00003	-0.07663	-0.00001	-0.14475	0.00009	0.20366
P	-0.05257	-1.76946	0.30099	-0.76640	-0.05053	0.00403
Q	2.46181	0.08166	0.93621	0.12011	-1.33744	-0.12984
R	0.00776	-0.18787	-0.45957	-0.06008	0.00643	-0.03976

LONGITUDINAL F-MATRIX IS:

	1	2	3	4
1	-0.04422	0.03283	-5.87152	-31.90770
2	0.21206	-0.27064	-32.46379	-4.32879
3	0.01045	-0.00731	-1.33744	0.00000
4	0.00000	0.00000	1.00000	0.00000

LONGITUDINAL G-MATRIX IS:

	1	2
1	0.12940	1.20437
2	-0.10331	-8.06621
3	0.32931	0.03615
4	0.00000	0.00000

LATERAL F-MATRIX IS:

	1	2	3	4
1	-0.78875	0.00000	-0.07810	-0.00690
2	1.00000	0.00000	0.17567	0.00000
3	-0.05677	0.00000	-0.04578	-0.00295
4	8.56387	31.90770	33.21213	-0.12523

LATERAL G-MATRIX IS:

	1	2
1	0.43262	-0.06659
2	0.00000	0.00000
3	0.04107	0.19853
4	1.15921	-0.07663

THE 8TH ORDER F-MATRIX IS:

	1	2	3	4	5	6	7	8
1	-0.04422	-0.00058	0.03283	-0.05257	-5.87152	0.00776	-31.90770	0.00000
2	-0.00151	-0.12523	0.00221	8.56387	0.08166	33.21213	0.02901	31.90699
3	0.21206	0.00570	-0.27064	0.30099	-32.46379	-0.45957	-4.32879	0.00000
4	-0.00062	-0.00690	0.00530	-0.78875	0.07115	-0.07810	0.00000	0.00000
5	0.01045	-0.00731	-0.00731	-0.05053	-1.33744	0.00643	0.00000	0.00000
6	0.00007	-0.00295	0.00073	-0.05677	-0.12436	-0.04578	0.00000	0.00000
7	0.00000	0.00000	0.00000	0.00000	0.39998	0.00570	0.00000	0.00000
8	0.00000	0.00000	0.00000	1.00000	0.00091	0.17566	0.00000	0.00000

THE 8TH ORDER G-MATRIX IS:

	1	2	3	4
1	0.12940	1.20437	0.00007	0.00000
2	-0.02766	0.05345	1.15921	-0.07663
3	-0.10331	-8.06621	-0.00050	-0.00001
4	-0.01773	-0.01208	0.41252	-0.06659
5	0.32931	0.03615	0.00001	0.00009
6	0.03812	-0.00349	0.04107	-0.01151
7	0.00000	0.00000	0.00000	0.00000
8	0.00000	0.00000	0.00000	0.00000

Figure G.9: Linear Model for Airspeed of -20 knots, Climb Rate 500 ft/min.

THIS IS DATA FOR ZDOT= 0 FT/MIN AND XDOT OR AIRSPEED=

	KNOTS					
	X	Y	Z	L	M	N
U	-0.04449	-0.00149	0.19817	-0.00059	0.00727	0.00023
V	-0.00075	-0.13255	0.00100	-0.00601	0.00054	-0.00254
W	0.03811	0.00238	-0.30703	0.00050	-0.00562	0.00026
DB	0.13262	-0.01824	-0.10291	-0.03269	0.33689	0.04375
DC	1.21170	0.05992	-8.12808	-0.01116	0.02013	-0.00218
DS	-0.00007	1.16217	0.00051	0.41715	0.00000	0.00782
DR	-0.00006	-0.07540	0.00014	-0.14475	-0.00012	0.20419
P	0.05290	-1.60055	-0.19944	-0.72706	0.05658	0.00866
Q	2.51458	0.05194	0.69186	0.12183	-1.31503	-0.14697
R	-0.12437	-0.17280	0.47219	-0.05530	-0.01058	-0.04088

LONGITUDINAL F-MATRIX IS:

	1	2	3	4
1	-0.04449	0.03811	2.51458	-31.90471
2	0.19817	-0.30703	-32.70814	-4.35079
3	0.00727	-0.00562	-1.31503	0.00000
4	0.00000	0.00000	1.00000	0.00000

LONGITUDINAL G-MATRIX IS:

	1	2
1	0.13262	1.21170
2	-0.10291	-8.12808
3	0.33689	0.02013
4	0.00000	0.00000

LATERAL F-MATRIX IS:

	1	2	3	4
1	-0.74630	0.00000	-0.07363	-0.00723
2	1.00000	0.00000	0.13637	0.00000
3	-0.04887	0.00000	-0.04656	-0.00310
4	-1.60055	31.90471	33.22720	-0.13255

LATERAL G-MATRIX IS:

	1	2
1	0.43338	-0.06638
2	0.00000	0.00000
3	0.04123	0.19907
4	1.16217	-0.07540

THE 8TH ORDER F-MATRIX IS:

	1	2	3	4	5	6	7	8
1	-0.04449	-0.00075	0.03811	0.05290	2.51458	-0.12437	-31.90471	0.00000
2	-0.00149	-0.13255	0.00238	-1.60055	0.05194	33.22720	0.03181	31.90385
3	0.19817	0.00100	-0.30703	-0.19944	-32.70814	0.47219	-4.35079	0.00000
4	-0.00052	-0.00723	0.00062	-0.74630	-0.06597	-0.07363	0.00000	0.00000
5	0.00727	0.00054	-0.00562	0.05658	-1.31503	-0.01058	0.00000	0.00000
6	0.00019	-0.00310	0.00031	-0.04887	-0.14188	-0.04656	0.00000	0.00000
7	0.00000	0.00000	0.00000	0.00000	0.99997	0.00731	0.00000	0.00000
8	0.00000	0.00000	0.00000	1.00000	0.00100	0.13637	0.00000	0.00000

THE 8TH ORDER G-MATRIX IS:

	1	2	3	4
1	0.13262	1.21170	-0.00007	-0.00006
2	-0.01824	0.05992	1.16217	-0.07540
3	-0.10291	-8.12808	0.00051	0.00014
4	-0.01395	-0.01239	0.43338	-0.06638
5	0.33689	0.02013	0.00000	-0.00012
6	0.04252	-0.00314	0.04123	-0.01151
7	0.00000	0.00000	0.00000	0.00000
8	0.00000	0.00000	0.00000	0.00000

Figure G.8: Linear Model for Airspeed of -20 knots, Climb Rate 0 ft/min.

THIS IS DATA FOR 6000 FT/min AND 6000 ft/min

SV	NOTS	Z	L	M	N
0	0.0000	0.0000	0.0000	0.0000	0.0000
1	0.0001	0.0001	0.0001	0.0001	0.0001
2	0.0002	0.0002	0.0002	0.0002	0.0002
3	0.0003	0.0003	0.0003	0.0003	0.0003
4	0.0004	0.0004	0.0004	0.0004	0.0004
5	0.0005	0.0005	0.0005	0.0005	0.0005
6	0.0006	0.0006	0.0006	0.0006	0.0006
7	0.0007	0.0007	0.0007	0.0007	0.0007
8	0.0008	0.0008	0.0008	0.0008	0.0008
9	0.0009	0.0009	0.0009	0.0009	0.0009
10	0.0010	0.0010	0.0010	0.0010	0.0010
11	0.0011	0.0011	0.0011	0.0011	0.0011
12	0.0012	0.0012	0.0012	0.0012	0.0012
13	0.0013	0.0013	0.0013	0.0013	0.0013
14	0.0014	0.0014	0.0014	0.0014	0.0014
15	0.0015	0.0015	0.0015	0.0015	0.0015
16	0.0016	0.0016	0.0016	0.0016	0.0016
17	0.0017	0.0017	0.0017	0.0017	0.0017
18	0.0018	0.0018	0.0018	0.0018	0.0018
19	0.0019	0.0019	0.0019	0.0019	0.0019
20	0.0020	0.0020	0.0020	0.0020	0.0020
21	0.0021	0.0021	0.0021	0.0021	0.0021
22	0.0022	0.0022	0.0022	0.0022	0.0022
23	0.0023	0.0023	0.0023	0.0023	0.0023
24	0.0024	0.0024	0.0024	0.0024	0.0024
25	0.0025	0.0025	0.0025	0.0025	0.0025
26	0.0026	0.0026	0.0026	0.0026	0.0026
27	0.0027	0.0027	0.0027	0.0027	0.0027
28	0.0028	0.0028	0.0028	0.0028	0.0028
29	0.0029	0.0029	0.0029	0.0029	0.0029
30	0.0030	0.0030	0.0030	0.0030	0.0030
31	0.0031	0.0031	0.0031	0.0031	0.0031
32	0.0032	0.0032	0.0032	0.0032	0.0032
33	0.0033	0.0033	0.0033	0.0033	0.0033
34	0.0034	0.0034	0.0034	0.0034	0.0034
35	0.0035	0.0035	0.0035	0.0035	0.0035
36	0.0036	0.0036	0.0036	0.0036	0.0036
37	0.0037	0.0037	0.0037	0.0037	0.0037
38	0.0038	0.0038	0.0038	0.0038	0.0038
39	0.0039	0.0039	0.0039	0.0039	0.0039
40	0.0040	0.0040	0.0040	0.0040	0.0040
41	0.0041	0.0041	0.0041	0.0041	0.0041
42	0.0042	0.0042	0.0042	0.0042	0.0042
43	0.0043	0.0043	0.0043	0.0043	0.0043
44	0.0044	0.0044	0.0044	0.0044	0.0044
45	0.0045	0.0045	0.0045	0.0045	0.0045
46	0.0046	0.0046	0.0046	0.0046	0.0046
47	0.0047	0.0047	0.0047	0.0047	0.0047
48	0.0048	0.0048	0.0048	0.0048	0.0048
49	0.0049	0.0049	0.0049	0.0049	0.0049
50	0.0050	0.0050	0.0050	0.0050	0.0050
51	0.0051	0.0051	0.0051	0.0051	0.0051
52	0.0052	0.0052	0.0052	0.0052	0.0052
53	0.0053	0.0053	0.0053	0.0053	0.0053
54	0.0054	0.0054	0.0054	0.0054	0.0054
55	0.0055	0.0055	0.0055	0.0055	0.0055
56	0.0056	0.0056	0.0056	0.0056	0.0056
57	0.0057	0.0057	0.0057	0.0057	0.0057
58	0.0058	0.0058	0.0058	0.0058	0.0058
59	0.0059	0.0059	0.0059	0.0059	0.0059
60	0.0060	0.0060	0.0060	0.0060	0.0060
61	0.0061	0.0061	0.0061	0.0061	0.0061
62	0.0062	0.0062	0.0062	0.0062	0.0062
63	0.0063	0.0063	0.0063	0.0063	0.0063
64	0.0064	0.0064	0.0064	0.0064	0.0064
65	0.0065	0.0065	0.0065	0.0065	0.0065
66	0.0066	0.0066	0.0066	0.0066	0.0066
67	0.0067	0.0067	0.0067	0.0067	0.0067
68	0.0068	0.0068	0.0068	0.0068	0.0068
69	0.0069	0.0069	0.0069	0.0069	0.0069
70	0.0070	0.0070	0.0070	0.0070	0.0070
71	0.0071	0.0071	0.0071	0.0071	0.0071
72	0.0072	0.0072	0.0072	0.0072	0.0072
73	0.0073	0.0073	0.0073	0.0073	0.0073
74	0.0074	0.0074	0.0074	0.0074	0.0074
75	0.0075	0.0075	0.0075	0.0075	0.0075
76	0.0076	0.0076	0.0076	0.0076	0.0076
77	0.0077	0.0077	0.0077	0.0077	0.0077
78	0.0078	0.0078	0.0078	0.0078	0.0078
79	0.0079	0.0079	0.0079	0.0079	0.0079
80	0.0080	0.0080	0.0080	0.0080	0.0080
81	0.0081	0.0081	0.0081	0.0081	0.0081
82	0.0082	0.0082	0.0082	0.0082	0.0082
83	0.0083	0.0083	0.0083	0.0083	0.0083
84	0.0084	0.0084	0.0084	0.0084	0.0084
85	0.0085	0.0085	0.0085	0.0085	0.0085
86	0.0086	0.0086	0.0086	0.0086	0.0086
87	0.0087	0.0087	0.0087	0.0087	0.0087
88	0.0088	0.0088	0.0088	0.0088	0.0088
89	0.0089	0.0089	0.0089	0.0089	0.0089
90	0.0090	0.0090	0.0090	0.0090	0.0090
91	0.0091	0.0091	0.0091	0.0091	0.0091
92	0.0092	0.0092	0.0092	0.0092	0.0092
93	0.0093	0.0093	0.0093	0.0093	0.0093
94	0.0094	0.0094	0.0094	0.0094	0.0094
95	0.0095	0.0095	0.0095	0.0095	0.0095
96	0.0096	0.0096	0.0096	0.0096	0.0096
97	0.0097	0.0097	0.0097	0.0097	0.0097
98	0.0098	0.0098	0.0098	0.0098	0.0098
99	0.0099	0.0099	0.0099	0.0099	0.0099
100	0.0100	0.0100	0.0100	0.0100	0.0100

Figure G.7: Linear Model for Airspeed of 60 knots, Climb Rate -500 ft/min.

Appendix I.

Flight Software

This appendix lists the flight computer software unique to this project. It is written in Sperry 1819A assembly code and internally documented. Three different sets of the code are shown. The initialization code was executed whenever the experimental control system was disengaged. It did such things as:

- reset the compensator states to zero
- set the trim values of controls and states to the current values of these variables in preparation for system engage

The experimental controller subroutines computed the control laws, described in Chapters 3 and 4, and were executed at 20 Hz. Both the longitudinal CAS and hover controller are shown. The last item shown in this appendix are the instructions which reserve memory for the variables and constants unique to the subroutines.

Initialization Code.

PAGE 32

1919A ASSEMBLER, VERSION 1.0 NOV643 10/02/84 SECTION 1

```

1379      0
1380      0
1381      0
1382      0
1383      0
1384      0
1385      0
1386      0
1387      0
1388      002800 120748      ENIAL      IPATH
1389      002601 442156      STRAL      MATH
1390      002602 442344      STRAL      MATH
1391      002603 442603      STRAL      OATH
1392      002604 442751      STRAL      PPATH
1393      002605 120753      ENIAL      INSMI
1394      002606 442804      STRAL      OATH
1395      002607 443152      STRAL      PPATH
1396      002610 120752      ENIAL      KNEPO
1397      002611 442157      STRAL      MATH
1398      002612 442344      STRAL      MATH
1399      002613 442605      STRAL      PPATH
1400      002614 442153      ENIAL      PPATH
1401      002615 120765      STRAL      VSI
1402      002616 442160      STRAL      MATH
1403      002617 442346      STRAL      MATH
1404      002620 442308      STRAL      PPATH
1405      002621 443154      STRAL      PPATH
1406      002622 121134      ENIAL      XPIT
1407      002623 442662      STRAL      OATH
1408      002624 442330      STRAL      PPATH
1409      002625 121147      ENIAL      XPCY
1410      002626 442603      STRAL      OATH
1411      002627 443231      STRAL      PPATH
1412      002630 121135      ENIAL      YPIT
1413      002631 442673      STRAL      OATH
1414      002632 443241      STRAL      PPATH
1415      002633 121130      ENIAL      YPCY
1416      002634 442674      STRAL      OATH
1417      002635 443242      STRAL      PPATH
1418      002636 121136      ENIAL      ZPIT
1419      002637 442704      STRAL      OATH
1420      002640 442322      STRAL      PPATH
1421      002641 402712      STRZ      OACI
1422      002642 402760      STRZ      PACT
1423      002643 402714      STRZ      OACI
1424      002644 402762      STRZ      PACT
1425      002645 402716      STRZ      OACI
1426      002646 402764      STRZ      PACT
1427      002647 402713      STRZ      OACI+1
1428      002650 402761      STRZ      PACT+1
1429      002651 402715      STRZ      OACI+1
1430      002652 402763      STRZ      PACT+1
1431      002653 402717      STRZ      OACI+1
1432      002654 402765      STRZ      PACT+1
1433      002655 402672      STRZ      OACLO
1434      002656 402740      STRZ      PACTLO
1435      002657 402703      STRZ      OACLO

```

GET THETA AT ENGAGE
 STORE THETA AT ENGAGE
 STORE THETA AT ENGAGE
 STORE THETA AT ENGAGE
 GET PHI AT ENGAGE
 STORE PHI AT ENGAGE
 STORE PHI AT ENGAGE
 GET THE AIRSPEED AT ENGAGE
 STORE AIRSPEED AT ENGAGE
 STORE AIRSPEED AT ENGAGE
 STORE AIRSPEED AT ENGAGE
 STORE AIRSPEED AT ENGAGE
 GET VERT VELOCITY AT ENGAGE
 STORE VERTICAL VELOCITY AT ENGAGE
 STORE VERTICAL VELOCITY AT ENGAGE
 STORE VERTICAL VELOCITY AT ENGAGE
 GET RUNWAY X POSITION
 STORE RUNWAY X POSITION
 GET BODY X POSITION
 STORE BODY X POSITION
 GET RUNWAY Y POSITION
 STORE RUNWAY Y POSITION
 GET BODY Y POSITION
 STORE BODY Y POSITION
 GET Z POSITION
 STORE Z POSITION
 GET P2 POSITION
 STORE P2 POSITION
 GET P1 POSITION
 STORE P1 POSITION
 GET P3 POSITION
 STORE P3 POSITION
 GET P4 POSITION
 STORE P4 POSITION
 GET P5 POSITION
 STORE P5 POSITION
 GET P6 POSITION
 STORE P6 POSITION
 GET P7 POSITION
 STORE P7 POSITION
 GET P8 POSITION
 STORE P8 POSITION
 GET P9 POSITION
 STORE P9 POSITION
 GET P10 POSITION
 STORE P10 POSITION
 GET P11 POSITION
 STORE P11 POSITION
 GET P12 POSITION
 STORE P12 POSITION
 GET P13 POSITION
 STORE P13 POSITION
 GET P14 POSITION
 STORE P14 POSITION
 GET P15 POSITION
 STORE P15 POSITION
 GET P16 POSITION
 STORE P16 POSITION
 GET P17 POSITION
 STORE P17 POSITION
 GET P18 POSITION
 STORE P18 POSITION
 GET P19 POSITION
 STORE P19 POSITION
 GET P20 POSITION
 STORE P20 POSITION
 GET P21 POSITION
 STORE P21 POSITION
 GET P22 POSITION
 STORE P22 POSITION
 GET P23 POSITION
 STORE P23 POSITION
 GET P24 POSITION
 STORE P24 POSITION
 GET P25 POSITION
 STORE P25 POSITION
 GET P26 POSITION
 STORE P26 POSITION
 GET P27 POSITION
 STORE P27 POSITION
 GET P28 POSITION
 STORE P28 POSITION
 GET P29 POSITION
 STORE P29 POSITION
 GET P30 POSITION
 STORE P30 POSITION
 GET P31 POSITION
 STORE P31 POSITION
 GET P32 POSITION
 STORE P32 POSITION
 GET P33 POSITION
 STORE P33 POSITION
 GET P34 POSITION
 STORE P34 POSITION
 GET P35 POSITION
 STORE P35 POSITION
 GET P36 POSITION
 STORE P36 POSITION
 GET P37 POSITION
 STORE P37 POSITION
 GET P38 POSITION
 STORE P38 POSITION
 GET P39 POSITION
 STORE P39 POSITION
 GET P40 POSITION
 STORE P40 POSITION
 GET P41 POSITION
 STORE P41 POSITION
 GET P42 POSITION
 STORE P42 POSITION
 GET P43 POSITION
 STORE P43 POSITION
 GET P44 POSITION
 STORE P44 POSITION
 GET P45 POSITION
 STORE P45 POSITION
 GET P46 POSITION
 STORE P46 POSITION
 GET P47 POSITION
 STORE P47 POSITION
 GET P48 POSITION
 STORE P48 POSITION
 GET P49 POSITION
 STORE P49 POSITION
 GET P50 POSITION
 STORE P50 POSITION
 GET P51 POSITION
 STORE P51 POSITION
 GET P52 POSITION
 STORE P52 POSITION
 GET P53 POSITION
 STORE P53 POSITION
 GET P54 POSITION
 STORE P54 POSITION
 GET P55 POSITION
 STORE P55 POSITION
 GET P56 POSITION
 STORE P56 POSITION
 GET P57 POSITION
 STORE P57 POSITION
 GET P58 POSITION
 STORE P58 POSITION
 GET P59 POSITION
 STORE P59 POSITION
 GET P60 POSITION
 STORE P60 POSITION
 GET P61 POSITION
 STORE P61 POSITION
 GET P62 POSITION
 STORE P62 POSITION
 GET P63 POSITION
 STORE P63 POSITION
 GET P64 POSITION
 STORE P64 POSITION
 GET P65 POSITION
 STORE P65 POSITION
 GET P66 POSITION
 STORE P66 POSITION
 GET P67 POSITION
 STORE P67 POSITION
 GET P68 POSITION
 STORE P68 POSITION
 GET P69 POSITION
 STORE P69 POSITION
 GET P70 POSITION
 STORE P70 POSITION
 GET P71 POSITION
 STORE P71 POSITION
 GET P72 POSITION
 STORE P72 POSITION
 GET P73 POSITION
 STORE P73 POSITION
 GET P74 POSITION
 STORE P74 POSITION
 GET P75 POSITION
 STORE P75 POSITION
 GET P76 POSITION
 STORE P76 POSITION
 GET P77 POSITION
 STORE P77 POSITION
 GET P78 POSITION
 STORE P78 POSITION
 GET P79 POSITION
 STORE P79 POSITION
 GET P80 POSITION
 STORE P80 POSITION
 GET P81 POSITION
 STORE P81 POSITION
 GET P82 POSITION
 STORE P82 POSITION
 GET P83 POSITION
 STORE P83 POSITION
 GET P84 POSITION
 STORE P84 POSITION
 GET P85 POSITION
 STORE P85 POSITION
 GET P86 POSITION
 STORE P86 POSITION
 GET P87 POSITION
 STORE P87 POSITION
 GET P88 POSITION
 STORE P88 POSITION
 GET P89 POSITION
 STORE P89 POSITION
 GET P90 POSITION
 STORE P90 POSITION
 GET P91 POSITION
 STORE P91 POSITION
 GET P92 POSITION
 STORE P92 POSITION
 GET P93 POSITION
 STORE P93 POSITION
 GET P94 POSITION
 STORE P94 POSITION
 GET P95 POSITION
 STORE P95 POSITION
 GET P96 POSITION
 STORE P96 POSITION
 GET P97 POSITION
 STORE P97 POSITION
 GET P98 POSITION
 STORE P98 POSITION
 GET P99 POSITION
 STORE P99 POSITION
 GET P100 POSITION
 STORE P100 POSITION

PAGE 33

1019A ASSEMBLER, VERSION 1.0 NOV64 10/02/84 SECTION 1

ADDRESS	DATA	INSTR	OP	COMMENT
1436	002660	003251	STRZ	PYDCLD=0
1437	002661	003252	STRZ	PYDCLD=0
1438	002662	003253	STRZ	PYDCLD=0
1439	002663	003254	STRZ	PYDCLD=0
1440	002664	003255	STRZ	PYDCLD=0
1441	002665	003256	STRZ	PYDCLD=0
1442	002666	003257	STRZ	PYDCLD=0
1443	002667	003258	STRZ	PYDCLD=0
1444	002668	003259	STRZ	PYDCLD=0
1445	002669	003260	STRZ	PYDCLD=0
1446	002670	003261	STRZ	PYDCLD=0
1447	002671	003262	STRZ	PYDCLD=0
1448	002672	003263	STRZ	PYDCLD=0
1449	002673	003264	STRZ	PYDCLD=0
1450	002674	003265	STRZ	PYDCLD=0
1451	002675	003266	STRZ	PYDCLD=0
1452	002676	003267	STRZ	PYDCLD=0
1453	002677	003268	STRZ	PYDCLD=0
1454	002678	003269	STRZ	PYDCLD=0
1455	002679	003270	STRZ	PYDCLD=0
1456	002680	003271	STRZ	PYDCLD=0
1457	002681	003272	STRZ	PYDCLD=0
1458	002682	003273	STRZ	PYDCLD=0
1459	002683	003274	STRZ	PYDCLD=0
1460	002684	003275	STRZ	PYDCLD=0
1461	002685	003276	STRZ	PYDCLD=0
1462	002686	003277	STRZ	PYDCLD=0
1463	002687	003278	STRZ	PYDCLD=0
1464	002688	003279	STRZ	PYDCLD=0
1465	002689	003280	STRZ	PYDCLD=0
1466	002690	003281	STRZ	PYDCLD=0
1467	002691	003282	STRZ	PYDCLD=0
1468	002692	003283	STRZ	PYDCLD=0
1469	002693	003284	STRZ	PYDCLD=0
1470	002694	003285	STRZ	PYDCLD=0
1471	002695	003286	STRZ	PYDCLD=0
1472	002696	003287	STRZ	PYDCLD=0
1473	002697	003288	STRZ	PYDCLD=0
1474	002698	003289	STRZ	PYDCLD=0
1475	002699	003290	STRZ	PYDCLD=0
1476	002700	003291	STRZ	PYDCLD=0
1477	002701	003292	STRZ	PYDCLD=0
1478	002702	003293	STRZ	PYDCLD=0
1479	002703	003294	STRZ	PYDCLD=0
1480	002704	003295	STRZ	PYDCLD=0
1481	002705	003296	STRZ	PYDCLD=0
1482	002706	003297	STRZ	PYDCLD=0
1483	002707	003298	STRZ	PYDCLD=0
1484	002708	003299	STRZ	PYDCLD=0
1485	002709	003300	STRZ	PYDCLD=0
1486	002710	003301	STRZ	PYDCLD=0
1487	002711	003302	STRZ	PYDCLD=0
1488	002712	003303	STRZ	PYDCLD=0
1489	002713	003304	STRZ	PYDCLD=0
1490	002714	003305	STRZ	PYDCLD=0
1491	002715	003306	STRZ	PYDCLD=0
1492	002716	003307	STRZ	PYDCLD=0
1493	002717	003308	STRZ	PYDCLD=0
1494	002718	003309	STRZ	PYDCLD=0
1495	002719	003310	STRZ	PYDCLD=0
1496	002720	003311	STRZ	PYDCLD=0
1497	002721	003312	STRZ	PYDCLD=0
1498	002722	003313	STRZ	PYDCLD=0
1499	002723	003314	STRZ	PYDCLD=0
1500	002724	003315	STRZ	PYDCLD=0
1501	002725	003316	STRZ	PYDCLD=0
1502	002726	003317	STRZ	PYDCLD=0
1503	002727	003318	STRZ	PYDCLD=0
1504	002728	003319	STRZ	PYDCLD=0
1505	002729	003320	STRZ	PYDCLD=0
1506	002730	003321	STRZ	PYDCLD=0
1507	002731	003322	STRZ	PYDCLD=0
1508	002732	003323	STRZ	PYDCLD=0
1509	002733	003324	STRZ	PYDCLD=0
1510	002734	003325	STRZ	PYDCLD=

Initialisation Code. (contd)

PAGE 34

1493	002746	564457	PSK	MACPI	IF P=MC-1 THEN SKIP A LINE
1494					ELSE INITIALIZE THE NEXT MUI
1495	002747	342745	JP	MINI11	CONTINUE MUI INITIALIZATION
1496	002750	360000	ENTBK	0	ICRI=0 START PZK,MZKPI INITIALIZATION
1497	002751	412114	MINI12	MZK	(PZK+ICRI)=0
1498	002752	412110	STGZB	MZKPI	(MZKPI+ICRI)=0
1499	002753	564454	PSK	MZKPI	IF B=PP-1 THEN SKIP A LINE
1500					CONTINUE INITIALIZATION
1501	002754	342751	JP	MINI12	ELSE GO INITIALIZE NEXT TERM, ICRI=ICRI+1
1502					NON DO THE CMSTR2 INITIALIZATIONS
1503	002755	501201	ENTBK	1	USE ICRI AS INDEX REGISTER
1504	002756	360000	ENTBK	0	ICRI=0
1505	002757	412111	MINI11	MUI	(MUI+ICRI)=0
1506	002760	503170	PSK	MZKPI	IF P=MC-1 THEN SKIP A LINE
1507					ELSE INITIALIZE THE NEXT MUI
1508	002761	342757	JP	MINI11	CONTINUE MUI INITIALIZATION
1509	002762	360000	ENTBK	0	ICRI=0 START MZK,MZKPI INITIALIZATION
1510	002763	412271	MINI12	MZK	(MZK+ICRI)=0
1511	002764	412274	STGZB	MZKPI	(MZKPI+ICRI)=0
1512	002765	503169	PSK	MZKPI	IF P=MC-1 THEN SKIP A LINE
1513					ELSE GO INITIALIZE NEXT TERM, ICRI=ICRI+1
1514	002766	342763	JP	MINI12	CONTINUE INITIALIZATION
1515					NON DO THE CMSTR3 INITIALIZATIONS
1516	002767	501201	ENTBK	1	USE ICRI AS INDEX REGISTER
1517	002770	360000	ENTBK	0	ICRI=0 START OZK,OZKPI INITIALIZATION
1518	002771	412491	MINI12	OZK	(OZK+ICRI)=0
1519	002772	412454	STGZB	OZKPI	(OZKPI+ICRI)=0
1520	002773	503676	PSK	OZKPI	IF B=MC-1 THEN SKIP A LINE
1521					ELSE GO INITIALIZE NEXT TERM, ICRI=ICRI+1
1522	002774	342771	JP	MINI12	CONTINUE INITIALIZATION
1523					NON DO THE CMSTR4 INITIALIZATIONS
1524	002775	501201	ENTBK	1	USE ICRI AS INDEX REGISTER
1525	002776	360000	ENTBK	0	ICRI=0 START PZK,PZKPI INITIALIZATION
1526	002777	415017	MINI12	PZK	(PZK+ICRI)=0
1527	003000	413024	STGZB	PZKPI	(PZKPI+ICRI)=0
1528	003001	506712	PSK	PZKPI	IF B=PP-1 THEN SKIP A LINE
1529					ELSE GO INITIALIZE NEXT TERM, ICRI=ICRI+1
1530	003002	342777	JP	MINI12	CONTINUE INITIALIZATION
1531	003003	343004	JP	MINI11	END THE INITIALIZATIONS
1532	003004	504000	MINI12	MOOP	END OF THE CMSTR INITIALIZATIONS
1533					*****
1534	003005	120793	ENTBK	100FMI	*****
1535	003006	411203	STGAL	MC18T	*****
1536	003007	402627	STGAL	16GL12	*****
1537	003010	400777	STGAL	PH3ENG	*****
1538	003011	400274	STGZ	16GL17	*****
1539	003012	400414	STGZ	16GL14	*****
1540	003013	401277	STGZ	RCUCLD	*****
1541	003014	401277	STGZ	PH3CLD	*****
1542	003015	401454	STGZ	WAPPLG	*****
1543	003016	400066	STGZ	LAPPEC	*****
1544	003017	400664	STGZ	A/PFLG	*****
1545	003018	400665	STGZ	M/APPG	*****
1546	003021	400663	STGZ	G/APLG	*****
1547	003022	502207	TOP	CLRM	*****
1548	003023	121366	CL1	ENTAL	*****
1549	003024	121366	CL1	VERCM	*****

Longitudinal CAS Subroutine.

```

1019A ASSEMBLER, VERSION 1.0  NOVPA3 10/02/84  SECTION 1  PAGE 62

2094 0
2095 0
2096 0
2097 0
2098 0
2099 0
2100 0
2101 0
2102 0
2103 0
2104 0
2105 0
2106 0
2107 0
2108 0
2109 0
2110 0
2111 0
2112 0
2113 0
2114 0
2115 0
2116 0
2117 0
2118 0
2119 0
2120 0
2121 0
2122 0
2123 0
2124 0
2125 0
2126 0
2127 0
2128 0
2129 0
2130 0
2131 0
2132 0
2133 0
2134 0
2135 0
2136 0
2137 0
2138 0
2139 0
2140 0
2141 0
2142 0
2143 0
2144 0
2145 0
2146 0
2147 0
2148 0
2149 0
2150 0
2151 0
2152 0
2153 0
2154 0
2155 0
2156 0
2157 0
2158 0
2159 0
2160 0
2161 0
2162 0
2163 0
2164 0
2165 0
2166 0
2167 0
2168 0
2169 0
2170 0
2171 0
2172 0
2173 0
2174 0
2175 0
2176 0
2177 0
2178 0
2179 0
2180 0
2181 0
2182 0
2183 0
2184 0
2185 0
2186 0
2187 0
2188 0
2189 0
2190 0
2191 0
2192 0
2193 0
2194 0
2195 0
2196 0
2197 0
2198 0
2199 0
2200 0
2201 0
2202 0
2203 0
2204 0
2205 0
2206 0
2207 0
2208 0
2209 0
2210 0
2211 0
2212 0
2213 0
2214 0
2215 0
2216 0
2217 0
2218 0
2219 0
2220 0
2221 0
2222 0
2223 0
2224 0
2225 0
2226 0
2227 0
2228 0
2229 0
2230 0
2231 0
2232 0
2233 0
2234 0
2235 0
2236 0
2237 0
2238 0
2239 0
2240 0
2241 0
2242 0
2243 0
2244 0
2245 0
2246 0
2247 0
2248 0
2249 0
2250 0
2251 0
2252 0
2253 0
2254 0
2255 0
2256 0
2257 0
2258 0
2259 0
2260 0
2261 0
2262 0
2263 0
2264 0
2265 0
2266 0
2267 0
2268 0
2269 0
2270 0
2271 0
2272 0
2273 0
2274 0
2275 0
2276 0
2277 0
2278 0
2279 0
2280 0
2281 0
2282 0
2283 0
2284 0
2285 0
2286 0
2287 0
2288 0
2289 0
2290 0
2291 0
2292 0
2293 0
2294 0
2295 0
2296 0
2297 0
2298 0
2299 0
2300 0
2301 0
2302 0
2303 0
2304 0
2305 0
2306 0
2307 0
2308 0
2309 0
2310 0
2311 0
2312 0
2313 0
2314 0
2315 0
2316 0
2317 0
2318 0
2319 0
2320 0
2321 0
2322 0
2323 0
2324 0
2325 0
2326 0
2327 0
2328 0
2329 0
2330 0
2331 0
2332 0
2333 0
2334 0
2335 0
2336 0
2337 0
2338 0
2339 0
2340 0
2341 0
2342 0
2343 0
2344 0
2345 0
2346 0
2347 0
2348 0
2349 0
2350 0
2351 0
2352 0
2353 0
2354 0
2355 0
2356 0
2357 0
2358 0
2359 0
2360 0
2361 0
2362 0
2363 0
2364 0
2365 0
2366 0
2367 0
2368 0
2369 0
2370 0
2371 0
2372 0
2373 0
2374 0
2375 0
2376 0
2377 0
2378 0
2379 0
2380 0
2381 0
2382 0
2383 0
2384 0
2385 0
2386 0
2387 0
2388 0
2389 0
2390 0
2391 0
2392 0
2393 0
2394 0
2395 0
2396 0
2397 0
2398 0
2399 0
2400 0
2401 0
2402 0
2403 0
2404 0
2405 0
2406 0
2407 0
2408 0
2409 0
2410 0
2411 0
2412 0
2413 0
2414 0
2415 0
2416 0
2417 0
2418 0
2419 0
2420 0
2421 0
2422 0
2423 0
2424 0
2425 0
2426 0
2427 0
2428 0
2429 0
2430 0
2431 0
2432 0
2433 0
2434 0
2435 0
2436 0
2437 0
2438 0
2439 0
2440 0
2441 0
2442 0
2443 0
2444 0
2445 0
2446 0
2447 0
2448 0
2449 0
2450 0
2451 0
2452 0
2453 0
2454 0
2455 0
2456 0
2457 0
2458 0
2459 0
2460 0
2461 0
2462 0
2463 0
2464 0
2465 0
2466 0
2467 0
2468 0
2469 0
2470 0
2471 0
2472 0
2473 0
2474 0
2475 0
2476 0
2477 0
2478 0
2479 0
2480 0
2481 0
2482 0
2483 0
2484 0
2485 0
2486 0
2487 0
2488 0
2489 0
2490 0
2491 0
2492 0
2493 0
2494 0
2495 0
2496 0
2497 0
2498 0
2499 0
2500 0
2501 0
2502 0
2503 0
2504 0
2505 0
2506 0
2507 0
2508 0
2509 0
2510 0
2511 0
2512 0
2513 0
2514 0
2515 0
2516 0
2517 0
2518 0
2519 0
2520 0
2521 0
2522 0
2523 0
2524 0
2525 0
2526 0
2527 0
2528 0
2529 0
2530 0
2531 0
2532 0
2533 0
2534 0
2535 0
2536 0
2537 0
2538 0
2539 0
2540 0
2541 0
2542 0
2543 0
2544 0
2545 0
2546 0
2547 0
2548 0
2549 0
2550 0
2551 0
2552 0
2553 0
2554 0
2555 0
2556 0
2557 0
2558 0
2559 0
2560 0
2561 0
2562 0
2563 0
2564 0
2565 0
2566 0
2567 0
2568 0
2569 0
2570 0
2571 0
2572 0
2573 0
2574 0
2575 0
2576 0
2577 0
2578 0
2579 0
2580 0
2581 0
2582 0
2583 0
2584 0
2585 0
2586 0
2587 0
2588 0
2589 0
2590 0
2591 0
2592 0
2593 0
2594 0
2595 0
2596 0
2597 0
2598 0
2599 0
2600 0
2601 0
2602 0
2603 0
2604 0
2605 0
2606 0
2607 0
2608 0
2609 0
2610 0
2611 0
2612 0
2613 0
2614 0
2615 0
2616 0
2617 0
2618 0
2619 0
2620 0
2621 0
2622 0
2623 0
2624 0
2625 0
2626 0
2627 0
2628 0
2629 0
2630 0
2631 0
2632 0
2633 0
2634 0
2635 0
2636 0
2637 0
2638 0
2639 0
2640 0
2641 0
2642 0
2643 0
2644 0
2645 0
2646 0
2647 0
2648 0
2649 0
2650 0
2651 0
2652 0
2653 0
2654 0
2655 0
2656 0
2657 0
2658 0
2659 0
2660 0
2661 0
2662 0
2663 0
2664 0
2665 0
2666 0
2667 0
2668 0
2669
```

Longitudinal CAS Subroutine. (contd)

PAGE 63

1019A ASSEMBLER, VERSION 1.0 MOVN43 10/02/84 SECTION 1

```

2953 005207 507310      ENTER  LC
2954 005210 445166      STRAL  MN
2955 005211 717776      ADDALR  -1
2956 005212 445169      STRAL  MPW1
2957 005213 445167      STRAU  MRB1
2958
2959
2960
2961
2962
2963
2964
2965
2966
2967
2968
2969
2970
2971
2972
2973
2974
2975
2976
2977
2978
2979
2980
2981
2982
2983
2984
2985
2986
2987
2988
2989
2990
2991
2992
2993
2994
2995
2996
2997
2998
2999
3000
3001
3002
3003
3004
3005
3006
3007
3008
3009

```

USE MEMORY BANK 0
 MRB1=MRCA1
 ALI=AL-1=MRDATA-1
 MRP1=MRCA1-1
 MRP1=MRP1

-----SECTION MRB0-----
 THIS SECTION PUTS MEASUREMENTS NEEDED BY THE CONTROLLER
 INTO THE MEASUREMENT VECTOR, MYS. IT ALSO PUTS THE ACTUAL
 VALUES OF THE DESIRED OUTPUTS INTO THE VECTOR, MYACT.

IN BASIC, THE CODE WOULD BE:

```

    FOR I=1 TO NM
      MYACT(I)=MYS(I)
    NEXT I
  
```

FOR I=1 TO MC
 MYACT(I)=MYS(I)
 NEXT I

MYSSEL IS A VECTOR CONTAINING, IN ORDER, THE INDEX NUMBERS
 OF THE SELECTED MEASUREMENTS. MYSSEL IS A VECTOR CONTAINING,
 IN ORDER, THE INDEX NUMBERS OF THE DESIRED MEASUREMENTS (THOSE
 BEING COMMANDS BY THE PILOT). THE MEASUREMENTS COME FROM BANK 3.
 THE INDEX NUMBERS AND THE RELATED POSSIBLE MEASUREMENTS ARE

SMCN BELOW:

INDEX NUMBER	PARAMETER
1	THETA(+MOSE UP, 500/DEG)
2	PHI(+RND, 500/DEG)
3	PSI(MAGNETIC, 500/DEG)
4	Q(+MOSE UP, 500/DEG/SEC)
5	P(+RND, 500/DEG/SEC)
6	R(+RIGHT, 500/DEG/SEC)
7	LONG. ACCEL.(NO GRAV, +FCRM, 128/(FT/SEC+92))
8	LAT. ACCEL.(NO GRAV, +FICRM, 128/(FT/SEC+92))
9	NORMAL ACCEL.(NO GRAV, +UP, 128/(FT/SEC+92))
10	DELTA FORW. VEL.(+FORW, 8/(FT/SEC))
11	VERT. VEL.(+UP, 32/(FT/SEC))
12	BARO. ALT.(16/FT)

NOTE THAT THETA AND AIRSPEED ARE PERTURBATION QUANTITIES AND HAVE
 THEIR VALUES SUBTRACTED FROM THEM.

-----SECTION MRP0-----
 USE MEMORY BANK 3
 ALI=AL+TH(PI) (PITCH ANGLE)
 MRP1=MRP1+TH(PI) (PERTURBATION PITCH ANGLE)
 MRP1=MRP1+TH(PI) (PERTURBATION PITCH ANGLE)

MRP1 IS RCLL, +RND, 500/DEG
 MRP1 IS MRP1, MAGNETIC, 500/DEG
 PITCH RATE, +MOSE UP, 500/DEG/SEC

Longitudinal CAS Subroutine. (contd)

PAGE 64

1019A ASSEMBLER, VERSION 1.0 NOV843 10/02/84 SECTION 1

```

3010 005227 442353      STRAL  NPOIPI
3011 005230 120769      STRAL  YNWP7C
3012 005231 442354      STRAL  NTAAP1
3013 005232 120767      STRAL  ACCING
3014 005233 442355      STRAL  NAI
3015 005234 120750      STRAL  ACCLAT
3016 005235 442356      STRAL  NAI
3017 005236 120751      STRAL  ACCRM
3018 005237 442357      STRAL  NA2
3019 005240 120752      STRAL  NIPSPD
3020 005241 120745      STRAL  NIPAS
3021 005242 442360      STRAL  NVEL
3022      0
3023 005243 120765      STRAL  TVSI
3024 005244 120746      STRAL  NIPPHD
3025 005245 442361      STRAL  NVPBL
3026 005246 120754      STRAL  SARC
3027 005247 442362      STRAL  NERT
3028      0
3029      0
3030      0
3031 005250 307201      ENTRC  1
3032 005251 360001      ENTRC  1
3033 005252 120723      NSTP01
3034 005253 441650      STRAL  TTP
3035 005254 307202      ENTRC  2
3036 005255 321650      ENTRC  TTP
3037 005256 120746      ENTRAL  NCTNET-1
3038 005257 307201      ENTRC  1
3039 005260 452234      STRALP  NTS-1
3040 005261 565172      PSN  NAREAS
3041      0
3042 005262 345252      JP  NSTF01
3043      0
3044      0
3045      0
3046 005263 507201      ENTRC  1
3047 005264 360001      ENTRC  1
3048 005265 120727      NSTP02
3049 005266 441650      STRAL  TTP
3050 005267 307202      ENTRC  2
3051 005270 321650      ENTRC  TTP
3052 005271 120746      ENTRAL  NCTNET-1
3053 005272 307201      ENTRC  1
3054 005273 452252      STRALB  NTACT-1
3055 005274 365171      PSK  NROTEL
3056      0
3057 005275 345265      JP  NSTP02
3058 005276 345277      JP  NSTF03
3059      0
3060      0
3061      0
3062 005277 120735      NSTP03
3063 005278 364600      ENTRAL  ZFLCH
3064 005301 442361      STRAL  NPL1
3065 005302 120760      ENTRC  CPMRY
3066 005303 504600      LTRAL  0

```

```

ROLL RATE, + RND, 500/(DEG/SEC)
YAW RATE, + RIGHT, 500/(DEG/SEC)
LONG. ACCEL., NO GRAV, +FORM, 128/(FT/SEC**2)
LAT. ACCEL., NO GRAV, +RIGHT, 128/(FT/SEC**2)
NORMAL ACCEL., NO GRAV, +UP, 128/(FT/SEC**2)
AL=ATRSPC-TRIM AIRSPEED
NVEL IS PERTURBATION VELOCITY,
VERT. SPEED, +UP, 32/(FT/SEC)
SUBTRACT WDOI AT ENGAGE
PERTURBFC VERT. SPEED, +UP, 32/(FT/SEC)
PARO. ALT., 16/FT

```

```

USE ICRI AS INDEX I
START WITH ICRI=1 SO (I=2)
AL=(NYSEL+ICRI-1)
TMP=NYSEL(I)
USE ICR2 AS INDEX
AL=NYSEL(I)
AL=NYSEL(I)
AL=INDEX REGISTER 1 AGAIN
AL=(NYSEL+ICRI-1)
IF BNNVARS DO NEXT LINE
CONTINUE

```

```

USE ICRI AS INDEX I
START WITH ICRI=1 SO (I=2)
AL=(NYSEL+ICRI-1)
TMP=NYSEL(I)
USE ICR2 AS INDEX
AL=NYSEL(I)
AL=NYSEL(I)
AL=INDEX REGISTER AGAIN
NYACT(I)=(NYACT+ICRI-1)
IF BNNVARS SKIP A LINE
GET NEXT NYACT
GO GET PILOT INPUTS

```

```

THIS SECTION PUTS EXPERIMENTAL PILOT COMMANDS INTO THE NPL1 VECTOR
AL=EP LONG STICK
SCALE THE INPUT OF LONG CYLIC
NPL1(1)=LONG STICK, 102488 IN, +AFT
NPL1(2)=LONG STICK, 102488 IN, +AFT
SCALE THE INPUT OF COLLECTIVE

```

Longitudinal CAS Subroutine. (contd)

[illegible]

PAGE 66

1019A ASSEMBLER, VERSION 1.0 NOV83 10/02/84 SFCTION 1

[illegible]

Longitudinal CAS Subroutine. (contd)

```

1019A ASSEMBLER, VERSION 1.0  MCVR43 10/02/84  SECTION 1  PAGE 67
3179      0
3180 005431 343416      0      ELSE DO NEXT LINE AND ICR3=ICR1+1
3181      0      JUMPS TO NEXT COLUMN OF MNC
3182 005432 370001      1      ICR1=ICR1+1
3183 005433 307203      3      USE ICR3 AS INDEX REG.(ROW INDEX)
3184 005434 305703      3      SCALING FOR MSTR3,24415
3185 005435 472215      0      MUC
3186 005436 363170      0      MNCPI
3187      0      ELSE DO NEXT LINE AND ICR3=ICR3+1
3188 005437 345441      0      GO RESET THE COUNTER
3189 005440 345451      0      GO TO NEXT MATRIX MULT IF DONE
3190 005441 307202      0      SAVE ROW INDEX AND START USING COLUMN INDEX
3191 005442 360000      0      RESET COLUMN INDEX TO ZERO
3192 005443 307310      0      BANK 0 TO USE MNCEND AND MNCtrl
3193 005444 125164      0      ALI=MNCEND
3194 005445 143171      0      ALI=MNCEND+MNCtrl-MNCEND+0 OF COLUMNS
3195 005446 443164      0      MNCEND=MNCEND+MNCtrl
3196 005447 307313      0      BANK 3 FOR DATA
3197 005450 345414      0      GO THE NEXT ROW
3198      0
3199      0      -----SECTION MSTR4-----
3200      0      THIS IS THE 2ND MATRIX MULTIPLY IN THE CMSTR2
3201      0      SUBROUTINE, I.E.
3202      0      MNCPI * MTS
3203      0
3204 005451 307310      0      MSTR4
3205 005452 307201      0      MSTR4
3206 005453 307000      0      MSTR4
3207 005454 400002      2      STR2
3208 005455 307003      3      STR3
3209 005456 307313      13     MSTR4
3210 005457 123334      0      MSTR4
3211 005460 117776      0      ADDALK
3212 005461 307310      0      MSTR4
3213 005462 443164      0      MSTR4
3214 005463 307313      13     MSTR4
3215 005464 700000      0      MSTR4
3216 005465 307300      0      MSTR4
3217 005466 300600      0      MSTR4
3218 005467 331850      0      MSTR4
3219 005470 307202      2      MSTR4
3220 005471 370001      1      MSTR4
3221 005472 132334      0      MSTR4
3222 005473 307201      1      MSTR4
3223 005474 252302      0      MSTR4
3224 005475 201850      0      MSTR4
3225 005476 305300      0      MSTR4
3226 005477 307000      0      MSTR4
3227 005480 565164      0      MSTR4
3228 005501 343466      0      MSTR4
3229 005502 370001      1      MSTR4
3230 005503 307203      3      MSTR4
3231 005504 305703      3      MSTR4
3232 005505 472214      0      MSTR4
3233 005506 363170      0      MSTR4
3234      0      ELSE DO NEXT LINE AND ICR3=ICR3+1

```


Longitudinal CAS Subroutine. (contd)

1019A ASSEMBLER, VERSION 1.0	NOV843	10/02/84	SECTION 1	PAGE 88
3291 005562 11650	ADDAL	TPP		
3292 005563 457387	STRAUS	TPP		
3293 005564 370001	ENTR8B	1		
3294				
3295 005565 345525	JP	MSF50		
3296 005566 380001	MSF54	ENTR8B		
3297				
3298				
3299 005567 132273	MSF55	ENTR8B		
3300 005570 132362	ADDALB	TPP		
3301 005571 452273	STRAUS	TPP		
3302 005572 565166	ENTR8B	1		
3303				
3304 005573 185587	JP	MSF55		
3305 005574 345575	JP	MSF56		
3306				
3307				
3308				
3309				
3310				
3311				
3312 005575 507310	MSF56	ENTR8B		
3313 005576 507201	ENTR8B	1		
3314 005577 380000	ENTR8B	0		
3315 005600 400002	STIRZ	2		
3316 005601 400003	STIRZ	3		
3317 005602 507313	ENTR8B	13		
3318 005603 122332	ENTR8B	MSF57		
3319 005604 717776	ADDALB	-1		
3320 005605 507310	ENTR8B	30		
3321 005606 445164	STIRAL	MSF58		
3322 005607 507313	ENTR8B	13		
3323 005610 700000	MSF59	ENTR8B		
3324 005611 507400	XPFLU	0		
3325 005612 500600	MSF60	STIRAL		
3326 005613 507350				
3327 005614 507202	ENTR8B	2		
3328 005615 370001	ENTR8B	1		
3329 005616 132373	ENTR8B	MSF61		
3330 005617 507201	ENTR8B	1		
3331 005620 252316	PULALB	MSF62		
3332 005621 201850	ADDAL	TPP		
3333 005622 505300	MSF63	ENTR8B		
3334 005623 507400	MSF64	ENTR8B		
3335 005624 505164	ENTR8B	1		
3336 005625 345612	JP	MSF65		
3337				
3338 005626 370001	ENTR8B	1		
3339 005627 507203	ENTR8B	3		
3340 005630 504700	LRTA	0		
3341 005631 472221	STRAUS	MSF66		
3342 005632 505170	ENTR8B	MSF67		
3343				
3344 005633 345635	JP	MSF68		
3345 005634 345635	JP	MSF69		
3346 005635 507202	MSF70	ENTR8B		

Longitudinal CAS Subroutine. (contd)

```

PAGE 70
1019A ASSEMBLER, VERSION 1.0  MOV#43 10/02/14 SECTION 1
3347 005636 360000  ENTBK 0
3348 005637 307370  ENTSL IC
3349 005640 125164  ENTAL MLEND
3350 005641 149166  ADDAL MPA
3351 005642 445164  STRAL MLEND
3352 005643 307319  ENTSL T3
3353 005644 345610  JUP MAXPH3
3354
3355 -----SECTION NS1P7-----
3356
3357 THIS STEP DOES THE ADDITION NUT = MUC + MUR + NUI
3358
3359 005645 507201  NS1P7  ENTICR 1
3360 005646 300001  ENTICR 1
3361 005647 132214  NS1P70  ENTALB MUC-1
3362 005648 152220  ADDALB MUR-1
3363 005651 152210  ADDALB NUI-1
3364 005652 305300  SHPROV
3365 005653 504000  MOOP
3366 005654 522224  STRALB MUR-1
3367 005655 565171  RSK MACTRL
3368
3369 005656 345647  JUP NS1P70
3370 005657 345660  JUP NS1P8
3371
3372 -----SECTION NS1P8-----
3373
3374 HERE GOES THE SECTION(NS1P8) WHICH WRITES NUT(ACTUATOR
3375 COMMANDS) IC THE LOCATION WHICH SENDS NUT IC THE
3376 ACTUATORS.
3377
3378 NS1P8
3379 005660 122223  NS1P8  ENTAL NUT
3380 005661 242340  PULAL MLENGC
3381 005662 660072  STRAU ORP1
3382 005663 122226  ENTAL NUI+1
3383 005664 242301  PULAL MCCISC
3384 005665 460075  STRAU ORP4
3385
3386 005666 122223  NS1P8  ENTAL NUT
3387 005667 242340  PULAL MLENGC
3388 005668 660072  STRAU ORP1
3389 005669 122226  ENTAL NUI+1
3390 005670 242301  PULAL MCCISC
3391 005671 460075  STRAU ORP4
3392
3393 005672 345647  JUP NS1P70
3394 005673 345660  JUP NS1P8
3395
3396 -----SECTION NS1P9-----
3397
3398 THIS SECTION CF (MS1P2 SETS THE PRESENT COMPENSATOR
3399 STATES(TEMP) TO OLD STATES(MK)
3400
3401 005674 307201  NS1P9  ENTICR 1
3402 005675 360001  ENTICR 1
3403 005676 132214  NS1P90  ENTALB MUR-1
3404 005677 152220  ADDALB MUR-1
3405 005678 305300  SHPROV
3406 005679 504000  MOOP
3407 005680 522224  STRALB MUR-1
3408 005681 565171  RSK MACTRL
3409
3410 005682 345647  JUP NS1P70
3411 005683 345660  JUP NS1P8
3412
3413 END THE CONTROLLER SUBROUTINE NUMBER 2

```

PAGE 06

10191 ASBESTHOLFR. VERSION 1.0 NOV843 10/02/84 SECTION 1

[illegible]

AD-A151 946

A MODERN CONTROL DESIGN METHODOLOGY WITH APPLICATION TO 3/3
THE CH-47 HELICOPTER(U) AIR FORCE INST OF TECH
WRIGHT-PATTERSON AFB OH R D HOLDRIDGE JAN 85

UNCLASSIFIED

AFIT/CI/NR-85-33D

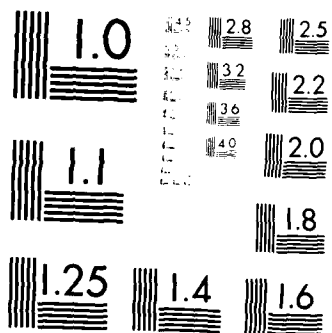
F/G 1/4

NL

END

FILED

ERIC



MICROCOPY RESOLUTION TEST CHART
NATIONAL BUREAU OF STANDARDS-1963-A

Hover Controller Subroutine. (contd)

```

18199  ASSEMBLER, VERSION 1.0  MOVN43  10/02/84  SECTION 1  PAGE 37

4237  006723  103137  ENTAU  PM  AU=(PMP)
4238  006724  507310  ENTSM  TC  USE MEMCRY BANK 0
4239  006725  466716  STRAL  PROTRL  ENCTRL=PNC
4240  006726  717798  ACCALK  *1  ALIMPNC=1
4241  006727  446715  STRAL  PACP1  ENCM1=PNC=1
4242  006730  806717  STRAU  PNEAS  ENPNEAS=PNC
4243  006731  507313  ENTSM  13  USE MEMCRY BANK 3
4244  006732  123135  ENTRL  PN  KLTN(PN)
4245  006733  103134  ENTAU  PPA1  AU=(PPF1)
4246  006734  507310  ENTSM  30  USE MEMCRY BANK 0
4247  006735  446713  STRAL  PPR  PPR=PPR
4248  006736  717778  RDBALR  *1  ALTRAL=PPR=1
4249  006737  446712  STRAL  PPA1  PPA1=PPR=1
4250  006740  806714  STRAU  PPA1  ENP1=PPR=1
4251
4252  *****SECTION P87P0*****
4253
4254  * THIS SECTION PUTS MEASUREMENTS NEEDED BY THE CONTROLLER
4255  * INTO THE MEASUREMENT VECTOR, PYS.
4256
4257  * IN BASIC, THE CODE WOULD BE:
4258
4259  * FOR I=1 TO NM
4260  *   PYS(I)=PERS(PTSSEL(I))
4261  * NEXT I
4262
4263  * PYSSEL IS A VECTOR CONTAINING, IN ORDER, THE INDEX NUMBERS
4264  * OF THE SELECTED MEASUREMENTS. THE MEASUREMENTS COME FROM BANK 3.
4265  * THE INDEX NUMBERS AND THE RELATED POSSIBLE MEASUREMENTS ARE
4266  * SHOWN BELOW:
4267
4268  * INDEX NUMBER  * PARAMETER
4269  1  THETA(+HOSE UP, 500/DEG)
4270  2  PHI(+HND, 500/DEG)
4271  3  PSI(MAGNETIC, 500/DEG)
4272  4  Q(+HOSE UP, 900/(DEG/SEC))
4273  5  P(+HND, 500/(DEG/SEC))
4274  6  R(+HND, 500/(DEG/SEC))
4275  7  LONG. ACCEL.(NC GRAY, +FCRM, 128/(FT/SEC+2))
4276  8  LAT. ACCEL.(MC GRAY, +RIGHT, 128/(FT/SEC+2))
4277  9  NORMAL ACCEL.(NO GRAY, +UP, 128/(FT/SEC+2))
4278  10  DELTA POS. VEL.(+FORW, 32/(FT/SEC))
4279  11  DELTA VERT. VEL.(+UP, 32/(FT/SEC))
4280  12  DRMO. VEL.(+FORW)
4281  13  X POSITION(+FCRM, 16/FT) IN HEADING INERTIAL AXIS
4282  14  Y POSITION(+RIGHT, 16/FT) IN HEADING INERTIAL AXIS
4283  15  Z POSITION(+DOWN, 16/FT) IN HEADING INERTIAL AXIS
4284  16  X INERTIAL VEL.(+FORW, 32/PPS) IN HEADING INERTIAL AXIS
4285  17  Y INERTIAL VEL.(+RIGHT, 32/PPS) IN HEADING INERTIAL AXIS
4286  18  Z INERTIAL VEL.(+DOWN, 32/PPS) IN HEADING INERTIAL AXIS
4287  19  X POSITION(+FCRM, 16/FT) IN RUNWAY FRAME
4288  20  Y POSITION(+RIGHT, 16/FT) IN RUNWAY FRAME
4289  21  X INERTIAL VEL.(+FORW, 32/PPS) IN RUNWAY FRAME
4290  22  Y INERTIAL VEL.(+RIGHT, 32/PPS) IN RUNWAY FRAME
4291
4292  * NOTE THAT THETA, VEL., VEL., AND DRMO ARE PERTURBATION QUANTITIES AND MAY

```

Hover Controller Subroutine. (contd)

-18194 1800		
---	--	--

Hover Controller Subroutine. (contd)

1019A ASSEMBLER, VERSION 1.0 NOV843 10/02/84 SECTION 1

PAGE 30

```

4403      0      PDIOPRDIOPDIOT
4404      0      PDIOPRDIOPRDIOT
4405      0      PDIOPRDIOPRDIOT
4406      0      PDIOPRDIOPRDIOT
4407      0      PDIOPRDIOPRDIOT
4408      0      PDIOPRDIOPRDIOT
4409      0      PDIOPRDIOPRDIOT
4410      0      PDIOPRDIOPRDIOT
4411      0      PDIOPRDIOPRDIOT
4412      0      PDIOPRDIOPRDIOT
4413      0      PDIOPRDIOPRDIOT
4414      0      PDIOPRDIOPRDIOT
4415      0      PDIOPRDIOPRDIOT
4416      0      PDIOPRDIOPRDIOT
4417      0      PDIOPRDIOPRDIOT
4418      0      PDIOPRDIOPRDIOT
4419      0      PDIOPRDIOPRDIOT
4420      0      PDIOPRDIOPRDIOT
4421      0      PDIOPRDIOPRDIOT
4422      0      PDIOPRDIOPRDIOT
4423      0      PDIOPRDIOPRDIOT
4424      0      PDIOPRDIOPRDIOT
4425      0      PDIOPRDIOPRDIOT
4426      0      PDIOPRDIOPRDIOT
4427      0      PDIOPRDIOPRDIOT
4428      0      PDIOPRDIOPRDIOT
4429      0      PDIOPRDIOPRDIOT
4430      0      PDIOPRDIOPRDIOT
4431      0      PDIOPRDIOPRDIOT
4432      0      PDIOPRDIOPRDIOT
4433      0      PDIOPRDIOPRDIOT
4434      0      PDIOPRDIOPRDIOT
4435      0      PDIOPRDIOPRDIOT
4436      0      PDIOPRDIOPRDIOT
4437      0      PDIOPRDIOPRDIOT
4438      0      PDIOPRDIOPRDIOT
4439      0      PDIOPRDIOPRDIOT
4440      0      PDIOPRDIOPRDIOT
4441      0      PDIOPRDIOPRDIOT
4442      0      PDIOPRDIOPRDIOT
4443      0      PDIOPRDIOPRDIOT
4444      0      PDIOPRDIOPRDIOT
4445      0      PDIOPRDIOPRDIOT
4446      0      PDIOPRDIOPRDIOT
4447      0      PDIOPRDIOPRDIOT
4448      0      PDIOPRDIOPRDIOT
4449      0      PDIOPRDIOPRDIOT
4450      0      PDIOPRDIOPRDIOT
4451      0      PDIOPRDIOPRDIOT
4452      0      PDIOPRDIOPRDIOT
4453      0      PDIOPRDIOPRDIOT
4454      0      PDIOPRDIOPRDIOT
4455      0      PDIOPRDIOPRDIOT
4456      0      PDIOPRDIOPRDIOT

```

IDENTICAL EXCEPT FOR THE Y AXIS (PDIOPRDIOT) IS LAT. CONTROL)
 IDENTICAL EXCEPT FOR THE Z AXIS (PDIOPRDIOT) IS COLLECTIVE)
 X AXIS **VELOCITY COMMAND/POSITION HOLD** LOGIC
 AL=PDIOPRDIOT(1)=PILOT LONG STICK
 GET ABS(PDIOPRDIOT(1))
 COMPARE PDIOPRDIOT(1) AND DETENT MAGNITUDE
 IF DETENT IS LARGER GO TO PID CALCULATIONS
 ELSE THE PILOT IS COMMANDING A VELOCITY AND
 WE DO THE FOLLOWING INSTRUCTIONS
 TURN OFF THE PITCH DETENT LIGHT
 PITCH BAR OUT OF VIEW IF NOT PID
 THESE TWO LINES FORCE THE REFERENCE POSITION
 TO FOLLOW
 ACTUAL POSITION WHILE THE PILOT IS COMMANDING
 A RATE.
 GO THE TRANSFORMATION FROM HEADING TO TURN
 GET XREF AND YREF IN THE A REGISTER
 AL=YREF*SCUT MULTIPLIER
 IF NOT RAPPED TO ZERO, GO DOWN AND CONTINUE R
 R
 IF WE'VE RAPPED TO ZERO, HOLD PDIOPRDIOT AT ZERO
 IF WE'VE RAPPED TO ZERO, KEEP RAMP AT ZERO
 SKIP AROUND THE FADE-OUT TO STRZ' COMMAND
 CONTINUE RAMP DOWN
 STORE THE RAMPED DOWN VALUE
 RAMP*PDIOPRDIOT
 DIVIDE BY NUMBER OF CYCLES IN RAMP DOWN
 PDIOPRDIOT*FADE-VALUE
 GET READY FOR PID FADE-IN
 STORE THE FADE-VALUE OF THE LAST PID
 COMMAND BEFORE COMING OUT OF DETENT
 ZERO THE INTEGRATOR
 AL=PDIOPRDIOT(1), PILOT LONG STICK
 IF CONTROL NEGATIVE, SKIP A LINE
 ELSE THE CONTROL IS POSITIVE SO SUBTRACT
 GO STORE THE DERIVED VALUE
 FOR NEG. CONTROL, ADD DETENT
 PUT THE MODIFIED CONTROL BACK IN PDIOPRDIOT
 GO TO THE Y AXIS

Hover Controller Subroutine. (contd)

PAGE 91

1019R ASSEMBLER, VERSION 1.0 HOVR43 10/02/84 SECTION 1

```

4457 007115 123230 PSIP11 ENIAL P1REF
4458 007116 103281 ENIAL P1REF
4459 007117 763366 RJP ACTATE
4460 007120 883287 STRAU P1REF
4461 007121 700001 ENIALK 1
4462 007122 880885 STRAL R/HFLC
4463 007123 602761 STR2 PDU1
4464 007124 123216 ENIAL P1BCD
4465 007125 163231 SUBAL P1REF
4466 007126 883232 STRAL P1ELX
4467 007127 506100 CPAL
4468 007130 780823 RJP SYNCNK
4469 007131 440111 STRAL DPK16
4470 007132 123232 ENIAL P1ELX
4471 007133 243195 PULAL P1P
4472 007134 506707 LTRN 7C
4473 007135 883233 STRAU P1DF
4474 007136 123232 ENIAL P1ELX
4475 007137 760333 RJP ABRAVAL
4476 007140 023178 CRIL PK240
4477 007141 657147 JPLEQ P8115
4478 007142 123232 ENIAL P1ELX
4479 007143 243160 PULAL P1X1
4480 007144 203260 ADDA P1D1
4481 007145 500800 STRA P1C1
4482 007146 033260 P8115 ENIAL P1C1
4483 007150 243163 PULAL P1X1
4484 007151 506708 LTRN 4C
4485 007152 463234 STRAU P1C1
4486 007153 123202 ENIAL P1C1
4487 007154 243166 PULAL P1X1
4488 007155 506704 LTRN 4C
4489 007156 463235 STRAU P1D1
4490 007157 123202 ENIAL P1D1
4491 007160 243170 PULAL P1P1
4492 007161 506704 LTRN 4C
4493 007162 883236 STRAU P1D1
4494 007163 123233 ENIAL P1D1
4495 007164 143281 ADDAL P1D1
4496 007165 143234 ADDAL P1C1
4497 007166 143235 ADDAL P1D1
4498 007167 143236 ADDAL P1D1
4499 007170 883237 STRAL P1D1
4500 007171 123208 ENIAL P1C1
4501 007172 710001 ADDAL 1
4502 007173 103201 ENIAL P1D1
4503 007174 760537 RJP LIMIT
4504 007175 143208 STRAL P1C1
4505 007176 243237 PULAL P1D1

```

DO THE TRANSFORMATION FROM RUNWAY TO HEADING
GET XREF AND YREF IN THE X REGISTER

TURN ON THE PITCH DETENT LIGHT

STORE ZERO IN PILOT COMMAND WHEN IN PID
THESE 3 LINES CALCULATE
THE POSITION ERROR, AL=POELX
STORE P1ELX
USE PITCH BAR TO SHOW XPOAN ERROR
IN PIC PCE
SCALING 3.33V=602 COUNTS=42.6 FEET=1 INCH
MULTIPLY F1P*POELX(DO PROPORTIONAL CONTROL)
SCALING ON XFP IS 1 FPS PER FT ENCR = 1024 B
116
STORE THE RESULT
GET POSITION ERROR TO BE INTEGRATED(IFT=16811
8)
HOLD INTEGRATOR TERM IF ERROR GT 15FT

MULTIPLY BY DIGITIZED INTEGRAL GAIN(1FPS/FT=2
V198115)
DO SUPPATION(THE INTEGRATION)
AU GOES TO P1K11, AL TO P1K1
DO DERIVATIVE CONTROL
F1D=PHAD*P1D01
SCALING ON P1D IS 1 FPS PER FPS = 1024 BYTES
STORE RESULT
GET YREF FOR 2ND DERIVATIVE CONTROL
F1D1=P1C1*P1D1
SCALING ON P1D1 IS 1 FPS PER DEC = 1048 BYTES
STORE THE RESULT
GET 2 FCM 2ND DERIVATIVE CONTROL
F1D1=P1D1*P1D1
SCALING ON P1D1 IS 1 FPS PER DEC/SEC = 1048
2178
STORE THE RESULT
BEGIN THE P1D1C EQUATION

F1D1C=F1C*P1D1+P1D1*P1D1+P1D1*P1D1

ACTN V1C1 MULTIPLIER
DO RAMP UP
USE 178 CYCLES AS THE RAMP UP TIME
LIMIT P1C1 TO P1K128 (LIMIT AL TO AU)
STORE V1C1 P1D1C VALUE
A1=RAMP*F1D1 CONTROL

Hover Controller Subroutine. (contd)

PAGE 53

10198 ASSEMBLER, VERSION 1.0 HCVR43 10/02/84 SECTION 1

LO THE TRANSFORMATION FROM RUNWAY TO HEADING
GET XREF AND YREF IN THE A REGISTERS

TURN ON THE ROLL DETENT LIGHT

STORE ZERO IN THE PILOT COMMAND WHEN IN PID
THESE 3 LINES CALCULATE
THE POSITION ERROR, AL-PEDELY
STORE PEELY
SUC= Y FCSM ERROR ON ROLL BAR
IF IN PID

MULTIPLY FRYPOLELY(DO PROPORTIONAL CONTROL)
SCALING CN RTP IS 1 F23 PER FT ERROR = 1034 6

116 STORE THE RESULT
GET POSITION ERROR TO BE INTEGRATED(1PT=16BIT
)

MULTIPLY BY DIGITIZED INTEGRAL GAIN(1PPS/FT=2
5019017E)

```

CPU DERIVATIVE CONTROL
PYDCC=RDV07D07
SCALING ON PYD0 IS 4 FPS PER FPS & 1045 BITS
STORE RESULT
GET P1(CLL ANGLE) FOR 2ND DERIVATIVE CONTROL
PYDPM=DM10PYPM
SCALING ON PYPM IS 1 FPS PER DEG & 1048 BITS
STORE THE RESULT
GET P FCM 2ND DERIVATIVE CONTROL
PYDAP=CLAP1PYAP
SCALING ON PYAP IS 1FPS PER DEG/SEC & 1048 B

```

176
STONY THE RESULY
BEGIN THE PYOPIC EQUATION

THE UNIVERSITY OF CHICAGO

ALU FACTOR MULTIPLIER

CO RAMP UP
USE 178 CYCLES IS THE NAME OF TIME
LIMIT PIECE TO PR126 (L1017 AL TC AU)
STONE NAME FADEN VALUE
ALSRAMP010 CONTROL
DIVIDE BY NUMBER OF CYCLES IN NAME
AND LAST PID COMMAND(FADED) TO AVCIO T

DO HAVE FADE-IN OF PID COMMAND WHEN THE PILOT
GOES BACK INTO DETENT

TWITC PYETCN

ADDALK 1

LIMP
LIMP

STREET **NO. 14**

PULAL PYDID
 PSHA 7E

ADOCAL PYC187

—

1
2
3
4
5
6
7
8
9
10
11
12
13
14
15
16
17
18
19
20
21
22
23
24
25
26
27
28
29
30
31
32
33
34
35
36
37
38
39
40
41
42
43
44
45
46
47
48
49
50
51
52
53
54
55
56
57
58
59
60
61
62
63
64
65
66
67
68
69
70
71
72
73
74
75
76
77
78
79
80
81
82
83
84
85
86
87
88
89
90
91
92
93
94
95
96
97
98
99
100
101
102
103
104
105
106
107
108
109
110
111
112
113
114
115
116
117
118
119
120
121
122
123
124
125
126
127
128
129
130
131
132
133
134
135
136
137
138
139
140
141
142
143
144
145
146
147
148
149
150
151
152
153
154
155
156
157
158
159
160
161
162
163
164
165
166
167
168
169
170
171
172
173
174
175
176
177
178
179
180
181
182
183
184
185
186
187
188
189
190
191
192
193
194
195
196
197
198
199
200
201
202
203
204
205
206
207
208
209
210
211
212
213
214
215
216
217
218
219
220
221
222
223
224
225
226
227
228
229
230
231
232
233
234
235
236
237
238
239
240
241
242
243
244
245
246
247
248
249
250
251
252
253
254
255
256
257
258
259
260
261
262
263
264
265
266
267
268
269
270
271
272
273
274
275
276
277
278
279
280
281
282
283
284
285
286
287
288
289
290
291
292
293
294
295
296
297
298
299
300
301
302
303
304
305
306
307
308
309
310
311
312
313
314
315
316
317
318
319
320
321
322
323
324
325
326
327
328
329
330
331
332
333
334
335
336
337
338
339
340
341
342
343
344
345
346
347
348
349
350
351
352
353
354
355
356
357
358
359
360
361
362
363
364
365
366
367
368
369
370
371
372
373
374
375
376
377
378
379
380
381
382
383
384
385
386
387
388
389
390
391
392
393
394
395
396
397
398
399
400
401
402
403
404
405
406
407
408
409
410
411
412
413
414
415
416
417
418
419
420
421
422
423
424
425
426
427
428
429
430
431
432
433
434
435
436
437
438
439
440
441
442
443
444
445
446
447
448
449
450
451
452
453
454
455
456
457
458
459
460
461
462
463
464
465
466
467
468
469
470
471
472
473
474
475
476
477
478
479
480
481
482
483
484
485
486
487
488
489
490
491
492
493
494
495
496
497
498
499
500
501
502
503
504
505
506
507
508
509
510
511
512
513
514
515
516
517
518
519
520
521
522
523
524
525
526
527
528
529
530
531
532
533
534
535
536
537
538
539
540
541
542
543
544
545
546
547
548
549
550
551
552
553
554
555
556
557
558
559
560
561
562
563
564
565
566
567
568
569
570
571
572
573
574
575
576
577
578
579
580
581
582
583
584
585
586
587
588
589
590
591
592
593
594
595
596
597
598
599
600
601
602
603
604
605
606
607
608
609
610
611
612
613
614
615
616
617
618
619
620
621
622
623
624
625
626
627
628
629
630
631
632
633
634
635
636
637
638
639
640
641
642
643
644
645
646
647
648
649
650
651
652
653
654
655
656
657
658
659
660
661
662
663
664
665
666
667
668
669
670
671
672
673
674
675
676
677
678
679
680
681
682
683
684
685
686
687
688
689
690
691
692
693
694
695
696
697
698
699
700
701
702
703
704
705
706
707
708
709
710
711
712
713
714
715
716
717
718
719
720
721
722
723
724
725
726
727
728
729
730
731
732
733
734
735
736
737
738
739
740
741
742
743
744
745
746
747
748
749
750
751
752
753
754
755
756
757
758
759
760
761
762
763
764
765
766
767
768
769
770
771
772
773
774
775
776
777
778
779
780
781
782
783
784
785
786
787
788
789
790
791
792
793
794
795
796
797
798
799
800
801
802
803
804
805
806
807
808
809
810
811
812
813
814
815
816
817
818
819
820
821
822
823
824
825
826
827
828
829
830
831
832
833
834
835
836
837
838
839
840
84

1

Journal of Management Inquiry 26(4) 399–417 399

Hover Controller Subroutine. (contd)

PAGE 58

1019A ASSEMBLER, VERSION 1.0 MCVR03 10/02/84 SECTION 1

PUT SUP BACK INTO PID COMMAND
STORE PID COMMAND FOR LATER FADE-OUT
GET READY FOR THE PI-OLD FADE-OUT ABOVE
PTECFF GET START OF FADE-OUT VALUE

2 AXIS ***VELOCITY COMMAND/POSITION HOLD***

ALIMPLT(2)PILDT COLLECTIVE
GET ABS(PPLT(2))
COMPARE PPLT(2) AND DETENT MAGNITUDE
IF DETENT IS LARGER GO TO PID CALCULATIONS

ELSE THE PILOT IS COMMANDING A VELOCITY AND
WE DO THE FOLLOWING INSTRUCTIONS

TURN OFF THE COLLECTIVE DETENT LIGHT
THESE TWO LINE FORCE THE REFERENCE POSITION 1
C PCLCN
ACTUAL POSITION WHILE THE PILOT IS COMMANDING
A RATE.

DO FADE OUT OF OLD PID CONTROL WHILE PILOT IS
COMMANDING A VELOCITY.

ALIMPLT(2)PILDT COLLECTIVE
IF NOT MAPPED TO ZERO, GO DOWN AND CONTINUE A
RAMP

IF WE'VE RAMPED TO ZERO, HOLD PZDCLC AT ZERO
IF WE'VE RAMPED TO ZERO, KEEP RAMP AT ZERO
SKIP AROUND THE FADE-OUT TO STR2' COMMAND
CONTINUE RAMP DOWN
STORE THE RAMPED DOWN VALUE
ALIMPLT(2)PILDT COLLECTIVE

DIVIDE BY NUMBER OF CYCLES IN RAMP DOWN
PZDCLC = PZDCLC / PZDCLC
GET READY FOR PID FADE-IN
STORE THE FADE-OUT VALUE OF THE LAST PID
COMMAND BEFORE COMING OUT OF DETENT
ZERO THE INTEGRATOR

NON DO THE DEADZONE CALCULATIONS

ALIMPLT(2)PILDT COLLECTIVE
IF CONTROL NEGATIVE, SKIP A LINE
ELSE THE CONTROL IS POSITIVE SO SUBTRACT

THE DETENT VALUE.

GO STORE THE DEADZONED PILOT COMMAND
FOR NEG. CONTROL, ADD DETENT
PUT THE DEADZONED CONTROL BACK IN PPLT(2)
GO TO THE PILOT SCALING ROUTINE
STORE ZERO IN THE PILOT COMMAND WHEN IN PID
TURN ON THE COLLECTIVE DETENT LIGHT

THESE 3 LINES CALCULATE
THE POSITION ERROR, ACWPOSIZ
STORE PCLZ
MULTIPLY PZDPPPOSIZ(00 PROPORTIONAL CONTROL)
SCALING ON K2P IS 1 FPS PER FT ERROR = 1024 B

ITG
STORE THE RESULT

4612 007331 43250 STRAL PZDCLC
4613 007332 43251 STRAL PZDCLC
4614 007333 123200 ENTAL PZDCLC
4615 007334 43252 STRAL PZDCLC
4616 007335 43253 STRAL PZDCLC

4617 007336 43254 STRAL PZDCLC
4618 007337 43255 STRAL PZDCLC

4619 007338 123201 ENTAL PZDCLC
4620 007339 700533 RJP ABSVAL
4621 007340 073174 CMAL PZDCLC
4622 007341 673372 JPMGR PZDCLC
4623 007342 43256 STRAL PZDCLC

4624 007343 000000 STR2 C7R7C
4625 007344 123220 ENTAL PZDCLC
4626 007345 123220 STRAL PZDCLC

4627 007346 43252 STRAL PZDCLC

4628 007347 43253 STRAL PZDCLC

4629 007348 43254 STRAL PZDCLC

4630 007349 43255 STRAL PZDCLC

4631 007350 43256 STRAL PZDCLC

4632 007351 43257 STRAL PZDCLC

4633 007352 43258 STRAL PZDCLC

4634 007353 43259 STRAL PZDCLC

4635 007354 43260 STRAL PZDCLC

4636 007355 43261 STRAL PZDCLC

4637 007356 43262 STRAL PZDCLC

4638 007357 43263 STRAL PZDCLC

4639 007358 43264 STRAL PZDCLC

4640 007359 43265 STRAL PZDCLC

4641 007360 43266 STRAL PZDCLC

4642 007361 43267 STRAL PZDCLC

4643 007362 43268 STRAL PZDCLC

4644 007363 43269 STRAL PZDCLC

4645 007364 43270 STRAL PZDCLC

4646 007365 43271 STRAL PZDCLC

Hover Controller Subroutine. (contd)

PAGE 95

[illegible]

Hover Controller Subroutine. (contd)

[illegible]

Hover Controller Subroutine. (contd)

PAGE 97

10198 ASSEMBLER, VERSION 1.0 NOV843 10/02/84 SECTION 1

```

4774      0
4775      0
4776      0
4777      0
4778      0
4779      0
4780      007330 507310 PSTP4 1C
4781      007331 507201 ENTIR 1C
4782      007332 360000 ENTIR 0
4783      007333 400002 STRZ 2
4784      007334 400003 STRZ 3
4785      007335 507313 ENTIR 13
4786      007336 123137 ENTAL PRM
4787      007337 717778 ADDALC -1
4788      007340 507310 ENTIR 1C
4789      007341 448711 STRAL PPNEND
4790      007342 507313 ENTIR 13
4791      007343 700000 PPNEND
4792      007344 507400 IPRLU
4793      007345 500000 PPNCL2 STRA TYP
4794      007346 031450 ENTIR 2
4795      007347 507202 ENTIR 1
4796      007350 370001 ENTIR 1
4797      007351 132764 ENTALC PPS-1
4798      007352 507201 ENTIR 1
4799      007353 753078 PULIR PPN
4800      007354 201450 ADDA TYP
4801      007355 503300 SKPROV
4802      007356 504000 NOOP
4803      007357 508711 PSK
4804      007358 347570 JP PRBL2
4805      007361 370001 ENTIR 1
4806      007362 507203 ENTIR 3
4807      007363 504704 LRTA 4C
4808      007364 473074 STRAUS PPRF1
4809      007365 566712 PSK PRM1
4810      007366 347570 JP PRBL2
4811      007367 347600 JP PSTP5
4812      007370 507202 PRBL2 ENTIR 2
4813      007371 360000 ENTIR 0
4814      007372 507310 ENTIR 1C
4815      007373 126711 ENTAL PPNEND
4816      007374 146717 ADDAL PPNEND
4817      007375 448711 STRAL PPNEND
4818      007376 507313 ENTIR 13
4819      007377 347570 JP PPNW2
4820      007378 347570
4821      0
4822      0
4823      0
4824      0
4825      0
4826      0
4827      0
4828      0
4829      007600 507202 PSTP5 ENTIR 2
4830      007601 507202 SELECT ICR2(J=JCR2)

```

USE MEMORY BANK 0
 USE ICR1 AS THE INDEX REG.(8)
 INITIALIZE THE 8 REG. TO 0
 ICR2=0, THE COLUMN INDEX
 ICR3=0, THE ROW INDEX
 USE MEMORY BANK 3
 ALI=NUMBER OF MEASUREMENTS
 ALI=PPN-1
 USE MEMORY BANK 0 SINCE PPNEND IS THERE
 PPNEND=PPN-1
 BACK TO MEMORY BANK 3 FOR DATA
 ALI=0
 ALI=AL-0
 TYP=1A

GET THE COLUMN INDEX
 INCREMENT COLUMN INDEX(ICR2=ICR2+1)
 ALI=(PPN-ICR2-1)
 USE ICR1 AS INDEX REG.(ELEMENT INDEX)
 STRL 9 (PPN-ICR1)
 ALI=ALI + (TYP,PPN+1)
 CHECK FOR OVERFLOW
 CALL OVERFLOW HANDLER
 IF ICR1=PPNEND THEN SKIP NEXT LINE
 ELSE DO NEXT LINE AND ICR1=ICR1+1

JUMP TO NEXT COLUMN OF PPN
 ICR1=ICR1+1
 USE ICR3 AS INDEX REG.(ROW INDEX)
 PSTP4 SCALING IS 2+014
 PPN=ICR3*(ALI)
 IF ICR3=PPN THEN SKIP NEXT LINE
 ELSE DO NEXT LINE AND ICR3=ICR3+1

GO RESET THE COUNTER
 GO TO NEXT MATRIX ROW IF DONE
 SAVE ROW INDEX AND START USING COLUMN INDEX
 RESET COLUMN INDEX TO ZERO
 BANK 0 TO USE PPNEND AND PPNENDS
 ALI=PPNEND
 PPNENDS=PPNENDS+PPNENDS+1 OF COLUMNS
 BACK TO MEMORY BANK 3 FOR DATA
 GO TO THE NEXT ROW

THIS STEP(PSTP5) DOES THE MATRIX MULTIPLICATION
 DESCRIBED BY
 PPNW2
 WHERE PPNW2 IS THE MINIMAL FORM OF THE COMPENSATOR
 DYNAMIC MATRIX

Hover Controller Subroutine. (contd)

```

PAGE 98
SECTION 1
MOVPR3 10/07/84
VERSION 1.0
ASSEMBLER,
4830 007601 360000 ENTBR 0
4831 007602 507201 ENTBR 1
4832 007603 360000 ENTBR 0
4833 007604 506713 PSTP50 PPR
4834 LINE ELSE ICR1=ICR1+(I1=I+1) AND DO NEXT LINE
4835 JP PETP51
4836 007606 347645 JP PETP54
4837 007607 507202 PSTP51 ENTBR 2
4838 007610 131140 ENTALB PADESC
4839 007611 023511 CMAC PCMP
4840 007612 617616 JPEQ PETP52
4841 007613 023512 CMAC PTMC
4842 007614 617623 JPEQ PETP53
4843 007615 506700 MOOP
4844 THIS IS THE SECTION FOR 1X1 BLOCKS OF AMIN
4845 007616 370001 PSTP52 ENTBR 1
4846 007617 507201 ENTBR 1
4847 007620 133030 ENTALB PAMIN=1
4848 007621 253016 PULALB PZK=1
4849 007622 506703 LTR 1
4850 007623 413276 STRAUB TPPEZ-1
4851 007624 347604 JP PETP50
4852 THIS IS THE SECTION FOR 2X2 BLOCKS OF AMIN
4853 007625 370001 PSTP53 ENTBR 1
4854 007626 507201 ENTBR 1
4855 007627 133017 ENTALB PZK
4856 007630 453276 STRALB TPPEZ-1
4857 007631 133030 ENTALB PAMIN-1
4858 007632 253016 PULALB PZM=1
4859 007633 504703 LATA 3
4860 007634 021650 STRAU TPP
4861 ENTBR 1
4862 007635 133031 ENTALB PAMIN
4863 007636 253017 PULALB PZK
4864 007637 504703 LATA 3
4865 007640 507500 XPRUD
4866 007641 141650 ADDAL TPP
4867 007642 453277 STRAUB TPPEZ
4868 007643 370001 ENTBR 1
4869 007644 370001 ENTBR 1
4870 007645 347604 JP PETP50
4871 007646 347604 ENTBR 1
4872 007647 360001 PSTP54 ENTBR 1
4873 THIS SECTION ACDS PBMIN*PXS + FAPIN*PZK
4874 AND PUTS THE RESULT IN THE PZM1 VECTOR
4875 007648 133023 PSTP55 ENTALB PZM1-1
4876 007649 133016 ADDALB TPPEZ-1
4877 007650 433023 STRALB PZM1-1
4878 007651 506713 FOR
4879 007652 347646 JP PETP55
4880 007653 347654 JP PETP56
4881 007654 347654 JP PETP56
4882 007655 347654 JP PETP56
4883 007656 347654 JP PETP56
4884 007657 347654 JP PETP56
4885 007658 347654 JP PETP56
4886 007659 347654 JP PETP56
4887 007660 347654 JP PETP56
4888 007661 347654 JP PETP56
4889 007662 347654 JP PETP56
4890 007663 347654 JP PETP56
4891 007664 347654 JP PETP56
4892 007665 347654 JP PETP56
4893 007666 347654 JP PETP56
4894 007667 347654 JP PETP56
4895 007668 347654 JP PETP56
4896 007669 347654 JP PETP56
4897 007670 347654 JP PETP56
4898 007671 347654 JP PETP56
4899 007672 347654 JP PETP56
4900 007673 347654 JP PETP56
4901 007674 347654 JP PETP56
4902 007675 347654 JP PETP56
4903 007676 347654 JP PETP56
4904 007677 347654 JP PETP56
4905 007678 347654 JP PETP56
4906 007679 347654 JP PETP56
4907 007680 347654 JP PETP56
4908 007681 347654 JP PETP56
4909 007682 347654 JP PETP56
4910 007683 347654 JP PETP56
4911 007684 347654 JP PETP56
4912 007685 347654 JP PETP56
4913 007686 347654 JP PETP56
4914 007687 347654 JP PETP56
4915 007688 347654 JP PETP56
4916 007689 347654 JP PETP56
4917 007690 347654 JP PETP56
4918 007691 347654 JP PETP56
4919 007692 347654 JP PETP56
4920 007693 347654 JP PETP56
4921 007694 347654 JP PETP56
4922 007695 347654 JP PETP56
4923 007696 347654 JP PETP56
4924 007697 347654 JP PETP56
4925 007698 347654 JP PETP56
4926 007699 347654 JP PETP56
4927 007700 347654 JP PETP56
4928 007701 347654 JP PETP56
4929 007702 347654 JP PETP56
4930 007703 347654 JP PETP56
4931 007704 347654 JP PETP56
4932 007705 347654 JP PETP56
4933 007706 347654 JP PETP56
4934 007707 347654 JP PETP56
4935 007708 347654 JP PETP56
4936 007709 347654 JP PETP56
4937 007710 347654 JP PETP56
4938 007711 347654 JP PETP56
4939 007712 347654 JP PETP56
4940 007713 347654 JP PETP56
4941 007714 347654 JP PETP56
4942 007715 347654 JP PETP56
4943 007716 347654 JP PETP56
4944 007717 347654 JP PETP56
4945 007718 347654 JP PETP56
4946 007719 347654 JP PETP56
4947 007720 347654 JP PETP56
4948 007721 347654 JP PETP56
4949 007722 347654 JP PETP56
4950 007723 347654 JP PETP56
4951 007724 347654 JP PETP56
4952 007725 347654 JP PETP56
4953 007726 347654 JP PETP56
4954 007727 347654 JP PETP56
4955 007728 347654 JP PETP56
4956 007729 347654 JP PETP56
4957 007730 347654 JP PETP56
4958 007731 347654 JP PETP56
4959 007732 347654 JP PETP56
4960 007733 347654 JP PETP56
4961 007734 347654 JP PETP56
4962 007735 347654 JP PETP56
4963 007736 347654 JP PETP56
4964 007737 347654 JP PETP56
4965 007738 347654 JP PETP56
4966 007739 347654 JP PETP56
4967 007740 347654 JP PETP56
4968 007741 347654 JP PETP56
4969 007742 347654 JP PETP56
4970 007743 347654 JP PETP56
4971 007744 347654 JP PETP56
4972 007745 347654 JP PETP56
4973 007746 347654 JP PETP56
4974 007747 347654 JP PETP56
4975 007748 347654 JP PETP56
4976 007749 347654 JP PETP56
4977 007750 347654 JP PETP56
4978 007751 347654 JP PETP56
4979 007752 347654 JP PETP56
4980 007753 347654 JP PETP56
4981 007754 347654 JP PETP56
4982 007755 347654 JP PETP56
4983 007756 347654 JP PETP56
4984 007757 347654 JP PETP56
4985 007758 347654 JP PETP56
4986 007759 347654 JP PETP56
4987 007760 347654 JP PETP56
4988 007761 347654 JP PETP56
4989 007762 347654 JP PETP56
4990 007763 347654 JP PETP56
4991 007764 347654 JP PETP56
4992 007765 347654 JP PETP56
4993 007766 347654 JP PETP56
4994 007767 347654 JP PETP56
4995 007768 347654 JP PETP56
4996 007769 347654 JP PETP56
4997 007770 347654 JP PETP56
4998 007771 347654 JP PETP56
4999 007772 347654
```

```
DATA FOR OPTSYS FOR THE CHAPTER 2 NAVION EXAMPLE
1 1 1Q INQ IR IOMF ISS IM ITF1 DM ITF3 IFDFW IE IDSTB IDBG ISET ILNG ISCLE IMIN
1 1 0 0 0 0 0 0 0 0 3 0 0 0 2 0 1 1 1
NS NC NM NPD NO NMOD IREG
4 2 3 2 2 0 0 0
IS MATRIX(NS)
1 0 1 0 01 01
IC MATRIX(NC)
01 1 0
ID MATRIX(NPD)
1 0 1 0
IM MATRIX(NM)
1 0 1 0 01
IP MATRIX(NO)
1 0 1 0
I MATRIX(NS X NS)
- 045 - 036 0 - 32 2
- 37 - 2 02 176 0 0
00191 - 0396 - 2 98 0
0 0 1 0 0
HO MATRIX(NO X NS)
1 0 0 0 0
0 - 1 0 0 176 0
PL MATRIX(NO X NC)
0 0
0 0
(AZ AM) MATRIX(NO)
1 1
G MATRIX(NS X NC)
0 1 0
- 28 2 0
- 11 0 0
0 0
B MATRIX(NC)
1 1
HM MATRIX(NM X NS)
1 0 0 0 0
0 - 1 0 0 176 0
0 0 0 1 0
PN MATRIX(NM X NPD)
0 0
0 0
0 0
GAMMA MATRIX(NS X NPD)
045 - 036
37 2 02
- 00191 0396
0 0
Q MATRIX(NPD)
24 6 3 98
R MATRIX(NM)
318 318 00039
```

ROPTSYS User's Manual. (contd)

FOR ONE REGULATOR SYNTHESIS USE
 F HO FM HS AM Q B
 FOR FILTER SYNTHESIS USE
 F HO GAM Q R
 DSTAB R ENTER DIAGONAL ELEMENTS ONLY
 (AT AM) B Q ARE DIAGONAL OR FULL (SELECT IR)
 WO IS A VECTOR

IF LAST CARD COL 1 IS * THEN CONTINUE TO NEXT CASE
 each case expects complete title lines options sizes and matrices

SUBROUTINE LISTING
 SETUP USER CAN SET UP OPEN LOOP DYNAMICS MATRIX
 INNER OPTIMAL CONTROLLER/OPTIMAL ESTIMATOR DESIGN
 ONE OPTIMAL MODEL FOLLOWING DESIGN OPTION
 COIV COMPLEX DIVISION
 RAUPRINT MATRIX PRINTING
 RGAIN REFORMATS EIGENVALUES CALCULATES MODAL SUBMATRICES
 MULT MATRIX MULTIPLICATION
 MADD MATRIX ADDITION
 MTRM MATRIX TRANSPOSITION
 MINV MATRIX INVERSION
 SLOV SOLVES LYAPUNOV EQUATION FOR SS COVARIANCE
 MODE COMPUTES MODAL COORDINATE MATRICES
 NFORM FORMATS EIGENVALUE/EIGENVECTOR OUTPUT
 TF COMPUTES TRANSFER FUNCTIONS
 CHECK CHECK CONSISTENCY OF INPUTS
 POLES PRINT OUT TF POLES
 ZEROS COMPUTE SISO TF ZEROS
 ACOMP COMPUTE ZEROS BY BROCKETT'S METHOD (3 SUBROUTINES)
 COOMP
 SCL FUNCTION
 RESID COMPUTE (TIME RESPONSE) RESIDUES
 BALANC FIND EIGENVALUES AND EIGENVECTORS VIA
 ORTHES THE QR ALGORITHM (6 SUBROUTINES)
 MTRM
 HOP2
 RALTRAK
 HOP
 MODCOM CALCULATES THE MODAL FORM OF THE COMPENSATOR (HOLLORIDGE)
 MINCOM CALCULATES THE MINIMAL FORM OF THE COMPENSATOR (HOLLORIDGE)

ROPTSYS User's Manual.

[illegible]

Appendix J.

ROPTSYS Computer Program

This appendix includes the users manual for the ROPTSYS computer program, which is located on the FSD VAX at NASA Ames Research center, and an example data file. The data file was used to calculate the full order compensator in the Navion example in Chapter 2. The lengthy FORTRAN listing is not shown.

Memory Allocation. (contd)

PAGE 165

10794 200000000, VERSION 1.0 NOV83 10/02/84 SECTION 3

RESERVE MEMORY FOR THE FADER RAMPS

7968 033266 000000 P1EZCH RESERV RESERV'ID
 7969 033267 000000 P1EZCH RESERV RESERV'ID
 7970 033270 000000 P1EZCH RESERV RESERV'ID
 7971 033271 000000 P1EZCH RESERV RESERV'ID
 7972 033272 000000 P1EZCH RESERV RESERV'ID
 7973 033273 000000 P1EZCH RESERV RESERV'ID
 7974 033274 000000 P1EZCH RESERV RESERV'ID
 7975 033275 000000 P1EZCH RESERV RESERV'ID
 7976 033276 000000 P1EZCH RESERV RESERV'ID
 7977 033277 000000 P1EZCH RESERV RESERV'ID
 7978 033278 000000 P1EZCH RESERV RESERV'ID

TEMPORARY USED IN PSTP52 AND PSTP53

CONSTANTS FOR CMSTRG SUBROUTINE

7980 033311 000001 PONE 1D
 7981 033312 000002 PONE 2D

COMPLEMENTARY FILTER FREQUENCIES AND DAMPINGS

7984 033313 000310 NFREQH 200D
 7985 033314 000320 NFREQH 400D
 7986 033315 000330 NFREQH 600D
 7987 033316 000340 NFREQH 800D
 7988 033317 000350 NFREQH 1000D
 7989 033318 000360 NFREQH 1200D
 7990 033319 000370 NFREQH 1400D
 7991 033320 000380 NFREQH 1600D
 7992 033321 000390 NFREQH 1800D
 7993 033322 000400 NFREQH 2000D
 7994 033323 000410 NFREQH 2200D
 7995 033324 000420 NFREQH 2400D

KALMAN FREQ 1000/RPS

KALMAN DAPPING 1000/UNIT

KALMAN CYCLE LIMITER

Memory Allocation. (contd)

10192 ASSEMBLY, VERSION 1.0				SECTION	
7911	033200	000100	PK64	CATA	64C
7912	033201	000200	PK78	CATA	128C
7913					
7914					
7915					
7916					
7917	033202	000300	PK92	RESERV	RESERV*1D
7918	033203	000400	PK106	RESERV	RESERV*1C
7919	033204	000500	PK120	RESERV	RESERV*1C
7920	033205	000600	PK134	RESERV	RESERV*1D
7921	033206	000700	PK148	RESERV	RESERV*1D
7922	033207	000800	PK162	RESERV	RESERV*1D
7923	033210	000900	PK176	RESERV	RESERV*1D
7924	033211	001000	PK190	RESERV	RESERV*1D
7925	033212	001100	PK204	RESERV	RESERV*1D
7926	033213	001200	PK218	RESERV	RESERV*1D
7927	033214	001300	PK232	RESERV	RESERV*1D
7928	033215	001400	PK246	RESERV	RESERV*1D
7929	033216	001500	PK260	RESERV	RESERV*1D
7930	033217	001600	PK274	RESERV	RESERV*1D
7931	033220	001700	PK288	RESERV	RESERV*1C
7932	033221	001800	PK302	RESERV	RESERV*1D
7933	033222	001900	PK316	RESERV	RESERV*1D
7934	033223	002000	PK330	RESERV	RESERV*1D
7935	033224	002100	PK344	RESERV	RESERV*1D
7936	033225	002200	PK358	RESERV	RESERV*1D
7937	033226	002300	PK372	RESERV	RESERV*1D
7938	033227	002400	PK386	RESERV	RESERV*1D
7939					
7940	033230	002500	PK400	RESERV	RESERV*1D
7941	033231	002600	PK414	RESERV	RESERV*1D
7942	033232	002700	PK428	RESERV	RESERV*1D
7943	033233	002800	PK442	RESERV	RESERV*1C
7944	033234	002900	PK456	RESERV	RESERV*1D
7945	033235	003000	PK470	RESERV	RESERV*1D
7946	033236	003100	PK484	RESERV	RESERV*1D
7947	033237	003200	PK498	RESERV	RESERV*1D
7948	033240	003300	PK512	RESERV	RESERV*1D
7949	033241	003400	PK526	RESERV	RESERV*1D
7950	033242	003500	PK540	RESERV	RESERV*1D
7951	033243	003600	PK554	RESERV	RESERV*1D
7952	033244	003700	PK568	RESERV	RESERV*1D
7953	033245	003800	PK582	RESERV	RESERV*1D
7954	033246	003900	PK596	RESERV	RESERV*1D
7955	033247	004000	PK610	RESERV	RESERV*1D
7956	033250	004100	PK624	RESERV	RESERV*1D
7957	033251	004200	PK638	RESERV	RESERV*1D
7958	033252	004300	PK652	RESERV	RESERV*1C
7959	033253	004400	PK666	RESERV	RESERV*1D
7960	033254	004500	PK680	RESERV	RESERV*1D
7961	033255	004600	PK694	RESERV	RESERV*1D
7962	033256	004700	PK708	RESERV	RESERV*1D
7963	033257	004800	PK722	RESERV	RESERV*1D
7964					
7965	033260	004900	PK736	RESERV	RESERV*2
7966	033262	005000	PK750	RESERV	RESERV*2
7967	033264	005100	PK764	RESERV	RESERV*2
7968					
7969					
7970					
7971					
7972					
7973					
7974					
7975					
7976					
7977					
7978					
7979					
7980					
7981					
7982					
7983					
7984					
7985					
7986					
7987					
7988					
7989					
7990					
7991					
7992					
7993					
7994					
7995					
7996					
7997					
7998					
7999					
8000					

64 CYCLE FADE VALUE
128 CYCLE FADE VALUE

THE FOLLOWING 22 VARIABLE DECLARATIONS MUST STAY IN
THE ORDER HERE TO MAKE THE MEASUREMENT SELECTION LOGIC
IN CPPS184 CORRECT

PENTURBATION PITCH ANGLE
ROLL ANGLE

YAW ANGLE
PITCH RATE
ROLL RATE

LONG. ACCELERATION

LATERAL ACCELERATION
NORMAL ACCELERATION

PENTURBATION AIRSPEED

VERTICAL VELOCITY

BAROMETRIC ALTITUDE

X POSITION IN HEADING INERTIAL FRAME

Y POSITION IN HEADING INERTIAL FRAME

Z POSITION IN HEADING INERTIAL FRAME

INERTIAL X VEL, IN HEADING INERTIAL FRAME

INERTIAL Y VEL, IN HEADING INERTIAL FRAME

INERTIAL Z VEL, IN HEADING INERTIAL FRAME

RUNWAY FRAME X POSITION

RUNWAY FRAME Y POSITION

RUNWAY FRAME X INERTIAL VELOCITY

RUNWAY FRAME Y INERTIAL VELOCITY

REFERENCE POSITION

ROTATED REFERENCE POSITION

X POSITION ERROR

X PROPORTIONAL CONTROL

X DERIVATIVE CONTROL

X 2ND DERIVATIVE CONTROL (THETA FEEDBACK)

X 3RD DERIVATIVE CONTROL (PITCH RATE FEEDBACK)

X TOTAL PID CONTROL

CLO X TOTAL PID CONTROL

REFERENCE POSITION

ROTATED REFERENCE POSITION

Y POSITION ERROR

Y PROPORTIONAL CONTROL

Y DERIVATIVE CONTROL

Y 2ND DERIVATIVE CONTROL (PHI FEEDBACK)

Y 3RD DERIVATIVE CONTROL (ROLL RATE FEEDBACK)

Y TOTAL PID CONTROL

CLO Y TOTAL PID CONTROL

REFERENCE POSITION

Z POSITION ERROR

Z PROPORTIONAL CONTROL

Z DERIVATIVE CONTROL

Z TOTAL PID CONTROL

CLO Z TOTAL PID CONTROL

X INTEGRAL CONTROL

Y INTEGRAL CONTROL

Z INTEGRAL CONTROL

Memory Allocation. (contd)

1019A ASSEMBLER, VERSION 1.0 MVR03 10/02/84 SECTION 3

PAGE 103

7076	033113	000325	DATA	213C,-76C,755C,2048C,229D																																																																																																																																																																																																																																																																																																																																																																																																																																																																																																																																																																																																																																																																																																																																																																																																																																																																																																																																																																																																																																																																																																																																																																																																																																																																																																																																																																																						
------	--------	--------	------	---------------------------	--	--	--	--	--	--	--	--	--	--	--	--	--	--	--	--	--	--	--	--	--	--	--	--	--	--	--	--	--	--	--	--	--	--	--	--	--	--	--	--	--	--	--	--	--	--	--	--	--	--	--	--	--	--	--	--	--	--	--	--	--	--	--	--	--	--	--	--	--	--	--	--	--	--	--	--	--	--	--	--	--	--	--	--	--	--	--	--	--	--	--	--	--	--	--	--	--	--	--	--	--	--	--	--	--	--	--	--	--	--	--	--	--	--	--	--	--	--	--	--	--	--	--	--	--	--	--	--	--	--	--	--	--	--	--	--	--	--	--	--	--	--	--	--	--	--	--	--	--	--	--	--	--	--	--	--	--	--	--	--	--	--	--	--	--	--	--	--	--	--	--	--	--	--	--	--	--	--	--	--	--	--	--	--	--	--	--	--	--	--	--	--	--	--	--	--	--	--	--	--	--	--	--	--	--	--	--	--	--	--	--	--	--	--	--	--	--	--	--	--	--	--	--	--	--	--	--	--	--	--	--	--	--	--	--	--	--	--	--	--	--	--	--	--	--	--	--	--	--	--	--	--	--	--	--	--	--	--	--	--	--	--	--	--	--	--	--	--	--	--	--	--	--	--	--	--	--	--	--	--	--	--	--	--	--	--	--	--	--	--	--	--	--	--	--	--	--	--	--	--	--	--	--	--	--	--	--	--	--	--	--	--	--	--	--	--	--	--	--	--	--	--	--	--	--	--	--	--	--	--	--	--	--	--	--	--	--	--	--	--	--	--	--	--	--	--	--	--	--	--	--	--	--	--	--	--	--	--	--	--	--	--	--	--	--	--	--	--	--	--	--	--	--	--	--	--	--	--	--	--	--	--	--	--	--	--	--	--	--	--	--	--	--	--	--	--	--	--	--	--	--	--	--	--	--	--	--	--	--	--	--	--	--	--	--	--	--	--	--	--	--	--	--	--	--	--	--	--	--	--	--	--	--	--	--	--	--	--	--	--	--	--	--	--	--	--	--	--	--	--	--	--	--	--	--	--	--	--	--	--	--	--	--	--	--	--	--	--	--	--	--	--	--	--	--	--	--	--	--	--	--	--	--	--	--	--	--	--	--	--	--	--	--	--	--	--	--	--	--	--	--	--	--	--	--	--	--	--	--	--	--	--	--	--	--	--	--	--	--	--	--	--	--	--	--	--	--	--	--	--	--	--	--	--	--	--	--	--	--	--	--	--	--	--	--	--	--	--	--	--	--	--	--	--	--	--	--	--	--	--	--	--	--	--	--	--	--	--	--	--	--	--	--	--	--	--	--	--	--	--	--	--	--	--	--	--	--	--	--	--	--	--	--	--	--	--	--	--	--	--	--	--	--	--	--	--	--	--	--	--	--	--	--	--	--	--	--	--	--	--	--	--	--	--	--	--	--	--	--	--	--	--	--	--	--	--	--	--	--	--	--	--	--	--	--	--	--	--	--	--	--	--	--	--	--	--	--	--	--	--	--	--	--	--	--	--	--	--	--	--	--	--	--	--	--	--	--	--	--	--	--	--	--	--	--	--	--	--	--	--	--	--	--	--	--	--	--	--	--	--	--	--	--	--	--	--	--	--	--	--	--	--	--	--	--	--	--	--	--	--	--	--	--	--	--	--	--	--	--	--	--	--	--	--	--	--	--	--	--	--	--	--	--	--	--	--	--	--	--	--	--	--	--	--	--	--	--	--	--	--	--	--	--	--	--	--	--	--	--	--	--	--	--	--	--	--	--	--	--	--	--	--	--	--	--	--	--	--	--	--	--	--	--	--	--	--	--	--	--	--	--	--	--	--	--	--	--	--	--	--	--	--	--	--	--	--	--	--	--	--	--	--	--	--	--	--	--	--	--	--	--	--	--	--	--	--	--	--	--	--	--	--	--	--	--	--	--	--	--	--	--	--	--	--	--	--	--	--	--	--	--	--	--	--	--	--	--	--	--	--	--	--	--	--	--	--	--	--	--	--	--	--	--	--	--	--	--	--	--	--	--	--	--	--	--	--	--	--	--	--	--	--	--	--	--	--	--	--	--	--	--	--	--	--	--	--	--	--	--	--	--	--	--	--	--	--	--	--	--	--	--	--	--	--	--	--	--	--	--	--	--	--	--	--	--	--	--	--	--	--	--	--	--	--	--	--	--	--	--	--	--	--	--	--	--	--	--	--	--	--	--	--	--	--	--	--	--	--	--	--	--	--	--	--	--	--	--	--	--	--	--	--	--	--	--	--	--	--	--	--	--	--	--	--	--	--	--	--	--	--	--	--	--	--	--	--	--	--	--	--	--	--	--	--	--	--	--	--	--	--	--	--	--	--	--	--	--	--	--	--	--	--	--	--	--	--	--	--	--	--	--	--	--	--	--	--	--	--	--	--	--	--	--	--	--	--	--	--	--	--	--	--	--	--	--	--	--	--	--	--	--	--	--	--	--	--	--	--	--	--	--	--	--	--	--	--	--	--	--	--	--	--	--	--	--	--	--	--	--	--	--	--	--	--	--	--	--	--	--	--	--	--	--	--	--	--	--	--	--	--	--	--	--	--	--	--	--	--	--	--	--	--	--	--	--	--	--	--	--	--	--	--	--	--	--	--	--	--	--	--	--	--	--	--	--	--	--	--	--	--	--	--	--	--	--	--	--	--	--	--	--	--	--	--	--	--	--	--	--	--	--	--	--	--	--	--	--	--	--	--	--	--	--	--	--	--	--	--	--	--	--	--	--	--	--	--	--	--	--	--	--	--	--	--	--	--	--	--	--	--	--	--	--	--	--	--	--	--	--	--	--	--	--	--	--	--	--	--	--	--	--	--	--	--	--	--	--	--	--	--	--	--	--	--	--	--	--	--	--	--	--	--	--	--	--	--	--	--	--	--	--	--	--	--	--	--	--	--	--	--	--	--	--	--	--	--	--	--	--	--	--	--	--	--	--	--	--	--	--	--	--	--	--	--	--	--	--	--	--	--	--	--	--	--	--	--	--	--	--	--	--	--	--	--

Memory Allocation. (contd)

1819A ASSEMBLER, VERSION 1.0 MOVF43 10/02/84 SECTION 3

PAGE 163

	033021	000000			
	033022	000000			
	033023	000000			
7868	033024	000000	PZKP1	CATA	0,0,0,0,0
	033025	000000			
	033026	000000			
	033027	000000			
	033028	000000			
	033029	000000			
7869	033031	715722	PAPIN	CATA	-25445D,97115D,29685C,31459C,23903C
	033032	157833			
	033033	671765			
	033034	075343			
	033035	056537			
7870	033036	753556	PBPIN	CATA	-11409D,4027D,-12415E,-217C,933D,342D,1960F,-35796E
	033037	007671			
	033040	747800			
	033041	777446			
	033042	001645			
	033043	000526			
	033044	003850			
	033045	672053			
7871	033046	747080		CATA	-12753D,-13925D,-14788D,-235E,932E,150E,1513E,-32809D
	033047	744632			
	033050	743123			
	033051	777424			
	033052	001864			
	033053	000226			
	033054	002751			
	033055	677726			
7872	033056	108077		CATA	359C3D,-8728D,14093C,-13D,-2031D,-1111D,-90E,6944D
	033057	756753			
	033060	033413			
	033061	77762			
	033062	774037			
	033063	775650			
	033064	777843			
	033065	015440			
7873	033066	780277		CATA	-8023D,168D,26173C,1D,131C,24E,52E,144E
	033067	000250			
	033070	083075			
	033071	000001			
	033072	000203			
	033073	000030			
	033074	000084			
	033075	000220			
7874	033076	813200		CATA	-55727D,19294D,1007E,109D,-12582D,2449E,-51995D,-30852D
	033077	045536			
	033080	001757			
	033101	000155			
	033102	747521			
	033103	004621			
	033104	872344			
	033105	703573			
7875	033106	770835	PTCWIN	CATA	-3682D,3740D,2048C,-337D,2048C
	033107	007234			
	033110	000000			
	033111	777256			
	033112	000000			

Memory Allocation. (contd)

PAGE 181

1019A ASSEMBLER, VERSION 1.0 NOV843 10/02/84 SECTION 3

7820	032710	000000	02CPIC	RESERV	RESERV'1D		Z TOTAL PID CONTROL
7821	032711	000000	02CCLD	RESERV	RESERV'1D		ELD Z TOTAL PID CONTROL
7822				01SET			
7823	032712	000000	0XCI	RESERV	RESERV'2		X INTEGRAL CONTROL
7824	032714	000000	0XCI	RESERV	RESERV'2		Y INTEGRAL CONTROL
7825	032716	000000	0XCI	RESERV	RESERV'2		Z INTEGRAL CONTROL
7826	032720	000000	0XZCN	RESERV	RESERV'1D		RESERVE MEMORY FOR THE PAGER RAMPS
7827	032721	000000	0XZCN	RESERV	RESERV'1D		
7828	032722	000000	0XZCN	RESERV	RESERV'1D		
7829	032723	000000	0XEOFF	RESERV	RESERV'1D		
7830	032724	000000	0XEOFF	RESERV	RESERV'1D		
7831	032725	000000	0XEOFF	RESERV	RESERV'1D		
7832	032726	000000	0XCLST	RESERV	RESERV'1D		
7833	032727	000000	0XCLST	RESERV	RESERV'1D		
7834	032730	000000	0XCLST	RESERV	RESERV'1D		
7835	032731	000000	1MPOZ	RESERV	RESERV'10C		TEMPORARY USED IN CSTEP2 AND CSTEP3
7836							
7837							
7838							
7839	032743	000001	UCNE	YD			
7840	032744	000001	0140	2D			
7841							
7842							
7843							
7844							
7845							
7846							
7847	032745	000000	PUC	RESERV	RESERV'4D		SET POINT BIAS COMMAND TO ACTUATOR
7848	032751	000000	PUR	RESERV	RESERV'4D		REGULATOR COMMANDS TO ACTUATOR
7849	032755	000000	PUR	RESERV	RESERV'4D		TOTAL ACTUATOR COMMANDS
7850							
7851							
7852							
7853							
7854	032761	000000	PPLT	RESERV	RESERV'4C		FILCT COMMANDS
7855							
7856							
7857							
7858							
7859	032765	000000	PVS	RESERV	RESERV'10D		MEASUREMENTS
7860	032777	000000	PVCS	RESERV	RESERV'4C		DESIRER OUTPUT VECTOR
7861	033003	001677	PVSCL	LATA	-400000,-200000,400000		LANG. CYCLIC SCALING(20000=10FPS/IN)
7862	033004	770737					
7863	033005	116100					
7864							
7865	033006	747214	PNN	LATA	-126590,-23650,-8730		COLLECTIVE SCALING
7866	033007	772772					LATERAL CYCLIC SCALING
7867	033010	776620					
7868	033011	001454					
7869	033012	727506					
7870	033013	001046					
7871	033014	771767					
7872	033015	776176					
7873	033016	076708					
7874	033017	000000	PZR	LATA	0,0,0,0,0		
7875	033020	000000					

THIS CODE RESERVES THE CONSTANTS AND
VARIABLES NEEDED BY THE CMSIR4 SUBROUTINE
WHICH IS ASSEMBLED IN MEMORY AREA 81.

7672	032344	000000	MIRMIN	0	THEIA AT ENGAGE			
7673	032345	000000	7674	032346	000000	MIRMC	0	AIRSPED AT ENGAGE
7675	032347	000000	NDTWT	RESERV	RESERV'1C	PERTURBATION PITCH ANGLE		NDOT AT ENGAGE
7676	032348	000000	MPH1	RESERV	RESERV'1C	ROLL ANGLE		
7677	032349	000000	MPH2	RESERV	RESERV'1D	YAW ANGLE		
7678	032350	000000	MPH3	RESERV	RESERV'1D	PITCH RATE		
7679	032351	000000	MPH4	RESERV	RESERV'1D	ROLL RATE		
7680	032352	000000	MPH5	RESERV	RESERV'1D	YAW RATE		
7681	032353	000000	MPH6	RESERV	RESERV'1D	LONG ACCELERATION		
7682	032354	000000	MPH7	RESERV	RESERV'1D	LATERAL ACCELERATION		
7683	032355	000000	MPH8	RESERV	RESERV'1D	WORLD ACCELERATION		
7684	032356	000000	MPH9	RESERV	RESERV'1C	PERFURNATION AIRSPEED		
7685	032357	000000	MPH10	RESERV	RESERV'1D	VERTICAL VELOCITY		
7686	032358	000000	MPH11	RESERV	RESERV'1D	BAROMETRIC ALTITUDE		
7687	032359	000000	MPH12	RESERV	RESERV'1D	TEMPORARY USED IN MSTEP2 AND MSTEP3		
7688	032360	000000	MPH13	RESERV	RESERV'1D			
7689	032361	000000	MPH14	RESERV	RESERV'1D			
7690	032362	000000	MPH15	RESERV	RESERV'1D			
7691	032363	000000	MPH16	RESERV	RESERV'1D			
7692	032364	000000	MPH17	RESERV	RESERV'1D			
7693	032365	000000	MPH18	RESERV	RESERV'1D			
7694	032366	000000	MPH19	RESERV	RESERV'1D			
7695	032367	000000	MPH20	RESERV	RESERV'1D			
7696	032368	000000	MPH21	RESERV	RESERV'1D			
7697	032369	000000	MPH22	RESERV	RESERV'1D			
7698	032370	000000	MPH23	RESERV	RESERV'1D			
7699	032371	000000	MPH24	RESERV	RESERV'1D			
7700	032372	000000	MPH25	RESERV	RESERV'1D			
7701	032373	000000	MPH26	RESERV	RESERV'1D			
7702	032374	000000	MPH27	RESERV	RESERV'1D			
7703	032375	000000	MPH28	RESERV	RESERV'1D			
7704	032376	000000	MPH29	RESERV	RESERV'1D			
7705	032377	000000	MPH30	RESERV	RESERV'1D			
7706	032378	000000	MPH31	RESERV	RESERV'1D			
7707	032379	000000	MPH32	RESERV	RESERV'1D			
7708	032380	000000	MPH33	RESERV	RESERV'1D			
7709	032381	000000	MPH34	RESERV	RESERV'1D			
7710	032382	000000	MPH35	RESERV	RESERV'1D			
7711	032383	000000	MPH36	RESERV	RESERV'1D			
7712	032384	000000	MPH37	RESERV	RESERV'1D			
7713	032385	000000	MPH38	RESERV	RESERV'1D			
7714	032386	000000	MPH39	RESERV	RESERV'1D			
7715	032387	000000	MPH40	RESERV	RESERV'1D			
7716	032388	000000	MPH41	RESERV	RESERV'1D			
7717	032389	000000	MPH42	RESERV	RESERV'1D			
7718	032390	000000	MPH43	RESERV	RESERV'1D			
7719	032391	000000	MPH44	RESERV	RESERV'1D			
7720								

Memory Allocation. (contd)

1819A ASSEMBLER, VERSION 1.0 MCVR43 10/02/84 SECTION 3				PAGE 136		
7444	032233	000000	WTS	RESERV	WTSERV-100	MEASUREMENTS DESIGNED OUTPUT VECTOR ACTUAL OUTPUTS CORRESPONDING TO MYTER COMMAND SCALING TERMS(20000=1 FPS PER INCH)
7445	032233	000000	WTS	RESERV	WTSERV-100	
7446	032233	000000	WTS	RESERV	WTSERV-100	
7447	032233	000000	WTS	RESERV	WTSERV-100	
7448	032233	000000	WTS	RESERV	WTSERV-100	MEASUREMENTS DESIGNED OUTPUT VECTOR ACTUAL OUTPUTS CORRESPONDING TO MYTER COMMAND SCALING TERMS(20000=1 FPS PER INCH)
7449	032233	000000	WTS	RESERV	WTSERV-100	
7450	032233	000000	WTS	RESERV	WTSERV-100	
7451	032233	000000	WTS	RESERV	WTSERV-100	
7452	032233	000000	WTS	RESERV	WTSERV-100	MEASUREMENTS DESIGNED OUTPUT VECTOR ACTUAL OUTPUTS CORRESPONDING TO MYTER COMMAND SCALING TERMS(20000=1 FPS PER INCH)
7453	032233	000000	WTS	RESERV	WTSERV-100	
7454	032233	000000	WTS	RESERV	WTSERV-100	
7455	032233	000000	WTS	RESERV	WTSERV-100	
7456	032233	000000	WTS	RESERV	WTSERV-100	MEASUREMENTS DESIGNED OUTPUT VECTOR ACTUAL OUTPUTS CORRESPONDING TO MYTER COMMAND SCALING TERMS(20000=1 FPS PER INCH)
7457	032233	000000	WTS	RESERV	WTSERV-100	
7458	032233	000000	WTS	RESERV	WTSERV-100	
7459	032233	000000	WTS	RESERV	WTSERV-100	
7460	032233	000000	WTS	RESERV	WTSERV-100	MEASUREMENTS DESIGNED OUTPUT VECTOR ACTUAL OUTPUTS CORRESPONDING TO MYTER COMMAND SCALING TERMS(20000=1 FPS PER INCH)
7461	032233	000000	WTS	RESERV	WTSERV-100	
7462	032233	000000	WTS	RESERV	WTSERV-100	
7463	032233	000000	WTS	RESERV	WTSERV-100	
7464	032233	000000	WTS	RESERV	WTSERV-100	MEASUREMENTS DESIGNED OUTPUT VECTOR ACTUAL OUTPUTS CORRESPONDING TO MYTER COMMAND SCALING TERMS(20000=1 FPS PER INCH)
7465	032233	000000	WTS	RESERV	WTSERV-100	
7466	032233	000000	WTS	RESERV	WTSERV-100	
7467	032233	000000	WTS	RESERV	WTSERV-100	
7468	032233	000000	WTS	RESERV	WTSERV-100	MEASUREMENTS DESIGNED OUTPUT VECTOR ACTUAL OUTPUTS CORRESPONDING TO MYTER COMMAND SCALING TERMS(20000=1 FPS PER INCH)
7469	032233	000000	WTS	RESERV	WTSERV-100	
7470	032233	000000	WTS	RESERV	WTSERV-100	
7471	032233	000000	WTS	RESERV	WTSERV-100	

Hover Controller Subroutine. (contd)

1019# ASSEMBLER, VERSION 1.0 MCVP43 10/02/80 SECTION 1

```

4942 007733 566716      PSK      PACTRL
4943      0
4944 007734 347726      JP      PSTF70
4945 007735 347736      JP      PSTF8
4946      0
4947      0
4948      0
4949      0
4950      0
4951      0
4952      0
4953 007736 327759      PSTP8
4954 007737 243145      ENTAL PUT
4955 007740 800072      PULAL PIMCSC
4956 007741 122756      ENTAL PUT+1
4957 007742 243148      PULAL PCO18C
4958 007743 460075      STRAU ORF4
4959 007744 122757      ENTAL PUT+2
4960 007745 243147      PULAL PLATSC
4961 007746 800073      STRAU ORF2
4962      0
4963      0
4964      0
4965      0
4966      0
4967      0
4968      0
4969      0
4970      0
4971 007747 507201      PSTP9
4972 007750 360001      ENTAL 1
4973 007751 122025      ENTALB PIM+1
4974 007752 453016      STRALB PZK-1
4975 007753 566713      PSK
4976      0
4977 007754 347751      JP      PSTP90
4978 007755 550720      LJP      CPSTR4

```

Hover Controller Subroutine. (contd)

PAGE 35

1019# A382MBLEP. VERSION 1.0 NOV84 10/02/84 SECTION 1

ADDRESS	DATA	COMMENT
4866		SUBROUTINE, I, I.
4867		PUR V ICWIN V PZKFI
4868	0	
4869	0	
4870	0	
4871	0	
4872	0	
4873	0	
4874	0	
4875	0	
4876	0	
4877	0	
4878	0	
4879	0	
4880	0	
4881	0	
4882	0	
4883	0	
4884	0	
4885	0	
4886	0	
4887	0	
4888	0	
4889	0	
4890	0	
4891	0	
4892	0	
4893	0	
4894	0	
4895	0	
4896	0	
4897	0	
4898	0	
4899	0	
4900	0	
4901	0	
4902	0	
4903	0	
4904	0	
4905	0	
4906	0	
4907	0	
4908	0	
4909	0	
4910	0	
4911	0	
4912	0	
4913	0	
4914	0	
4915	0	
4916	0	
4917	0	
4918	0	
4919	0	
4920	0	
4921	0	
4922	0	
4923	0	
4924	0	
4925	0	
4926	0	
4927	0	
4928	0	
4929	0	
4930	0	
4931	0	
4932	0	
4933	0	
4934	0	
4935	0	
4936	0	
4937	0	
4938	0	
4939	0	
4940	0	
4941	0	

Appendix K.

RSANDY Computer Program

The RSANDY computer program is a modified version of the SANDY computer program written by Uy-Loi Ly as part of his PhD dissertation at Stanford [3] and later modified first by Gardner [16]. It is stored on the FSD VAX at NASA Ames Research Center. Ly also wrote a user's guide for the SANDY program.[8] This appendix gives the input format changes to make the SANDY user's guide correct for the RSANDY program. The major capabilities added by the RSANDY program are:

- an optional gradient step-size reducer from Gardner [16]
- a linear discrete model of the closed loop system can be created for later simulation studies
- a leading free line and free lines before all the data items are included to help in documenting the data files

The changes which follow apply to page numbers in the SANDY User's Guide. Other than these changes, the program is exactly like the SANDY program. Also included here is an example data set for running the program. This data was used to find the reduced order Navion compensator in Chapter 2. In the following changes, the new variables needed by the program are italicized.

Change 1, page 117a. Running the RSANDY Program

@RSANDY Infile Outfile Simfile

where:

RSANDY- A VMS command file which runs the *RSANDY.EXE* file with *Infile*, *Outfile*, and *Simfile* as data files.

Infile- A file containing the input data; an example is shown at the end of this appendix.

Outfile- A filename where the program will write the output.

Simfile- A filename written by program, if *IPLOT=1*, which contains the linear simulation models used by the *SIMPLOT* program, described in Appendix M.

Change 2, page 119a. Item 1

Np,n,m,m',p,p',p'',r,flag,NNS,IPPSS,ICF,ISS

where:

NNS- Set to 0.

IPPSS- Set to 0.

ICF- Set to 0.

ISS- Set to 0.

Change 3, page 119a. Item 2

Maxfn,Nvar,Tol,MSTEP,Nlinear,Tf,Print,IDPRN,ICLPRN,MAPRN,IPLOT,DT,IBG

where:

MSTEP- Maximum step size for the gradient algorithm. Start at 100 and make it smaller if there are convergence problems.

IDPRN- = 0 for no input data printout.

ICLPRN- = 0 for no closed loop data printout.

MAPRN- = 0 for no modal analysis printout.

IPLOT- = 0 for not creating a simulation model. = *N* for creating a simulation model of the N^{th} plant condition.

DT- Cycle time for the discrete simulation model. Rule of Thumb, $DT \approx .2(\frac{2\pi}{\omega_{fastest}})$.

Change 4, page 126. Add Item 9

Data: *XO*

Description:

XO- A vector with $(n + r + m')$ zeros.

[illegible]

```

0
F MATRIX(N X N)U W Q.THETA
.045 .036 0. 32 2
.37 2.02 176 0.0
00191. 0396. 2 98 0
0 0 1 0 0
C MATRIX( N X m )
0 1 0
.28 2 0
11 0 0
0 0
GAMMA MATRIX( n X m' )
.045. .036.0.0
37 2 02.0.0
.00191. 0396.0.0
0 0 0 0
HS MATRIX( p X n )VELOCITY.HDOT
1 0 0 0 0
0 .1 0 0 .176 0
DSU MATRIX( p X m )
0 0
0 0
DSW MATRIX( p X m' )
0 0 1 0 0
0 0 0 1 0
HC MATRIX( p' x n )VELOCITY.HDOT
1 0 0 0 0
0 .1 0 0 .176 0
DCU MATRIX( p' x m )
0 0
0 0
DSW MATRIX( p' x m' )
0 0 0 0 0
0 0 0 0 0
HP MATRIX( p' ' x n )U W Q.THETA HDOT
1 0 0 0 0
0 1 0 0 0
0 0 57 3 0
0 0 0 57 3
0 .1 0 0 .176 0
DPU MATRIX( p' ' x m )
0 0
0 0
0 0
0 0
0 0
DPSW MATRIX( p' ' ' x m' )
0 0 0 0 0
0 0 0 0 0
0 0 0 0 0
0 0 0 0 0
0 0 0 0 0
UW NOISE TYPE ORDER RMS
2 1 2 3
FILTER CONSTANT
43
WV NOISE TYPE ORDER RMS
2 1 2 3

```

```

FILTER CONSTANT
1 06
U MEAS NOISE TYPE.ORDER RMS
2 1 1 0
FILTER CONSTANT(HZ)
6 28
HDOT MEAS NOISE TYPE.ORDER RMS
2 1 1 0
FILTER CONSTANT
6 28
ALPHA
0 DO
Q MATRIX( p' x p' ) VELOCITY.HDOT
1 0 0
0 1 0
0 0 1
R MATRIX( m x m ) ELEVATOR.THROTTLE
10000 0 0
0 1 0
A MATRIX
O OOOOOO
1 000 -13 59 -16 93
B MATRIX
O 1366 O 2124
2 676 -3 241
C MATRIX
O OOOOOO
-13 14 -1 228
[ DVAR( Nvar )
3 4 5 6 7 8 11 12
ITEM # XO
0 0 0 0 0 0 0 0 0 0 0 0
0 0 0 0 0 0 0 0 0 0 0 0

```


Appendix L.

SETPNT Computer Program

This appendix lists the computer program which calculates the feedforward matrix described in Appendix D. This version does not have the G_z matrix. The data formats and data sequence are described at the beginning of the program. Also included is an example data set (the full-order Navion of Chapter 2).

SETPNT Computer Program. (contd)

[illegible]

SETPNT Computer Program. (contd)

```

1000  RM(1:1) BTRM(1)RM(1:1)
1010  PRINT THE RESULTS
1020  (CALL MATINT(RM,NP,R,M,RM))
1030  RETURN
1040  END

SUBROUTINE TNAVAL(A,B,C,M,P,R)
THIS SUBROUTINE FINDS THE MATRIX POLYNOMIAL AND RESIDUE POLE
REPRESENTATION OF THE COMPENSATOR DYNAMIC SYSTEM SHOWN BELOW
      ZDET = A * Z + B * Y S
      U = C * Z

THE SUBROUTINE CALLS ARE BASED ON DOUG BERNARD'S
"CONTROLS PLAYERS" LIBRARY
      IMPLICIT REAL*8(A-H,O-Z)
      INTEGER DA(20),DB(20),DC(20),DN(20),DM(20),DMM(20)
      DIMENSION LAMBDA(20),MAT(20),NO(20),CLASS(64),RO(20)
      DIMENSION A(8,8),B(8,8),C(8,8),M(8,8),P(8,8),R(8,8)
      DIMENSION LDDIM1:1
      DIMENSION LDDIM2:1
      DIMENSION LDDIM3:1
      DIMENSION LDDIM4:1
      DIMENSION LDDIM5:1
      DIMENSION LDDIM6:1
      DIMENSION LDDIM7:1
      DIMENSION LDDIM8:1
      DIMENSION LDDIM9:1
      DIMENSION LDDIM10:1
      DIMENSION LDDIM11:1
      DIMENSION LDDIM12:1
      DIMENSION LDDIM13:1
      DIMENSION LDDIM14:1
      DIMENSION LDDIM15:1
      DIMENSION LDDIM16:1
      DIMENSION LDDIM17:1
      DIMENSION LDDIM18:1
      DIMENSION LDDIM19:1
      DIMENSION LDDIM20:1
      DIMENSION LDDIM21:1
      DIMENSION LDDIM22:1
      DIMENSION LDDIM23:1
      DIMENSION LDDIM24:1
      DIMENSION LDDIM25:1
      DIMENSION LDDIM26:1
      DIMENSION LDDIM27:1
      DIMENSION LDDIM28:1
      DIMENSION LDDIM29:1
      DIMENSION LDDIM30:1
      DIMENSION LDDIM31:1
      DIMENSION LDDIM32:1
      DIMENSION LDDIM33:1
      DIMENSION LDDIM34:1
      DIMENSION LDDIM35:1
      DIMENSION LDDIM36:1
      DIMENSION LDDIM37:1
      DIMENSION LDDIM38:1
      DIMENSION LDDIM39:1
      DIMENSION LDDIM40:1
      DIMENSION LDDIM41:1
      DIMENSION LDDIM42:1
      DIMENSION LDDIM43:1
      DIMENSION LDDIM44:1
      DIMENSION LDDIM45:1
      DIMENSION LDDIM46:1
      DIMENSION LDDIM47:1
      DIMENSION LDDIM48:1
      DIMENSION LDDIM49:1
      DIMENSION LDDIM50:1
      DIMENSION LDDIM51:1
      DIMENSION LDDIM52:1
      DIMENSION LDDIM53:1
      DIMENSION LDDIM54:1
      DIMENSION LDDIM55:1
      DIMENSION LDDIM56:1
      DIMENSION LDDIM57:1
      DIMENSION LDDIM58:1
      DIMENSION LDDIM59:1
      DIMENSION LDDIM60:1
      DIMENSION LDDIM61:1
      DIMENSION LDDIM62:1
      DIMENSION LDDIM63:1
      DIMENSION LDDIM64:1
      DIMENSION LDDIM65:1
      DIMENSION LDDIM66:1
      DIMENSION LDDIM67:1
      DIMENSION LDDIM68:1
      DIMENSION LDDIM69:1
      DIMENSION LDDIM70:1
      DIMENSION LDDIM71:1
      DIMENSION LDDIM72:1
      DIMENSION LDDIM73:1
      DIMENSION LDDIM74:1
      DIMENSION LDDIM75:1
      DIMENSION LDDIM76:1
      DIMENSION LDDIM77:1
      DIMENSION LDDIM78:1
      DIMENSION LDDIM79:1
      DIMENSION LDDIM80:1
      DIMENSION LDDIM81:1
      DIMENSION LDDIM82:1
      DIMENSION LDDIM83:1
      DIMENSION LDDIM84:1
      DIMENSION LDDIM85:1
      DIMENSION LDDIM86:1
      DIMENSION LDDIM87:1
      DIMENSION LDDIM88:1
      DIMENSION LDDIM89:1
      DIMENSION LDDIM90:1
      DIMENSION LDDIM91:1
      DIMENSION LDDIM92:1
      DIMENSION LDDIM93:1
      DIMENSION LDDIM94:1
      DIMENSION LDDIM95:1
      DIMENSION LDDIM96:1
      DIMENSION LDDIM97:1
      DIMENSION LDDIM98:1
      DIMENSION LDDIM99:1
      DIMENSION LDDIM100:1
      DIMENSION LDDIM101:1
      DIMENSION LDDIM102:1
      DIMENSION LDDIM103:1
      DIMENSION LDDIM104:1
      DIMENSION LDDIM105:1
      DIMENSION LDDIM106:1
      DIMENSION LDDIM107:1
      DIMENSION LDDIM108:1
      DIMENSION LDDIM109:1
      DIMENSION LDDIM110:1
      DIMENSION LDDIM111:1
      DIMENSION LDDIM112:1
      DIMENSION LDDIM113:1
      DIMENSION LDDIM114:1
      DIMENSION LDDIM115:1
      DIMENSION LDDIM116:1
      DIMENSION LDDIM117:1
      DIMENSION LDDIM118:1
      DIMENSION LDDIM119:1
      DIMENSION LDDIM120:1
      DIMENSION LDDIM121:1
      DIMENSION LDDIM122:1
      DIMENSION LDDIM123:1
      DIMENSION LDDIM124:1
      DIMENSION LDDIM125:1
      DIMENSION LDDIM126:1
      DIMENSION LDDIM127:1
      DIMENSION LDDIM128:1
      DIMENSION LDDIM129:1
      DIMENSION LDDIM130:1
      DIMENSION LDDIM131:1
      DIMENSION LDDIM132:1
      DIMENSION LDDIM133:1
      DIMENSION LDDIM134:1
      DIMENSION LDDIM135:1
      DIMENSION LDDIM136:1
      DIMENSION LDDIM137:1
      DIMENSION LDDIM138:1
      DIMENSION LDDIM139:1
      DIMENSION LDDIM140:1
      DIMENSION LDDIM141:1
      DIMENSION LDDIM142:1
      DIMENSION LDDIM143:1
      DIMENSION LDDIM144:1
      DIMENSION LDDIM145:1
      DIMENSION LDDIM146:1
      DIMENSION LDDIM147:1
      DIMENSION LDDIM148:1
      DIMENSION LDDIM149:1
      DIMENSION LDDIM150:1
      DIMENSION LDDIM151:1
      DIMENSION LDDIM152:1
      DIMENSION LDDIM153:1
      DIMENSION LDDIM154:1
      DIMENSION LDDIM155:1
      DIMENSION LDDIM156:1
      DIMENSION LDDIM157:1
      DIMENSION LDDIM158:1
      DIMENSION LDDIM159:1
      DIMENSION LDDIM160:1
      DIMENSION LDDIM161:1
      DIMENSION LDDIM162:1
      DIMENSION LDDIM163:1
      DIMENSION LDDIM164:1
      DIMENSION LDDIM165:1
      DIMENSION LDDIM166:1
      DIMENSION LDDIM167:1
      DIMENSION LDDIM168:1
      DIMENSION LDDIM169:1
      DIMENSION LDDIM170:1
      DIMENSION LDDIM171:1
      DIMENSION LDDIM172:1
      DIMENSION LDDIM173:1
      DIMENSION LDDIM174:1
      DIMENSION LDDIM175:1
      DIMENSION LDDIM176:1
      DIMENSION LDDIM177:1
      DIMENSION LDDIM178:1
      DIMENSION LDDIM179:1
      DIMENSION LDDIM180:1
      DIMENSION LDDIM181:1
      DIMENSION LDDIM182:1
      DIMENSION LDDIM183:1
      DIMENSION LDDIM184:1
      DIMENSION LDDIM185:1
      DIMENSION LDDIM186:1
      DIMENSION LDDIM187:1
      DIMENSION LDDIM188:1
      DIMENSION LDDIM189:1
      DIMENSION LDDIM190:1
      DIMENSION LDDIM191:1
      DIMENSION LDDIM192:1
      DIMENSION LDDIM193:1
      DIMENSION LDDIM194:1
      DIMENSION LDDIM195:1
      DIMENSION LDDIM196:1
      DIMENSION LDDIM197:1
      DIMENSION LDDIM198:1
      DIMENSION LDDIM199:1
      DIMENSION LDDIM200:1
      DIMENSION LDDIM201:1
      DIMENSION LDDIM202:1
      DIMENSION LDDIM203:1
      DIMENSION LDDIM204:1
      DIMENSION LDDIM205:1
      DIMENSION LDDIM206:1
      DIMENSION LDDIM207:1
      DIMENSION LDDIM208:1
      DIMENSION LDDIM209:1
      DIMENSION LDDIM210:1
      DIMENSION LDDIM211:1
      DIMENSION LDDIM212:1
      DIMENSION LDDIM213:1
      DIMENSION LDDIM214:1
      DIMENSION LDDIM215:1
      DIMENSION LDDIM216:1
      DIMENSION LDDIM217:1
      DIMENSION LDDIM218:1
      DIMENSION LDDIM219:1
      DIMENSION LDDIM220:1
      DIMENSION LDDIM221:1
      DIMENSION LDDIM222:1
      DIMENSION LDDIM223:1
      DIMENSION LDDIM224:1
      DIMENSION LDDIM225:1
      DIMENSION LDDIM226:1
      DIMENSION LDDIM227:1
      DIMENSION LDDIM228:1
      DIMENSION LDDIM229:1
      DIMENSION LDDIM230:1
      DIMENSION LDDIM231:1
      DIMENSION LDDIM232:1
      DIMENSION LDDIM233:1
      DIMENSION LDDIM234:1
      DIMENSION LDDIM235:1
      DIMENSION LDDIM236:1
      DIMENSION LDDIM237:1
      DIMENSION LDDIM238:1
      DIMENSION LDDIM239:1
      DIMENSION LDDIM240:1
      DIMENSION LDDIM241:1
      DIMENSION LDDIM242:1
      DIMENSION LDDIM243:1
      DIMENSION LDDIM244:1
      DIMENSION LDDIM245:1
      DIMENSION LDDIM246:1
      DIMENSION LDDIM247:1
      DIMENSION LDDIM248:1
      DIMENSION LDDIM249:1
      DIMENSION LDDIM250:1
      DIMENSION LDDIM251:1
      DIMENSION LDDIM252:1
      DIMENSION LDDIM253:1
      DIMENSION LDDIM254:1
      DIMENSION LDDIM255:1
      DIMENSION LDDIM256:1
      DIMENSION LDDIM257:1
      DIMENSION LDDIM258:1
      DIMENSION LDDIM259:1
      DIMENSION LDDIM260:1
      DIMENSION LDDIM261:1
      DIMENSION LDDIM262:1
      DIMENSION LDDIM263:1
      DIMENSION LDDIM264:1
      DIMENSION LDDIM265:1
      DIMENSION LDDIM266:1
      DIMENSION LDDIM267:1
      DIMENSION LDDIM268:1
      DIMENSION LDDIM269:1
      DIMENSION LDDIM270:1
      DIMENSION LDDIM271:1
      DIMENSION LDDIM272:1
      DIMENSION LDDIM273:1
      DIMENSION LDDIM274:1
      DIMENSION LDDIM275:1
      DIMENSION LDDIM276:1
      DIMENSION LDDIM277:1
      DIMENSION LDDIM278:1
      DIMENSION LDDIM279:1
      DIMENSION LDDIM280:1
      DIMENSION LDDIM281:1
      DIMENSION LDDIM282:1
      DIMENSION LDDIM283:1
      DIMENSION LDDIM284:1
      DIMENSION LDDIM285:1
      DIMENSION LDDIM286:1
      DIMENSION LDDIM287:1
      DIMENSION LDDIM288:1
      DIMENSION LDDIM289:1
      DIMENSION LDDIM290:1
      DIMENSION LDDIM291:1
      DIMENSION LDDIM292:1
      DIMENSION LDDIM293:1
      DIMENSION LDDIM294:1
      DIMENSION LDDIM295:1
      DIMENSION LDDIM296:1
      DIMENSION LDDIM297:1
      DIMENSION LDDIM298:1
      DIMENSION LDDIM299:1
      DIMENSION LDDIM300:1
      DIMENSION LDDIM301:1
      DIMENSION LDDIM302:1
      DIMENSION LDDIM303:1
      DIMENSION LDDIM304:1
      DIMENSION LDDIM305:1
      DIMENSION LDDIM306:1
      DIMENSION LDDIM307:1
      DIMENSION LDDIM308:1
      DIMENSION LDDIM309:1
      DIMENSION LDDIM310:1
      DIMENSION LDDIM311:1
      DIMENSION LDDIM312:1
      DIMENSION LDDIM313:1
      DIMENSION LDDIM314:1
      DIMENSION LDDIM315:1
      DIMENSION LDDIM316:1
      DIMENSION LDDIM317:1
      DIMENSION LDDIM318:1
      DIMENSION LDDIM319:1
      DIMENSION LDDIM320:1
      DIMENSION LDDIM321:1
      DIMENSION LDDIM322:1
      DIMENSION LDDIM323:1
      DIMENSION LDDIM324:1
      DIMENSION LDDIM325:1
      DIMENSION LDDIM326:1
      DIMENSION LDDIM327:1

```


SETPNT Computer Program. (contd)

[illegible]

SETPNT Computer Program. (contd)

[illegible]

SETPNT Computer Program Example Data Set.

```

N M.P.R.SAMPLE TIME FOR SPROVS DAT
4 2,3,4, 5
F MATRIX( n X n )--U,W,Q,THETA
- 045, 036, 0, -32.2
- 37, -2.02, 176 0,0
00191, -0396, -2.98, 0
0,0,1,0,0
G MATRIX( n X m )
0,1
-28.2,0
-11,0,0
0,0
HS MATRIX( p X n )--U,HDOT,THETA
1,0,0,0,0
0, -1,0,0,176,0
0,0,0,1,0
DSU MATRIX, PXM
0,0
0,0
0,0
A MATRIX
0.0000E+00 1.000 0.0000E+00 0.0000E+00
-14.69 -6.072 0.0000E+00 0.0000E+00
0.0000E+00 0.0000E+00 -11.34 0.0000E+00
0.0000E+00 0.0000E+00 0.0000E+00 -1.816
B MATRIX
-0.2781 -0.8863E-01 6.515
1.485 0.8725 -33.66
-0.1334E-01 -2.622 2.441
0.7711 -0.4641E-01 -10.10
C MATRIX
0.000 -0.1000E-01 -0.1000E-01 0.3600E-02
-0.1978 -0.2163E-01 0.3446E-01 -1.000
D MATRIX, MXP
0,0,0
0,0,0
HD MATRIX, M X N+R, --U,HDOT,THETA
1,0,0,0,0,0,0,0,0
0, -1,0,0,176 0,0,0,0,0
LD MATRIX, M X M
0,0
0,0

```

SCALEM2 Computer Program. (contd)

[illegible]

SCALEM2 Computer Program.

[illegible]

SCALEM1 Computer Program. (contd)

```

1170 INPUT "PLEASE TYPE IN THE DESIRED SCALING AS INHER OR 2" ZSCALE2
1180 SCALE 2 ZSCALE2
1190 REM NOW DO THE CALCULATION OF THE MATRICES IN COMPUTER SCALED
1200 REM VARIABLES
1210 REM
1220 REM
1230 REM
1240 MATB=0
1250 MATC=0
1260 MATD=0
1270 MARK=0
1280 FOR J=1 TO NM
1290   B=1
1300   NEXT J
1310 NEXT J
1320 FOR J=1 TO NM
1330   C=1
1340   NEXT J
1350 FOR J=1 TO NM
1360   D=1
1370   NEXT J
1380 FOR J=1 TO NM
1390   E=1
1400   NEXT J
1410 FOR J=1 TO NM
1420   F=1
1430   NEXT J
1440 FOR J=1 TO NM
1450   G=1
1460   NEXT J
1470 FOR J=1 TO NM
1480   H=1
1490   NEXT J
1500 FOR J=1 TO NM
1510   I=1
1520   NEXT J
1530 FOR J=1 TO NM
1540   J=1
1550   NEXT J
1560 FOR J=1 TO NM
1570   K=1
1580   NEXT J
1590 FOR J=1 TO NM
1600   L=1
1610   NEXT J
1620 FOR J=1 TO NM
1630   M=1
1640   NEXT J
1650 FOR J=1 TO NM
1660   N=1
1670   NEXT J
1680 FOR J=1 TO NM
1690   O=1
1700   NEXT J
1710 FOR J=1 TO NM
1720   P=1
1730   NEXT J
1740 FOR J=1 TO NM
1750   Q=1
1760   NEXT J
1770 FOR J=1 TO NM
1780   R=1
1790   NEXT J
1800 FOR J=1 TO NM
1810   S=1
1820   NEXT J
1830 FOR J=1 TO NM
1840   T=1
1850   NEXT J
1860 FOR J=1 TO NM
1870   U=1
1880   NEXT J
1890 FOR J=1 TO NM
1900   V=1
1910   NEXT J
1920 FOR J=1 TO NM
1930   W=1
1940   NEXT J
1950 FOR J=1 TO NM
1960   X=1
1970   NEXT J
1980 FOR J=1 TO NM
1990   Y=1
2000   NEXT J
2010 FOR J=1 TO NM
2020   Z=1
2030   NEXT J
2040 FOR J=1 TO NM
2050   A=1
2060   NEXT J
2070 FOR J=1 TO NM
2080   B=1
2090   NEXT J
2100 FOR J=1 TO NM
2110   C=1
2120   NEXT J
2130 FOR J=1 TO NM
2140   D=1
2150   NEXT J
2160 FOR J=1 TO NM
2170   E=1
2180   NEXT J
2190 FOR J=1 TO NM
2200   F=1
2210   NEXT J
2220 FOR J=1 TO NM
2230   G=1
2240   NEXT J
2250 FOR J=1 TO NM
2260   H=1
2270   NEXT J
2280 FOR J=1 TO NM
2290   I=1
2300   NEXT J
2310 FOR J=1 TO NM
2320   J=1
2330   NEXT J
2340 FOR J=1 TO NM
2350   K=1
2360   NEXT J
2370 FOR J=1 TO NM
2380   L=1
2390   NEXT J
2400 FOR J=1 TO NM
2410   M=1
2420   NEXT J
2430 FOR J=1 TO NM
2440   N=1
2450   NEXT J
2460 FOR J=1 TO NM
2470   O=1
2480   NEXT J
2490 FOR J=1 TO NM
2500   P=1
2510   NEXT J
2520 FOR J=1 TO NM
2530   Q=1
2540   NEXT J
2550 FOR J=1 TO NM
2560   R=1
2570   NEXT J
2580 FOR J=1 TO NM
2590   S=1
2600   NEXT J
2610 FOR J=1 TO NM
2620   T=1
2630   NEXT J
2640 FOR J=1 TO NM
2650   U=1
2660   NEXT J
2670 FOR J=1 TO NM
2680   V=1
2690   NEXT J
2700 FOR J=1 TO NM
2710   W=1
2720   NEXT J
2730 FOR J=1 TO NM
2740   X=1
2750   NEXT J
2760 FOR J=1 TO NM
2770   Y=1
2780   NEXT J
2790 FOR J=1 TO NM
2800   Z=1
2810   NEXT J
2820 FOR J=1 TO NM
2830   A=1
2840   NEXT J
2850 FOR J=1 TO NM
2860   B=1
2870   NEXT J
2880 FOR J=1 TO NM
2890   C=1
2900   NEXT J
2910 FOR J=1 TO NM
2920   D=1
2930   NEXT J
2940 FOR J=1 TO NM
2950   E=1
2960   NEXT J
2970 FOR J=1 TO NM
2980   F=1
2990   NEXT J
3000 FOR J=1 TO NM
3010   G=1
3020   NEXT J
3030 FOR J=1 TO NM
3040   H=1
3050   NEXT J
3060 FOR J=1 TO NM
3070   I=1
3080   NEXT J
3090 FOR J=1 TO NM
3100   J=1
3110   NEXT J
3120 FOR J=1 TO NM
3130   K=1
3140   NEXT J
3150 FOR J=1 TO NM
3160   L=1
3170   NEXT J
3180 FOR J=1 TO NM
3190   M=1
3200   NEXT J
3210 FOR J=1 TO NM
3220   N=1
3230   NEXT J
3240 FOR J=1 TO NM
3250   O=1
3260   NEXT J
3270 FOR J=1 TO NM
3280   P=1
3290   NEXT J
3300 FOR J=1 TO NM
3310   Q=1
3320   NEXT J
3330 FOR J=1 TO NM
3340   R=1
3350   NEXT J
3360 FOR J=1 TO NM
3370   S=1
3380   NEXT J
3390 FOR J=1 TO NM
3400   T=1
3410   NEXT J
3420 FOR J=1 TO NM
3430   U=1
3440   NEXT J
3450 FOR J=1 TO NM
3460   V=1
3470   NEXT J
3480 FOR J=1 TO NM
3490   W=1
3500   NEXT J
3510 FOR J=1 TO NM
3520   X=1
3530   NEXT J
3540 FOR J=1 TO NM
3550   Y=1
3560   NEXT J
3570 FOR J=1 TO NM
3580   Z=1
3590   NEXT J
3600 FOR J=1 TO NM
3610   A=1
3620   NEXT J
3630 FOR J=1 TO NM
3640   B=1
3650   NEXT J
3660 FOR J=1 TO NM
3670   C=1
3680   NEXT J
3690 FOR J=1 TO NM
3700   D=1
3710   NEXT J
3720 FOR J=1 TO NM
3730   E=1
3740   NEXT J
3750 FOR J=1 TO NM
3760   F=1
3770   NEXT J
3780 FOR J=1 TO NM
3790   G=1
3800   NEXT J
3810 FOR J=1 TO NM
3820   H=1
3830   NEXT J
3840 FOR J=1 TO NM
3850   I=1
3860   NEXT J
3870 FOR J=1 TO NM
3880   J=1
3890   NEXT J
3900 FOR J=1 TO NM
3910   K=1
3920   NEXT J
3930 FOR J=1 TO NM
3940   L=1
3950   NEXT J
3960 FOR J=1 TO NM
3970   M=1
3980   NEXT J
3990 FOR J=1 TO NM
4000   N=1
4010   NEXT J
4020 FOR J=1 TO NM
4030   O=1
4040   NEXT J
4050 FOR J=1 TO NM
4060   P=1
4070   NEXT J
4080 FOR J=1 TO NM
4090   Q=1
4100   NEXT J
4110 FOR J=1 TO NM
4120   R=1
4130   NEXT J
4140 FOR J=1 TO NM
4150   S=1
4160   NEXT J
4170 FOR J=1 TO NM
4180   T=1
4190   NEXT J
4200 FOR J=1 TO NM
4210   U=1
4220   NEXT J
4230 FOR J=1 TO NM
4240   V=1
4250   NEXT J
4260 FOR J=1 TO NM
4270   W=1
4280   NEXT J
4290 FOR J=1 TO NM
4300   X=1
4310   NEXT J
4320 FOR J=1 TO NM
4330   Y=1
4340   NEXT J
4350 FOR J=1 TO NM
4360   Z=1
4370   NEXT J
4380 FOR J=1 TO NM
4390   A=1
4400   NEXT J
4410 FOR J=1 TO NM
4420   B=1
4430   NEXT J
4440 FOR J=1 TO NM
4450   C=1
4460   NEXT J
4470 FOR J=1 TO NM
4480   D=1
4490   NEXT J
4500 FOR J=1 TO NM
4510   E=1
4520   NEXT J
4530 FOR J=1 TO NM
4540   F=1
4550   NEXT J
4560 FOR J=1 TO NM
4570   G=1
4580   NEXT J
4590 FOR J=1 TO NM
4600   H=1
4610   NEXT J
4620 FOR J=1 TO NM
4630   I=1
4640   NEXT J
4650 FOR J=1 TO NM
4660   J=1
4670   NEXT J
4680 FOR J=1 TO NM
4690   K=1
4700   NEXT J
4710 FOR J=1 TO NM
4720   L=1
4730   NEXT J
4740 FOR J=1 TO NM
4750   M=1
4760   NEXT J
4770 FOR J=1 TO NM
4780   N=1
4790   NEXT J
4800 FOR J=1 TO NM
4810   O=1
4820   NEXT J
4830 FOR J=1 TO NM
4840   P=1
4850   NEXT J
4860 FOR J=1 TO NM
4870   Q=1
4880   NEXT J
4890 FOR J=1 TO NM
4900   R=1
4910   NEXT J
4920 FOR J=1 TO NM
4930   S=1
4940   NEXT J
4950 FOR J=1 TO NM
4960   T=1
4970   NEXT J
4980 FOR J=1 TO NM
4990   U=1
5000   NEXT J
5010 FOR J=1 TO NM
5020   V=1
5030   NEXT J
5040 FOR J=1 TO NM
5050   W=1
5060   NEXT J
5070 FOR J=1 TO NM
5080   X=1
5090   NEXT J
5100 FOR J=1 TO NM
5110   Y=1
5120   NEXT J
5130 FOR J=1 TO NM
5140   Z=1
5150   NEXT J
5160 FOR J=1 TO NM
5170   A=1
5180   NEXT J
5190 FOR J=1 TO NM
5200   B=1
5210   NEXT J
5220 FOR J=1 TO NM
5230   C=1
5240   NEXT J
5250 FOR J=1 TO NM
5260   D=1
5270   NEXT J
5280 FOR J=1 TO NM
5290   E=1
5300   NEXT J
5310 FOR J=1 TO NM
5320   F=1
5330   NEXT J
5340 FOR J=1 TO NM
5350   G=1
5360   NEXT J
5370 FOR J=1 TO NM
5380   H=1
5390   NEXT J
5400 FOR J=1 TO NM
5410   I=1
5420   NEXT J
5430 FOR J=1 TO NM
5440   J=1
5450   NEXT J
5460 FOR J=1 TO NM
5470   K=1
5480   NEXT J
5490 FOR J=1 TO NM
5500   L=1
5510   NEXT J
5520 FOR J=1 TO NM
5530   M=1
5540   NEXT J
5550 FOR J=1 TO NM
5560   N=1
5570   NEXT J
5580 FOR J=1 TO NM
5590   O=1
5600   NEXT J
5610 FOR J=1 TO NM
5620   P=1
5630   NEXT J
5640 FOR J=1 TO NM
5650   Q=1
5660   NEXT J
5670 FOR J=1 TO NM
5680   R=1
5690   NEXT J
5700 FOR J=1 TO NM
5710   S=1
5720   NEXT J
5730 FOR J=1 TO NM
5740   T=1
5750   NEXT J
5760 FOR J=1 TO NM
5770   U=1
5780   NEXT J
5790 FOR J=1 TO NM
5800   V=1
5810   NEXT J
5820 FOR J=1 TO NM
5830   W=1
5840   NEXT J
5850 FOR J=1 TO NM
5860   X=1
5870   NEXT J
5880 FOR J=1 TO NM
5890   Y=1
5900   NEXT J
5910 FOR J=1 TO NM
5920   Z=1
5930   NEXT J
5940 FOR J=1 TO NM
5950   A=1
5960   NEXT J
5970 FOR J=1 TO NM
5980   B=1
5990   NEXT J
6000 FOR J=1 TO NM
6010   C=1
6020   NEXT J
6030 FOR J=1 TO NM
6040   D=1
6050   NEXT J
6060 FOR J=1 TO NM
6070   E=1
6080   NEXT J
6090 FOR J=1 TO NM
6100   F=1
6110   NEXT J
6120 FOR J=1 TO NM
6130   G=1
6140   NEXT J
6150 FOR J=1 TO NM
6160   H=1
6170   NEXT J
6180 FOR J=1 TO NM
6190   I=1
6200   NEXT J
6210 FOR J=1 TO NM
6220   J=1
6230   NEXT J
6240 FOR J=1 TO NM
6250   K=1
6260   NEXT J
6270 FOR J=1 TO NM
6280   L=1
6290   NEXT J
6300 FOR J=1 TO NM
6310   M=1
6320   NEXT J
6330 FOR J=1 TO NM
6340   N=1
6350   NEXT J
6360 FOR J=1 TO NM
6370   O=1
6380   NEXT J
6390 FOR J=1 TO NM
6400   P=1
6410   NEXT J
6420 FOR J=1 TO NM
6430   Q=1
6440   NEXT J
6450 FOR J=1 TO NM
6460   R=1
6470   NEXT J
6480 FOR J=1 TO NM
6490   S=1
6500   NEXT J
6510 FOR J=1 TO NM
6520   T=1
6530   NEXT J
6540 FOR J=1 TO NM
6550   U=1
6560   NEXT J
6570 FOR J=1 TO NM
6580   V=1
6590   NEXT J
6600 FOR J=1 TO NM
6610   W=1
6620   NEXT J
6630 FOR J=1 TO NM
6640   X=1
6650   NEXT J
6660 FOR J=1 TO NM
6670   Y=1
6680   NEXT J
6690 FOR J=1 TO NM
6700   Z=1
6710   NEXT J
6720 FOR J=1 TO NM
6730   A=1
6740   NEXT J
6750 FOR J=1 TO NM
6760   B=1
6770   NEXT J
6780 FOR J=1 TO NM
6790   C=1
6800   NEXT J
6810 FOR J=1 TO NM
6820   D=1
6830   NEXT J
6840 FOR J=1 TO NM
6850   E=1
6860   NEXT J
6870 FOR J=1 TO NM
6880   F=1
6890   NEXT J
6900 FOR J=1 TO NM
6910   G=1
6920   NEXT J
6930 FOR J=1 TO NM
6940   H=1
6950   NEXT J
6960 FOR J=1 TO NM
6970   I=1
6980   NEXT J
6990 FOR J=1 TO NM
7000   J=1
7010   NEXT J
7020 FOR J=1 TO NM
7030   K=1
7040   NEXT J
7050 FOR J=1 TO NM
7060   L=1
7070   NEXT J
7080 FOR J=1 TO NM
7090   M=1
7100   NEXT J
7110 FOR J=1 TO NM
7120   N=1
7130   NEXT J
7140 FOR J=1 TO NM
7150   O=1
7160   NEXT J
7170 FOR J=1 TO NM
7180   P=1
7190   NEXT J
7200 FOR J=1 TO NM
7210   Q=1
7220   NEXT J
7230 FOR J=1 TO NM
7240   R=1
7250   NEXT J
7260 FOR J=1 TO NM
7270   S=1
7280   NEXT J
7290 FOR J=1 TO NM
7300   T=1
7310   NEXT J
7320 FOR J=1 TO NM
7330   U=1
7340   NEXT J
7350 FOR J=1 TO NM
7360   V=1
7370   NEXT J
7380 FOR J=1 TO NM
7390   W=1
7400   NEXT J
7410 FOR J=1 TO NM
7420   X=1
7430   NEXT J
7440 FOR J=1 TO NM
7450   Y=1
7460   NEXT J
7470 FOR J=1 TO NM
7480   Z=1
7490   NEXT J
7500 FOR J=1 TO NM
7510   A=1
7520   NEXT J
7530 FOR J=1 TO NM
7540   B=1
7550   NEXT J
7560 FOR J=1 TO NM
7570   C=1
7580   NEXT J
7590 FOR J=1 TO NM
7600   D=1
7610   NEXT J
7620 FOR J=1 TO NM
7630   E=1
7640   NEXT J
7650 FOR J=1 TO NM
7660   F=1
7670   NEXT J
7680 FOR J=1 TO NM
7690   G=1
7700   NEXT J
7710 FOR J=1 TO NM
7720   H=1
7730   NEXT J
7740 FOR J=1 TO NM
7750   I=1
7760   NEXT J
7770 FOR J=1 TO NM
7780   J=1
7790   NEXT J
7800 FOR J=1 TO NM
7810   K=1
7820   NEXT J
7830 FOR J=1 TO NM
7840   L=1
7850   NEXT J
7860 FOR J=1 TO NM
7870   M=1
7880   NEXT J
7890 FOR J=1 TO NM
7900   N=1
7910   NEXT J
7920 FOR J=1 TO NM
7930   O=1
7940   NEXT J
7950 FOR J=1 TO NM
7960   P=1
7970   NEXT J
7980 FOR J=1 TO NM
7990   Q=1
8000   NEXT J
8010 FOR J=1 TO NM
8020   R=1
8030   NEXT J
8040 FOR J=1 TO NM
8050   S=1
8060   NEXT J
8070 FOR J=1 TO NM
8080   T=1
8090   NEXT J
8100 FOR J=1 TO NM
8110   U=1
8120   NEXT J
8130 FOR J=1 TO NM
8140   V=1
8150   NEXT J
8160 FOR J=1 TO NM
8170   W=1
8180   NEXT J
8190 FOR J=1 TO NM
8200   X=1
8210   NEXT J
8220 FOR J=1 TO NM
8230   Y=1
8240   NEXT J
8250 FOR J=1 TO NM
8260   Z=1
8270   NEXT J
8280 FOR J=1 TO NM
8290   A=1
8300   NEXT J
8310 FOR J=1 TO NM
8320   B=1
8330   NEXT J
8340 FOR J=1 TO NM
8350   C=1
8360   NEXT J
8370 FOR J=1 TO NM
8380   D=1
8390   NEXT J
8400 FOR J=1 TO NM
8410   E=1
8420   NEXT J
8430 FOR J=1 TO NM
8440   F=1
8450   NEXT J
8460 FOR J=1 TO NM
8470   G=1
8480   NEXT J
8490 FOR J=1 TO NM
8500   H=1
8510   NEXT J
8520 FOR J=1 TO NM
8530   I=1
8540   NEXT J
8550 FOR J=1 TO NM
8560   J=1
8570   NEXT J
8580 FOR J=1 TO NM
8590   K=1
8600   NEXT J
8610 FOR J=1 TO NM
8620   L=1
8630   NEXT J
8640 FOR J=1 TO NM
8650   M=1
8660   NEXT J
8670 FOR J=1 TO NM
8680   N=1
8690   NEXT J
8700 FOR J=1 TO NM
8710   O=1
8720   NEXT J
8730 FOR J=1 TO NM
8740   P=1
8750   NEXT J
8760 FOR J=1 TO NM
8770   Q=1
8780   NEXT J
8790 FOR J=1 TO NM
8800   R=1
8810   NEXT J
8820 FOR J=1 TO NM
8830   S=1
8840   NEXT J
8850 FOR J=1 TO NM
8860   T=1
8870   NEXT J
8880 FOR J=1 TO NM
8890   U=1
8900   NEXT J
8910 FOR J=1 TO NM
8920   V=1
8930   NEXT J
8940 FOR J=1 TO NM
8950   W=1
8960   NEXT J
8970 FOR J=1 TO NM
8980   X=1
8990   NEXT J
9000 FOR J=1 TO NM
9010   Y=1
9020   NEXT J
9030 FOR J=1 TO NM
9040   Z=1
9050   NEXT J
9060 FOR J=1 TO NM
9070   A=1
9080   NEXT J
9090 FOR J=1 TO NM
9100   B=1
9110   NEXT J
9120 FOR J=1 TO NM
9130   C=1
9140   NEXT J
9150 FOR J=1 TO NM
9160   D=1
9170   NEXT J
9180 FOR J=1 TO NM
9190   E=1
9200   NEXT J
9210 FOR J=1 TO NM
9220   F=1
9230   NEXT J
9240 FOR J=1 TO NM
9250   G=1
9260   NEXT J
9270 FOR J=1 TO NM
9280   H=1
9290   NEXT J
9300 FOR J=1 TO NM
9310   I=1
9320   NEXT J
9330 FOR J=1 TO NM
9340   J=1
9350   NEXT J
9360 FOR J=1 TO NM
9370   K=1
9380   NEXT J
9390 FOR J=1 TO NM
9400   L=1
9410   NEXT J
9420 FOR J=1 TO NM
9430   M=1
9440   NEXT J
9450 FOR J=1 TO NM
9460   N=1
9470   NEXT J
9480 FOR J=1 TO NM
9490   O=1
9500   NEXT J
9510 FOR J=1 TO NM
9520   P=1
9530   NEXT J
9540 FOR J=1 TO NM
9550   Q=1
9560   NEXT J
9570 FOR J=1 TO NM
9580   R=1
9590   NEXT J
9600 FOR J=1 TO NM
9610   S=1
9620   NEXT J
9630 FOR J=1 TO NM
9640   T=1
9650   NEXT J
9660 FOR J=1 TO NM
9670   U=1
9680   NEXT J
9690 FOR J=1 TO NM
9700   V=1
9710   NEXT J
9720 FOR J=1 TO NM
9730   W=1
9740   NEXT J
9750 FOR J=1 TO NM
9760   X=1
9770   NEXT J
9780 FOR J=1 TO NM
9790   Y=1
9800   NEXT J
9810 FOR J=1 TO NM
9820   Z=1
9830   NEXT J
9840 FOR J=1 TO NM
9850   A=1
9860   NEXT J
9870 FOR J=1 TO NM
9880   B=1
9890   NEXT J
9900 FOR J=1 TO NM
9910   C=1
9920   NEXT J
9930 FOR J=1 TO NM
9940   D=1
9950   NEXT J
9960 FOR J=1 TO NM
9970   E=1
9980   NEXT J
9990 FOR J=1 TO NM
10000   F=1
10010   NEXT J
10020 FOR J=1 TO NM
10030   G=1
10040   NEXT J
10050 FOR J=1 TO NM
10060   H=1
10070   NEXT J
10080 FOR J=1 TO NM
10090   I=1
10100   NEXT J
10110 FOR J=1 TO NM
10120   J=1
10130   NEXT J
10140 FOR J=1 TO NM
10150   K=1
10160   NEXT J
10170 FOR J=1 TO NM
10180   L=1
10190   NEXT J
10200 FOR J=1 TO NM
10210   M=1
10220   NEXT J
10230 FOR J=1 TO NM
10240   N=1
10250   NEXT J
10260 FOR J=1 TO NM
10270   O=1
10280   NEXT J
10290 FOR J=1 TO NM
10300   P=1
10310   NEXT J
10320 FOR J=1 TO NM
10330   Q=1
10340   NEXT J
10350 FOR J=1 TO NM
10360   R=1
10370   NEXT J
10380 FOR J=1 TO NM
10390   S=1
10400   NEXT J
10410 FOR J=1 TO NM
10420   T=1
10430   NEXT J
10440 FOR J=1 TO NM
10450   U=1
10460   NEXT J
10470 FOR J=1 TO NM
10480   V=1
10490   NEXT J
10500 FOR J=1 TO NM
10510   W=1
10520   NEXT J
10530 FOR J=1 TO NM
10540   X=1
10550   NEXT J
10560 FOR J=1 TO NM
10570   Y=1
10580   NEXT J
10590 FOR J=1 TO NM
10600   Z=1
10610   NEXT J
10620 FOR J=1 TO NM
10630   A=1
10640   NEXT J
10650 FOR J=1 TO NM
10660   B=1
10670   NEXT J
10680 FOR J=1 TO NM
10690   C=1
10700   NEXT J
10710 FOR J=1 TO NM
10720   D=1
10730   NEXT J
10740 FOR J=1 TO NM
10750   E=1
10760   NEXT J
10770 FOR J=1 TO NM
10780   F=1
10790   NEXT J
10800 FOR J=1 TO NM
10810   G=1
10820   NEXT J
10830 FOR J=1 TO NM
10840   H=1
10850   NEXT J
10860 FOR J=1 TO NM
10870   I=1
10880   NEXT J
10890 FOR J=1 TO NM
10900   J=1
10910   NEXT J
10920 FOR J=1 TO NM
10930   K=1
10940   NEXT J
10950 FOR J=1 TO NM
10960   L=1
10970   NEXT J
10980 FOR J=1 TO NM
10990   M=1
11000   NEXT J
11010 FOR J=1 TO NM
11020   N=1
11030   NEXT J
11040 FOR J=1 TO NM
11050   O=1
11060   NEXT J
11070 FOR J=1 TO NM
11080   P=1
11090   NEXT J
11100 FOR J=1 TO NM
11110   Q=1
11120   NEXT J
11130 FOR J=1 TO NM
11140   R=1
11150   NEXT J
11160 FOR J=1 TO NM
11170   S=1
11180   NEXT J
11190 FOR J=1 TO NM
11200   T=1
11210   NEXT J
11220 FOR J=1 TO NM
11230   U=1
11240   NEXT J
11250 FOR J=1 TO NM
11260   V=1
11270   NEXT J
11280 FOR J=1 TO NM
11290   W=1
11300   NEXT J
11310 FOR J=1 TO NM
11320   X=1
11330   NEXT J
11340 FOR J=1 TO NM
11350   Y=1
11360   NEXT J
11370 FOR J=1 TO NM
11380   Z=1
11390   NEXT J
11400 FOR J=1 TO NM
11410   A=1
11420   NEXT J
11430 FOR J=1 TO NM
11440   B=1
11450   NEXT J
11460 FOR J=1 TO NM
11470   C=1
11480   NEXT J
11490 FOR J=1 TO NM
11500   D=1
11510   NEXT J
11520 FOR J=1 TO NM
11530   E=1
11540   NEXT J
11550 FOR J=1 TO NM
11560   F=1
11570   NEXT J
11580 FOR J=1 TO NM
11590   G=1
11600   NEXT J
11610 FOR J=1 TO NM
11620   H=1
11630   NEXT J
11640 FOR J=1 TO NM
11650   I=1
11660   NEXT J
11670 FOR J=1 TO NM
11680   J=1
11690   NEXT J
11700 FOR J=1 TO NM
11710   K=1
11720   NEXT J
11730 FOR J=1 TO NM
11740   L=1
11750   NEXT J
11760 FOR J=1 TO NM
11770   M=1
11780   NEXT J
11790 FOR J=1 TO NM
11800   N=1
11810   NEXT J
11820 FOR J=1 TO NM
11830   O=1
11840   NEXT J
11850 FOR J=1 TO NM
11860   P=1
11870   NEXT J
11880 FOR J=1 TO NM
11890   Q=1
11900   NEXT J
11910 FOR J=1 TO NM
11920   R=1
11930   NEXT J
11940 FOR J=1 TO NM
11950   S=1
11960   NEXT J
11970 FOR J=1 TO NM
11980   T=1
11990   NEXT J
12000 FOR J=1 TO NM
12010   U=1
12020   NEXT J
12030 FOR J=1 TO NM
12040   V=1
12050   NEXT J
12060 FOR J=1 TO NM
12070   W=1
12080   NEXT J
12090 FOR J=1 TO NM
12100   X=1
12110   NEXT J
12120 FOR J=1 TO NM
12130   Y=1
12140   NEXT J
12150 FOR J=1 TO NM
12160   Z=1
12170   NEXT J
12180 FOR J=1 TO NM
12190   A=1
12200   NEXT J
12210 FOR J=1 TO NM
12220   B=1
12230   NEXT J
12240 FOR J=1 TO NM
12250   C=1
12260   NEXT J
12270 FOR J=1 TO NM
12280   D=1
12290   NEXT J
12300 FOR J=1 TO NM
12310   E=1
12320   NEXT J
12330 FOR J=1 TO NM
12340   F=1
12350   NEXT J
12360 FOR J=1 TO NM
12370   G=1
12380   NEXT J
12390 FOR J=1 TO NM
12400   H=1
12410   NEXT J
12420 FOR J=1 TO NM
12430   I=1
12440   NEXT J
12450 FOR J=1 TO NM
12460   J=1
12470   NEXT J
12480 FOR J=1 TO NM
12490   K=1
12500   NEXT J
12510 FOR J=1 TO NM
12520   L=1
12530   NEXT J
12540 FOR J=1 TO NM
12550   M=1
12560   NEXT J
12570 FOR J=1 TO NM
12580   N=1
12590   NEXT J
12600 FOR J=1 TO NM
12610   O=1
12620   NEXT J
12630 FOR J=1 TO NM
12640   P=1
12650   NEXT J
12660 FOR J=1 TO NM
12670   Q=1
12680   NEXT J
12690 FOR J=1 TO NM
12700   R=1
12710   NEXT J
12720 FOR J=1 TO NM
12730   S=1
12740   NEXT J
12750 FOR J=1 TO NM
12760   T=1
12770   NEXT J
12780 FOR J=1 TO NM
12790   U=1
12800   NEXT J
12810 FOR J=1 TO NM
12820   V=1
12830   NEXT J
12840 FOR J=1 TO NM
12850   W=1
12860   NEXT J
12870 FOR J=1 TO NM
12880   X=1
12890   NEXT J
12900 FOR J=1 TO NM
12910   Y=1
12920   NEXT J
12930 FOR J=1 TO NM
12940   Z=1
12950   NEXT J
12960 FOR J=1 TO NM
12970   A=1
12980   NEXT J
12990 FOR J=1 TO NM
13000   B=1
13010   NEXT J
13020 FOR J=1 TO NM
13030   C=1
13040   NEXT J
13050 FOR J=1 TO NM
13060   D=1
13070   NEXT J
13080 FOR J=1 TO NM
13090   E=1
13100   NEXT J
13110 FOR J=1 TO NM
13120   F=1
13130   NEXT J
13140 FOR J=1 TO NM
13150   G=1
13160   NEXT J
13170 FOR J=1 TO NM
13180   H=1
13190   NEXT J
13200 FOR J=1 TO NM
13210   I=1
13220   NEXT J
13230 FOR J=1 TO NM
13240   J=1
13250   NEXT J
13260 FOR J=1 TO NM
13270   K=1
13280   NEXT J
13290 FOR J=1 TO NM
13300   L=1
13310   NEXT J
13320 FOR J=1 TO NM
13330   M=1
13340   NEXT J
13350 FOR J=1 TO NM
13360   N=1
13370   NEXT J
13380 FOR J=1 TO NM
13390   O=1
13400   NEXT J
13410 FOR J=1 TO NM
13420   P=1
13430   NEXT J
13440 FOR J=1 TO NM
13450   Q=1
13460   NEXT J
13470 FOR J=1 TO NM
13480   R=1
13490   NEXT J
13500 FOR J=1 TO NM
13510   S=1
13520   NEXT J
13530 FOR J=1 TO NM
13540   T=1
13550   NEXT J
13560 FOR J=1 TO NM
13570   U=1
13580   NEXT J
13590 FOR J=1 TO NM
13600   V=1
13610   NEXT J
13620 FOR J=1 TO NM
13630   W=1
13640   NEXT J
13650 FOR J=1 TO NM
13660   X=1
13670   NEXT J
13680 FOR J=1 TO NM
13690   Y=1
13700   NEXT J
13710 FOR J=1 TO NM
13720   Z=1
13730   NEXT J
13740 FOR J=1 TO NM
13750   A=1
13760   NEXT J
13770 FOR J=1 TO NM
13780   B=1
13790   NEXT J
13800 FOR J=1 TO NM
13810   C=1
13820   NEXT J
13830 FOR J=1 TO NM
13840   D=1
13850   NEXT J
1
```

SCALEM1 Computer Program.

[illegible]

Appendix N.

SCALEM1 and SCALEM2 Computer Programs

This appendix lists the computer programs for doing the fixed point scaling described in Appendix E. Also included are two example sets of data. These programs are written in VAX BASIC. The SCALEM1 computer program does the scaling for the longitudinal CAS controller. The SCALEM2 computer program does the scaling for the hover controller. The description of required data is at the beginning of each program. The SCALEM1 data is for the 6th order compensator with integral control. The SCALEM2 data is for the final hover controller.

SIMPLOT Example Data File.

```
4.8,0.1,15.0,0.0
18.22,20.21,16.17,18.22
'NAVION WITH FULL ORDER COMP HDOT COM = 10 FT/SEC '
'FORWARD VEL (FT/SEC) '
'CLIMB RATE (FT/SEC) '
' PITCH RATE (DEG/SEC) '
' THETA (DEG) '
' ELEVATOR (DEGREES) '
' THROTTLE (FT/SEC**2) '
'FORWARD VEL (FT/SEC) '
'CLIMB RATE (FT/SEC) '
0.0,0.0,0.0,10.0,0.0,0.0,0.0,0.0,0.0,0.0,0.0,0.0,0.0,0.0,0.0,0.0
```


SIMPLOT Computer Program. (contd)

```

DO 3100 I=1, NPNTS
  YARAY(I)=DAT(NCNT+1,I)
  IF (YARAY(I) GT YMAX) YMAX=YARAY(I)
  IF (YARAY(I) LT YMIN) YMIN=YARAY(I)
3100 CONTINUE
CALL PHYSOR(XJORG(NCIVE), YJORG(NCIVE))
CALL AREA2D(6, 0, 2, 7)
CALL XNAME('TIME(sec)', 9)
CALL YNAME(XREF(PLTIT(NCNT)), 20)
CALL CROSS
CALL GRAF(0, 'SCALE', TIME(NPNTS), YMIN, 'SCALE', YMAX)
CALL CURVE(TIME, YARAY, NPNTS, 0)
CALL ENDOR(NPONT)
3400 CONTINUE
CALL ENDPL(NPONT)
3500 CONTINUE
GO TO 5000

THIS IS THE PART THAT DOES 4 PLOTS/PAGE
3600 DO 4500 NPONT=1, NPAGE
  CALL PAGE(11, 0, 8, 5)
  CALL PHYSOR(1, 1)
  IF (NPLTR EQ 0) CALL HMROT('MOVIE')
  CALL NOBRDR
  CALL AREA2D(9, 0, 6, 0)
  CALL HEADIN(XREF(ORTIT), 50, 2, 1)
  CALL ENDOR(NPONT)

  NOW START THE LOOP FOR PLOTTING THE 4 CURVES
  DO 4400 NCIVE=1, 4
    NCNT IS THE COLUMN OF THE VECTOR IN DAT BEING PLOTTED
    NCNT=(4*NPONT-4)+NCIVE
    YMAX=DAT(NCNT+1,1)
    YMIN=YMAX
    DO 4100 I=1, NPNTS
      YARAY(I)=DAT(NCNT+1,I)
      IF (YARAY(I) GT YMAX) YMAX=YARAY(I)
      IF (YARAY(I) LT YMIN) YMIN=YARAY(I)
    4100 CONTINUE
    CALL PHYSOR(XJORG(NCIVE), YJORG(NCIVE))
    CALL AREA2D(4, 1, 2, 7)
    CALL XNAME('TIME(sec)', 9)
    CALL YNAME(XREF(PLTIT(NCNT)), 20)
    CALL CROSS
    CALL GRAF(0, 'SCALE', TIME(NPNTS), YMIN, 'SCALE', YMAX)
    CALL CURVE(TIME, YARAY, NPNTS, 0)
    CALL ENDOR(NPONT)
  4400 CONTINUE
  CALL ENDPL(NPONT)
  4500 CONTINUE
  GO TO 5000
3600 CALL DONEPL
  RETURN
  END

```

SIMPLOT Computer Program. (contd)

```

C      WRITE(6,'*)YMAX
C      C USE HORIZONTAL PAGE FORMAT FOR VERTICATEL
C      C FOR VECTOR FOR THE VT12S
C      CALL PAGE(11,8,5)
C      IF (NPLTR EQ 0) CALL TABR(T,NMVE,T)
C      C SUPPRESS PAGE BORDER OUTLINE
C      CALL NBRDR
C      C SET UP PLOTTING AREA
C      CALL AREA(9,0,6,0)
C      C PUT THE TITLE ON THE GRAPH
C      CALL HEADIN(ORIT,CRITTI,SO,2,1)
C      C THE X AXIS WITH TIME IN SECONDS
C      CALL XNAME('TIME(sec)',9)
C      C LABEL THE ORIGINATE WITH THE VARIABLE NAME
C      CALL YNAME(YREF,PLITIT(NPAGE),20)
C      C SET UP THE GRAPH TYPE USING SELF SCALING
C      AND PUT THE AXIS AT Y=0
C      CALL CROSS
C      CALL GRAF(0,SCALE,TIME(NPMTS),YMIN,SCALE,YMAX)
C      C PLOT THE DATA
C      CALL CURVE(TIME,YVAR,NPMTS,0)
C      C END ONE PAGE OF ONE PLOT
C      CALL ENDPG(NMNT)
C      C 1500 CONTINUE
C      GO TO 5000
C      C THIS IS THE PART THAT DOES 3 PLOTS/PAGE
C      3000 DO 3500 NPMT=1,NPAGE
C          CALL PAGE(8,5,11)
C          CALL NBRDR(1,1)
C          CALL AREA(6,0,8,5)
C          CALL HEADIN(YREF,CRITTI,SO,2,1)
C          CALL ENDPG(NPMT)
C      C NOW START THE LOOP FOR PLOTTING THE 3 CURVES
C      DO 3400 NMVE=1,3
C      C NMVE IS THE COLUMN OF THE VECTOR IN DAT BEING PLOTTED
C      NMVE=(3*NPMT+3)+NMVE
C      YMAX=DAT(NMVT-1,1)
C      YMIN=YMAX

```

SIMPLOT Computer Program. (contd)

[illegible]

SIMPLOT Computer Program.

```

86 continue
14.1
101 if (idfr ne 0) go to 78
102 format (1x f11.4 14 (f12.4))
103 write (1) 1
104 do 6 k=1,nc
105 do 6 k=1,ns
106 x=y(k)
107 y(ns+1)=y(ns+1)+CFB(1,k)*x
108 continue
109 do 7 j=1,nc
110 u(1)=y(ns+1)
111 continue
112 if (idfr ne 0) go to 10
113 do 7 j=1,nc
114 do 7 k=1,ns
115 y(ns+nc+1)=y(ns+nc+1)+heat(1,k)*y(k)
116 continue
117 do 8 i=1,nc
118 do 8 k=1,ns
119 y(ns+nc+1)=y(ns+nc+1)+dent(1,k)*u(k)
120 continue
121 if (nd eq 0) go to 9
122 do 9 i=1,nc
123 do 9 k=1,ns
124 y(ns+nc+1)=y(ns+nc+1)+dent(1,k)*u(k)
125 continue
126 do 200 i=1,nc
127 opt(1)=y(ns+nc+1)
128 continue
129 do 201 i=1,nc
130 opt(nc+1)=u(1)
131 continue
132 C WRITE DATA TO THE DAT ARRAY
133 C
134 DAT(1,K4)=T-NBLT
135 DO 1100 DAT(1+1,K4)=Y(NPARAM(11))
136 t=t+dt
137 continue
138 K4=17
139 do 17 i=1,ns
140 y(i)=0
141 continue
142 if (nd le 0) go to 413
143 if (id eq 0) go to 22
144 do 6 k=1,ns
145 do 6 i=1,nc
146 if (idfr eq 0) adjust (k,k4)=dist(k)
147 continue
148 do 30 i=1,ns
149 do 30 k=1,ns
150 y(i)=y(i)+heat(1,k)*y(k)
151 continue
152 do 40 i=1,ns
153 do 40 k=1,ns
154 yp(i)=yp(i)+heat(1,k)*y(k)
155 do 50 i=1,ns
156 if (idfr ne 0) go to 133
157 if (idfr ne 0) go to 133
158 y(ns+1)=0
159 y(ns+1)=0

```

```

.....
..... PROGRAM DISCUSSION .....
..... A DISCRETE TIME SIMULATION OF A LINEAR SYSTEM .....
..... WRITTEN BY BRUCE E. GARDNER .....
..... LAST REVISED 11 FEB 63 BY RICK HALLIDAY .....
.....
..... implicit real*8 (a-h,o,z)
.....
NOTE: DAT IS ONLY SINGLE PRECISION
REAL DAT(13,5000)
INTEGER L(10)
CHARACTER*20 PLTIT
CHARACTER*20 PLTIT(12)
dimension y(75), yp(75), tsw(20), del(1,20), opt(75)
dimension dist(20), at(20), w(20)
dimension heat(40,40), dent(40,6), heat(20,40), dent(20,6)
dimension w(40,20), dent(20,20), dist(20,20), adjust(20,6000)
dimension u(6), NPARAM(12)
real adjust(20), av(20,6000), raw(20), sav(20), cav(20,20)

READ THE PLOT DATA
READ(30,*)NTYPE,NBLT,NBLT,DTH,THAX,IDE,TR
READ(30,*)NPARAM(1),1,1,NPLT
READ(30,*)IDFR,ITIT(1),1,1,NPLT
read(01,*)ns,nc,nd,no,dt
if (idfr eq 0) go to 1
if (itit(1) j=1,ns) 1=1,ns
read(01,*)heat(1,j) 1=1,ns
read(01,*)dent(1,j) 1=1,ns
read(01,*)dent(1,j) 1=1,ns
if (nd eq 0) go to 404
read(01,*)w(1,j) 1=1,ns
read(01,*)dent(1,j) 1=1,ns
read(01,*)dent(1,j) 1=1,ns
data (dist(1),1,1,20)/20*0.0/
write(5,600) 'IF DIST IS RANDOM, TYPE 1. IF NOT, TYPE 0.'
format(1,2x)
read(1,2x) id=5001,d
if (id eq 0) go to 404
write(5,602)
format(1,2x) 'INPUT SCALE FACTORS FOR DISTURBANCES'
read(1,2x) id=601,SE(1),1,1,nd
write(5,603)
format(1,2x) 'IF DESIRE NEW SEEDS, TYPE ANY ODD INTEGER. IF NOT,
+TYPE 0.'
read(5,*) id=603,ISEED

C INITIALIZE SEEDS
DO 21 I=1,10
L(I)=10000+2*I-1
IF ISEED EQ 0) GO TO 4
L(I)=L(I)-ISEED
CONTINUE

C READ IN THE INITIAL CONDITIONS FOR THE SIMULATIONS
14 read(30,*)y(1),1=1,ns
do 86 i=1,nc,no
y(ns+1)=0
21

```

m - Number of controls.

p'' - Number of performance variables.

Item 3

GRTIT, PLTIT(NPLT)

where:

GRTIT - A 50 character variable containing the title which will be put on all *NPLT/NTYPE* pages of plots.

PLTIT - An array of *NPLT* 20 character variables containing the y-axis labels for the plots. The x-axis is always time.

Note: These character variables must be exactly 50 and 20 characters long.

Item 4

XCO(n + r + ns)

XCO is an array containing $n + r + ns$ initial conditions on the simulation states in the following order:

State	Parameter
x_1	plant states
\downarrow	
x_n	compensator states
z_1	
\downarrow	
z_r	
w_1	noise filter states
\downarrow	
w_{ns}	

Description of "Plotdata" File inputs

Item 1

NTYPE, NPLT, NPLTR, DT1, TMAX, IDF, TR

where:

NTYPE- "1" for 1 plot per page, horizontal. "3" for 3 plots per page, vertical. "4" for 4 plots per page, horizontal.

NPLT- The total number of plots to be made *NPLT/NTYPE* must be an integer less than 13.

NPLTR- "1" for immediate results on a VT125 screen. "0" to create plot files, VECTR1.PLV and PARM.PLV.

DT1- The data point interval, *DT1/DT*(from RSANDY) must be an integer.

TMAX- Final time of the simulation, *TMAX/DT1* must be less than 5000.

IDF- "1" to run the simulation *TR* seconds prior to recording data for plotting. This is used to allow filtered noise to reach a steady covariance. "0" to start taking plot data at time= 0.

TR- The number of seconds to wait prior to recording and plotting data.

Item 2

Plot parameter ID's, the array *NPARM**NPARM* is an array containing *NPLT* identification numbers of the variables to be plotted.

The parameters are identified in the following sequence:

ID number	Parameter
1	x_1
↓	↓ plant states
n	x_n
$n + 1$	z_1
↓	↓ compensator states
$n + r$	z_r
$n + r + 1$	w_1
↓	↓ noise filter states
$n + r + ns$	w_{ns}
$n + r + ns + 1$	u_1
↓	↓ controls
$n + r + ns + m$	u_m
$n + r + ns + m + 1$	y_1
↓	↓ performance variables(from RSANDY)
$n + r + ns + m + p''$	$y_{p''}$

where:

n - Order of the plant.

r - Order of the compensator.

ns - Number of states in all the noise filters.

Running SIMPLOT

@SIMPLOT *Plotdata Simfile*

where:

SIMPLOT- A VMS command file which runs the SIMPLOT.EXE file with *Plotdata* and *Simfile* as data files.

Plotdata- A users created file containing data used by SIMPLOT. The input item descriptions are shown on following pages.

Simfile- The simulation model file previously created by an RSANDY run.

The SIMPLOT program will ask 3 questions:

1. "Are the disturbances random?"

Type "1" for yes or "0" for no. If no noise was modeled in the RSANDY run which created the *Simfile*, you must type "0". If you had noise in the RSANDY run but want a clean time response, you can type "0" and no noise will show up in the time responses. If you answered "0" to this question, the simulation will be run. If you answered "1", the program will ask:

2. "Input new random number generator seed?"

Type in any odd integer for a new seed or type in zero for the default seed.

3. "Input scale factors for disturbances"

To force the simulation to be driven by noise having the same RMS as the RSANDY data, type "1,1,1...1" where there are as many 1's as there were random inputs in the RSANDY data, i.e. m' . If you want to scale the RMS of the noise, change the "1's" accordingly. For example, typing "2,.5" will make the first noise source twice the RMS of the RSANDY data and will make the second source half as large.

Appendix M.

SIMPLOT Computer Program

This appendix is the user's guide for the SIMPLOT computer program. The simulation part of the code was written by Bruce Gardner. It uses models created by the RSANDY program to run simulations of the closed loop designs. The program has the option of including the random disturbances used in the RSANDY design. Up to 12 variables can be plotted versus time and displayed on a VT125 screen or sent to a file for later plotting. The listing of the program and an example data set (Navion with full-order compensator from Chapter 2) are shown at the end of the appendix. The user's guide begins on the next page.

SCALEM2 Computer Program. (contd)

```

EXT I
2240 PRINT TAB(10), "THE N MATRIX IS"
2250 FOR I=1 TO NC\ FOR J=1 TO NC\ PRINT TAB(J*8).FNR(N(I,J)).\ NEXT J\ PRINT\ N
EXT I
2260 PRINT
2270 PRINT TAB(10), "THE COMPUTER SCALED VARIABLE MATICES ARE"
2280 PRINT TAB(10), "THE COMPUTER SCALED B MATRIX IS"
2290 FOR I=1 TO NR\ FOR J=1 TO NR\ PRINT TAB(J*8).FNR(BCS(I,J)).\ NEXT J\ PRINT\
NEXT I
2300 PRINT TAB(10), "THE COMPUTER SCALED C MATRIX IS"
2310 FOR I=1 TO NC\ FOR J=1 TO NR\ PRINT TAB(J*8).FNR(CCS(I,J)).\ NEXT J\ PRINT\
NEXT I
2320 PRINT TAB(10), "THE COMPUTER SCALED N MATRIX IS"
2330 FOR I=1 TO NC\ FOR J=1 TO NC\ PRINT TAB(J*8).FNR(NCS(I,J)).\ NEXT J\ PRINT\
NEXT I
2340 PRINT
2350 PRINT TAB(10), "THE COMPLETELY SCALED MATICES ARE"
2360 PRINT TAB(10), "THE AFINAL MATRIX IS"
2370 FOR I=1 TO NR\ PRINT TAB(I*8).FNR(AFINAL(I)).\ NEXT I
2380 PRINT TAB(10), "THE BFINAL MATRIX IS"
2390 FOR I=1 TO NR\ FOR J=1 TO NR\ PRINT TAB(J*8).FNR(BFINAL(I,J)).\ NEXT J\ PRI
NT\ NEXT I
2400 PRINT TAB(10), "THE CFINAL MATRIX IS"
2410 FOR I=1 TO NC\ FOR J=1 TO NR\ PRINT TAB(J*8).FNR(CFINAL(I,J)).\ NEXT J\ PRI
NT\ NEXT I
2420 PRINT TAB(10), "THE NFINAL MATRIX IS"
2430 FOR I=1 TO NC\ FOR J=1 TO NC\ PRINT TAB(J*8).FNR(NFINAL(I,J)).\ NEXT J\ PRI
NT\ NEXT I
2440 PRINT TAB(10), "THE KXIFINAL MATRIX IS"
2450 FOR I=1 TO NC\ PRINT TAB(I*8).FNR(KXIFINAL(I)).\ NEXT I
2460 PRINT TAB(10), "THE KXIFINAL MATRIX IS"
2470 FOR I=1 TO NC\ PRINT TAB(I*8).FNR(KXIFINAL(I)).\ NEXT I
2472 PRINT TAB(10), "THE KODIFINAL MATRIX IS"
2474 FOR I=1 TO NC\ PRINT TAB(I*8).FNR(KODIFINAL(I)).\ NEXT I
2480 PRINT
2490 PRINT "THE A MATRIX REQUIRES A LRTA'3 THEN STRAU IN 1819 ASSEMBLY"
2500 PRINT "THE B MATRIX REQUIRES A LRTA'3.18-SCALEB2." THEN STRAU"
2510 PRINT "THE C MATRIX REQUIRES A LRTA'3.18-SCALEC2." THEN STRAU"
2520 PRINT "THE N MATRIX REQUIRES A LRTA'3.18-SCALEN2." THEN STRAU"
2530 PRINT "THE KX(1) ELEMENT REQUIRES A LRTA'3.18-SCALEKX(1)." THEN STRAU"
2540 PRINT "THE KX(2) ELEMENT REQUIRES A LRTA'3.18-SCALEKX(2)." THEN STRAU"
2550 PRINT "THE KX(3) ELEMENT REQUIRES A LRTA'3.18-SCALEKX(3)." THEN STRAU"
2560 PRINT "THE KXI(1) ELEMENT REQUIRES A LRTA'3.18-SCALEKXI(1)." THEN STRAU"
2570 PRINT "THE KXI(2) ELEMENT REQUIRES A LRTA'3.18-SCALEKXI(2)." THEN STRAU"
2580 PRINT "THE KXI(3) ELEMENT REQUIRES A LRTA'3.18-SCALEKXI(3)." THEN STRAU"
2582 PRINT "THE KXD(1) ELEMENT REQUIRES A LRTA'3.18-SCALEKXD(1)." THEN STRAU"
2584 PRINT "THE KXD(2) ELEMENT REQUIRES A LRTA'3.18-SCALEKXD(2)." THEN STRAU"
2586 PRINT "THE KXD(3) ELEMENT REQUIRES A LRTA'3.18-SCALEKXD(3)." THEN STRAU"
2590 END

```

SCALEM1 Computer Program Example Data.

```

"NR,NM,NC,TP"
6,4,2,05
"A MATRIX(NR)"
-.23081, .89831, -.23642, 1.17826, .43492, .88649
"B MATRIX(NR X NM) MEASUREMENTS DISTRIBUTION MATRIX "
-16.358, -456.87, -.2653, .05456
-8.274, -230.9, -.15366, .012246
10.224, 195.99, .02073, -.005186
2.39548, 49.65, .00599, .000614
2.749, 160.16, .17429, .00936
1.04027, -.01363, -.00002, .00428
"C MATRIX(NC X NR) COMPENSATOR STATE TO CONTROL DISTRIBUTION MATRIX "
0.0, 1.0, 0.0, 0.1, 0.1, 0.0, .688186
-.91396, 2.70164, -.90986, 4.64211, .56013, 1.0
"N MATRIX(NC X NC) COMMAND DISTRIBUTION MATRIX"
-.08369, -.037896
-.164, .07336
"KI MATRIX(NC X NC) INTEGRAL GAIN MATRIX"
-.0042511, -.049046
-.0040024, -.042269
"BSCALE(NM) ----- THE SCALING FACTORS ON SPECIFIC COLUMNS OF B."
.017452, .017452, 1.1
"CSCALE(NR) ----- THE SCALING FACTORS ON SPECIFIC COLUMNS OF C."
1.1, 1.1, 1.1
"NSCALE(NC) ----- THE SCALING FACTORS ON SPECIFIC COLUMNS OF N."
1.1
"KISCALE(NC) ----- THE SCALING FACTORS ON SPECIFIC COLUMNS OF KI "
1.1
"YSCALE(NM) ----- THE SCALING ON EACH MEASUREMENT."
500, 500, 32.8
"CNTRLSCALE(NC) --- THE COMPUTER SCALING ON EACH CONTROL."
1024, 1024
"YDSCALE(NC) ----- THE COMPUTER SCALING ON EACH DESIRED OUTPUT."
8, 32
"YMAX(NM) ----- THE VECTOR OF MAX VALUES OF THE MEASUREMENTS."
20, 20, 20, 30
"YDMAX(NC) ----- THE VECTOR OF MAX VALUES OF THE DESIRED OUTPUTS."
30, 20

```

SCALEM2 Computer Program Example Data.

```

"NR,NM,NC,TP"
5 8,3,05
"THE MINIMAL DISCRETE COMPENSATOR DYNAMICS MATRIX, PHI, IS:"
-O 78263,1 74302,0 90592,0 96006,0 72946
"THE MINIMAL DISCRETE COMPENSATOR INPUT MATRIX, GAMMAMIN, IS:"
-O 00068,0 00024,-0 00074,-0 01160,0 04977,0 01823,0 10458,-1 910236
-O 00076,-0 00083,-0 00088,-0 01252,0 04972,0 00800,0 08074,-1 750846
-O 00214,-0 00052,0 00084,-0 00071,-0 10784,-0 05930,-0 00479,0 370566
-O 00048,0 00001,0 00156,0 00007,0 00701,0 00129,0 00276,0 007696
-O 00356,0 00115,0 00006,0 00581,-0 67143,0 13067,-2 77471,-1 64643
"THE MINIMAL COMPENSATOR OUTPUT MATRIX, HMIN, IS:"
-1 79786,1 82597,1 00000,-0 16434,1 000006
-O 10394,-0 03719,0 36894,1 00000,0 111846
-O 00000,1 00000,0 79317,0 03578,0 09061
"N MATRIX(NC X NC) COMMAND DISTRIBUTION MATRIX"
-4 829E-02,-9 785E-03,-2 378E-036
7 004E-03,-7 883E-02,2 098E-036
-1 175E-02,-3 420E-03,5 886E-02
"THE KX MATRIX"
-26522,-19939,-1 2212
"THE KXI MATRIX"
-0000864,-0001028,-17365
"THE KXD MATRIX"
-094118,-72424,-3 0
"BSCALE(NM)----- THE SCALING FACTORS ON SPECIFIC COLUMNS OF B."
1 1 1 017452 017452 017452 017452 017452
"CSCALE(NR)----- THE SCALING FACTORS ON SPECIFIC COLUMNS OF C."
1 1 1 1 1 1
"NSCALE(NC)----- THE SCALING FACTORS ON SPECIFIC COLUMNS OF N."
1 1 1 1
"YSCALE(NM)----- THE SCALING ON EACH MEASUREMENT."
32 32 32 500 500 500 500 500
"CNTRLSCALE(NC)--- THE COMPUTER SCALING ON EACH CONTROL."
1024 1024 1024
"YDSCALE(NC)----- THE COMPUTER SCALING ON EACH DESIRED OUTPUT."
32 32 32
"YMAX(NM)----- THE VECTOR OF MAX VALUES OF THE MEASUREMENTS."
50 50 30 10 10 30 20 30
"YDMAX(NC)----- THE VECTOR OF MAX VALUES OF THE DESIRED OUTPUTS."
20 20 20

```

END

FILMED

5-85

DTIC